UNIVERSITY OF TWENTE.

**Faculty of Engineering Technology,
Mechanical Engineering &
Sustainable Energy Technology**

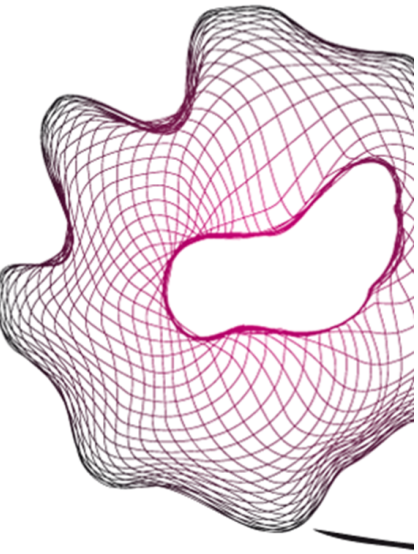

Transitioning to cost-optimal renewable energy systems under uncertainty

Seth van Wieringen

Master Thesis
December 1, 2021

Supervisors:
dr. S. Trip
E. van Druten MSc.
dr. S. Hajimolana
dr. J.B.W. Kok
dr. G.M. Bonnema

Mechanical Engineering
Sustainable Energy Technology
Faculty of Engineering Technology,
University of Twente
P.O. Box 217
7500 AE Enschede
The Netherlands

In memory of Gerbrant van Vledder.

Preface

This report is the result of a year-long graduation period at Witteveen+Bos and serves as a thesis for the Sustainable Energy Techology and Mechanical Engineering masters at the University of Twente. Even though I've had to spend most of the time at home due to the worldwide pandemic, which has been challenging at times, looking back I can say that I've really enjoyed working on my thesis project in a corporate environment.

During my time at Witteveen+Bos, I wasn't limited to working only on my thesis project. I got the opportunity to co-author a large project called "Systeemstudie Gelderland" together with a team consisting of colleagues from Witteveen+Bos and Berenschot. The report presents insight into the impact of the integration of higher shares of renewable energy along with various relevant demographic and technological developments. It was awesome to be able to work on such a meaningful project and I'm grateful for this learning experience.

The experience from this real-life project was combined with the research goals of the Systems Integration research theme within the Thermal Fluid Engineering department. With the help of my daily supervisor Sebastian Trip, the direction of the thesis was formed such that it would provide a sophisticated modelling framework and generate relevant insights into the scope of the Dutch energy transition. I am thankful for his involvement because, without his guidance, feedback and insights, this research would not have been the same.

I would like to thank my supervisor and future colleague at Witteveen+Bos Emiel van Druten for his enthusiasm, knowledge and support. I do not know of any other students that have had the opportunity to go for a ride on the racing bike on a sunny afternoon with their supervisor. I look forward to continuing our teamwork during future projects at Witteveen+Bos.

Every Monday, the "Keek op de Week" would kick-start my week. Because of this moment with colleagues from both Deventer and Den Haag, I was sure to start my week with at least a laugh or two. And, when we could, I've enjoyed our real-life encounters at the office and the occasional food and drinks afterwards. Thank you guys, for your interest, support and insights.

My friends and family have supported me during the writing of this thesis. I am lucky for having such great parents and awesome brothers, thank you for your love and support at all times. Hanneke, thank you for your unwavering support and your ability to comfort me whenever I needed you. I look forward to spending more time together in another way than staring at each of our screens. All my friends, rowing squad, Magnus — thank you for making my time as a student as unforgettable as it was! Onto the next chapter.

Seth van Wieringen, *Olst, December 2021*

Summary

In light of the need for increased climate action, various countries are in the process of decreasing greenhouse gas emissions from the energy system. Policymakers and energy planners are tasked with making high-impact strategic decisions under uncertainty. Energy system modelling and analysis is considered a vital instrument for informing decision-makers of transition pathways. The Dutch energy transition is informed mainly by descriptive energy models used to evaluate the performance of predefined systems in distinct scenarios. In contrast to energy system optimisation models, this approach lacks the ability to provide insight into the optimality of the defined scenario.

Optimisation models entail a high level of complexity and cannot be validated. As a consequence, model outcomes cannot be considered normative by policymakers, and results remain indicative. Various methods to decrease structural uncertainty have been introduced. The near-optimal design space is discovered by applying these methods, allowing policymakers to obtain insight into energy system design trade-offs. Other than statistical methods, there is no method to deal with parametric uncertainties. A novel approach to deal with parametric uncertainty is to apply exploratory modelling analysis.

By applying this method to several case studies within the province of Gelderland using the optimisation model developed in this thesis, insight is obtained into the effect of exogenous cost uncertainties. In addition to this systematic method, clustering is used to visualise patterns in optimal system configurations and are consequently analysed to determine synergies and dynamics. It is concluded that this approach is valuable for increasing policy relevance of energy system optimisation models.

Contents

List of acronyms

API	Application Programming Interface
BOS	Balance Of System
CSF	Capacity Scaling Factor
CRF	Capital Recovery Factor
CRD	Climate Reanalysis Data
CNES	Climate-neutral Energy Scenarios
DSO	Distribution System Operator
DCA	Dutch Climate Agreement
ETM	Energy Transition Model
EVs	Electric Vehicles
ETRI	Energy Technology Reference Indicator
EMA	Exploratory Modelling Analysis
ETS	Emissions Trading System
ESOMs	Energy System Optimisation Models
GHG	Greenhouse Gases
LCOE	Levelised Cost Of Electricity
LP	Linear Programming
LESO	Local Energy Systems Optimizer
MAA	Modelling All Alternatives
MGA	Modelling to Generate Alternatives
MILP	Mixed Integer Programming
NLP	Non-Linear Programming
NCA	National Climate Agreement
OSC	Overnight System Cost
PPA	Power Purchase Agreement

RVO	Rijksoverheid voor Ondernemend Nederland
RES	Regional Energy Strategy
SOC	State of Charge
STC	Standard Testing Conditions
TMY	Typical Meteorological Year
TSO	Transport System Operator
VRE	Variable Renewable Energy
WACC	Weighted Average Cost of Capital

Chapter 1

Introduction

This chapter is an introduction to this thesis. It does not serve as an introduction to the subject itself. This thesis forms the conclusion to two masters: Sustainable Energy Technology and Mechanical Engineering. In section 1.1 a brief description of the two master programmes in relation to this thesis is given. After this, section 1.2 declares the scope of this research and section 1.3 introduces the research questions. Finally, section 1.4 contains a readers guide aimed at presenting an overview of this thesis' content.

1.1 Two masters, one thesis

After obtaining my bachelor's degree in Mechanical Engineering, I wanted to focus more on the subject that sparked my interest the most: the energy transition. As a result, I enrolled in the master's programme of Sustainable Energy Technology at the University of Twente. This master covers nearly all technical aspects associated with the energy transition and even mixes in the required economic and societal subjects. In my second year, I decided to also take up the master of Mechanical Engineering in conjunction with Sustainable Energy Technology. I choose the Design Engineering track, as I always felt that understanding the technical design processes was at least as important as the technical skills themselves.

This thesis was conducted based on knowledge and experience from both masters. The sustainable energy domain knowledge mostly comes from Sustainable Energy technology. Courses such as Wind Energy, Solar Energy and Energy Storage were each quite literally qualifying factors to be able to conduct this research. Without the specific technical ability obtained in those courses, it would not have been possible to write this thesis. Additionally, other courses from the program such as Energy, Sustainability and Society have made me realise the societal implications of technology, for instance through policies.

The courses from the Mechanical Engineering - Design Engineering master have served a more supportive role. This thesis aims to contribute to a complex part of the energy transition: optimal system integration of renewable energy. Without the insights from courses like Modelling Technical Design Processes and Engineering Project Management, it would have been very difficult to form an actionable approach that incrementally validates and improves the research and model. Moreover, from courses like Electric Vehicle System Design and, from the Mechanical Engineering bachelor, Systems Engineering I have learned to adopt a mindset that supports the design and integration of more complex systems.

Finally, I would like to conclude by saying that I believe this thesis is a good reflection of the skills I have developed during my education and that I have enjoyed working hard to contribute a small part to the Dutch energy transition and academic research.

1.2 Scope

This thesis is the result of a graduation project in collaboration with Witteveen+Bos. This company of consulting engineers is one of the players in the energy transition that provides key insights for policymakers and offer engineering services for realising projects. In this sense, Witteveen+Bos is heavily intertwined with the Dutch energy transition.

The scope of this thesis is in part aligned with a project at Witteveen+Bos and in part with an ongoing research project at the University of Twente. This research project is conducted within the Thermal and Fluid Engineering department. The chair of Energy Technology has a project called *Smart Energy Grid Regio Nijmegen* within the research theme "Energy Systems Integration". One of the research goals of the Smart Energy Grid Regio Nijmegen project is to develop sophisticated models to identify innovative local energy system configurations. At the same time, Witteveen+Bos has an ongoing project on system integration of regional energy strategies within the province of Gelderland. The goal of this project is to generate insights for policymakers and energy planners based on the planned deployment of renewable energy assets and demand development of the regional energy strategies.

To align the two aforementioned goals, this thesis develops an energy systems model and subsequently applies this model in the context of Gelderland system study to generate insights for policymakers. In the Dutch energy transition, similar integration studies are carried now and will be carried out in the years to come. Therefore, the research has been generalised to fit the Dutch context. Only in the application of the model in the case studies the scope of Gelderland is applied.

1.3 Research questions

Based on the research scope and research goals of both Witteveen+Bos and the Energy Technology department at the University of Twente a set of research questions is formulated. Below an overview of the research questions is given. In the mind of continuous improvement, these have been updated during the thesis when new insights were obtained. The research questions still reflect the original intention but are reformulated to better represent the final content of this thesis.

1. How is Dutch energy transition policy formed and how do energy system modelling studies contribute? *(chapter 2)*

    1.1. In what way can energy system modelling approaches currently underutilized in the Dutch energy policy be applied to present new information? *(chapter 2)*

2. What do cost-optimisation studies reveal about the deployment of renewable generation and storage required for decarbonising energy/electricity systems/sector? *(chapter 3)*

    2.1. What methodology can be applied to optimisation models to explore the robustness of optimisation results in relation to uncertainties? *(chapter 3)*

3. What design considerations are imperative to create an optimisation model that can be used to explore uncertainties and policy effects? *(chapter 4 and discussion)*

    3.1. How can the optimisation model be coupled to existing models to reflect the effect of (inter)national energy policies? *(chapter 3 and chapter 5)*

4. How can exploring energy system optimisation models under uncertainty provide insights into cost-optimal system configurations to support (robust) energy transition policy? *(chapters 7-9 and discussion)*

    4.1. How can optimization models be utilized such that, in addition to uncertainty, the impact of various scenarios can be assessed? *(discussion)*

    4.2. Which cost-optimal system configurations can be identified for case studies within the province of Gelderland? *(chapters 7-9 and discussion)*

Answers to the research questions are provided in the conclusion section of the chapters. The chapters that contain the answers to the questions can be found next to the respective questions. At the end of this thesis, an overview of all research questions and respective answers is omitted within the conclusions to preserve conciseness. However, the research questions and respective answers are used as a basis to formulate the main conclusions.

1.4 Readers guide

In this section, an overview of the content of this thesis is given. An graphical overview is shown in figure 1.1. This thesis has two introductory chapters. Chapter 2 is an introduction to the Dutch energy transition and associated processes and policies oriented towards the regional energy strategies and system integration studies. In this chapter, it is identified how energy systems modelling can be implemented to generate new insights for supporting policymakers. Chapter 3 introduces a specific energy systems modelling approach based on analysis of literature and reveals model design considerations and introduces the gap in the literature on explorative use of energy system optimisation models under uncertainty.

The developed energy systems optimisation modelling framework and submodels are introduced in chapters 4 and 5, respectively. Chapter 4 provides an overview of the framework capabilities while chapter 5 presents a detailed description of each of the component submodels.

Chapter 6 describes the methodology applied to the various case studies within the province of Gelderland. Consequently, chapter 7 presents the results obtained on the local energy projects: the cable pooling project and electric mobility hub. Chapters 8 and 9 presents results obtained for regional energy strategies and the province of Gelderland in 2030 and 2050, respectively.

In chapter 10, the case study results are related to the research questions, implications of the applied modelling methodology and following from that, recommendations for future research are discussed. Finally, chapter 11 concludes this thesis and concisely presents the main findings and recommendations of this research.

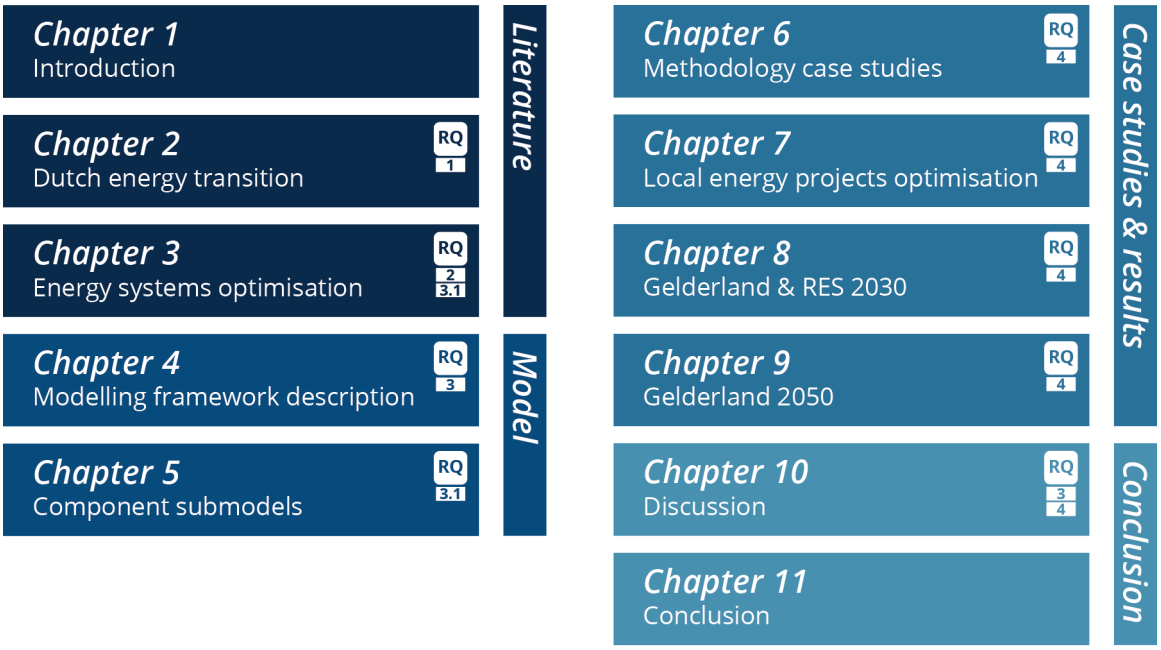

Figure 1.1: Graphical overview of the content of this thesis. RQ stands for research question and can be used to find which chapters answer the research questions in the respective conclusive section.

Chapter 2

Dutch energy transition

Across academics, politics, and society, little doubt remains on climate change's adverse effects and causes. The current system of energy, production and consumption is not sustainable. Transitioning from the polluting and damaging status quo to a climate-neutral and sustainable future is vital and imminent.

This chapter provides a comprehensive overview of the energy transition in the Dutch context. Various parties are involved in the energy transition. Each party has a unique perspective and is dedicated to specific tasks, possibly secured or enforced by legislation. An overview of involved parties and their respective roles is presented based on a review of relevant legislation, governmental proceedings and grey literature. Processes and policies that support and govern the transition of the Dutch energy system are discussed. Therefore, this chapter provides the overview, context, and knowledge to propose the experimental content included in this thesis. Additionally, by analysing the energy systems modelling methodology applied, a gap in current policy supporting processes is identified.

The energy transition is complex and multi-disciplinary. It entails any direct or indirect energy-consuming sector, from households to industry. The scope of this thesis is limited to the power system. An overview of parties involved with the transition of the Dutch energy system is given in section 2.1, with a specific focus on the power system's transition. Processes, policies, and associated publications relevant to the Dutch energy transition are presented in section 2.2. Finally, this chapter is concluded in section 2.3.

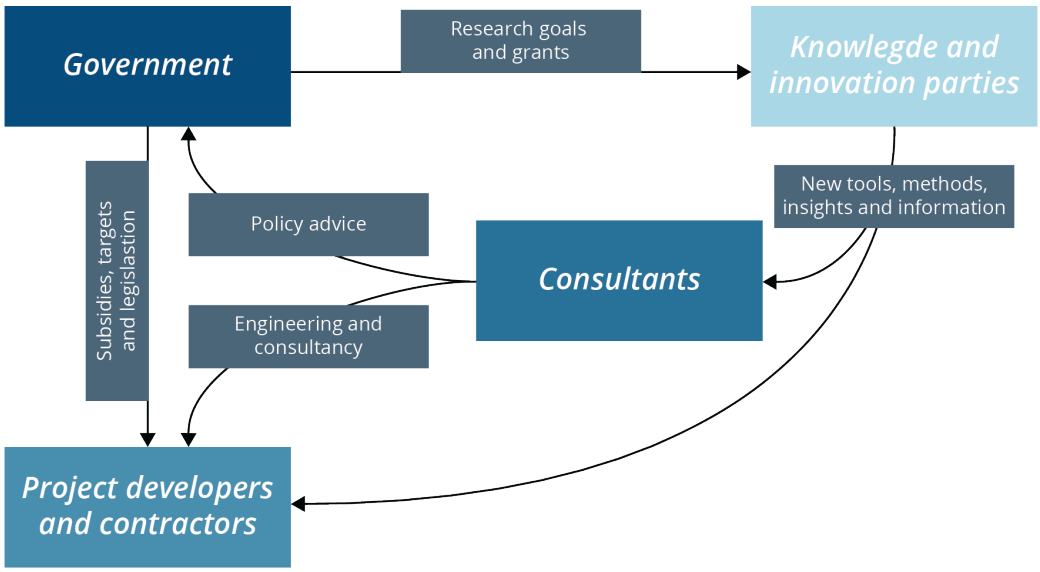

Figure 2.1: An abstract overview of the various parties involved in the Dutch energy transition, based on their role.

2.1 Involved parties

To obtain insight into the playing field of the Dutch energy transition it is vital to know what parties are involved and what their respective role or perspective is. It is recognised that providing a comprehensive overview scoped towards this thesis' content will in some respect negate the complexity of the organisation, policies and legislation of the transition. Unmistakably, without providing any specific context the societal relevance of this research cannot be pinpointed. Societal relevance is favoured, as it allows to align this work with the mission of the University of Twente: *"The University of Twente is the ultimate people-first university of technology. We empower society through sustainable solutions."* [1] In other words, the UT aims to provide solutions to real-world problems through its research.

Parties that play a significant role in the Dutch energy transition have been established based on literature review and subsequently curated based on expert opinion with help of the colleagues at Witteveen+Bos. Four categories of parties are used to provide some taxonomy, i.e. a systematic classification of the parties. The identified categories are (local) government (i.e. the demanding party), project developers and contractors (i.e. the executive parties), consultants and knowledge and innovation parties (i.e. research institutes and universities). The government set goals, decides on subsidies, provides legislation and warrant compliance with goals and legislation. Project developers and contractors realise the energy projects that contribute to reaching the targets and are incentivised by legislation and subsidies. Consultants are parties that are able to provide unbiased specialist knowledge to support policymakers and decision-makers with information or on complex challenges in realising goals. Knowledge and innovation parties generate and/or combine new domain knowledge through fundamental or applied research. An abstract overview of the identified groups is shown in figure 2.1.

Depending on the scope, perspective and system level, the exact parties in this process overview change. From an international perspective, all national governments could be regarded as the demanding party through the Paris agreement. An executive party would then be the European Parliament, which consults the European Commission to support decisions and policies. Innovative parties would entail academics, industry and consortia alike on an international level.

Since this thesis is tailored towards the Dutch energy transition specifically, an overview of the parties on a national level is given below. The boundaries chosen are based on the current organisation of the energy transition within the Netherlands. Per category, publications and documents that fulfil a substantial role in the Dutch energy transition are listed. These will be further elaborated and connected in section 2.2.

1. **Government**
   Dutch national government, provinces, municipalities, regional energy strategies, National Program regional energy strategies
   Relevant publications: Klimaatakkoord (climate agreement), RES goals, PBL's climate and energy outlooks.
2. **Executive parties**
   Grid operators (TSO and DSO), renewable energy project developers, RVO, etc.
   Relevant publications: System studies, infrastructure outlooks.
3. **Consulting parties**
   CE Delft, Witteveen+Bos, Kalavasta, DNV, Royal HaskoningDHV, Quintel Intelligence, OverMorgen, Berenschot, etc.
   Relevant publications: RES offers, system studies, infrastructure outlooks
4. **Knowledge and innovation parties**
   TNO, TU Delft (Engineering Systems and Services), TU Eindhoven (NEON Research) & University of Twente (Energy Systems Integration), etc.

This thesis is the result of a graduation internship at Witteveen+Bos, one of the consulting parties in the Dutch energy transition. The University of Twente is one of the innovative parties in the energy transition, that generates knowledge by conducting research. This offers a unique value proposition, by connecting the knowledge and functions of both domains. It should be possible to adapt energy system modelling methodologies developed by research institutes effectively by leveraging on the practical domain knowledge of Witteveen+Bos in an effort to bridge the gap between academics and society. As a result, consulting parties will be better equipped to inform executive parties while novel modelling methodologies can be developed and tested on real-life cases. This will in turn hone the societal relevance of academic energy system modelling. To be able to stipulate where and how such a contribution can be made, the current process, policies and relevant publications are analysed in section 2.2.

2.2 Current process, policies and publications

Global warming results from anthropogenic activities that the emit Greenhouse Gases (GHG), such as carbon dioxide and methane [2]. After recognising the validity of climate change, 195 national governments committed to severely reducing emissions to address the pressing issue. This international assembly of countries named the conference of parties (COP), signed the by now well-known Paris agreement [3]. While writing this thesis, COP26 in Glasgow is taking place. Leading to this major event, several countries have raised their Nationally Determined Commitments illustrating the perceived urgency of rising to the climate change challenge [4]. The European Union has recently increased its emission reduction ambition from 40% to 55% by 2030, relative to 1990 levels [5]. The increased emission reduction ambition is received well and is supported throughout the EU [6]. It is recognised that large scale deployment and integration of renewable energy sources play a major role in reaching decarbonisation goals because 75% of GHG emissions in the EU come from the energy sector. The target share of renewables in the European energy mix by 2030 is increased from 32% to 40% in the new renewable energy directive, while this share was 20% in 2019 [7].

To organise and realise emission reduction on a national level, the Dutch government passed the climate law and published the National Climate Agreement (NCA) which outlines the organisation and sector-specific targets [8] [9]. This law was passed before the European Green deal and set a goal of 49% emission reduction by 2030, although it is expected that the reduction goal will be aligned with the new European target. Monitoring whether the current policy is sufficiently effective for reaching the renewability goals across all policies is done by PBL. This is done based on a yearly publication: Klimaat en Energieverkenning (Climate and energy outlook) [10]–[13]. Moreover, the NCA sets clear renewable electricity generation goals for 2030. A target of 35 TWh annually generated electricity is set for large-scale onshore renewables. To achieve this goal while respecting local constraints, taking into consideration of spatial integration and societal support the Netherlands is divided into 30 regions. These regions are tasked with establishing a Regional Energy Strategy (RES). Each of these regions is tasked with determining how much renewable electricity can be generated within that region by 2030, and with what technologies this is achieved. A framework for procedures and communication between the regions is secured by a higher-level organisational body called the National Program RES.

However, it is not trivial that from the combination of a very abstract top-down goal of energy generation (i.e. climate agreement target) and bottom-up approach of spatial integration and societal support (i.e. the RES) a robust and optimal transition to the future system integration is achieved. The regional energy strategies do not consider the effect of spatial dispersion of renewables on the grid infrastructure nor does it consider consequences or cost impacts on the national system. As the European Commission [14] states: "*Without robust policy action, the energy system of 2030 will be more akin to that of 2020 than a reflection of what is needed to achieve climate-neutrality by 2050.*". It is therefore vital that policymakers are well-informed on the impact of the transformation from the current centralised, dispatchable energy generators to geographically distributed, time-variant, renewable energy sources on a system level.

Therefore, system integration studies are carried out on a provincial level. These system studies aggregate the RES within a province and analyse the challenges and opportunities on a system level if all regional plans become reality. A central topic in the system integration studies is the effect of increased supply of renewable energy sources as well as increased electrification of various sectors on existing energy infrastructure. In contrast to the RES, this approach forms a more clear overview and allows the assessment of the system impact of the multiple RES' and formulate advice that enables the mitigation of possible negative effects while identifying possible regional opportunities. A literature study is carried out to obtain more insight into the system integration studies specifically. The analysis of the system integration studies methodologies is presented in section 2.2.1.

2.2.1 System integration studies

The system integration studies aggregate all RES' within provinces to obtain an overview of local decisions in terms of renewable energy generation and establish the balance of supply and demand by 2030 and 2050. The focus of system integration studies is on the changing and increasing demand on energy infrastructure, and where ever possible map possibilities of systems integration. Each of these reports includes a grid study carried out by the Dutch Transport System Operator (TSO) TenneT, and Distribution System Operator (DSO) within that province. As a whole, these reports aim to highlight the regional plans within the provincial context, which allows for a more coordinated system approach between regions without diminishing the intentions of detailed regional studies.

As of now, eight provinces have already published their system studies. The provinces Groningen and Drenthe together have published their system study together, so a total of seven reports is available now. During this thesis work, I co-authored the system study for the province of Gelderland. By contributing to the system studies, I obtained insight into the process and methodologies applied in system studies. During this period, the system study for the province of Utrecht was also under development. The authors of this study (Quintel Intelligence) were contacted to obtain insight into their process and methodology.

The two remaining provinces needed to cover 12 provinces within the Netherlands are the province of Flevoland and Friesland. Both these provinces are also their own RES region and have not carried out system integration studies yet. Friesland states that the methodology followed in the RES publication lacks an integral approach and focuses only on the realisation of renewable energy and plans to carry out a system study [15]. The province of Flevoland consulted the TSO and DSO directly in the RES publication, which results in a set of qualitative descriptions for the mitigation of possible net congestion [16].

All reviewed provincial system studies follow a generally similar methodology. First, scenarios are created for 2030 and 2050. The scenarios are detailed using the RES, region-specific information (e.g. data on industry or mobility within the province) and apply the latest projections (e.g. technology adaption rates, demographic changes, etc) to obtain a scenario that aims to provide a realistic representation of the province in 2030. For the 2050 scenarios, the aim is no longer to provide a representation that is as realistic as possible but rather to examine the effects of diverse future system configurations. To this end, the provincial studies use one of two sets of scenarios that have been developed by the party of Dutch system operators, NetbeheerNL, covered in more detail in section 2.2.2. To quantitatively interpret the effects of those scenarios, simulation tools and models are employed to determine the energy balance and flows of various energy carriers on an hourly basis for the horizon year. Based on the modelled scenarios, the grid operators test the current infrastructure against the developed scenarios. Finally, the system studies are able to provide key information on a system-level based on the obtained results. An overview of the utilised scenarios and applied tools per provincial system study is given in table 2.1.

From table 2.1 it can be concluded that there is some agreement in the scenarios and tools utilised in the system studies. The studies on the province of Noord-Holland and Zeeland are slightly different from the rest, applying the older scenarios ”Net voor de Toekomst” scenarios [26], while other studies apply the newer ”Klimaatneutrale Energiescenario’s” [27]. Both Noord-Holland and Zeeland use the corresponding 2030 scenarios, instead of scenarios based on the RES (and/or climate agreement). Moreover, as laid out in section 2.2.2, the two sets of scenarios are very similar. It can therefore be concluded that these scenarios are widely used to investigate possible future configurations of the energy system to inform policymakers.

On top of this, nearly all scenarios used in the system studies have been modelled using the Energy Transition Model (ETM). This scenario-based modelling tool offers an integral, independent and transparent platform to model energy systems. It is completely open-source, including the underlying data sets. It has been developed by Quintel Intelligence with the support of numerous parties, including grid operators and the Dutch Ministry of Economic Affairs and Climate Policy. It is used by (local) government, consulting parties and research institutes. Through a web-based graphical interface, assumptions and predictions about developments between the reference year and the horizon year can be implemented in the model. The ETM calculates the energy demand, energy production, electricity prices, import and export, etc on an hourly basis. It is also able to present the impact of the

Table 2.1: Overview of the scenarios and tools implemented in the provincial system studies.

Provincial	Scenarios			Tools			
system study	RES 2030	KNES 2050	NvdT	ETM	CE tools	Other	ref.
Gelderland	x	x		x			[17]
Groningen & Drenthe	x	∼	∼	x	x[a]		[18]
Limburg	x	x		x	x[b]		[19]
Noord-Brabant		∼		∼		x[c]	[20]
Noord-Holland			x		x[d]		[21]
Overijssel	x	x		x			[22]
Utrecht	x	x		x			[23]
Zeeland			x		x[e]		[24]
Zuid-Holland	x	x		x			[25]

x marks that this study uses the specified tool or scenario while ∼ represents a processed or interpreted version of that tool/scenario. KNES 2050, "Klimaatneutrale energiescenario's 2050" (climate-neutral scenarios 2050). NdvT, "Net voor de toekomst" (Grid for the future scenarios, both 2030 and 2050).

[a] *CEGOIA*

[b] *CE PowerFlex*

[c] ETM scenario demand curves are used in internal undisclosed model.

[d] *CE explorer, CEGOIA*

[e] *CEGOIA, CELINE, CE PowerFlex*

modelled parameters in terms of system cost, emission reduction and regional energy balances. Due to the ease of interaction and open-source nature of the ETM, the model is transparent and fulfils a key role in bridging the gap between policymakers and energy system modellers. It is concluded that by modelling future energy system configurations in the ETM a wide support base can be established.

2.2.2 Integral infrastructure outlooks

The exact configuration of the Dutch energy system of the future is uncertain and subject to political decisions, societal support and technological innovations. To be able to somehow assess the demands of possible configurations on energy infrastructure, the Dutch party of grid operators have studied future energy systems based on energy scenarios. These scenarios are diverse in terms of global developments (e.g. the emergence of a global hydrogen economy), energy demand (e.g. industrial growth, electrification of heat and mobility) and national energy self-sufficiency. As such, these uniquely different scenarios aim to provide insight into the required infrastructure for the corresponding energy systems. In reality, the transition from one system to a future state results from the complex dynamics of politics, society and economics [28]. Therefore, the designed energy system scenarios are not a reflection of the most realistic future energy configurations. However, by using this descriptive modelling approach the performance of a given future outcome can be analysed [29].

In 2017 NetbeheerNL released the "Net voor de Toekomst" (grid for the future) publication [26]. Later, a consortium named the "Integrale Infrastructuurverkenning 2030-2050" (integral infrastructure outlook, II3050) was formed which published a series of reports on future energy system configurations. Since the provincial system studies use scenarios for 2050 based on both, a brief introduction and overview is given below.

Net voor de Toekomst

In this publication, four possible future energy system scenarios are introduced depending on different societal and political directions. They are defined based on the level of scale the energy transition is governed and on the level of self-sufficiency on a (sub)national level. From this approach, the following scenarios are defined.

1. **Regional**
   High level of regional control, e.g. municipalities and provinces take initiative. Electricity and heat are generated locally as much as possible. A combination of on-shore wind, solar PV, biomass and geothermal determine the energy mix.
2. **National**
   The government takes a leading position and steers towards energy autarky on the Dutch national level by taking control in the deployment of more centralised and large-scale energy sources, mainly off-shore wind.
3. **Generic**
   A natural transformation of the energy system is assumed. No government interference other than a strong incentive to decarbonise through CO2 prices and other taxes.
4. **International**
   In this scenario, the Dutch energy transition is strongly intertwined and dependent on the global energy transition. Cross-border trade in renewable electricity and energy carriers such as hydrogen is typical for this scenario. The resulting energy mix is a combination of renewables and fossil with carbon capture.

Integral infrastructure outlook 2030-2050

The Dutch Climate Agreement (DCA) recognises the significance of infrastructural changes required to facilitate the Dutch energy transition. Industrial demand development and the increase in decentralised, variable energy production is assessed to obtain insight into the required infrastructural investments [8]. As a result the Netbeheer Nederland consortium consisting of TenneT, GasUnie and the regional grid operators (Liander, Stedin, Enexis, Coteq, Rendo, Westland Infra and Enduris) was tasked in 2019 with delivering an integral infrastructure outlook.

This outlook was organised in several phases. Firstly, the existing future energy scenarios were revised based on the latest trends, projections and insights. These scenarios were then used by the grid operators to determine the effects of those scenarios on the infrastructure. Finally, a report bringing forth relevant conclusions and insights based on the carried out infrastructural calculations and analysis was published [30].

Similarly to the Net voor de Toekomst scenarios, four future energy system scenarios were published for the integral infrastructure outlook. These are called the ”Klimaatneutrale Energiescenario’s” (climate-neutral energy scenarios, CNES) [27]. The scenarios follow a similar but slightly different structure, as detailed below.

1. **Regional**
   This scenario is focused on regional control and energy autarky. Key concepts are high levels of decentralised power generation, by deploying high shares of on-land wind turbines and solar PV. The energy demand from industry is assumed to shrink and electrify where possible. This results in a substantial reduction in energy demand.

2. **National**
   This scenario assumes strong leadership by the Dutch government. This allows for more centralised renewable energy sources, mainly an expanded capacity of offshore wind production. The industry remains roughly the same size. Energy self-sufficiency is achieved on a national level.
3. **European**
   Significantly less renewable energy is generated within the Netherlands leading to low self-sufficiency on a national level. Additionally, this scenario assumes a growing industry. The import of hydrogen, biomass and fossil fuels closes the energy balance. The scenario is centred around biomass and highly dependent on CO2 capturing technologies to mitigate or reduce emissions from fossil energy sources.
4. **International**
   This scenario displays the lowest self-sufficiency and renewability. This energy system configuration relies very heavily on the availability and import of green hydrogen. Additionally, this scenario assumes a growing industry and is the only scenario where the final energy demand increases. In this scenario, hydrogen and bio-gas could be feasible alternative energy sources for natural gas in gas plants.

The CNES scenarios are used for the integral infrastructure outlook, making them more valuable than other generic scenarios. Moreover, all scenarios are modelled in the ETM, making them highly accessible and transparent. As a result, the CNES are used throughout the provincial system studies. However, this descriptive modelling approach only produces four possible corner piece scenarios for 2050. It is reasoned that these can be used to assess the bandwidth of required energy infrastructure and to identify no-regret investment decisions. As such, the scenarios were never meant to represent optimised or desired future energy system configurations that policymakers should choose between. Instead, a realistic and feasible, well-balanced energy system is expected to be somewhere in solution space between the four corners. There are no insights into solutions existing in the plausible solution space nor where an optimal system might be found. This insight is vital to support policymakers in establishing a desired future system which the transition should lead to. Combinations of the four scenarios do not exist nor do they contain continuous variables that can be used to determine tipping points or trade-offs.

2.2.3 On the lack of optimisation studies

Dutch national and regional government is tasked with the transition to a clean, affordable and dependable energy system. The Dutch climate agreement and law, and subsequently the regional energy strategies, are tasked with realising this transition. This transformation ideally is managed by policy measures that ensure an orchestrated transition to the desired state of the future energy system. However, the scale and complexity of national and regional energy systems and the mutual interaction require robust long-term planning which has introduced increasing reliance on energy system modelling [31].

Lund et al. [29] defines two distinct categories of energy system models that can be used to analyse energy systems and generate insight using modelling. Descriptive models that are based on predefined system configuration are referred to as simulation models. Prescriptive models that are used to find the optimal configuration given a set of decision-variables such as technology deployment are defined as optimisation models. Based on the review of the Dutch energy transition policy, process and relevant publications it can be concluded that simulation models are mainly used through prescribing distinct energy system scenarios. However, it is recognised that optimisation models are more suited to support policy makers and energy planners in achieving robust long-term policy [31].

The current approach can be summarised by the top-down renewable electricity generation target, enforced by the climate agreement, which is subsequently realised by bottom-up spatial integration through the regional energy strategies. Effects of regional policy decisions to realise the imposed targets are only reactively assessed in the provincial system studies. This distributed approach with regional renewable energy deployment pledges does not inherently consider system integration. As such, it is not a strategically orchestrated transition. This lack of insight into the optimality of the future energy system that emerges from this approach has been recognised by politicians, calling for "*optimisation studies to gain insight in cost-optimal energy configurations, as scenario-based studies have been carried out but optimisation studies are missing*" [32]. Therefore, it can be established that there is a distinct demand for applying energy system optimisation models to help inform energy planners and policymakers in the Dutch energy transition.

2.3 Conclusion

This chapter analysed the parties, policies, processes and publications governing the Dutch energy transition. Based on a review of relevant proceedings and publications in grey literature, involved parties have been mapped. Using a taxonomy, these parties have been assigned to groups that each fulfil distinct functions in the Dutch energy transition. This thesis is a product of a graduation internship at Witteveen+Bos, one of the consulting parties of the transition, and its practical domain knowledge is utilised to come to a societal value proposition while bridging the gap between academics and consulting parties.

Moreover, through the review of the grey literature, the first research question can be answered. *How is Dutch energy transition policy formed and how do energy system modelling studies contribute?* Dutch energy transition policies are developed in three phases. First, the national Dutch government sets a renewable energy target with the aim to reduce emissions to comply with international and European agreements and laws. This goal is subsequently imposed on local governments by organising municipalities into regional energy strategies. These regional energy strategies are tasked with mapping the possible quantities of renewable energy generation deployment within that region, based on spatial integration, societal support and local integration opportunities. Lastly, the pledged and/or proposed renewable energy generation deployment resulting from the regional energy strategies is evaluated in the provincial system studies. These studies assess the impact and effect of the pledges on a provincial level and focus mostly on system effects, such as grid infrastructure congestion.

Moreover, prescriptive energy modelling is applied to generate insight for energy planning and policymakers into the effect of possible future energy system configurations. To this end, climate-neutral energy scenarios have been modelled in the Energy Transition Model. Consequently, these scenarios have been used to carry out infrastructure studies both on a national and provincial level. Considering the research question: *In what way can energy system modelling approaches currently underutilised in the Dutch energy policy be applied to present new information?* it can be stated that optimisation studies are underutilised in the current process. Energy system optimisation models are marked in academic literature as more suited for supporting robust policies for long-term energy systems planning. In the parliament, this lack of optimisation studies on future Dutch energy systems has been recognised, and a motion stipulating this concern is passed.

However, it should be recognised that completely steering away from the current process will negatively impact the support base for energy optimisation model outcomes. Leveraging on the fact that there is already a consensus in terms of the future scenarios to use and the descriptive model that is used as a platform, the optimisation studies should align with the current methodology to expand knowledge and societal relevance. By coupling the energy system optimisation model to the existing descriptive models, i.e. the climate-neutral energy scenarios modelled in the Energy Transition Model, optimisation models can be used to generate new insights on the Dutch energy transition.

Chapter 3

Energy systems optimization models

As outlined in chapter 2, there is an opportunity to apply energy system optimisation models to provide new insight for energy planners and policymakers involved in the Dutch energy transition. Based on a review of the current process, it was found that descriptive modelling is predominantly used. This category of models is very suitable for evaluating an energy system based on a predefined configuration but lacks the ability to find optimal configurations.

This chapter provides a comprehensive review of the literature published in the energy systems modelling niche, with a specific focus on energy system optimisation models. Before attempting to apply optimisation models in the Dutch context, it is vital to obtain insight into key modelling considerations in terms of formulation of the model, such as the spatial and temporal resolution or geographic scope of the model. Other than the technical validity of the modelling approach, care should be taken that the modelling approach and decisions on corresponding assumptions are aligned with the purpose and intended use of the model.

In section 3.1, a brief introduction to optimisation modelling for energy systems is given. Section 3.2 present a brief overview of the landscape of existing energy systems optimisation models and analyses model outcomes from present studies. Based on the publications surrounding energy system optimisation modelling methodologies, section 3.3 presents insight into design considerations when applying optimisation models for long-term planning of energy systems. The validity and uncertainty associated with model outcomes are addressed in section 3.4. Finally, section 3.5 concludes this section.

3.1 Optimisation

International action on climate change has initiated the transition of energy systems based on sustainable energy resources. However, the optimal configuration of future energy systems remains largely unknown [33]. To obtain insight into the possible configurations of future energy systems based on renewable energy, energy modelling analysis has been adopted to model complex relationships and interdependencies, temporal variability and spatial dispersion [29]. Governments, policymakers and energy planners tasked with making required strategic planning decisions are increasingly dependent on the development and implementation of energy modelling tools [34]. Energy System Optimisation Models (ESOMs) specifically, are widely used to generate insights to inform energy and environmental policymakers [35].

The term optimisation is used to describe methodologies that either maximise or minimise the objective function (e.g. minimal cost) by varying a set of design variables. In ESOMs, the objective function often represents system cost and the design variables represent deployment and operation of technologies. ESOMs outcomes will therefore be able to determine the optimal configuration and operation of a given energy system [36]. The energy balance is implemented as constraint equation. As a result, the determined energy system is scaled such that during the operation over the predefined time horizon the system is capable of delivering the power needed to meet the demand for energy at every time step.

Optimisation models can be formulated using various mathematical programming methodologies. Linear Programming (LP) is the most simple and considers (piece-wise) linear relations and (in)equalities. The addition of binary variables yields Mixed Integer Programming (MILP). When the model purpose requires the inclusion of more complex and non-linear relations the model will be formulated using Non-Linear Programming (NLP). If the design variables of the optimisation model are based on components that exhibit complex dynamics (e.g. ramping speed, partial load efficiencies, minimal up-time of thermal plants) the model can be best formulated using either MILP or NLP to achieve sufficient accuracy. For modelling purposes that are less focused on exact dispatch dynamics or that do not consider design variables based on such complex dynamics LP is favoured for computational tractability [37].

ESOMs can be further divided into ”snapshot” and ”evolution” categories [34]. Models in the snapshot category can be used determine to optimal system configuration and operation for a given time period somewhere in the future. As a result, this formulation is representative of a long-term equilibrium optimal outcome under predefined conditions [38]. Evolutionary models start with the existing power system at the reference year and incrementally optimise technological deployment over the modelled time horizon. As a result, models that use this approach can also be used to describe the pathway to the optimal configuration of the energy system [33] [39].

3.2 Existing models

In literature, plenty of review papers can be found that present a clear overview of existing energy system models [39]–[48]. This section does not aim to provide a similar overview that categorises, compares or ranks existing models. Rather, it presents a select number of high-level insights based on the diversity of models found in the literature.

In general, it was determined that there is a diverse landscape of developed models. These models are diverse in various aspects, which can be used to explain the co-existence of many models. Firstly, there is the origin of the model. Some models are (in part) realised by commercial parties while others are developed by academics, often impacting the specific application area. Then there is the purpose of the model, i.e. what is the research question to be answered. Based on the purpose of the model, various model design considerations can be decided. This is further unpacked in section 3.3.

One challenge that is repeatedly addressed in literature is the availability and reproducibility of energy system models. This is covered separately in section 3.2.1. This thesis is oriented towards providing insights into the Dutch regional energy strategies. Therefore, studies that have applied ESOMs to determine energy system configurations at the national, sub-national or regional levels with high shares of renewable energy generation and storage are of special interest. Observations and conclusions of those studies are analysed in section 3.2.2.

3.2.1 Transparency and traceability

The development of increasingly complex energy modelling tools has been accompanied by criticism regarding the transparency, responsibility and accessibility of models [40]. Historically, energy systems have been dominated by only a few players. There was no obligation for large commercial parties or government agencies to reveal data, assumptions or methodologies utilized in energy systems planning. The rapid deployment of decentralised energy generating or storing technologies in the advent of liberalised markets and increasing pressure on decarbonisation has introduced a large number of new market players, making centralised orchestration historically controlled by a few parties no longer feasible. Additionally, more transparency is advantageous by facilitating collaboration across the policy-science boundary [49]. This opens up decision processes and offers insight into the reasoning behind policies, improving the social acceptance of new legislation and energy infrastructure [50].

In an attempt to open the black box of energy systems modelling various initiatives exist. In 2003, the first open-source energy model was released [51]. Researchers and analysts have since recognized and underlined the importance of open access, open data and open source in the field of energy modelling. Freely accessible code repositories and specific snapshots provide the possibility for third parties to inspect and verify model outcomes [52]. The conditions encountered in modern energy planning display a disruptive character in a fast-changing environment. Moreover, public acceptance becomes increasingly important in an era of expanding information technology. Additionally, the energy transition can have major implications for the overall economy that results in an increasing demand for energy system analysis to provide guidance [53]. Open and collaborative development of the Open Energy Modelling Framework (oemof) was aimed at achieving maximum levels of transparency and participation [54]. Furthermore, in a response to the rising challenges of energy modelling in terms of transparency, participation and accessibility the Open Energy Modelling Initiative (openmod) was initiated. This is a community of modellers and energy system experts alike, devoted to promoting an open approach in energy systems modelling and analysis [51].

Not only the accessibility (e.g. open source, open access) of energy system models and tools is important for transparency. Modellers are tasked with addressing the growing complexity of energy systems by balancing various model design considerations, such as resolving spatial and temporal dimensions or the trade-off between incorporating uncertainty and clarity of model outcomes [48]. Supporting the decisions of the modeller should be the recognition of the fact that more complex

models do not necessarily guarantee more accurate results [55], while they pose the risk of further obfuscating model internal workings [34]. This can possibly negatively impact the perceived policy relevance of the model [41].

3.2.2 Renewable energy and storage deployment

More than 500 peer-reviewed articles have used energy modelling and analysis to provide insight into the possibilities of fully renewable energy systems [56]. Although these studies are generally well-received and show a steady increase of publications on the topic [57] [56], studies on 100% renewable energy systems have received criticism [58]. It was reported that publications did not sufficiently meet novel feasibility criteria, such as compliance with mainstream energy-demand forecasts and the use of adequately modelled time resolution. However, this criticism was consequently debunked [59]. It should be stressed that even when more strenuous feasibility and viability criteria are imposed it is indeed possible to meet 100% of future energy demand based on energy systems with high shares of renewable energy.

Based on the technical potential of renewable generation it was determined that it is possible to meet local demand in most sub-national regions in Europe, based on energy generation of photovoltaics and wind turbines alone [60]. The trade-offs between various geographic scales of balancing and autarky were investigated based on a fully renewable energy system at a European scale. It was concluded that the continental scale of supply of balancing is most cost-effective but requires large coordinated efforts to expand grid capacity. Regional self-sufficiency is feasible for most regions but introduces a higher total system cost [61]. By varying the deployment of on-shore and offshore wind, rooftop and open-field photovoltaics, it was shown that land use of renewable energy generation can be halved at a minimal cost penalty [62].

Overall, several studies have found economically viable energy systems that are largely based on solar and wind-based energy generation [63]. Moreover, at least 16 studies have revealed that 100% renewable energy systems are possible on a global level although the relative contribution of solar and wind-powered generation was very dependent on technology cost assumptions. The conservative attitude towards technological adaptation has led to a failure to anticipate steep cost declines [56]. The resilience of 100% renewable energy systems to extended periods of the scarce supply of wind and solar revealed that single year approaches underestimate storage requirements although renewable dispatchable sources (e.g. hydro or bio-based thermal plants) can greatly reduce this impact [64].

However, there is no real consensus on the role of storage versus flexible assets. Some studies found that incremental deployment of dispatchable generation can greatly displace the need for storage, reducing overall system cost [65]. Other studies imply lesser importance for dispatchable technologies, either based on the cost reduction potential of modern storage technologies such as lithium-ion [38] [66] or based on the potential of demand response and senatorial coupling (e.g. power-to-gas or power-to-heat) [67] [68].

Overall, it is concluded that energy systems that are based on renewable energy are technologically feasible and economically viable. What the exact optimal system configuration is, remains inconclusive. As such, normative policy advice cannot be condensed from the literature. The obtained system configuration is greatly impacted by the used model. Therefore, section 3.3 covers model design considerations as well as uncertainty which is both integral for achieving policy relevance with energy systems modelling and analysis.

3.3 Model design considerations

During the development of a model, it is inevitable to make decisions on what sectors, technologies and representations to include or exclude. It is important to highlight the most important parts of reality to be represented in the model that is fundamental to reach the specific modelling purpose [29]. This section describes four of such model design considerations: time resolution, geographical scope, data sources and finally, components and functionalities.

3.3.1 Time resolution

The time resolution used in the model should align with the geographic scope, the weather conditions within the area of interest and the research questions at hand. When optimising to find reliable energy system configurations, the time resolution should be sufficiently high to account for the variability of energy demand and renewable energy generation. Models used to generate long-term planning insights can in general safely be based on hourly simulations [59]. Correspondingly, the majority of models used presented in section 3.2 are based on hourly resolution.

Several studies have shown that sub-hourly optimisation does not lead to substantially different results. Decreasing the temporal resolution from 1 hour to as little as 5 minutes only increased system cost by 1% for Ireland, an isolated power system that can be expected to be more susceptible to small fluctuations [69]. Also for smaller energy systems hourly simulation is valid. Only small differences in models outcome are reported by comparing results based on 60 and 15-minute intervals for a district heating network based on high shares of wind, subsequently concluding that there is 'no need for higher resolution modelling' [70]. It should be noted that modelling on an hourly basis can underestimate the starting and ramping of dispatchable assets required to maintain intra-hour supply and demand balance, although energy storage dispatch and other forms of flexibility can counter this underestimation [71].

Increasing the time interval, however, should be treated carefully because downsampling to longer periods can lead to vastly different results [72]. On the other hand, time series aggregation methods can be used to reduce the size of the model input data while remaining representative of the original signal. Methods such as k-medoids and hierarchical clustering can be implemented to select a small set of typical time periods (e.g. days or weeks), each consisting of multiple hours. When used in optimisation models, these lead to similar model outcomes at a substantial decrease in computation time [73]. When the systems under study are dependent on storage, this method is no longer applicable because the typical days are independent and cannot exchange energy. It is possible to "couple" typical periods. In this method, the power balance is solved based on the typical periods while energy is solved based on the original hourly simulation [74]. Applying this method in the optimisation of multi-sector energy systems reduced computational time from 19 hours to five minutes, while model outputs were within a reasonable error range compared to the outputs of the original hourly optimisation [75].

3.3.2 Spatial resolution

Applying high temporal and spatial resolution in ESOMs results in model complexity that becomes nearly insolvable. Therefore, it is important to reduce the level of spatial detail while still remaining representative of the spatial dispersion within the geographical scope of the model [76]. One approach to reducing spatial resolution through spatial aggregation is the single-node approximation.

The single-node approximation assumes that within the system boundary, all components are connected to each other through a copperplate; thus, assuming infinite conductivity. This means that all system components within the geographic scope are spatially aggregated to a single virtual point called a node, even though in reality they are spatially dispersed. Several studies and models exist that implement the single-node or copper plate representation [64] [45].

By linking several energy systems represented as a single node, a multi-node representation is obtained. These models allow to include a representation of grid infrastructure by dividing the system into nodes based on political boundaries, which are subsequently integrated into a network and allowed to exchange energy through power flow between nodes [61] [77] [52]. Some models are capable of simulating the flow of power within the grid in great detail but still represent whole countries as a single node [78]. The political regions that these models consider are often at the national level or regional (provincial) level. Within any of those regions, all supply and demand are approximated as a single point system. Based on the required grid capacities and backup as a function of spatial aggregation, it can be concluded that single node approximations up to the national level are sufficiently detailed to represent the spatial variation of energy demand and variable renewable energy generation [79].

Although multi-node models are more representative of the energy system as a whole, it lacks the ability to provide insights into the preferred actions of a single region. Optimisation for an interconnected system as a whole implicitly assumes that central coordination of all individual regions is possible. In other words, the global or continental optimum can often only be achieved if all regions act on fulfilling their contribution in the system-wide optimal configuration. Since this study is aimed at generating insights for the regional energy strategies, a single-node approximation of those regions should suffice as these are of a sub-national size. However, care should be taken in representing the system boundary to correctly represent the energy market and interconnectivity of that region [42] [29].

3.3.3 Components and functionalities

Given that the renewable energy strategies are mainly concerned with planning the deployment of wind and solar PV it seems intuitive to only implement wind and solar PV generation as design variables. On the other hand, the Climate-neutral Energy Scenarios (CNES) scenarios for 2050 consider the plausibility that the global economy converges towards green hydrogen or biomass-based energy systems. This would allow dispatchable thermal power plants to be fully renewable [22]. The exclusion of such dispatchable power plants could lead to slightly higher Levelised Cost Of Electricity (LCOE) because the incremental deployment of dispatchable generation has the potential to substantially decrease the required amount of storage capacity [65]. However, more recent publications have found that future energy systems might be even cheaper with storage than with dispatchable peaking plants if current cost projections for storage technologies become a reality [38] [66]. Moreover, including these technologies would give the false impression that regional governments can act on those opportunities while whether those hydrogen or biomass-based economies will emerge is outside the influence of regional or even national politics [80].

How predicted or assumed future energy demand is implemented into the model is another important functionality consideration. Two distinct approaches exist. The first and most direct implementation of demand profiles is to model it as a must-meet load. This means that the given demand should be met for any time step over the modelled time horizon. Demand loads should always be met by generation, import/export or storage. This can be achieved by deploying more renewable energy

generation, utilising storage components, or importing or exporting energy. In this sense, this approach does not allow any demand-side driven optimisation; only the deployment and operation of generation and storage components is considered a controllable design variable [81].

On the other hand, there is the implementation of slack variables, shiftable loads, demand-side management or demand curtailment. Demand-side management has been found significant in terms of reducing overall system cost, as rescheduling peak loads reduces the overall need for system redundancy [67] [68] [82] [83]. It is possible to implement demand-side management but it introduces a higher degree of time-coupling, negatively impacting computational demands [84]. Even though demand response shows potential, challenges regarding the exact implementation of demand-side management algorithms in terms of technology, ownership and integration level are not yet overcome. New technology such as block-chain could allow for an innovative and decentralised implementation if common legislation and standardisation can be achieved [85].

3.3.4 Data sources

For effective use of ESOMs, the models should not be designed exclusively based on the desired outcome and model purpose. Other key phases of energy system modelling and analysis should be considered, such as data gathering and result interpretation [35]. Based on a survey under model developers and users, it was found that the data-gathering phase consumed a large portion of the time needed to come to results. Moreover, the acquisition of consistent and high-quality data sources is considered a complex and time-consuming part of the modelling work [86].

Considering that energy planners and policymakers face the responsibility of making robust decisions under increasing pressure to act in rapidly changing environments [53], it is concluded that energy system models should be designed integral with open data acquisition. This allows modellers to more rapidly respond while upholding data quality and accessibility, increasing policy relevance.

3.4 Validation and uncertainty

The use of ESOMs can generate crucial insight for the energy planning and policymaking process. However, the long-term development of energy systems is subject to a large number of uncertainties. As a result, long-term policy or system planning based analysis requires decision making under deep uncertainty [87]. Energy modelling and analysis can lead to potentially misleading conclusions as a result of a combination of errors in predicting future energy demand, relevant technology prices, effects of policies and socio-economic dynamics. Therefore, model outcomes should not be treated as normative, where single model outcomes are presented as the only desirable system configuration. Instead, energy modellers should focus on generating insights that are robust to underlying uncertainty instead of providing single-point estimates [52]. Addressing this uncertainty associated when applying ESOMs for decision support is considered one of the main challenges [48].

To better address the issue of uncertainty in energy modelling, a distinction between parametric and structural uncertainty should be made. Parametric uncertainty relates to the uncertainty of the validity of certain empiric values assumed in the model. These can be further subdivided into *epistemic* and *aleatory*, where the former assumes resolvable uncertainty e.g. through the gathering of more or better quality data. If uncertainties cannot be reduced through extended research or data gathering, these uncertainties should be classified as the latter [88].

Structural uncertainty is associated with the functioning of a model as a result of the formulation [89]. Since ESOMs are often applied to optimise energy systems several decades from now, it is nearly impossible to compare model outcomes to observations. As a result, it is nearly impossible to create a feedback loop to increase model accuracy [90] [91]. Still, uncertainty assessment and characterization are rarely addressed integrally in the published literature or it is treated in comparatively low urgency [88]. Moreover, most studies only introduce the effects of uncertainty by prescribing distinct scenarios. This is considered an adequate method to deal with deep uncertainty associated with energy systems modelling in general by some [92]. On the other hand, scenarios are known to be cognitively biased i.e. scenarios form compelling but misleading storylines [93].

To overcome the barrier of creating policy relevance without removing structural uncertainty in ESOMs – considered impossible due to the complexity associated with public planning problems – formal methods have been introduced to obtain insight into the near-optimal solution space. By applying these methods the effects of unmodeled objectives and structural uncertainties can in part be alleviated [93]. Modelling to Generate Alternatives (MGA) stems from operations research and is used to explore the sub-optimal feasible solution region [89]. The optimal solution is used as an initial anchor point. By relaxing the optimal solution by implementing a slack variable (e.g. up to 5% higher system cost) and reformulating the problem to yield maximally different solutions, feasible and acceptably cost-effective alternatives to the optimal solution can be found [94].

An extension to MGA (SPORES) can be used to generate spatially explicit, practically optimal results which can support policymakers in deciding on transition paths that are socially and politically acceptable [95]. MGA has been applied in various papers on energy systems and is improved by introducing more rigorous routines. Additionally, iterative applying MGA to identify the sub-optimal solutions with maximum and minimum deployment considered technologies can be used to identify the extremities of the near-optimal solution space [96]. However, it lacks the ability to provide insight into the near-optimal solution space itself. Modelling All Alternatives (MAA) is able to overcome through its capability to determine the continuum of the near-optimal solution space [97].

It can be concluded that efforts to address structural uncertainty have resulted in complete methods and are still improving. To obtain insight into the effects of parametric uncertainty, several possible approaches exist that are sparsely applied in energy systems modelling [93]. Monte Carlo sampling can be used to reveal model sensitives, providing insight into *what* parameters have the highest impact on model outcomes. Stochastic programming can be used to obtain insight into how to hedge against risks propagating from uncertainties but is computationally expensive (exponential with the number of uncertainties) and hedging strategies are fully based on underlying distributions - which themselves in turn are uncertain [88]. Robust optimisation overcomes the computational burden encountered with stochastic programming but is less informative about correlations between inputs and outputs, and it does not provide a unified hedging strategy [98].

Conclusively, it can be stated that all aforementioned methods serve the purpose of quantifying how robust a given optimisation result is, often by varying input parameters over arbitrary positions. This can be interpreted as an approach to validate the role of optimisation models in a prescriptive manner. The tension between exploratory and prescriptive use of ESOMs was identified and subsequently validated through ex-post analysis, concluding that cost optimisation poorly reflects the real-world transition. Although models are not able to perfectly predict the transition of energy systems, near-optimal scenarios – driven both by structural and parametric uncertainty – are useful for determining an envelope of predictability [99].

Moreover, although several methods exist that are able to determine *that* a model is indeed sensitive to a given uncertainty there is currently no method that can be used to obtain insight into *how* models behave under parametric uncertainty. In other words, there is a proposition to research methods that are able to combine uncertainty and sensitivity analysis to provide insight into the behaviour of ESOMs when exposed to parametric uncertainty. By generating a range of model outcomes, the misleading effect of providing a singular model outcome is mitigated [100].

This exploratory use of energy system models aligns with the philosophy of decision making under uncertainty. This can be defined as situations where policymakers and planners are incapable of agreeing on a model, associated uncertainties or how to value the model outcomes [28]. Instead of generating a very complex model that produces a singular result, which is typical for optimisation models, many variations on parameters and model formulations are generated, yielding a series of experiments. Based on analysis of the large set of model outcomes, modellers and analysts can draw conclusions useful for decision making without implying that they are able to predict that which is unpredictable [101]. This approach is called Exploratory Modelling Analysis (EMA). Recently, EMA was applied on a multi-year, investment optimisation model. It was concluded that the use of EMA on ESOMs was promising to produce policy insights [100].

3.5 Conclusion

This chapter analysed the literature on energy systems modelling with a specific focus on optimisation models to provide insights for policymakers and energy planners in the transition to renewable energy systems. There is agreement that energy modelling and analysis is a valuable tool for providing insights for policy. Energy system optimisation models are favoured for investigating the transition to future energy systems, as they work prescriptively in contrast to scenario models that are descriptive. Based on the obtained insights in the literature, the following are the answers to relevant research questions.

What do cost-optimisation studies reveal about the deployment of renewable generation and storage required for decarbonising energy/electricity systems/sector? The main takeaway from the literature is that, although contested, it is indeed possible to determine technologically feasible and economically viable energy systems based completely on renewable energy sources. Although many models and corresponding studies exist, the conclusions are highly dependent on the design considerations of the model. Based on analysis of various cost-optimal configurations of (highly) renewable energy systems presented in the literature, it was found that even though such systems are viable and feasible no real consensus on the exact optimal system configuration. As a result, the model outcomes of existing studies cannot be used to generate normative policy advice.

This is a result of the fact that the energy transition is intrinsically complex, making it infeasible to formulate models that perfectly represent reality. As such, modellers are tasked with considering various assumptions and approximations that align with the goal of the research while addressing trade-offs such as complexity and computational demand or completeness and transparency of results. An important effort that aims to overcome this barrier is the open-source, open access and open data initiative, that increases accessibility, transparency and traceability.

Still, energy systems optimisation models assume perfect foresight, e.g. the optimal solution is only valid when all assumptions are fully resolved ex-ante. While on the other hand, strategic decisions that have to be made now will potentially impact the energy systems for decades to come. Policymakers and planners cannot assume that uncertainty is resolved nor can they wait for it to resolve.

Modellers should focus on aligning model design considerations with the purpose of the research to generate relevant policy advice. Moreover, uncertainty should be addressed as an integral part of energy system optimisation models.

What methodology can be applied to optimisation models to provide insight into the robustness of optimisation results in relation to uncertainties? Two types of uncertainty exist. Structural uncertainty is related to the formulation and mathematical representation of the model. Various research efforts have addressed this topic, resulting in methodologies that can be used to generate insight into the structural uncertainties of energy systems optimisation models. Methods such as modelling to generate alternatives, spatially explicit and practically optimal solutions and modelling all alternatives can be used to inform policymakers about the alternative, sub-optimal system configurations that exist in the near-optimal solution space.

The other type of uncertainty is parametric uncertainty, which is the uncertainty surrounding the validity of assumed values in the model e.g. fuel prices, cost of technologies, etc. Various methodologies exist that aim to overcome this uncertainty, such as robust optimisation, stochastic programming and sensitivity analysis. However, these methodologies are often used to support the normative nature of optimisation model outcomes. As already developed for structural uncertainty, a method to explore cost-optimal configurations as a result of parametric uncertainties should be applied. This aims to provide decision making under deep uncertainty with more insight by applying energy system optimisation models in an explorative manner instead of the typical normative manner.

A structured manner of approaching this explorative use of energy systems optimisation is by applying explorative modelling and analysis, a methodology more often applied to obtain insight or generate advice for decision making under deep uncertainty. Explorative modelling and analysis were applied to an energy system using a multi-year, investment optimisation model on a yearly time resolution [100]. However, as laid out in section 3.3.1, the time resolution used has great implications for the obtained results. It has been shown that a lower temporal resolution leads to an underestimation of investments needed in renewable energy generation technologies by overestimating renewable energy penetration [102]. This can be related to the variability inherent to renewable energy sources, which if excluded only poorly reflect the system integration dynamics and thus do not fairly represent the required effort for the energy transition [103].

The identified gap in literature can be described as the lack of rigorous methods that support the explorative use of energy system optimisation models with regard to parametric uncertainty. This can be aligned with the opportunity of applying optimisation models for generating policy advice for the Dutch energy transition, identified in chapter 2.

Moreover, energy optimisation models could further be utilized by overcoming barriers that remain in the accessibility, tool coupling and policy relevance [41]. This can be related to the research question: *How can the optimisation model be coupled to existing models to reflect the effect of (inter)national energy policies?* Chapter 2 revealed that a specific part of the Dutch energy transition, the regional energy strategies and corresponding system studies, are well-aligned in terms of what simulation model and subsequently what scenario is used. This is the Energy Transition Model and is used to determine the impact on the energy system as a whole, including various other sectors such as housing, heating and transport. Scenarios for 2030 are modelled based on the respective regional energy strategies while scenarios for 2050 are based on a well-defined set of scenarios called the climate-neutral energy scenarios. By coupling an energy system optimisation model to the Energy Transition Model, accessibility and perceived policy relevance can both be expected to increase.

Chapter 4

Model description

This chapter will introduce the optimisation framework developed during this thesis work. Chapter 3 introduced the current landscape of modelling tools, model design considerations and the remaining gap in addressing parametric uncertainty. This chapter explains how this thesis contributes to filling this gap. A framework with a low-code interface to support multi-modal analysis of cost-optimal renewable energy systems is introduced. The presented modelling framework contributes by making explorative uncertainty assessment accessible to consulting engineers and policymakers in the energy transition to make informed decisions about future energy systems under uncertainty.

The developed framework is released as open-source software under the MIT license of use [104]. It was named Local Energy Systems Optimiser (LESO) due to its single node representation of local or regional (subnational-level) energy systems and its core competence: optimisation. It can be installed through the Python standard package handler pip, and the source code is openly available through Github [105].

Section 4.1 sets out by stating the design goals that were used during the development of the framework. In section 4.2 an overview of the model scope is presented, along with deliberation of the implications embedded in the applied scope. The main features of LESO - simulation, optimisation, parametric uncertainty exploration - are introduced in section 4.3. Section 4.4 presents a brief overview of the components currently included in the LESO component library. Finally, section 4.5 concludes this chapter.

Figure 4.1: Logo of the Local Energy Systems Optimiser (LESO) framework.

4.1 Model design goals

Based on the literature research in chapters 2 and 3 the design goals have been formulated to support the development of this framework.

- **Minimal complexity for computational tractability**
  Optimisation problems can become quite exhaustive to solve when complexity is not considered a design constraint, while increased complexity does not necessarily lead to higher accuracy [55]. In keeping with the philosophy of increasing the accessibility and transparency of optimisation models to reach better support, they should not require a high-performance cluster to be used [50]. Low complexity is increasingly important when parametric research using uncertainty sampling is applied, as the computational time required for a single model is multiplied by the number of experiments.
- **Flexibility and extensibility**
  LESO is built around an objected orient approach, which forms a comprehensible modelling structure. In addition, LESO is designed with extensibility in mind. This is achieved by defining a universal interface to extend the component library with new components. As a result, LESO can be used to describe nearly any arbitrary energy system configuration in a straightforward object-based approach.
- **Low-code interface**
  A result of defining LESO components using an objected-oriented approach is that it results in an intuitive workflow. Within LESO, each component defined in the energy system has its own distinct object. Using this notation relieves engineers or modellers of learning and understanding Python's syntax and programming specifics completely. Instead, they need only to know how to interact with the LESO components to generate optimisation studies.
- **Automation of exogenous data integration**
  If input data used for modelling is wrong or inaccurate, this will lead to unexpected and unreliable behaviour. Therefore, it is essential to integrate validated sources of such data. Automatic data integration removes the burden of both time-consuming and error-prone work, customarily done manually by the researcher. LESO aims to overcome this burden by automating this input data acquisition by integrating interfaces to various databases.
- **Multi-modal approach**
  LESO is implemented with more than one approach to finding the optimal solution. Modellers can implement exploratory synthesis and optimisation based on linear programming in the same model following a nearly identical process.
- **Integration with existing tools**
  Integrating existing models and tools makes it possible to leverage the functionality and support base of validated and broadly applied models. The ETM is integrated to generate scenarios for future energy systems using a bottom-up in a highly interactive environment. To implement the before mentioned uncertainty sampling and exploratory modelling LESO is integrated with the EMA workbench [106].

4.2 Model scope

This section introduces the scope of the introduced model, which is based on the analysis presented in chapter 3. LESO is designed with certain flexibility towards multiple energy carriers. However, for the case studies within this thesis only power systems are considered, e.g. electric generation and demand. As a result, all components that have currently been implemented in the LESO component library are electric, such as wind turbines, solar photovoltaic and domestic electric demands.

Systems modelled within LESO are represented as a single node e.g. all components are connected with infinite transport capacity. In reality, grid constraints may apply, limiting the energy exchange between various elements in the energy system. Such constraints can be a result of the spatial dispersion of components and respective connectivity between several members. Grid conditions (capacity and prices) can be still considered within LESO models but only as a boundary condition based on the geographic scope. As discussed in section 3.3.2, multi-node systems include nodes on the scale from municipality to country connected by a stylized representation of grid infrastructure that only considers inter-connectivity between regions. This further substantiates the single-node approach implemented in LESO, as long as it remains at or below the national level. Also, the goal of LESO is to provide a snapshot of cost-optimal deployment of renewable energy technologies in future energy systems, not to investigate technical specifics of grid congestion in existing infrastructure.

However, this means that LESO is currently not able to represent a network of multiple nodes using a single model. Instead, LESO can be used to optimise every sub-region separately by defining separate models for every region. The interface between the sub-region and the larger region is reflected by including specific boundary conditions such as import/export capacity or electricity price levels at that node. Future research could be conducted to implement multi-node energy systems by implementing power flow optimisation using semidefinite programming [107].

For now, LESO only includes wind and solar as electricity-generating components. As discussed in section 3.2, multiple studies exist that demonstrate that a fully renewable energy system based on wind and solar power is possible. Moreover, the purpose of this model is to generate insights for policymakers in the regional energy strategies that are tasked with the orchestrated deployment of wind and solar asses ts within their regions.

Finally, LESO considers electrical demand as a must-meet load. This means that demand should be met for any hour of the year. Demand loads should always be met by generation, import/export or storage.

4.3 Features

In this section, a high-level overview of the features available within LESO is presented. For programming specifics, please refer to the associated repository that is released in conjunction with this thesis [105]. Although more functionalities are captured within the LESO framework, three distinct features are discussed here:

- Configuration and simulation
- Optimisation
- Parametric uncertainty exploration

4.3.1 Configuration and simulation

The core feature that enables LESO to represent a wide range of energy systems is the object-oriented programming approach. Every component in the LESO component library is reflective of a real component in an energy system, such as PV modules, wind turbines and battery systems. Each of these components should be able to correctly reflect the unique dynamic behaviour of a component in a specific configuration. What components exist and how they can be configured is discussed in section 4.4. How the behaviour of those components is modelled is detailed in chapter 5. In general, components are configured with certain relevant parameters (e.g. tilt, hub height, turbine type, storage duration, etcetera) and simulated based on their respective models.

In Python, such a component approach can be programmed using a `class`. Relevant parameters and data is connected to the `class` object using `attributes`. Models that simulate that components behaviour is contained by the `class` object in the form of object-specific functions called `methods`. This programming paradigm allows for a convenient and explicit manner of formulating component objects in Python.

```python
from LESO import System, PhotoVoltaic

modelname = "PV code snippet"
lat, lon = 52.24, 6.19 # latitude and longitude Arnhem

system = System(
    lat=lat,
    lon=lon,
    model_name=modelname)

pv_south = PhotoVoltaic(
    "South-PV",
    azimuth=180, # deg
    tilt=40,     # deg
    installed=2, # MW
)

system.add_components([pv_south])
system.fetch_input_data()
system.calculate_time_series()
```

Figure 4.2: A code snippet depicting the low-code interface used to configure and simulate a south-oriented PV system in the LESO framework.

For illustrative purposes, a code snippet configuring a PV-system is shown in figure 4.2 . First, the location of the project site is configured by defining the latitude and longitude. Then an `instance` is created of the `System class`, that will contain these parameters as `attributes` which will be used for any of the subsequent `methods`. Then an `instance` of the `PhotoVoltaic class` is initialized. This object will contain the component-specific parameters (tilt, azimuth and installed capacity in this case) as `attributes`. Using the `methods` which are part of `system object`, the PV component is placed within the system context, relevant data is retrieved and finally, the time-series for all components within the system are calculated. This will result in LESO fetching historical meteorological data from the PVGIS server through an API, which is subsequently parsed and used in the `PhotoVoltaic` simulation model to deliver a time-series containing the power output of the configured PV system for every hour of the year.

This is the only explicitly shown code in this thesis report. This is done to maintain readability in this thesis and to focus on the possibilities of using the framework and not the pragmatics of programming the developed framework. Documentation, programming specifics and examples can be found in the repository on Github [105]. In addition, appendix E can be used to find specific versions and files used to generate the results shown in this thesis.

4.3.2 Optimisation

Finding the optimal system configuration through synthesis processes is a complicated task due to the multiple large time series that need to be considered. Components that are not only dynamic in time, but flexible in operation such as batteries further complicate this matter. When components require to be time-coupled as with storage, it becomes even more complex [108]. Traditionally, similar design challenges would be tackled through iterative synthesis. However, as introduced in section 3.1, energy system design problems can be best approached through optimisation.

To determine optimal technology deployment i.e. installed capacities of solar, wind and storage a mathematical representation of the system can be made that approximates real-life system dynamics. The optimal solution is either the most or the least of a certain unit of measure. These goals are defined in the objective function, with a declaration to either maximise or minimise the objective function. In essence, the algorithm also considers all possible solutions, but the algorithms in themselves are able to determine the best configuration based on the objective value and satisfaction of constraint functions.

The context of the problem is taken into account by optimisation by the introduction of boundary conditions in the form of constraint functions. These boundary conditions must be met by the optimum for the solution to be valid. Conditions are used to introduce real-life limitations to quantities or dynamics to the mathematical formulation.

General formulation of optimisation problems — Starting at an abstract formulation of the optimisation problem, we obtain the formulation as shown in equation 4.1. Generally speaking, the objective function is a sum of over the considered components given the product of some cost or benefit associated to a certain quantity of the design variable. The objective function is given by $f(x)$, this function is used to relate the design variable x, to a variable that should be optimised. In this case; to minimise by changing x. In this notation, x represents a vector of parameters. Equation 4.2 and equation 4.3 represent equality and inequality constraints, respectively. Constraint functions $g_i(x)$ and $h_i(x)$ are in place to ensure the obtained results are valid within the restrictions of the problem its context. The function $g_i(x)$ forms the relation between parameter x and equality value b_i for the set of all equality constraints m. This equality denotes the equality to a value but equality constraint equations can also relate two dynamic quantities to each other, e.g. to include charging dynamics. $g_i(x)$ on the other hand, defines the inequality constraints of parameters x for all inequality constraints n. An inequality function can for example be used to guarantee no negative deployment of assets is applied by the optimisation algorithm.

$$\min_{x} \quad f(x) \tag{4.1}$$

$$\text{subject to:} \quad g_i(x) = b_i \quad \forall i = 1, m \tag{4.2}$$

$$h_j(x) \geq 0 \quad \forall j = 1, n \tag{4.3}$$

A less generic depiction of the objective function and its constraints is shown in equation 4.4. In this, some variable x must be optimised over components j such that the resultant of all components and respective costs c_j is maximal. Solutions are only valid in the domain where the constraint equations are met (eq. 4.5 and eq. 4.6).

It can easily be imagined that the term $c_j x_j$ represents the total investment cost and thus the objective function is to minimise investment cost. The associated constraint functions could represent the

systems energy balance and prevent the algorithm from implementing deploying negative quantities of a certain component.

$$\min_{x} \quad \sum_{j=1}^{n} c_j x_j \tag{4.4}$$

$$\text{subject to:} \quad \sum_{j=1}^{n} a_{ij} x_j \leq b_i \quad \forall i = 1, m \tag{4.5}$$

$$x_j \geq 0 \quad \forall j = 1, n \tag{4.6}$$

The mathematics associated with formulating the optimisation can become lengthy. To maintain readability, the specific mathematics applied to define the optimisation problem is excluded from this chapter but is included in the appendix. Readers interested in the specific mathematical formulation applied in LESO are encouraged to read appendix A.

Linear programming — A specific form of optimisation can be classified as linear programming. In this form of optimisation, the objective function is a linear equation. In most cases, this is a sum of cost times quantity overall design variables, which should include all fixed and variable component costs. All constraint functions should either pose linear equality or inequality. As such, the resulting solution space will be an n-dimensional polygon encapsulated by a finite amount of linear constraint functions.

The optimal solution is found at the point where either the minimal or maximal value of the objective function is calculated. Various methods exist to find this optimum and include (meta) heuristics or stochastic approximations. Solving LP problems, and optimisation in general is a specialist area within mathematics. Therefore, further detailed analysis of solving algorithms is out of scope during this thesis work. It is however important to note that implementing the optimisation problem as LP will greatly improve solvability and decrease computation time.

Objective function — Perhaps this function has the single most impact on the outcome of the optimisation problem. This thesis concerns only cost-optimal configurations and therefore only has a monetary unit. Models exist that allow for linear combinations of multiple objective functions (i.e. carbon dioxide emissions, land use, etcetera) [109]. The optimality solution is used to provide a snapshot of a future energy system in a cost-optimal configuration, an objective function fitting to this goal should be implemented. The objective function is shown in equation 4.7. Derivation and detailed explanation can be found in appendix A. In short, this objective function sums the annualised investment cost and variable operating costs based on the optimisation variables component capacity deployment D_j and dispatched energy $E_{j,t}$, for every component j in component set m, for every moment in time t.

$$\min_{D_j, E_{j,t}} \quad f(D_j, E_{j,t}) = \sum_{j=1}^{m} c'_j D_j + \sum_{j=1}^{m} \sum_{t} V_{j,t} \Delta t \tag{4.7}$$

This objective function reflects an 'instantaneous' yearly cost often referred to as Overnight System Cost (OSC). As such, this objective function is analogue to the annualised investment cost plus the total variable cost for the optimised year, if the found optimal configuration would be created in that year. Investment costs are annualised using the Capital Recovery Factor (CRF), which depends on the weighted cost of capital, expected inflation and component lifetime. It implicitly includes a linear replacement and decommissioning assumption which is applied on components that have a shorter

lifetime than the system. Variable costs (with negative cost resembling income) are considered for all energy dispatched or absorbed by components on an hourly basis. As a result, the total equation is the objective function that is used to find the cost-optimal system with the lowest yearly total costs.

4.3.3 Parametric uncertainty exploration

J. Decarolis et. al. stated: ”Insights generated with ESOM should — to the degree possible — be robust to large future uncertainties. If not, they are of questionable value to policy planners and decision-makers.” [52]

Robustness to uncertainty can be assessed in various approaches. In the spirit of generating more insight through exploration, LESO is set up to integrate well with Explanatory Modelling Analysis (EMA). To this end, an already existing Python module called EMA workbench is selected [106]. This toolbox has already been applied to the Dutch energy transition before, albeit not based on optimisation [28]. More recently, this toolbox has first been applied to a multi-year, investment optimisation framework in the context of the energy transition [100].
Moreover, the few papers published on cost-optimal future energy systems using ESOM that include uncertainty or sensitivity analysis have found that the cost of components has a substantial effect on the optimal system configuration, which further motivates the necessity of exploratory analysis [110] [82] [111].

By incorporating the EMA workbench, it is possible to use LESO to explore parametric uncertainty, i.e. how do investment decisions respond to various technology cost assumptions. This is highly relevant since there is a significant amount of uncertainty to be considered when dealing with future energy systems. Another advantage of using the EMA workbench is the support for testing discrete policies. In this way, the EMA workbench can be used to construct alternative model configurations in which LESO should be executed. This allows modellers to access the effect of certain boundary conditions effectively.
In a nutshell, EMA is connected to LESO using a standard approach for Python models as described in EMA. In this approach, the LESO model is wrapped in a function called a ”handshake”. This function has the responsibility of translating the values EMA delivers to inputs for the LESO model and that the model results are returned in the prescribed EMA format.

To run experiments, the modeller defines the uncertainties to be assessed based on the range of uncertainty and their respective names (e.g. cost of solar PV). In addition, EMA supports the use of policy levers. These are different from uncertainties because levers from an alternate configuration of boundary conditions. As a result, these form a unique system problem configuration which can best be interpreted as an alternate reality over which uncertainties are sampled. This is shown in equation 4.8

$$\text{number of experiments} = \text{number of uncertainty samples} \times \text{number of policies} \tag{4.8}$$

From a programming perspective, it is important to note that the handshake function is in turn wrapped in a decorator that casts the types to native Python types (e.g. floats). Otherwise, LESO will not even start solving due to a type based compatibility error between EMA and the Pyomo module. This is the package LESO uses to formulate the optimisation problem, by defining objective and constraint functions.

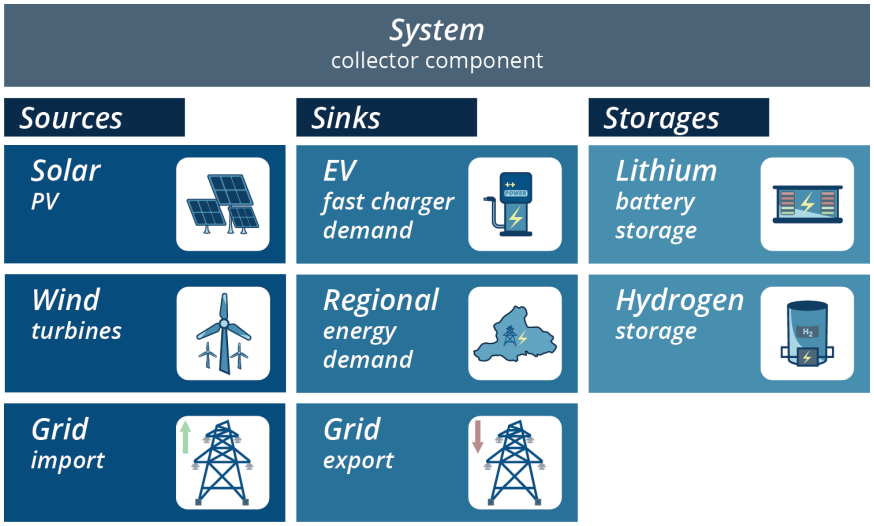

Figure 4.3: Overview of the components included in the LESO component library based on the categories of the components.

4.4 Components

As briefly introduced in section 4.3.1, LESO treats energy components based on an object oriented approach. E.g. solar PV components are defined based on their respective parameters and generate electricity based on the parameters, the component object itself contains the associated model and relevant data.

LESO components are defined based on generic objects as proposed in the modelling approach [112], with some small deviations. The collector object is replaced by the system object, as all components are part of a system. The single-node approximation implemented in LESO also makes it so that all components are collected to the same single system, superseding the need for a collector object. Lindberg distinguishes between sources and sinks, but in LESO these are implemented as the same generic object. The differentiation between sources and sinks is maintained using sign convention, negative power is a sink and positive power is a source. A generic transformer object is included as converter object. This object is unused in the current electricity-only implementation of LESO but could be used to include other energy carriers.

The following subsections introduce the components that are currently included in the LESO framework. An overview of the components is given in figure 4.3. Relevant parameters of specific components can be found in sections 4.4.1-4.4.4. A detailed description of the modelling approach for each of the components is covered in chapter 5. Component specific parameters are included in the following sections. However, the following generic parameters apply to any object:

1. **Component installed capacity**
   This variable denotes the capacity of a certain technology that is deployed, e.g. peak-power or storage volume. During model definition, it can be used to assign a predetermined value to components in the energy system and can for example be used to define legacy components.
2. **Option to set installed capacity as optimisation parameter**
   This is a boolean variable used to mark this component's installed capacity as an optimisation parameter. If set to true, this option allows the optimisation algorithm to override the component's installed capacity to determine the cost-optimal solution.

3. **The data source that is used to retrieve historical meteorological data**
   This variable can be used to declare the data source to be used for retrieving meteorological data. The possible sources are PVGIS, DOWA and renewables.ninja which is covered in depth in section 5.1.
4. **Component technical lifetime**
   This variable declares the component technical lifetime, which is used to determine the component's annuity in financial calculations which in turn is used to construct the objective function.
5. **Investment cost per installed capacity**
   This parameter denotes the investment cost related to installing a certain capacity of a component, i.e. euros per megawatt.
6. **Fixed operational cost per installed capacity**
   This variable reflects the yearly operational cost that scale with installed capacity but do not scale with the usage of a component. These costs are fixed and include posts such as maintenance and service but exclude posts such as fuel cost.
7. **Variable operational cost per unit of dispatched energy**
   This variable is used to determine the marginal cost associated with dispatching a certain asset. This includes battery degradation costs due to discharging and the cost of imported electricity.
8. **Variable operational cost absorbed energy**
   This variable is used to determine the marginal cost associated with energy absorbed by a certain asset. This includes battery degradation cost due to charging and income (negative cost) due to exported electricity.

4.4.1 System

The system object acts as the centre piece. All components within the scope of a certain optimisation model configuration are added to a system. The system connects them to the power balance, forms relevant constraints and defines the optimisation problem matrices. This system contains parameters relevant to all components, i.e. it provides the context to the components. For example, the location is determined by the latitude and longitude contained in the system object. It is also more convenient to only call a single method on the system (e.g. `system.calculate_timeseries()`) instead of having to call these methods on every component individually.

4.4.2 Sources

Currently, there are three source objects defined in the component library of LESO. Below a brief overview of the most relevant parameters of each object is given. For details on the submodels in these components, refer to sections 5.2 and 5.3 for photovoltaics and wind, respectively.

1. **Wind**
   Determines the feed-in curve for wind turbines using a height correction method and manufacturers power curves.
   Parameters:
   (a) **Turbine type**
   The turbine type is used to specify the manufacturer and make of the turbine. It is used by the component submodel to determine the power curve of the turbine.
   (b) **Hub height**
   Is used to determine the height of the hub of the turbine and to determine the wind speed at that height to determine the power output.
   (c) **Surface roughness**
   This is a unitless parameter that reflects the effect of surface obstacles on the wind speed.

2. **Photovoltaics**
   Determines the feed-in curve for solar PV for various configurations using irradiance transposition.
   Parameters:
   (a) **Tilt**
   This represents the angle between the horizontal plane and the plane of array. This affects the irradiance on the plane and therefore the power output.
   (b) **Azimuth**
   This is the angle in the horizontal plane and is thus is the orientation of the plane of array against the compass (e.g. North-oriented or South-oriented). This affects the irradiance on the plane and therefore the power output.
   (c) **Efficiency**
   A dimensionless factor is used to denote the efficiency at which the PV array converts incident light to energy and includes all efficiency losses in the PV system. It is applied proportionately to the irradiance in the plane of array.
3. **Grid**
   Can be both a source and a sink through export and import
   Has no unique parameters outside the general parameters already covered.

4.4.3 Sinks

Currently, there are three sink objects defined in the component library of LESO. Below a brief overview of the most relevant parameters of each object is given. For details on the submodels in these components, refer to sections 5.5 and 5.6 for fast charging demand and ETM regional demand, respectively.

1. **Fast charging demand**
   Converts typical weekday and weekend day traffic data into an electrical charging demand.
   Parameters:
   (a) **Average charged volume**
   This is the amount of energy that is charged by an EV when stopping at the fast charger. It is used in combination with the charging duration and charging efficiency to determine the maximum hourly energy demand coming from a single charger.
   (b) **Charging duration**
   This variable denotes the time it takes an EV to stop, connect, charge and disconnect to a fast charger. It includes the time that is lost due to queuing inefficiencies.
   (c) **Traffic data files**
   For this object to generate a time series, two CSV files containing traffic volume intensities on an hourly basis should be supplied. One file contains a typical weekday and the other a typical weekend day.
   (d) **Charging efficiency**
   This parameter is used to determine the actual electric load on the energy system. This factor is included to reflect electrical losses during charging, such as generated heat.
2. **ETMdemand**
   API integration to the ETM allows feeding load curves from any ETM scenario to LESO.
   Parameters:
   (a) **Scenario ID**
   Every scenario created in the ETM can be traced using a unique scenario ID. Typically, these are session IDs that are not guaranteed to be persistent. By saving the scenario to an account it can be stored safely.

(b) **Generation whitelist**
This is a list of all generation keys that should be included when determining the residual load curve that is used in LESO. This is used to allow other sources of renewable energy that are not in the scope of LESO to contribute to the energy balance.

3. **Grid**
Can be both a source and a sink through export and import
Has no unique parameters outside the general parameters already covered.

4.4.4 Storages

Currently, there are two storage objects defined in the component library of LESO. Below a brief overview of the most relevant parameters of each object is given. For details on the submodels in these components, refer to section 5.4 for both objects.

1. **Lithium**
This is the short-term storage and is typically modelled in 2, 4, 8 and 10-hour storage duration configurations.
Parameters:
   (a) **Round-trip efficiency**
   This efficiency factor is used to determine the charging and discharging energy losses. In the current implementation, these are assumed to be symmetrical and irrespective of the charging rate.
   (b) **Self-discharge rate**
   Using this parameter the discharge of stored energy over time is scaled proportionally to the amount of stored energy. For lithium batteries, self-discharge is caused by unwanted chemical reactions without an established connection between the electrodes.
   (c) **Energy-to-power ratio**
   Storage components can be defined based on their charge/discharge power and energy capacity. In LESO, storage components can be configured in arbitrary ratios between power and energy capacity using the energy-to-power ratio. This can be interpreted as the duration a battery can deliver energy at maximum discharge power.

2. **Hydrogen**
This is the long-term storage and is typically modelled in 350 or 700-hour storage duration configurations.
Parameters:
   (a) **Round-trip efficiency**
   This efficiency factor is used to determine the charging and discharging energy losses. In the current implementation, these are assumed to be symmetrical and irrespective of the charging rate.
   (b) **Self-discharge rates**
   Using this parameter the discharge of stored energy over time is scaled proportionally to the amount of stored energy. For hydrogen storage, self-discharge is caused by leaking hydrogen.
   (c) **Energy to power ratio**
   Hydrogen storage components are typically configured for higher storage duration due to the relatively low cost associated with increased energy capacity. Seasonal storage is a typical application area that requires around 700 hours of storage duration.

4.5 Conclusion

In this chapter, the optimisation framework developed based on the information about modelling decision considerations learned from chapter 3 was introduced. From now on out, it will be referred to under the acronym LESO, which stands for Local Energy Systems Optimizer. The design of the framework constitutes the first contribution to the research question: *What design considerations are imperative to create an optimisation modelling framework that can be used to explore uncertainties and policy effects?* After applying the developed framework on the case studies, it will be evaluated whether the framework is able to deliver the purpose or whether further improvements should be made.

The framework is tailored to solving multi-dimensional synthesis problems, e.g. determining the optimal deployment of various competing and synergistic energy technologies in a local energy system. It is built keeping flexibility, extensibility and minimal complexity in mind. LESO offers optimisation and parametric uncertainty exploration through a low-code interface. Exogenous data such as meteorological data is automatically retrieved from various data sources. By integrating LESO with the ETM, it is possible to find cost-optimal configurations of renewable energy assets and storage for validated scenarios that are currently used by policymakers.

Components are modelled and connected using a single-node, copper-plate representation. Only electric energy is currently considered. Variable Renewable Energy (VRE) sources, e.g. solar PV arrays and wind turbines, are currently included. Dispatchable renewable energy sources such as thermal bio-mass plants are not included. Demand-side management is also not included. Both dispatchable renewable energy sources and demand-side management have been reported to potentially decrease the total system redundancy. It is therefore recommended these features are included in later research.

LESO offers a library of components that can be used to define and later optimise energy systems. Components that are currently included are solar PV arrays, wind turbine, grid connection, fast charger, regional energy demand, lithium-ion storage and hydrogen storage. All components are collected and controlled by the system object.

Chapter 5

Component submodels

This chapter describes key steps, mathematical formulation, and data sources used for modelling the components within the scope of the optimisation model. The optimisation model operates on an hourly basis, typically 8760 hours within a year. Thus, every component has to express its hourly contribution to the energy system. It is important to properly incorporate variable energy resource dynamics as it substantially impacts the performance of future energy systems with high penetration of such energy sources [113]. As a result, components have various specific methods and models to generate such time series that describe their behaviour over time.

Since LESO determines cost-optimal configurations of energy systems, another important aspect to consider is the cost of technologies. For all technologies covered in section 4.4, this chapter touches on cost projections in every respective section. An exception is the price curve that is applied in the grid component, which is covered separately in section 5.6.2.

Variable renewable energy sources such as wind and solar are represented by applying physical models and approximations on historical meteorological data. Photovoltaics are covered in section 5.2. Section 5.3 describes the equations governing power generation based on wind speed.

Storage components exhibit dynamic behaviour which is captured by introducing specific constraint equations in the optimisation problem, as already briefly discussed in section 4.3.2. Charging, discharging and efficiency losses are included in such constraint equations. This is covered in section 5.4.

Within this research, two sorts of demand are considered. The load generated by fast-charging infrastructure used by EV's is approximated by stochastically sampling traffic data. The details of this approach are described in section 5.5. Section 5.6 covers the regional energy demand that is included through coupling the optimisation framework to the Energy Transition Model. Finally, section 5.7 concludes this chapter.

5.1 Meteorological data sources

Intermittent renewable energy sources such as wind and photovoltaics are intermittent due to the fact that they depend on certain meteorological conditions to generate energy. Since weather is dynamic, so is the power output of wind and photovoltaics.

Before the feed-in models are covered, it should be noted that these models are only able to transform a certain time series of historical or synthetic meteorological information to power output (e.g. wind speed to wind power). Without a source of such time series, it is not possible to predict the associated power output for a given PV or wind system. For this purpose, three data sources have been selected and integrated into the component submodels and therewith the optimisation framework. These data sources can be selected at the respective component submodel and the framework will consequently automatically integrate that data source through an Application Programming Interface (API). In this thesis, two sources have been found that allow use through an API integration and are well-known in the field of renewable energy.

PVGIS — This source is very well known within the solar community and stands out due to its user-friendly interactive mode, as well as its participation in various studies that have contributed to better PV system performance estimations. Performance metrics and meteorological data available through this interface are either mathematical estimations based on satellite images from METEOSAT through SARAH or CMSAF or based on Climate Reanalysis Data (CRD) such as ERA-5 or COSMO-REA [114] [115]. It has been validated extensively and is frequently updated to include the latest improvements in relevant modelling techniques [116] [117] [118]. This data source is able to deliver time series with an hourly resolution for any location within Europe and Africa that include the following parameters:

- Temperature at 2 metres
- Relative humidity
- Total/global horizontal irradiance
- Beam/direct normal irradiance
- Diffuse horizontal irradiance
- Wind speed at 10 metres
- Wind direction at 10 metres
- Surface air pressure

This data source can be used as a source of time series for both the PV power model and the wind power model. PVGIS has the merit of being able to provide location-specific meteorological data in Typical Meteorological Year (TMY) format. This is a synthetic method to determine representative composite years based on long term historic data, that better reflects historic observations than a single consecutive year would [119] [120].

Renewables.ninja — This data source also includes an interactive tool interface as well as an API. Its authors have introduced this data source to help modellers with the challenge of credibly integrating the variable nature of solar PV and wind [72]. It uses both CRD based on MERRA-2 and satellite-based data set CM-SAF SARAH. Validation of the PV modelling approach is done by correcting for a systematic bias by matching the simulated output against over 1000 PV systems [121]. Wind power output is based only on the MERRA-2 reanalysis model data and is spatially bias-corrected on a national level for 23 European countries [122]. Wind power simulations based on reanalyses with bias-correction have been widely studied and validated [123]–[127].

Renewables.ninja can be used to predict PV and wind output on an hourly resolution at a specified location depending on the configuration of the system given. E.g. tilt, azimuth and system losses of a PV system and turbine type and hub height for a wind generator. In addition, it can also provide the raw meteorological input data which is processed by its power models. In summary, the following parameters can be accessed through renewables.ninja:

- PV power output
- Temperature at 2 metre
- Beam/direct horizontal irradiance
- Diffuse horizontal irradiance
- Cloud cover fraction
- Wind power output
- Wind speed
- Air density
- Precipitation

Dutch Offshore Wind Atlas — The DOWA-project was initiated specifically for Dutch off-shore power production estimations and is the successor of the KNMI North Sea Wind Atlas, which are both downscaled from global scale reanalyses using the mesoscale weather model HARMONIE. It can be accessed through the KNMI Data Centre [128] and offers wind-related parameters for a 2.5km spaced grid spanning the North Sea at 17 height levels from 10 to 600 metres [129]. This source was originally introduced because PVGIS only includes wind speeds at 10 metres height, and thus introduces unwanted error when wind speed is extrapolated to the hub height of a turbine. In addition, PVGIS excludes sea bodies from its data set. To be able to reflect energy production from offshore wind parks, DOWA was coupled to the optimisation framework. It offers the following parameters on an hourly resolution at 17 height levels for periods between 2008-2018:

- Wind speed
- Wind direction
- Air pressure
- Air density
- Relative humidity

5.2 Photovoltaics

Photovoltaics or solar energy technology converts irradiance into power through photoactive material. It is variable in nature due to natural variability of solar irradiance, as shown in figure 5.1. To be able to simulate this dynamic behaviour as a function of the variability of solar irradiance over time for any system configuration (e.g. tilt and orientation), several mathematical transformations and physical models can be applied. This section formulates a comparatively simple model which is used to approximate power production from solar PV based on irradiance time series. This is later validated against more detailed and bias-adjusted models. Lastly, cost developments of photovoltaics are analysed as cost-based optimisation of future greatly depends on future technology cost assumptions used in the optimisation model.

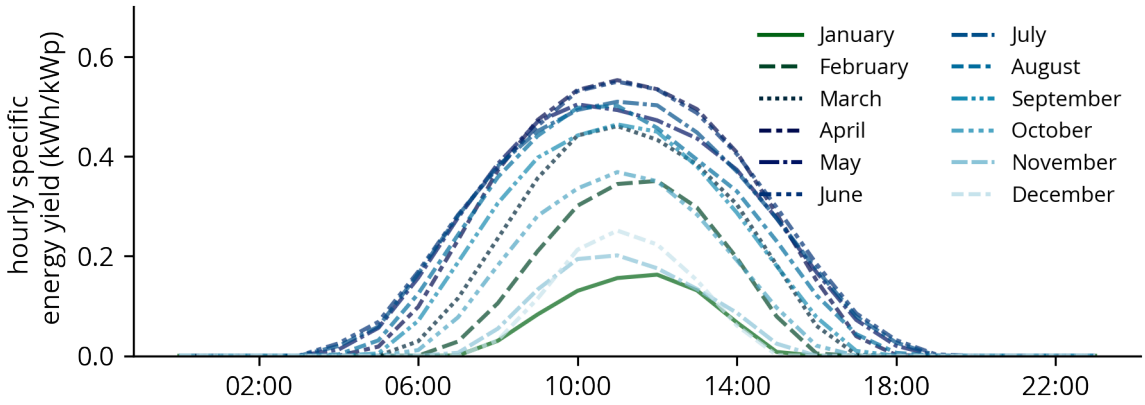

Figure 5.1: Monthly averaged daily PV power curves for a south-oriented, 40 ° tilted array.

5.2.1 Submodel description

It is possible to describe the total (or global) irradiance on an arbitrary plane by dissecting the total irradiance into various components as shown in figure 5.2 and corresponding equation 5.1. Beam radiation constitutes of all direct light emitted by the sun reaching the surface of the plane without having been scattered by the atmosphere. As a result, all irradiance contributing to this radiation component originates from the solar position relative to the plane at that moment of time. Diffuse radiation reaches the surface from nearly any direction, as it is the component that reflects light that has been scattered by the atmosphere. Lastly, there is the ground radiation component. This irradiance is a result of the direct beam radiation component which reaches the plane after reflecting on the nearby ground.

$$I_{\text{total}} = I_{\text{beam}} + I_{\text{diffuse}} + I_{\text{ground}} \tag{5.1}$$

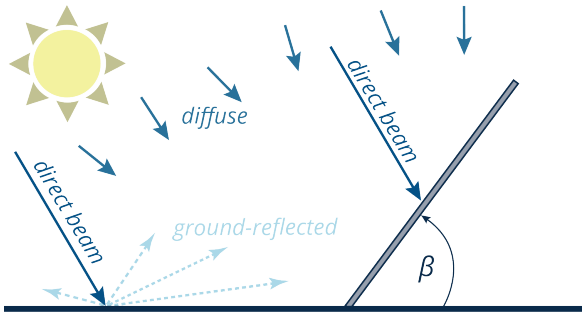

Figure 5.2: Irradiance components and their effect on a tilted plane

$$I_{\text{total, poa}} = I_{\text{beam},\,n} \cos\beta + f(I_{\text{diffuse},\,h},\ \beta) + g(I_{\text{global},\,h},\ \rho,\ \beta) \tag{5.2}$$

Since historical meteorological data is typically only captured for a horizontal plane, it is key to be able to transpose the irradiance to any arbitrary orientation to reflect the various configurations of solar PV arrays. For statically mounted PV arrays, two parameters define the orientation to the radiation components. These are the tilt of the module (β), and the azimuth (γ) angle of the array which is the orientation of the array with respect to the compass (e.g. South oriented). These two components define the plane-of-array (poa). The effect of various tilts on the energy yield of a PV power system is shown in figure 5.3. Since the beam component is defined as a function of the solar position, it can be

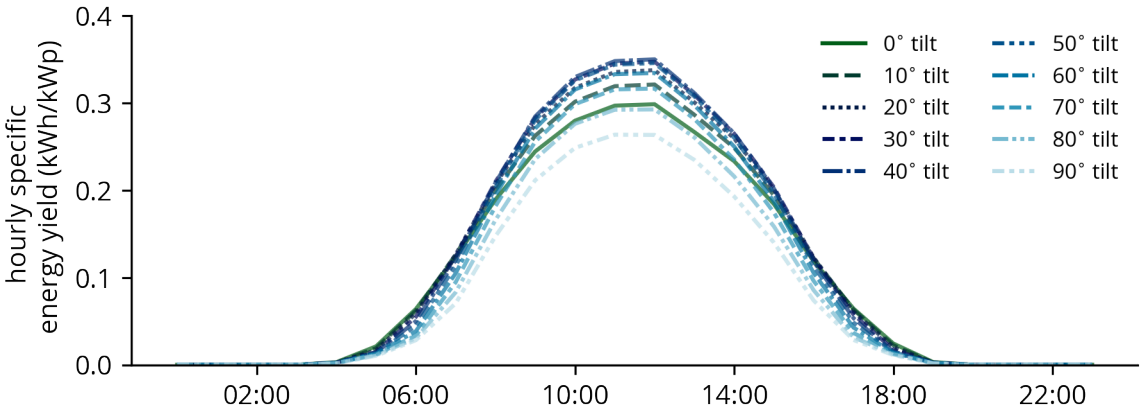

Figure 5.3: Year average daily PV power curves for a south-oriented PV array over various tilts.

transposed to the poa using geometry. The diffuse and ground radiation components require specific transposition functions, as shown in equation 5.2. In this equation, the diffuse irradiance on the poa is a function of the horizontal diffuse irradiance and the tilt of the module. The reflected irradiance is a function of the global irradiance, the tilt of the module and the ground-reflectance, called albedo and denoted by ρ.

Various models exist that transpose the various radiation components for a given tilt to an arbitrarily angled plane [130]. A typical approach is the isotropic transposition [131]. This model approximates the actual irradiance in the poa of diffuse and ground radiation using equation 5.3 and equation 5.4, respectively. Ground radiation includes an empirical factor representing the reflectivity of nearby surfaces called albedo (ρ_{ground}), where various surface types have distinguished albedo values. From both isotropic transposition equations, a similar component can be distilled, which is called the view factor. In the case of ground reflectance, this represents the fraction of diffuse radiation emitted from the ground surface projected on the poa surface. For the diffuse radiation component, the view factor represents the projection of the horizontal surface to the poa surface.

$$f(I_{\text{diffuse},\,h},\ \beta) = I_{\text{diffuse},\,h}\ \frac{1+\cos\beta}{2} \tag{5.3}$$

$$g(I_{\text{global},\,h},\ \rho,\ \beta) = I_{\text{global},\,h} \cdot \rho_{\text{ground}}\ \frac{1-\cos\beta}{2} \tag{5.4}$$

By substituting equation 5.3 and equation 5.4 back into equation 5.2 the formula is shown in equation 5.5 is achieved. This formula enables the approximation of irradiance on arbitrarily oriented PV arrays based on historical meteorological data.

$$I_{\text{total, poa}} = I_{\text{beam},\,n}\cos\beta + I_{\text{diffuse},\,h}\ \frac{1+\cos\beta}{2} + I_{\text{global},\,h} \cdot \rho_{\text{ground}}\ \frac{1+\cos\beta}{2} \tag{5.5}$$

To determine the power output of an arbitrarily oriented PV array, a formula relating the irradiance on the array to the power output of the given array. A linear relationship between the power output of a given PV array based on the module specification (P_{STC}) under Standard Testing Conditions (STC) (I_{STC}) and module area (A_{module}). In addition, an system efficiency factor (η_{system}) is introduced to allow for approximation of various system losses - including anything from DC cable losses to soiling losses. All module specific factors can be included in a single term $\eta_{\text{conversion}}$ that denotes the total conversion efficiency of the PV system from irradiance to power. Finally, equation 5.6 is reached.

$$P = I_{\text{total}} \cdot A_{\text{module}} \cdot \frac{P_{STC}}{I_{STC}} \cdot \eta_{\text{system}} = I_{\text{total}} \cdot \eta_{\text{conversion}} \tag{5.6}$$

Table 5.1: PV model statistics of deviation

	Yearly specific yield [kWh/kWp]	Yearly deviation [-]	Largest deviation		
			Month	kWh	Relative
Simple PV model	975	-	-	-	-
Advanced PV model	997	2%	January	-5	-17%
Renewables.ninja	961	-1%	June	-19	-29%

5.2.2 Submodel validation

As described in the previous section, the model used to determine the power output of PV systems based on historical irradiance data entails various approximations and simplifications. It is however of vital importance that the resulting power output curves are sufficiently accurate in representing the actual power output of PV systems. To this end, the PV submodel is validated against two models. The first model is based on a similar method as introduced in the previous section but entails a bias correction based on a statistical comparison between the modelled result and actual production data from various PV power plants in Europe over decades of data [72]. The second model is an advanced PV modelling approach, which introduces a much higher level of detail in capturing PV system-specific dynamics and a more complex transposition model [132]. This advanced modelling approach is introduced in more detail in appendix B.1.

Figure 5.4 shows the results of the comparison of these various approaches against the simple PV model. Table 5.1 contains statistical information on the deviation on a yearly basis and the largest monthly deviation. From figure 5.4a it can be seen that there is a generally good agreement between the various models.

When comparing the simple PV model against the advanced PV model, two things stand out. Firstly, the simple PV model slightly overestimates the energy production during the summer months while underestimating the energy production during the winter months. This can be mainly contributed to the lack of temperature modelling in the simple model approach. As a result of higher air temperatures during summer days, the power output of the modules is comparatively lower than during winter months when the air temperatures are lower.

Secondly, the effect of clipping due to a DC to AC power ratio above 1 (i.e. inverter maximum rated power is lower than the output of all PV modules) can be seen in figure 5.4c. While the simple model approach reaches a smooth maximum, the advanced model reaches a certain value at which the smooth rise of the power output is capped. This reflects the clipping effect which is included in the advanced model. The total yearly output shows only an error of 2% between the two models. Considering the fact that the advanced model requires about 7-10 times the computational time for only a limited accuracy gain, the simple PV model is a valid approach.

When comparing the simple model to the renewables.ninja again two things should be noted. Firstly, the bias correction approach is driven by error minimisation against data of existing PV power plants. Due to the spatial sparsity of those PV power plants, some local specificity of the irradiance time series is lost such as the passing of cloud cover. Therefore, the curves from renewables.ninja are very smooth when compared to the two other models, as can be seen from figure 5.4b and figure 5.4c.

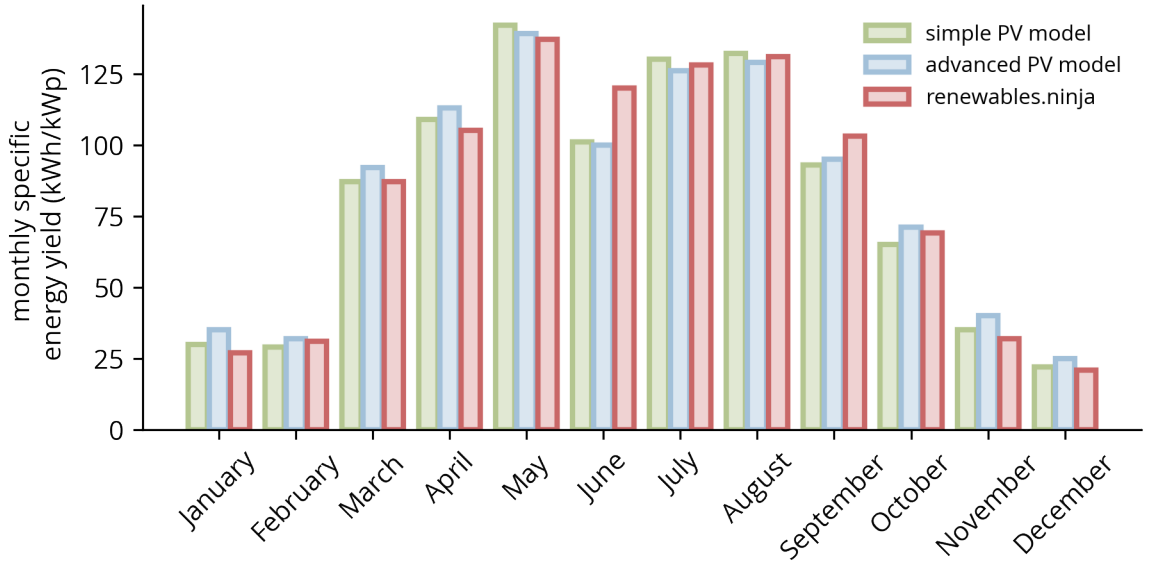

(a) Monthly specific energy yield of the three models

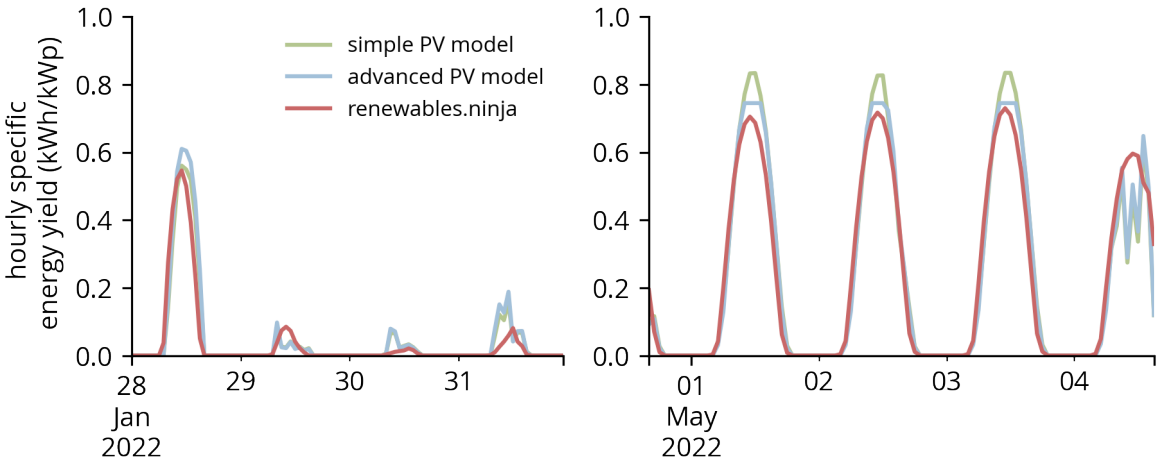

(b) Four winter days winter generated by each model

(c) Four spring days winter generated by each model

Figure 5.4: PV model validation against advanced PV model and renewables.ninja model

Secondly, while the deviation on a yearly basis is as little as 1%, there is a large deviation of 29% over the month of June. Both the simple and the advanced models show a substantially lower production in June. This could be a result of the difference between the large scale meteorological data reanalysis behind the approaches. Where the renewables.ninja model bases its calculation on the global MERRA-2 reanalysis, the two other models are based on European scale PVGIS-SARAH data which is based on satellite images.

In conclusion both the simple and the renewables.ninja PV models are found to be acceptably accurate approaches to produce PV production profiles needed to fairly represent PV technology in the optimisation problem. The simple model approach is based on PVGIS data which has the merit of being able to provide a TMY compliant year, which is a synthetically generated year that is representative of a longer time period [115] [119].

On the other hand, the renewables.ninja approach has been bias-corrected to enhance its hindcasting performance. If a specific year of interest is to be investigated, this approach is favourable. An exemplary case would be the integration of time series from another model which itself is based on a specific historic year.

5.2.3 PV cost development

Due to the cost-based optimisation nature of the framework in this thesis, it is of vital importance that substantiated assumptions about future costs are in place. For this reason, literature was studied to find sources of such projections which are often referred to in optimisation studies. Figure 5.5 shows three of those projections, both in absolute and in normalised values. Energy Technology Reference Indicator (ETRI) 2014 and 2017 are publications as part of the European Strategic Energy Technology Plan [133] [134]. Fraunhofer ISE is considered one of the leading parties in terms of information on the European solar market [135].

There are similar reports offering such reference or baseline values, but these contain a very complete range of information sources - from academic literature to consulting publications - and are specifically tailored to the European Union. The three projections have roughly the same reference value in the same reference year (2015). As a result, the normalised projections show nearly the same behaviour.

All three reference (or mean/baseline) scenarios show good agreement. Fraunhofers projection shows the tightest range, while ETRI 2017 shows the largest range of possible future prices. This is in part due to the different methodologies. ETRI 2017 is based on scenario-based cost projections, each reflecting a different future energy system with varying shares of renewable technology. As ETRI 2017 is the most recent study and distinguishes between various PV set-ups and scales it was used to determine realistic values for optimisation of future energy systems. In addition, the given range is also used to determine the PV cost development uncertainty ranges for parametric experiments.

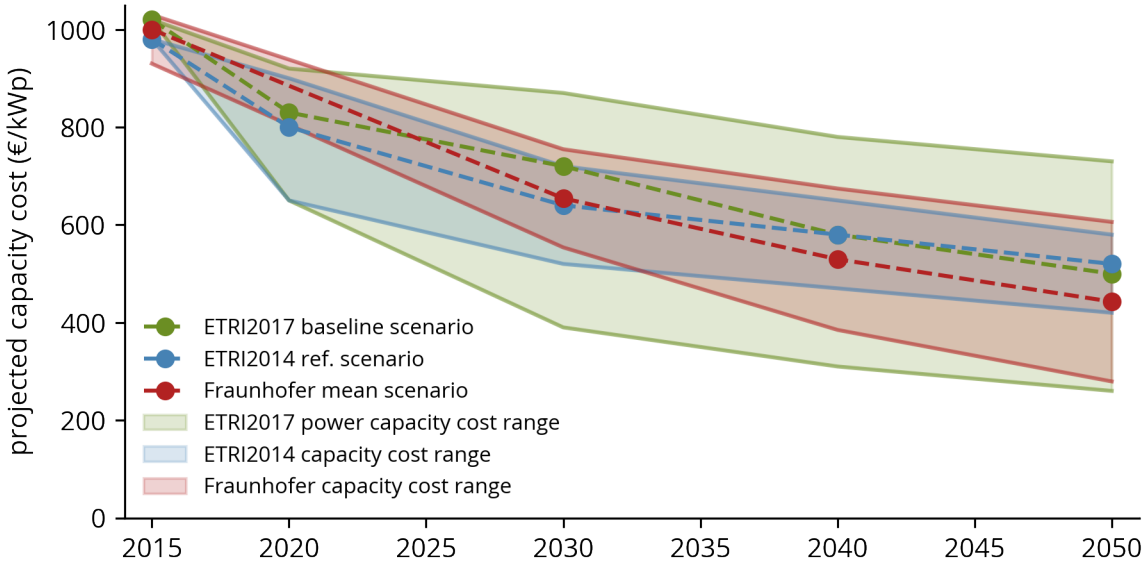

(a) Absolute capacity cost development

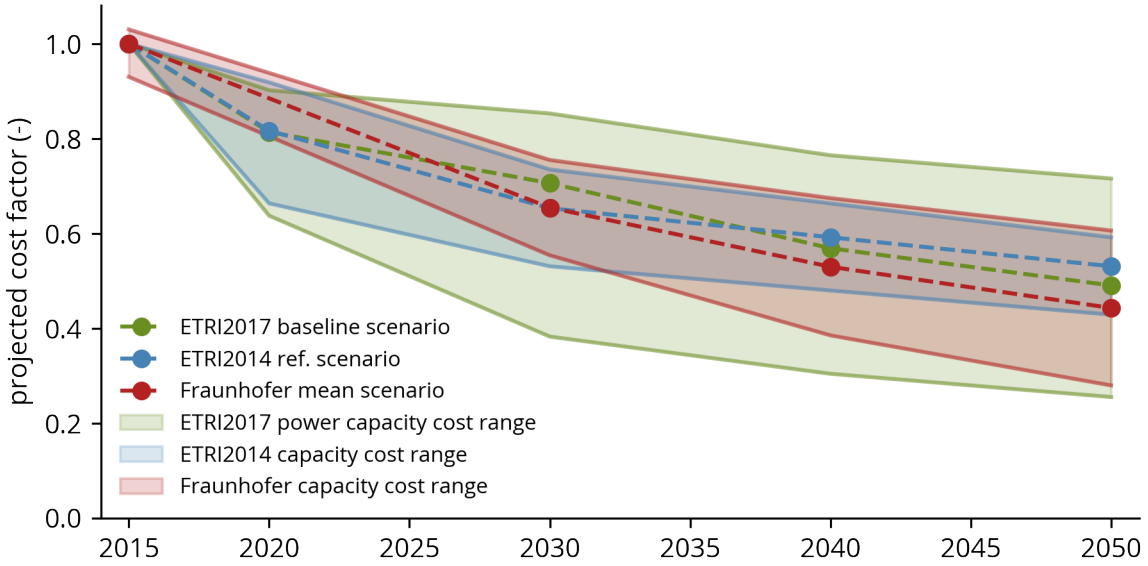

(b) Normalized capacity cost development

Figure 5.5: Utility-scale PV capacity cost development [133] [134] [135]

5.3 Wind

Another important source of intermittent renewable energy is wind power. Through the use of turbine blades placed in moving wind, the kinetic energy of the moving air is first converted to mechanical shaft power after which a generator converts the shaft energy to electrical energy. As with solar PV systems, the output of a wind turbine depends on the local meteorological conditions.

5.3.1 Submodel description

To correctly incorporate the intermittent and dynamic behaviour of wind power production, a wind power model is formulated. Wind power systems can be modelled with fewer meteorological conditions to consider compared to solar PV. Equation 5.7 shows the fundamental relation between wind

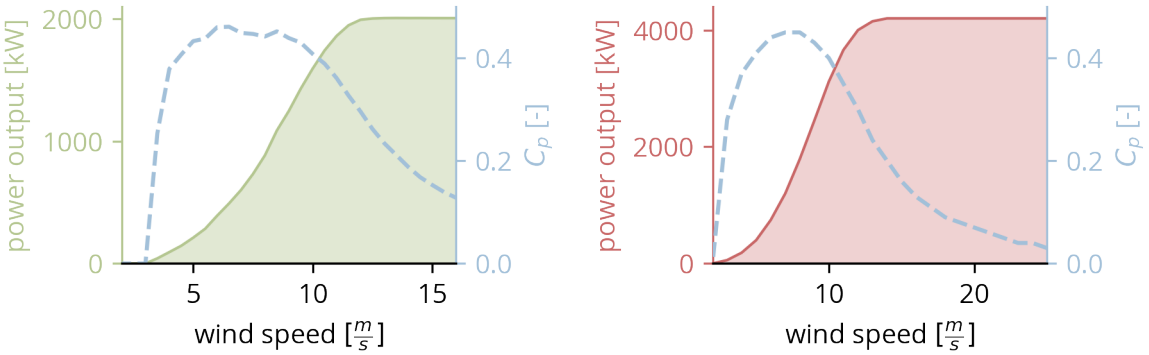

(a) Vestas V90 2 MW turbine power curve

(b) Enercon e126 4.2 MW turbine power curve

Figure 5.6: Wind power curves for two example turbines

speed and output power. In this equation, ρ denotes the specific gravity of the air, A represents the effective rotor area, v is the wind speed at the hub height, c_p is the power coefficient, and η is the conversion efficiency factor. This equation relates the kinetic energy contained in the wind $E_{ki} = \frac{1}{2}mv^2$ to power output. This is achieved by back-substitution of mass flux $\frac{dm}{dt} = \rho A v$ traveling through the effective rotor area.

$$P_{wind} = \frac{1}{2}\rho A v^3 \eta c_p \tag{5.7}$$

Aerodynamic losses are included by applying the power coefficient c_p and the system conversion losses are reflected in the efficiency η. The power coefficient is dynamic in function of the wind speed and determined by the design of the turbine blades. This coefficient cannot exceed the Betz limit of $c_p = 16/27$ [136]. Typically, wind turbine manufacturers supply a power curve and/or the power coefficient as a function of wind speed under standard conditions. This has been collected for various manufacturers and makes in an open database accessible under the Open Energy Platform [137]. Two of such power curves are shown in figure 5.6.

The parameter with the largest effect on the power output is the wind speed, which has a cubic relationship to the power output. The other parameters are proportional. Rotor area is a turbine specific parameter and a constant. The density is a function of temperature and relative humidity and is dynamic, albeit at a reasonably tight range. The efficiency is also turbine specific and can be considered dynamically as a function of the load relative to nominal capacity.

Due to shear between the nearly stationary air at the surface and higher layers of moving air, the wind speed gradually increases with the height. As a result, wind speeds at a certain height should be transformed to the hub height of the turbine. The increase in wind speed depends on various factors, including surface roughness and the temperature gradient [138]. Equation 5.8 shows the logarithmic relation used to determine the vertical wind profile [136]. It is assumed that the surface roughness length z_0 equals 0.03, which is analogue to an open field.

$$v(H) = \mathrm{v_{ref}} \frac{\ln\left(H/z_0\right)}{\ln\left(\mathrm{H_{ref}}/z_0\right)} \tag{5.8}$$

5.3.2 Submodel validation

Within the framework, three approaches to modelling wind power are possible: 1) described model based on meteorological data from PVGIS 2) described model based on meteorological data from DOWA and 3) requesting a calculated power curve from renewables.ninja. Both DOWA and renewables.ninja have the merit of containing multiple height levels due to the fact that both are submodels of the MERRA-2 reanalysis. These two approaches will therefore better capture location-specific vertical wind profiles. Throughout this thesis, the DOWA data is not used, as no of the studies require off-shore wind production curves.

Therefore, approach 1) and approach 3) are compared against each other for a Vestas V90 2 MW wind turbine on a specified location. The result is shown in figure 5.7. Generally, there is good agreement in the monthly energy yields with an exception for October. In this month, the wind modelling approach based on PVGIS underestimates the expected yield by 52% when compared to renewables.ninja. Due to the fact that these models are each based on different data sources, it is likely that this is a result of the difference between satellite driven models against reanalysis models. On a yearly basis, there is a good agreement ($<$2% error) between the two modelling approaches, as shown in table 5.2.

When looking at the winter and summer days generated by both models, shown in figure 5.7b and fig 5.7c, respectively, the behaviour is in general quite similar. However, it becomes apparent that the model based on the PVGIS data behaves more erratically, showing a more irregular pattern with large spikes. The profile of renewables.ninja on the contrary shows a more smooth pattern. In addition, the number of values in extremities seem substantially lower.

This is concluded to be indeed the case, by analysing the histogram shown in figure 5.8. In this figure, the x-axis denotes the hourly capacity factor (e.g. output power for that hour relative to the nominal capacity). The y-axis shows the corresponding frequency (in hours per year) of that hourly capacity factor. From this figure, it is concluded that the PVGIS based model seems to switch in a quite binary manner between no production and peak production. This is assumed to be an artefact of the logarithmic height extrapolation applied.

In conclusion, both models show reasonable results and have each been validated in existing literature [138] [122]. Renewables.ninja shows more realistic and smooth behaviour, while PVGIS is more erratic. This can be attributed to the availability of various height levels in the renewables.ninja, which is a more realistic reflection of the vertical wind profile at and around the turbine hub height.

PVGIS only produces wind speeds at a height of 10 meters, where near-surface effects and surrounding objects can substantially affect the wind speed. Moreover, this margin of error is further increased due to the extrapolation errors from applying the height correction. PVGIS has the merit of being able to produce output in a TMY format, which better reflects historical meteorological conditions than a single year would [115] [119] [120].

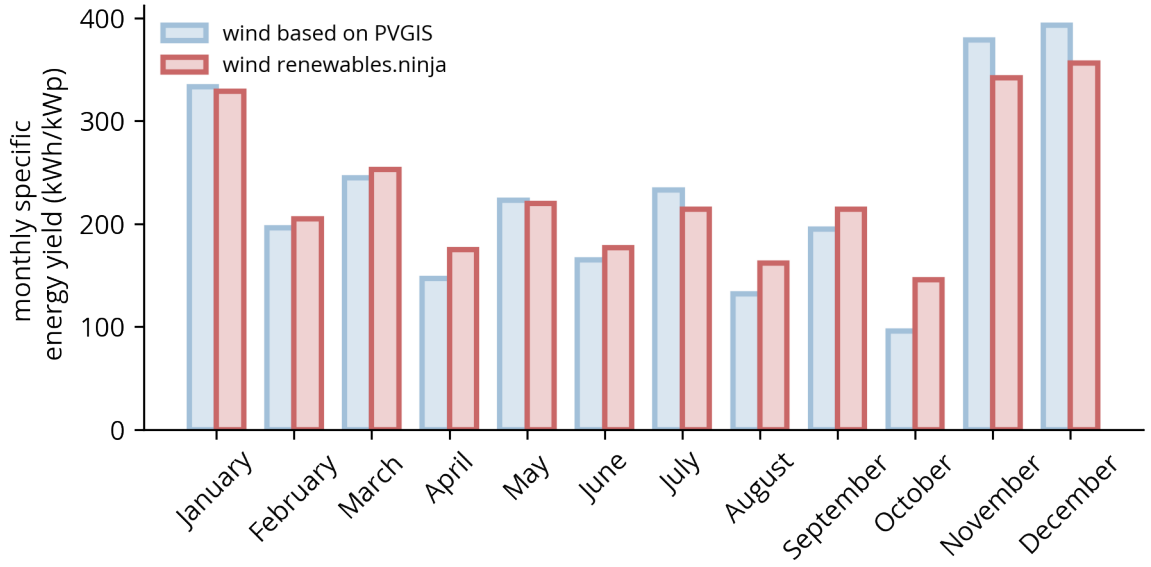

(a) Monthly specific energy yield of the two models

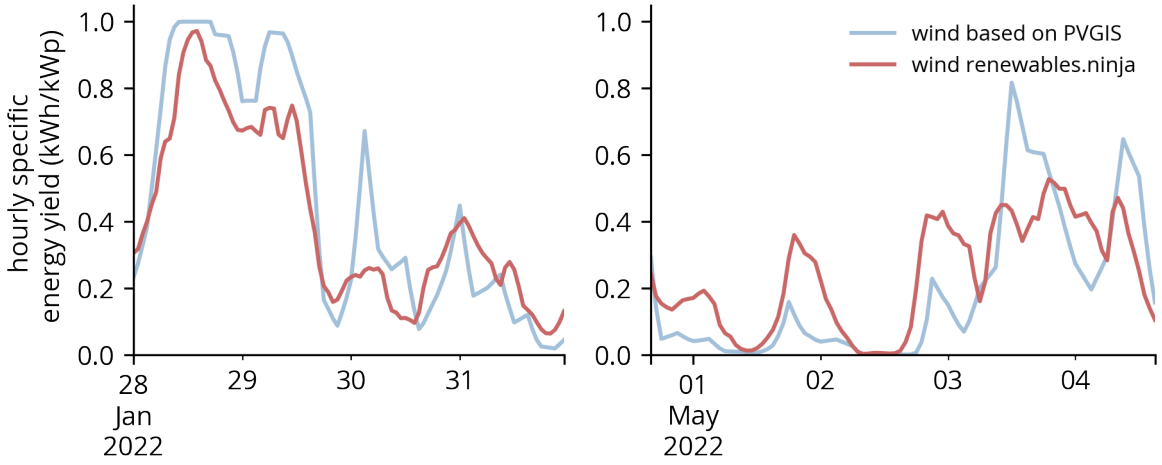

(b) Four winter days winter generated by each model

(c) Four spring days winter generated by each model

Figure 5.7: Wind model based on PVGIS wind data validation against renewables.ninja wind model

Table 5.2: Wind model statistics of deviation

	Yearly specific yield [kWh/kWp]	Yearly deviation [-]	largest deviation		
			Month	kWh	relative
PVGIS	2737	-	-	-	-
renewables.ninja	2793	2%	October	-50	-52%

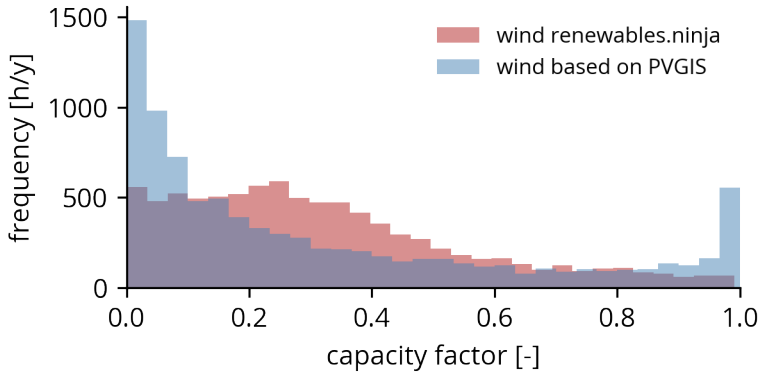

Figure 5.8: Histogram $n_{bins} = 30$ depicting the frequency of wind capacity factors through the year based on two models

5.3.3 Wind cost development

Figure 5.9 shows two projections - of which the specifics have been described in 5.2.3 - both in absolute and in normalised values. These projections show great discrepancies in terms of the uncertainty range. This is mainly due to the fact that ETRI 2014 does not distinguish between different configurations of on-land wind systems, whereas ETRI 2017 does include this distinction. As a result, ETRI 2014 generalises all current cost and projections to a singular value; regardless of the hub height or rated power of the wind turbine. ETRI 2017 includes an update, which classifies wind turbines into three bins both in terms of the power rating and the hub height of that turbine. For this thesis, medium-medium turbines were selected. This roughly reflects the current landscape, where wind turbines have around 100m hub height and are rated around 2-3 MW. For this reason and the fact that ETRI 2017 is more recent, this cost projection will be used for the determination of the future cost of wind as well as provide the uncertainty range for the parametric experiments.

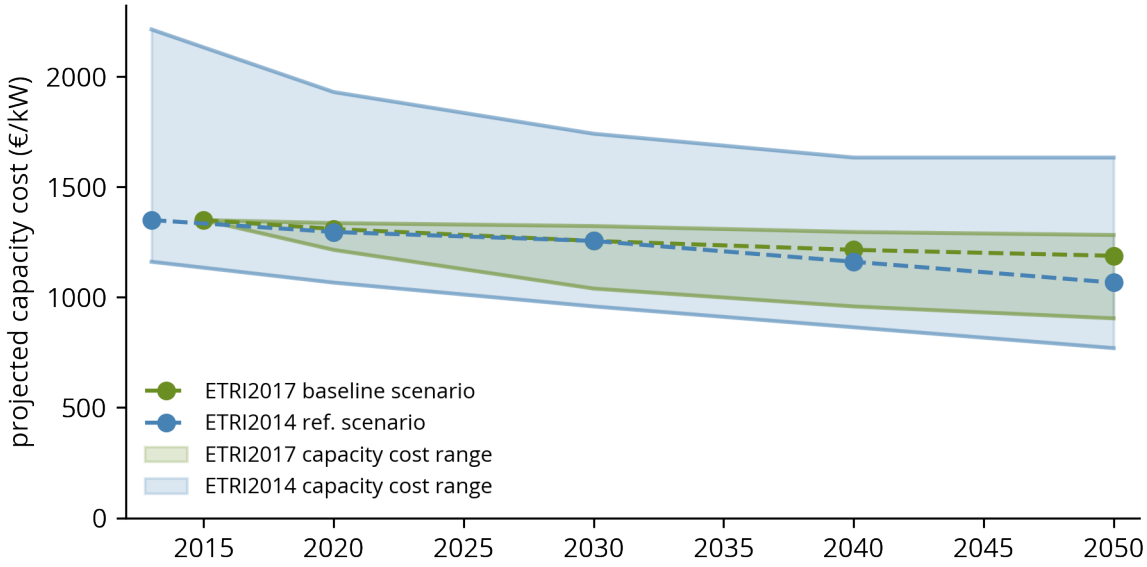

(a) Absolute capacity cost development

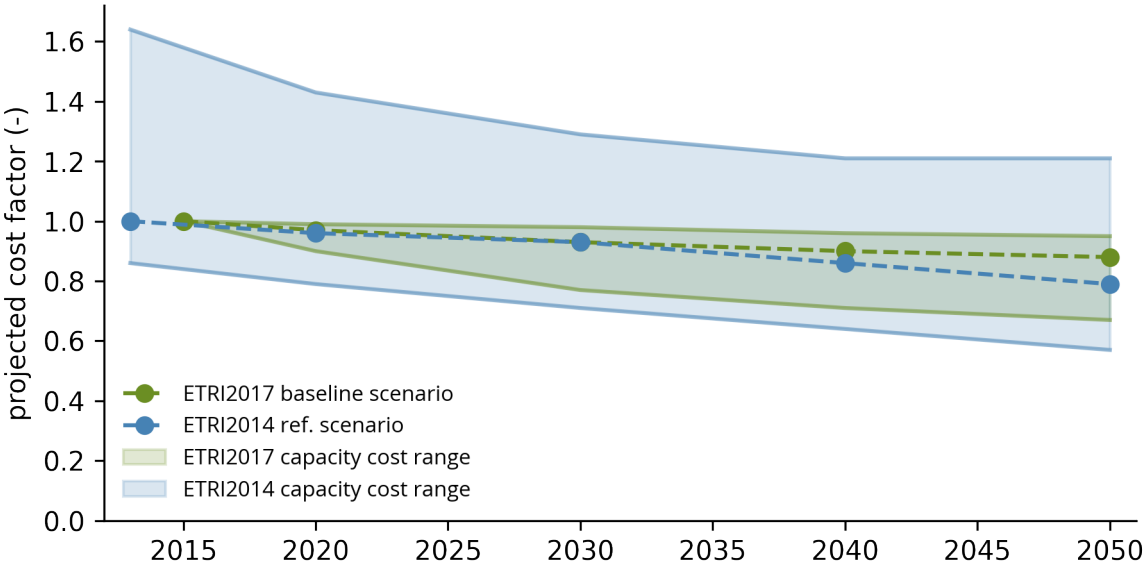

(b) Normalized capacity cost development

Figure 5.9: onshore wind capacity cost development [133] [134]

5.4 Storage components

Throughout literature, it is concluded that storage of energy will be crucial in supporting energy systems highly dependent on intermittent renewable sources of energy [83] [139]–[143]. With increasing shares of non-dispatchable sources of renewable energy, storage offers operation flexibility and greatly reduces the required installed capacity of wind and solar [144]. Requirements for successful implementation of energy storage solutions in future energy systems have been studied intensively [145] [146]. Use cases such as reserve capacity, operational flexibility and balancing services are out of scope in this thesis, in part due to the hourly time-step used.

Based on the definitions of use-cases for storage in future energy systems [145] and corresponding outcomes from cost projection, it can be concluded that at least two distinct storage technologies should be considered to correctly reflect cost optimisation of future energy systems. These two technology are lithium-ion battery storage and hydrogen storage.

Currently, lithium storage technology is considered cost-effective most cost-effective for storage applications around 1 hour storage duration and less than 500 discharges per year. Towards 2050 the application range is expected to increase to nearly 16 hours storage duration [145]. These applications include gas peaker plant replacement and black start capacity but are also related to the management of grid congestion and investment deferral due to mitigating peak flow load on existing infrastructure. Lithium battery storage should be considered in various power-to-energy ratios configurations, allow to most cost-effectively meet the demand of a specific task in closing the intra-day energy balance [38].

Hydrogen storage is expected to be the most cost-effective technology for seasonal storage, as early as 2025 [145]. Seasonal storage is described as a crucial component for buffering and storing seasonal excesses and shortages related to high shares of renewable energy [147]. This segment requires the storage component to store energy for extended periods, from weeks to months.

5.4.1 Submodel description

Both hydrogen and lithium, or any arbitrary storage component, can be described using the same general storage dynamics. These are used to correctly reflect charging, discharging, self-discharge losses and conversion efficiency losses. The maximum amount of energy contained in a storage component can never exceed its maximum energy (E_{max}) content as shown in equation 5.9. This is defined by component-specific installed capacity ($P_{installed}$) and EP (energy-to-power) ratio (EP_{ratio}), as shown in equation5.11.

$$E(t) \leq E_{max} \tag{5.9}$$

$$\text{with:} \quad t, \text{time} \quad \forall t \in [t_{min}, t_{max}] \tag{5.10}$$

$$E_{max} = P_{installed} \cdot EP_{ratio} \tag{5.11}$$

To define the charging and discharging dynamics, equation 5.12. In this equation, the η denotes single direction efficiency which is determined based on the round-trip efficiency. The round-trip efficiency is assumed at 85% and 40%, for lithium battery storage [148] and hydrogen storage [145], respectively. Due to the recursive behaviour of this formula, an initial value ($E_{t_{min}}$) and final value ($E_{t_{max}}$) should be set. This is implemented through equation 5.14 and equation 5.15, respectively. In these equations, E_{max} denotes the maximum storage capacity and SOC_{init} is the initial state-of-charge of the storage component.

$$E_t = E_{t-1} + \eta P_t \tag{5.12}$$

$$\text{with:} \quad t, \text{time} \quad \forall t \in [t_{min} + 1, t_{max} - 1] \tag{5.13}$$

$$E_{t_{min}} = E_{max} \cdot SOC_{init} \tag{5.14}$$

$$E_{t_{max}} = E_{t_{min}} \tag{5.15}$$

Charging losses require a more sophisticated implementation to correctly reflect the charging and discharging dynamics. To be able to do this, charging power should be split to a positive and a negative component, as shown in equation 5.16. Substituting this back into equation 5.12 yields equation 5.17. Through this implementation, conversion losses are rightfully reflected. For instance, the storage component state of charge will increase to a higher energy level than it will be able to contribute again to the system energy balance, due to discharge conversion losses.

$$P = P_{pos} + P_{neg} \tag{5.16}$$

$$E_t = E_{t-1} + \eta P_{neg,t} + \eta P_{pos,t} \tag{5.17}$$

with:

$$P_{pos}, \quad \text{Positive charge component} \quad \forall P_{pos} \in [0, \infty) \tag{5.18}$$

$$P_{neg}, \quad \text{Negative charge component} \quad \forall P_{neg} \in (-\infty, 0] \tag{5.19}$$

$$t, \quad \text{time} \quad \forall t \in [t_{min} + 1, t_{max} - 1] \tag{5.20}$$

Finally, self-discharge losses should be implemented to represent the loss of charge over time. This is determined by using equation 5.21. Here $\eta_{\text{self-discharge}}$ should be always implemented as the hourly rate of discharge. For lithium battery storage and hydrogen storage these hourly discharge rates are assumed at 0.9995 and 1 [145], respectively.

$$E_t = \eta_{\text{self-discharge}} \cdot E_{t-1} \tag{5.21}$$

with:

$$t, \text{time} \quad \forall t \in [t_{min} + 1, t_{max} - 1] \tag{5.22}$$

All derived equations can be implemented into the optimisation problem as linear (in-)equalities and thus will contribute to the system of equations as linear constraint functions. By substituting the storage technology and component-specific parameters, these equations can be used to reflect any arbitrary storage component added to the energy system under analysis.

5.4.2 Lithium battery storage data and cost development

The cost projections for lithium-ion storage technology is based on the Annual Technology Baseline published by NREL [148]. This study is relevant specifically due to the fact that it includes separate price projections for both the power and energy component of lithium storage, as can be seen from figure 5.10.

Even though the normalised projections show a similar lower range (figure 5.10b), the moderate scenario and upper range are substantially higher for the power component of cost. This is augmented by the researchers based on the fact that the energy component (lithium cells) is still in the early stages of development, allowing for larger gains in cost-effectiveness. The power component on the other hand is mainly dependent on Balance Of System (BOS), which are power electronics such as wires, switches and inverters. Since this market is readily mature, large cost improvements are less likely.

Due to the fact that the storage cost component and power cost component are supplied separately, it is possible to accurately determine the cost of arbitrary configured battery storage system. Driven by the EP ratio of the lithium battery, investment cost can be determined, as shown in equation 5.23. In this equation, C' denotes the specific investment cost for a cost component. C_{power} denotes the total investment cost per installed power capacity for a given battery configuration. Identically, equation 5.24 can be used to determine the total investment cost per kWh, denoted by C_{energy}. For example,

lithium battery storage configured at 2 hours storage duration would result in a cost per kWh of 245 euros ($(197 + 147 \cdot 2)/2$) when the centre values of the 2030 cost range are assumed.

$$C_{power} = C'_{power} + C'_{energy} \cdot EP_{ratio} \tag{5.23}$$

$$C_{energy} = \frac{C'_{power} + C'_{energy} \cdot EP_{ratio}}{EP_{ratio}} \tag{5.24}$$

For lithium storage future cost projections applied in this thesis, it is assumed that storage and power cost scenarios are related and occur together. The storage component cost range is sampled and the cost component for power is linearly mapped to match that cost scenario. In reality, these events are disjoint and not do not strictly correlate. However, applying this simplification greatly reduces the variability of possible future cost outcomes resulting in a more clear overview and enhanced computation tractability.

5.4.3 Hydrogen data and cost development

Cost development of hydrogen is more difficult to predict, as it is still in an early stage of adoption and therefore still in the early stages of the experience curve. This is determined based on the global cumulative installed capacity of technologies. When comparing hydrogen storage to pumped hydrogen storage, the installed capacity is almost three orders of magnitude lower [145].

The projected costs for hydrogen can be seen in figure 5.11. The absolute costs are depicted for two different configurations. Seasonal storage and sub-seasonal storage with a storage duration of 700 and 350 hours, respectively. The cost of such a configuration is based using a combination of the power cost component and storage cost component, as shown in equation 5.24.

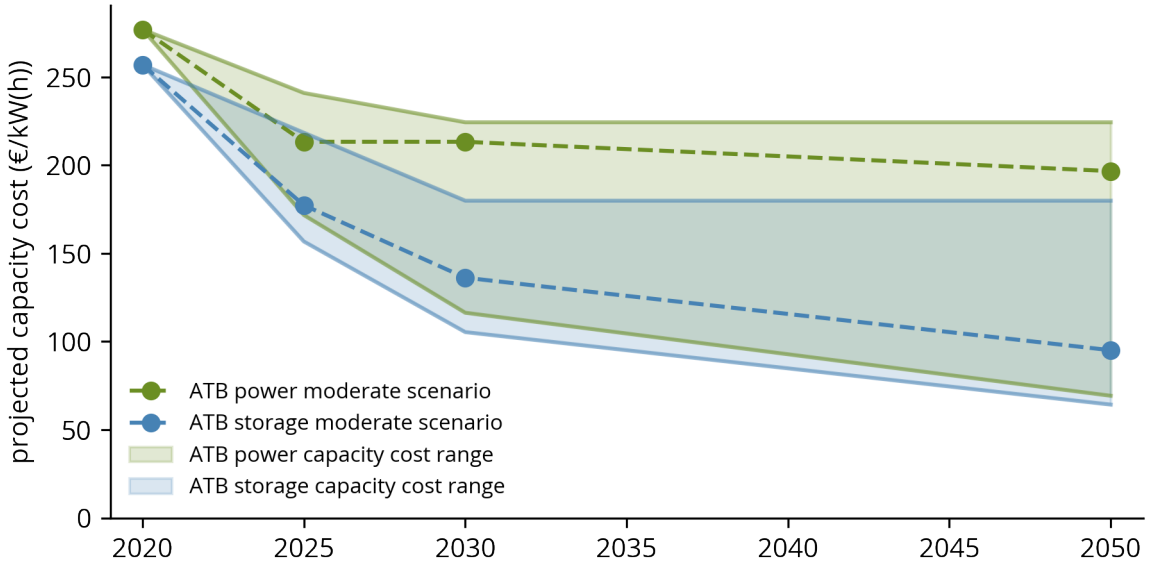

(a) Absolute capacity cost development

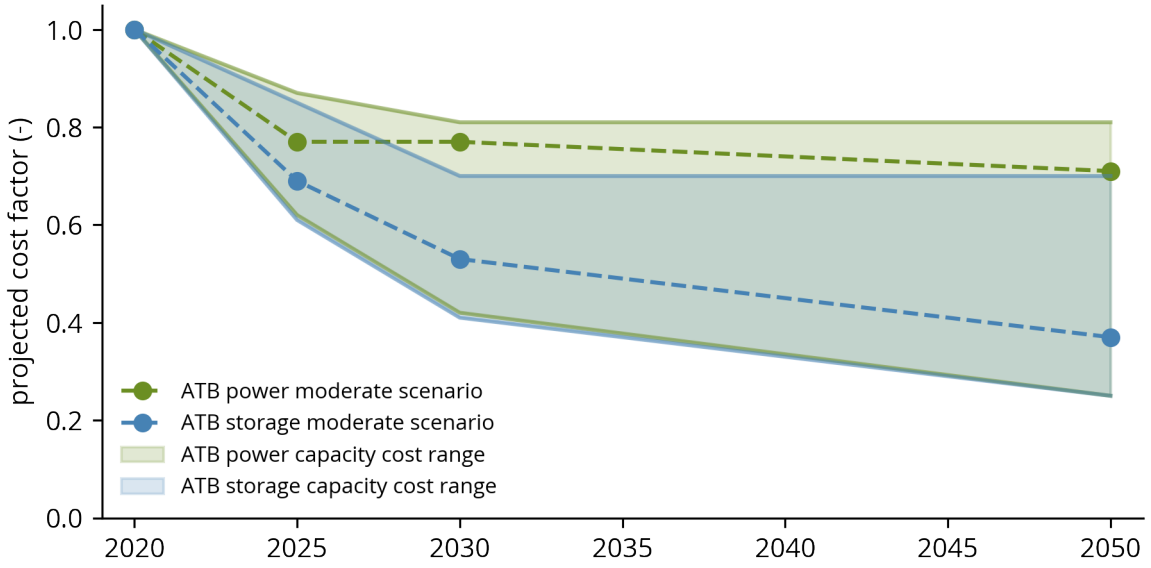

(b) Normalized capacity cost development

Figure 5.10: Utility-scale lithium-ion based storage cost development [148]

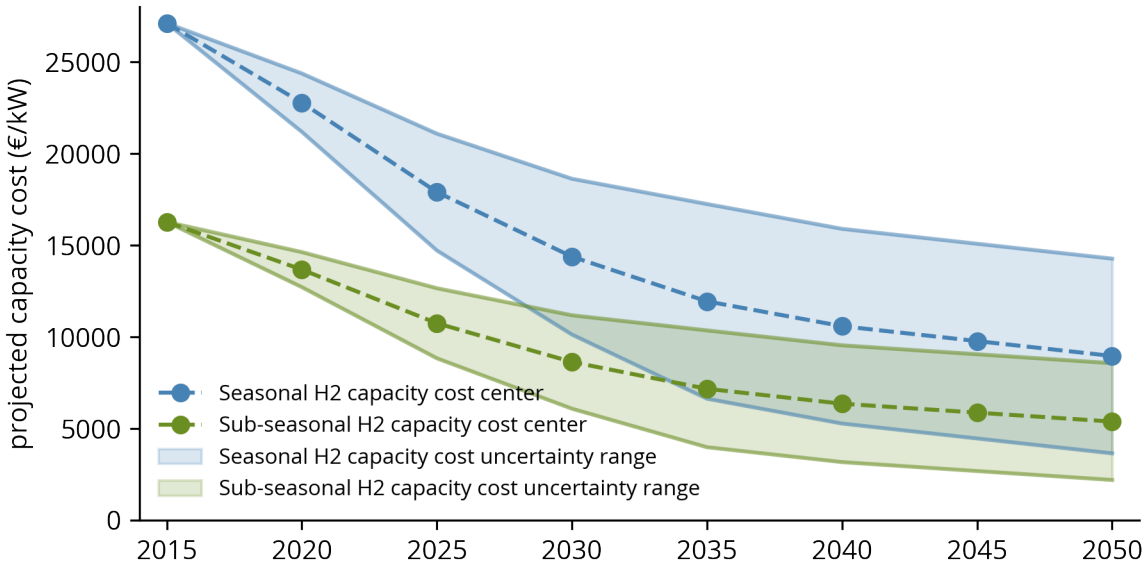

(a) Absolute capacity cost development

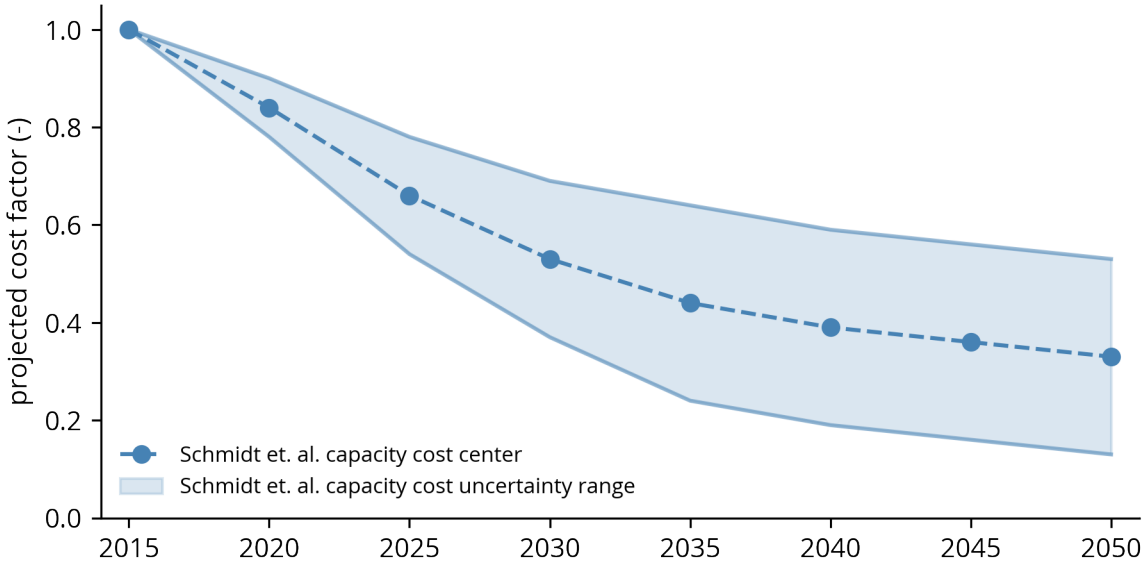

(b) Normalized capacity cost development

Figure 5.11: Utility-scale hydrogen-based storage cost development [145]

5.5 Electric mobility hub charging demand

One of the case studies in this thesis explores the possibilities for the deployment of energy systems based on renewable energy generation to facilitate charging infrastructure for a rapidly increasing share of Electric Vehicles (EVs). Funke [149] identifies two distinct use cases for fast charging infrastructure. The first is fast charging within urban areas as an alternative to overnight charging at home. The second is intermittent charging during travel, mostly on highway stops. The latter poses a greater demand on existing grid infrastructure as EVs will only stop for a relatively short period of time to charge using high power DC fast charging infrastructure. This use case is dynamic within the hour due to the fact that fast charging on highways is very time-constrained [149].

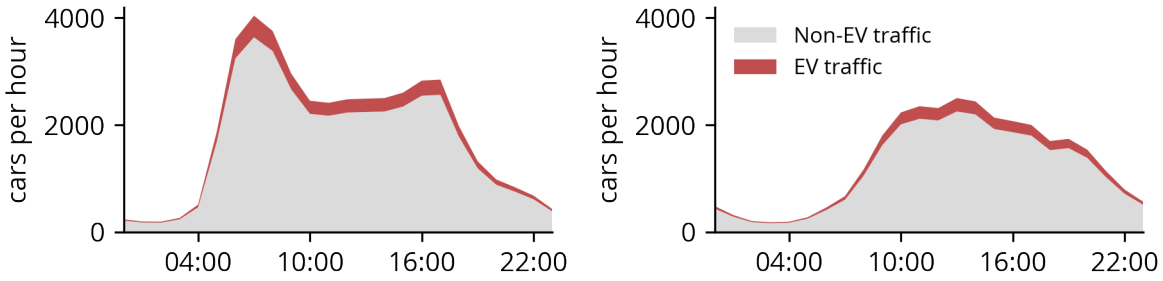

(a) Typical weekday

(b) Typical weekend day

Figure 5.12: Traffic and proportion of EV at Deventer highway segment A1 westbound

All time series used in LESO are on an hourly basis therefore, it is reasonable to include the charging behaviour on an hourly basis. Even though shorter peak loads will not be reflected correctly, the hourly energy balance will still reflect such a demand profile sufficiently to include in energy system optimisation [150].

Since no suitable data sources are publicly available on EV charging demand specifically for highway charging infrastructure, it was decided to stochastically approximate the time series. This is based on real traffic data, supplied by the Dutch National data portal for traffic data [151]. Unfortunately, it is not possible to extract a whole year of hourly traffic data. Instead, a typical weekday is created based on an average of all weekdays in the year - excluding holidays. In addition, a typical weekend day is created based on an average of all weekend days in the year - including holidays.

Combining the two to form every week of the year yields an hourly traffic profile of light traffic passing a certain highway segment for every hour of the year. Based on projections for EV uptake in the Netherlands [152], a certain (constant) share of this traffic is assumed to be electric. This is shown in figure 5.12 for the A1 highway segment near Deventer.

It is out of scope to model the origin and destination of the passing EVs as a basis to determine the State of Charge (SOC) when passing the charging opportunity. Instead, a stochastic approximation is implemented. To this end, a truncated exponential normal distribution is randomly sampled. This is applicable due to the higher likelihood of a lower state of charge than a nearly fully charged EV.

Due to the random sampling, the time series becomes more diverse, because the rigidity of using only two representative days is relaxed. It should be noted that for parametric studies conducted, for instance, to investigate cost development uncertainties, this random sampling is connected to a specific random seed to maintain reproducibility over many experiments.

After this, it can be decided which EVs are eligible for charging at this location. This is decided based on the energy content and fast-charging power of the batteries found in the EVs. This is assumed to be around 70 kWh and 150 kW, respectively. If a user would stop for about 10 minutes on average, this would mean that EVs should be able to charge at least 25 kWh. The upper region for fast charging is typically up to a SOC of 80% [153]. As a result, only EVs with a SOC below 40% are considered candidates for using the fast charger. Of those EVs that could charge, a certain share will use this charging opportunity while others might find alternatives, as shown in figure 5.13.

Due to starting, stopping and connecting activities taking place before and after charging the maximum amount of EVs per charger per hour is capped to four EV's per charger per hour. Combining the

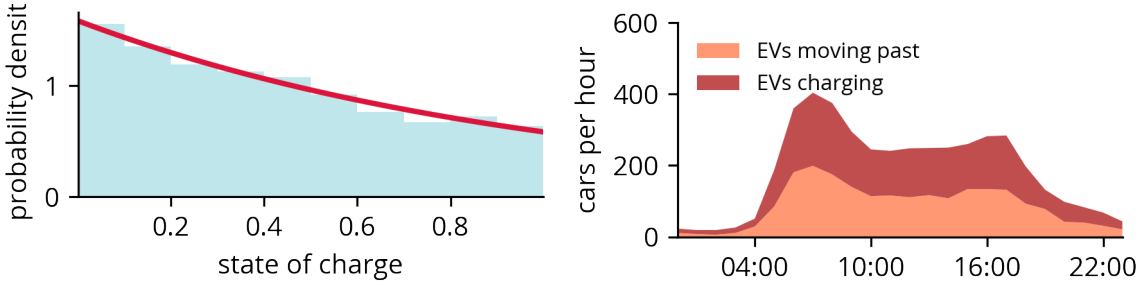

(a) Truncated exponential pdf and histogram

(b) Fraction of EVs charging on a typical weekday

Figure 5.13: Stochastic approximation of charging behaviour of EVs

maximum capacity of the charging infrastructure at a location with the stochastically sampled traffic data, an energy demand profile is generated. This profile is translated into an electric load profile by using the charging efficiency, which is set at 85% [153]. As a result, the load acting on the energy system is higher than the energy transferred into the EV batteries due to electrical and heat losses. The resulting load is shown in figure 5.14.

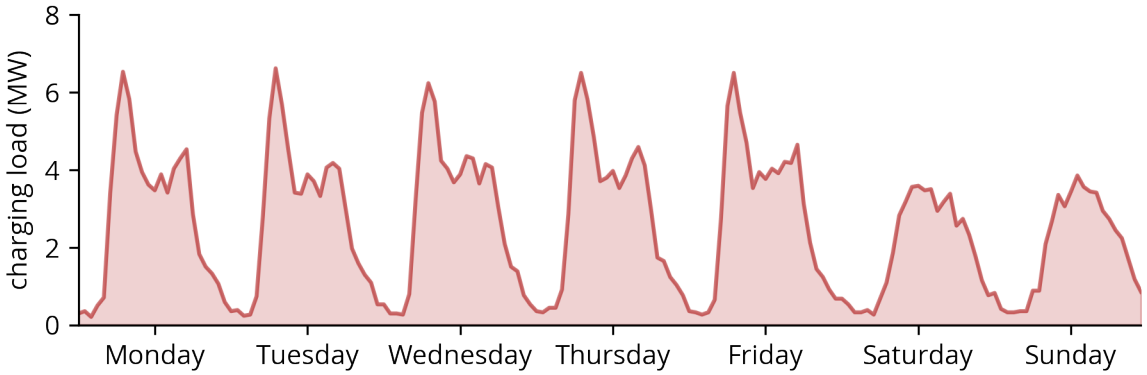

Figure 5.14: Load on the system as a result of EV charging demand

5.6 Regional electric demand from ETM

Since Local Energy Systems Optimizer (LESO) aims to optimise local energy systems, it is relevant to have a dependable source for regional energy demand curves. As stated in section2.2.1, the ETM is used numerously throughout RES and system integration studies on a provincial level. Impacts assessments of future energy systems carried out by DSOs and TSOs are also (in part) based on the ETM and resulting demand curves [154] [30] [17]. The reasoning of the scenarios and the implementation in the Dutch energy transition is covered in more detail in chapter 2. The advantages of using ETM as a source for regional demand curves:

1. **Transparency**
   Online graphic interface, customisable through sliders (e.g. share of heat pumps, growth of industry, etc), direct results, browsable
2. **Regionallity**
   ability to switch between scales from neighbourhoods to national level

3. **Diverse energy carriers, sectors and components are modelled**
   i.e. heat, mobility, gas, industry, electricity, etc.

This section focuses on how ETM scenario models and their respective hourly curves are integrated in LESO.

5.6.1 Scenario-based demand curves

It is possible to query the yearly demand curves on a hourly resolution for any existing ETM scenario using the public API. This return a file containing each individual curve contributing to the energy balance in the model. In total there are [1] 171 categories modelled. Of which 68 are production curves and 103 are demand curves. Depending on the inputs given by the user, these curves contribute a larger or smaller share to the total. For some specific curves, user settings affect the curve produced by the ETM (e.g. merit order).

An example of such curves is shown in fig 5.15. These curves belong to the 49% emission reduction scenario for the province of Gelderland by 2030. This scenario includes the most recent projections on 2030 in the context of Gelderland [17].

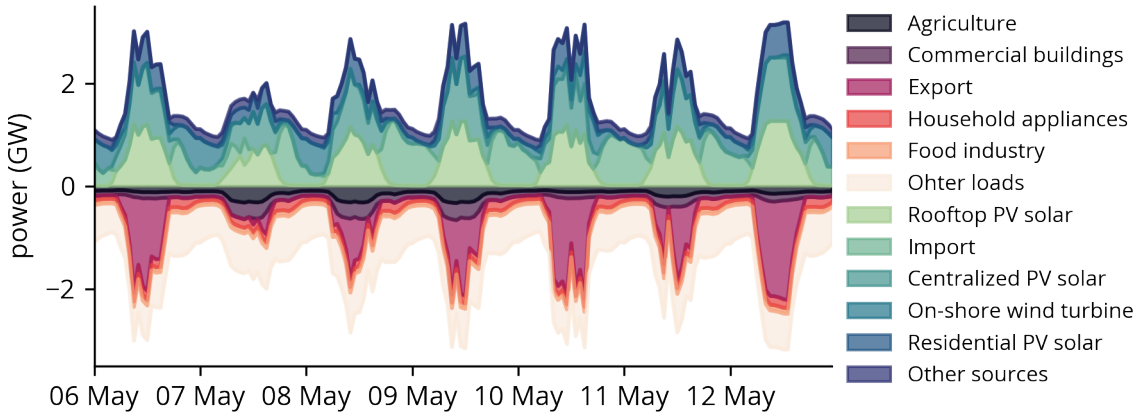

Figure 5.15: An example of demand and supply curves that can be queried from the ETM using the API from the 2030 49% reduction Gelderland scenario. Any scenario in the ETM can be queried using this approach. Only the top 5 contributing categories are shown for both the loads and sources, the rest is summed to the ”other” category.

The ETM models more technologies than included in the scope of LESO. To determine the residual load to use for the optimisation, certain technologies are allowed to contribute to the future energy system without being simulated within LESO. These are technologies such as waste incinerators or biogas fueled combined heat and power plants (CHPs). Wind and solar PV production curves are excluded from the residual because these technologies fall within the scope of LESO and should therefore be simulated and optimised within the framework. The original residual load curve (normally resolved with import/export, which was excluded for illustration purposes) and the demand curve after applying the aforementioned technology group filters are shown in figure 5.16.

[1] at moment of writing, release ”production-2021-09-07” [https://github.com/quintel/etengine/releases/tag/production-2021-09-07]

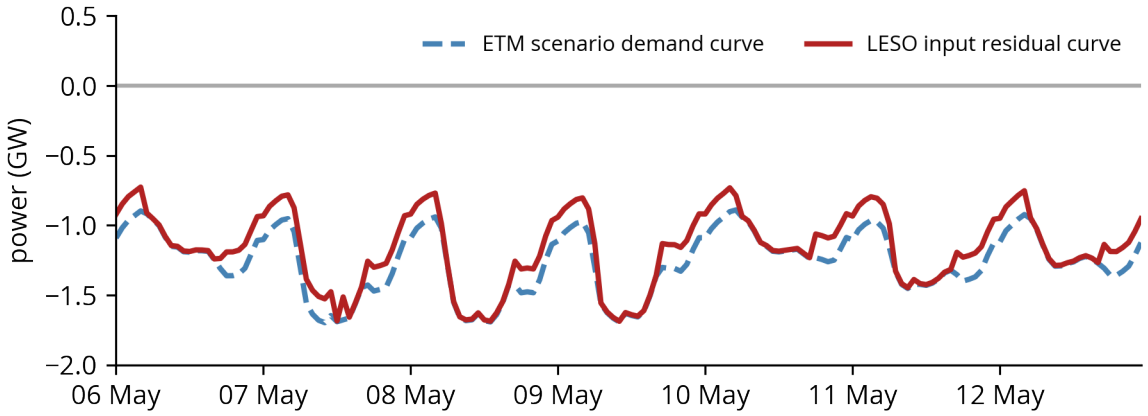

Figure 5.16: Residual and scenario demand curve for the 2030 49% reduction Gelderland scenario.

The shape of the determined residual does not necessarily match the residual curve one could imagine from looking at figure 5.15. This is because export is on of the largest demand categories, which is not included as a must-meet load. In addition, this scenario includes an already high share of renewable energy. On the other hand, the region of Gelderland does not contain any centralised dispatchable power plants in this scenario (e.g. hydrogen CCGT or CCGT with CC(U)S) other than a comparatively small waste incinerator and some decentral CHPs used for agriculture heat. By combining figure 5.15 and figure 5.16 it is possible to also observe the merit order on which the ETM solves the energy balance and unit dispatch. During hours where renewable energy production significantly outsizes the demand, observable from the high share of export in figure 5.15, it can be seen that the residual curve (red line) nearly equals the scenario demand curve (blue dashed line). This is due to the fact that the renewable dispatchable energy sources in this scenario are below the variable renewable energy sources in the merit order based on variable costs of operation and are therefore switched off.

5.6.2 Scenario-based price curves

Another capability of the ETM is to generate synthetic price curves. It does so based on resolving a merit order, which determines which generation technologies are dispatched during hours of the year. This merit order leads to dispatch based on marginal costs of technology groups. This is shown in figure 5.17. The displayed merit order is from the Climate Agreement 2030 National scenario.

This approach oversimplifies the actual electricity market due to a few reasons. First of all, all power plants based on the same generation technology are assumed to offer their capacity at the same marginal price level. In reality, such a marginal cost of operation is dependent on factors such as the location and configuration of the plant. As a result, the price level switches between the various cost of technology groups discontinuously. A real market would reach equilibrium on a significantly larger amount of marginal costs. In addition, it is based on the assumption that wind and PV power plants bid at zero marginal cost. Although this is approximately true for subsidised projects, it will no longer hold for subsidy-free projects [155].

An example of a price curve generated with the ETM is shown in figure 5.18a. The discrete switching as a result of the merit order dispatch approach can be recognised in the squareness of the original signal. As stated, this does not correctly reflect a real market, where more continuous equilibria would be reached. Therefore, it is proposed to smooth the original curve from the ETM by applying a Savitzky-Golay (savgol) filter. This is in essence a least-square error fit of a low-order polynomial

within a moving window [156]. When the points within the window are equally spaced it is possible to find an analytical solution, making this a fast algorithm even when applied to a year of hourly values. The applied window size is equivalent to a day (actually 25 hours, due to the odd number requirement) and a quintic polynomial function is fitted.

As can be seen from the detail in figure 5.18b, this smooth curve still reflects the original signal tendency very adequately while reducing the discontinuous switching contained in the original signal. The result is a continuous signal, which is illustrated by the histogram in figure 5.18c. From this figure it can be seen that the original signal has two very distinct equilibria points. Both occur for about 3000 hours per year, determining the price of electricity for a large share of the time. The first equilibrium can be explained based on the overproduction of wind and solar compared to the demand within the Netherlands, leading to a zero marginal cost for electricity. The second equilibrium is the situation in which the national renewable energy production is insufficient to meet national demand and the electricity price is determined by the marginal cost of conventional fossil plants (mostly gas CCGT) and import. The price of interconnected imports is assumed constant. It was investigated what effect a dynamic price of impact has on the national electricity price, but this was found to be neglectable.

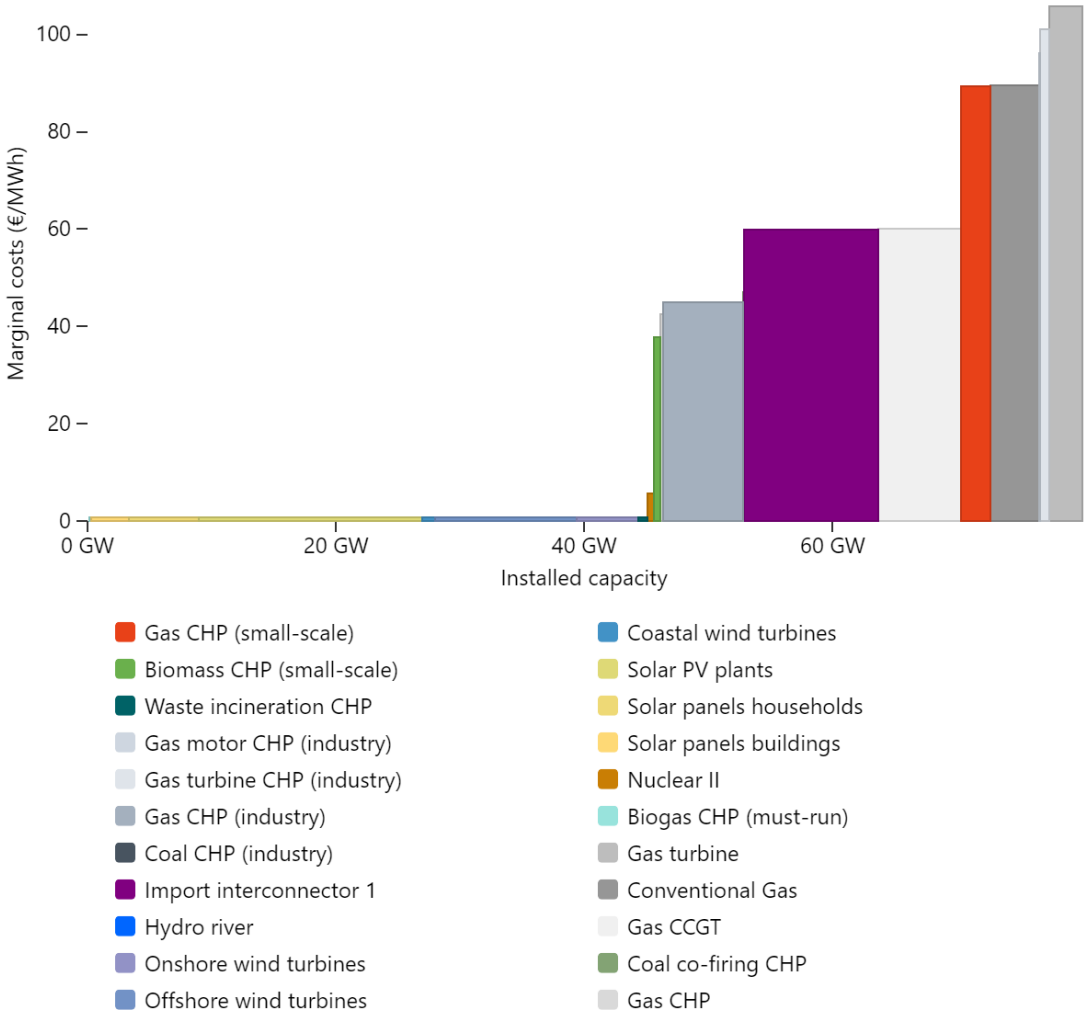

Figure 5.17: Merit order capacities and marginal costs. This figure is taken from the ETM front-end web application. This merit order determines unit dispatch based on the marginal cost and installed capacities of technology groups.

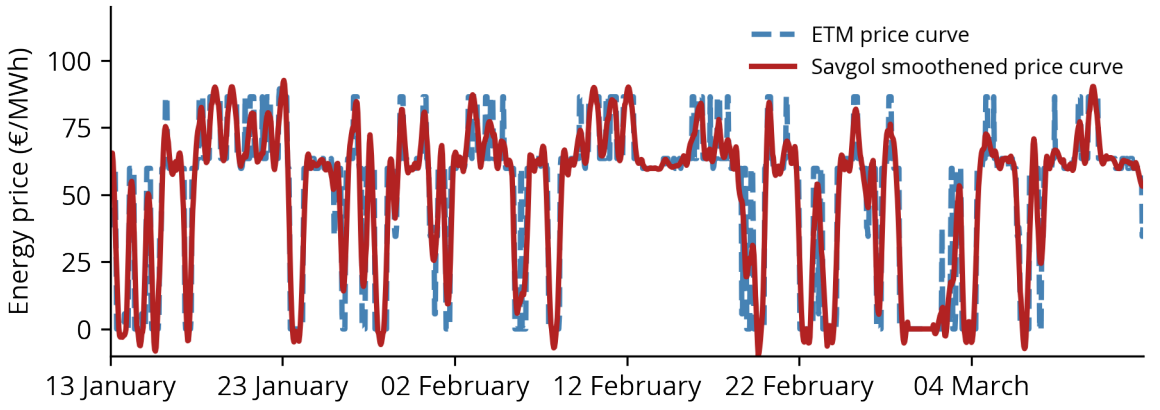

(a) 60 day snippet of the (filtered) ETM price curve

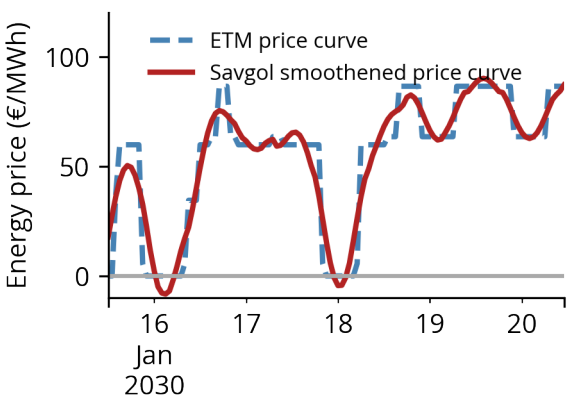

(b) Detail of the (filtered) ETM price curve

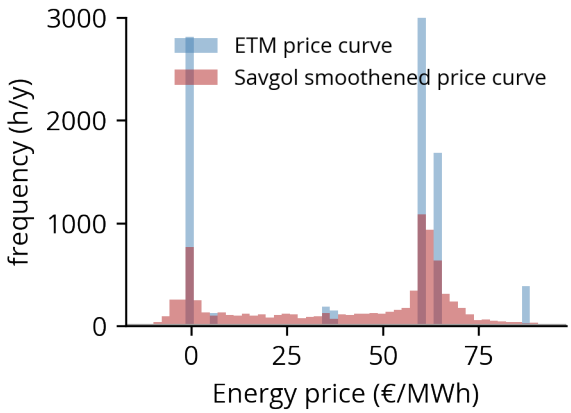

(c) Histogram of the (filtered) ETM price curve

Figure 5.18: Wind model based on PVGIS wind data validation against renewables.ninja wind model

5.7 Conclusion

In this chapter, the key steps, mathematical formulation and data sources used for modelling the components within the scope of the LESO were introduced.

Three sources have been integrated within the framework that allow for automatic retrieval of location specific historical meteorological time series, namely PVGIS, DOWA and renewables.ninja. Relevant information from the meteorological time series is fed to the feed-in power models.

The photovoltaic component uses global, normal beam, and horizontal diffuse irradiance to determine the irradiance on the plane-of-array. This is subsequently converted to power output by applying a conversion efficiency factor. Assessment of the cost development of photovoltaics reveals that investment cost could drop to as low as 260 €$/kWp$ by 2050, a reduction of 75% compared to the reference year 2015. Studies do reveal a large range of uncertainty.

The wind component is based on the wind speed, the pressure, temperature and relative humidity. Wind speed is extrapolated to the hub height using the logarithmic law. Using the power curve of the specified turbine type the wind speed is converted into electrical power. Cost projections show a smaller range of improvement when compared to photovoltaics. Still, costs are projected to drop to 900 €$/kW$ by 2050, a reduction of 33% compared to the reference year 2015.

Storage components are modelled using recursive equations that account for (dis)-charging and self-discharge losses. Lithium will very likely become the most cost-effective storage solution for intraday balancing, while hydrogen is most the cost-effective solution for seasonal storage, according to projections. Both components can be configured in various storage duration by setting the energy-to-power ratio. Lithium storage cost are expected to reduce by about 75%, while hydrogen storage cost might reduce by as much as 87%. Both lithium and hydrogen cost display a wide range of uncertainty.

The electrical demand curve resulting from fast charger infrastructure was introduced, which is formulated based on stochastically sampled traffic data.

Finally, the ETM component in LESO was covered in detail. This relates to research question 3.1: *How can the optimisation model be coupled to existing models to reflect the effect of (inter)national energy policies?* In chapter 3, it was concluded that coupling to the ETM and to the available energy scenarios was desirable. In this chapter, the method for coupling was introduced. Scenarios that reflect possible future energy systems that result from diverse energy policies are constructed in the ETM. These can subsequently be used in LESO to generate regional load curves that reflect the regional demand under certain assumptions on (inter)national energy policy such as the CNES. In addition, this component can be used to construct a synthetic price profile based on national models of the Dutch energy system.

Chapter 6

Methodology

This chapter covers the methodology that is applied in the case studies to discover cost-optimal energy systems configuration under uncertainty. In the case studies, LESO is implemented to explore the effect of cost uncertainty on optimal configurations for various energy systems. Because the case studies have distinctly different energy systems configuration of the model is relevant and covered in section 6.1.

Parametric uncertainty exploration is applied based on the projected respective technology cost ranges. Each uniquely configured model is referred to as an experiment. Many experiments are obtained by sampling the uncertain parameters and policy levers (e.g. renewability targets, maximum allowed grid connectivity or subsidy schemes). The terms used to describe parameters and methods in parametric uncertainty exploration are consistent with the nomenclature used in EMA. As such, section 6.2 describes how uncertainty sampling is applied in the case studies. Section 6.3 covers how policy levers are implemented in the parametric experiments.

Section 6.4 reveals the implementation of policy levers and uncertainties to produce an attributable set of experiments per case study. To close this chapter, section 6.5 presents a clear overview of the case studies and their corresponding chapters.

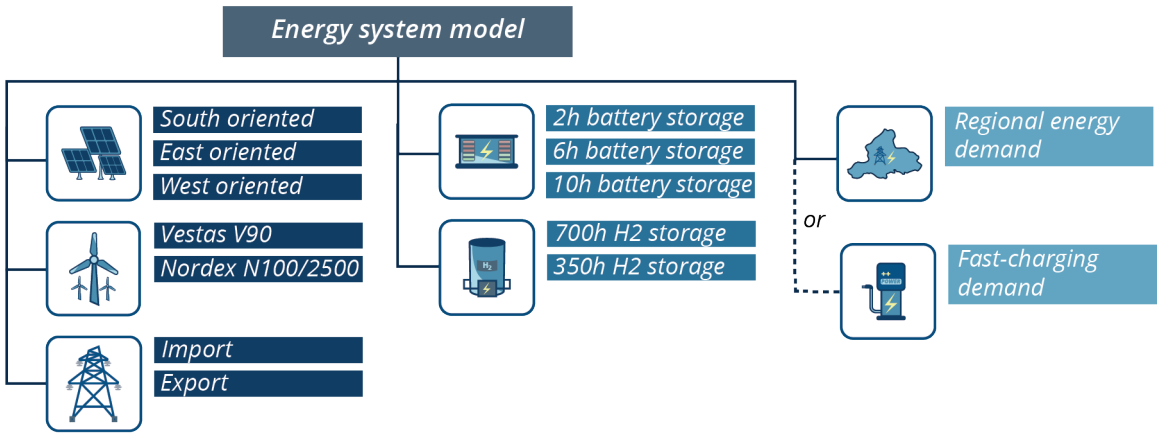

Figure 6.1: Diagram of a configured energy system model

6.1 Initial model configuration

The LESO energy systems model is set up in a similar manner throughout the various case studies. That is to say, the components that the optimisation algorithm has to determine the optimal amount of deployment for, are defined as a set of standard configured components. This allows for comparison between the various optimisation results, due to the uniform model set-up. A graphical representation of the initial model configuration is shown in figure 6.1 and is discussed in more detail in the remainder of this section.

6.1.1 Components

Source components — Three distinct solar PV configurations are considered. All of these configurations are set at a tilt of 37 degrees. The azimuth is set to varying angles to produce East, South and West oriented arrays (see section 5.2). These configurations are based on the mounting strategies used by the industry for open-field projects and large scale rooftop projects. They are thus assumed to sufficiently reflect the possible production curves to consider.

The wind component is included in only one specific configuration. The wind turbine type used in this configuration is the Vestas V-90. This turbine type has been deployed throughout the Netherlands and falls within the medium-medium category as discussed in section 5.3.3. This turbine has a hub height of 80 metres. Although the power capacities of modern turbines are trending towards greater capacities, this trend is mostly relevant for offshore wind farms. Onshore wind turbines are more constrained, due to the landscape disruption and, resulting from that, civil resistance, which is a topic in itself [157]. To refrain from such political and social concerns, the Vestas V-90 is applied, arguably the best reflection of the current industry standard in the Netherlands.

Both the wind and solar components are configured to use renewables.ninja as data source since this allows for the selection of a single historical year. The selected year is 2015. This is in line with the default meteorological data used by the ETM. As a result, the relationship between e.g. temperature and heat demand, irradiance or wind speed and power production are kept aligned.

Storage components — Lithium-based storage is included in three distinct storage duration configurations. This yields a set of 2, 6 and 10-hour storage duration lithium batteries.

Hydrogen-based storage is configured in two variants in terms of storage duration. A 700-hour storage duration hydrogen component reflects seasonal storage, while sub-seasonal storage is based on a 350-hour storage duration. Whether hydrogen is included in the model depends on the scope of the study.

Sink components — The grid component is always included as a part of the energy system model, as all case studies are connected to the electricity grid. The installed capacity of the grid components depends on the context of the case study. In the Gelderland studies, the grid capacity is based on the current transformer capacity between the regional distribution net and the high-voltage (150 kV) transportation infrastructure. The ETM is used to determine this value by querying this value from its corresponding data-model; the etsource [158]. This procedure is carried for every region under analysis.

The regional demand component is included in all studies on Gelderland, as well as its RES regions. It is configured such that the API connection to the corresponding scenario is triggered whenever the load curve or other relevant parameters are queried from the ETM. The specific scenarios used are listed in their respective chapters and sections. All regional ETM scenarios used in these sections are a result of the very recent system study on Gelderland [17].

Finally, the fast-charging demand component is included in only one study and is discussed in the respective section.

6.1.2 Electricity price curves

National scale ETM scenarios are used to determine the energy market price curves used in the grid component. The method applied to obtain and process these curves is discussed in detail in section 5.6.2. Using an ETM model on a national scale, the corresponding price curve results from the marginal costs of energy generation corresponding to the conditions of a future Dutch energy system if current policies remain in place. This is thus a suitable method to represent a synthetic price curve that acts as an exogenous factor on the energy systems under study in these case studies.

For studies in 2030, this is based on the ETM scenario constructed by Kalavasta [159], which in turn is based on the National Energy Report and Climate and Energy Report [9] [10]. In this scenario, the electricity mix is 74% renewable, based on projections of current policies. Three model settings have been changed, however. This is the fuel cost of natural gas, the carbon price and the free allocation setting for carbon emission rights. Natural gas is set to $40€/MWh$ in line with the most recent EU reference scenario projection for 2030 [160]. It should be noted that the current gas market is highly volatile as the price for natural gas contracts is $90€/MWh$ at the moment of writing. The Emissions Trading System (ETS) carbon price is assumed at $85€/tonne$, which is based on more recent and opinionated projections [161]. Free allocation of carbon rights is set at 0%, in line with current European policy for the electricity sector.

For studies in 2050, this is based on the ETM scenario constructed by Kalavasta [159], which in turn is based on the National Energy Report and National Climate Agreement [10] [9]. For the case studies in 2050, the national model used is one of the four II3050 scenarios as composed

by Kalavasta and Berenschot [27], depending on the specific case study. These scenarios have subsequently been extended and detailed by NetbeheerNL as part of the integral infrastructure study phases 2&3 [30] [162]. See section 2.2.2 for more details on the integration studies.

6.2 Uncertainty sampling: technology cost development

In this thesis, the uncertainty that has been addressed is the cost development of various technologies. For case studies on which the static approach is applied, component cost settings are based on the centre values (or mean, moderate or reference depending on the nomenclature of the source used) of the cost development projections. The cost development is discussed in detail in chapter 5, in each respective subsection. The static method is used in this thesis to validate and compare the aggregation of the RES regions in Gelderland to the province of Gelderland as a whole.

As discussed in section 4.3.2 and 4.3.3, the optimisation algorithms implemented in LESO are designed to solve various tipping points and trade-offs between the considered technologies. Insight into those tipping points and trade-offs is achieved by sampling the uncertainty range of all involved technologies. As a result, many uniquely configured optimisation variants of the same energy system are acquired. LESO is integrated into EMA to apply Latin hypercube sampling on uncertainties. This statistical method generates a set of random samples of the multi-dimensional uncertainty space that ensures a good representation of the original space, unlike typical random sampling. This sampling approach is more efficient than generating a full factorial which is exponential with the dimensions of the sampling space.

6.3 Policy sampling: model exogenous factors and boundary conditions

Policy levers are parameters that could possibly impact the outcome of the experiment but are not inherently uncertain but rather deterministic of nature. That is to say, these parameters reveal the outcome of a specifically determined configuration if actions were taken to reach that configuration. This implies that only parameters which can in totality be controlled through policies, actions or processes qualify as a policy lever. Examples of policy levers include features such as the application of an energy subsidy, extended grid capacity at a certain location or maximum/minimum allowed ratio of wind-to-solar. Design parameters or exogenous factors can also be sampled in a discrete manner to investigate the sensitivity of outcomes to a prescribed change in those parameters.

6.4 Experiments

To produce a set of parametric experiments both the uncertainties and policies are sampled. The total number of experiments is the product of the number of samples over the uncertainties and the number of policies to be investigated. The set of samples that defines the uncertainties are exactly the same for all policy variants. Otherwise, it would not be possible to assess the effect of the policies separately over the same set of uncertainties.

In practice, if 100 samples are taken from the uncertainty space in combination with a set of six policies, a total of 600 experiments need to be solved. This means 600 model configurations that each

produce an optimisation problem accordingly and each yielding a possible energy system configuration that is cost-optimal under those assumptions.

By applying (statistical) analysis on the results of the experiments, insight is obtained into how the configuration of cost-optimal future energy systems depend on the cost development of solar, wind, lithium and hydrogen storage. In addition, the effect of policies levers and exogenous model factors can be addressed separately.

6.5 Case studies overview

To conclude this chapter, an overview of all case studies is given. The case studies are split up into three main chapters to better distinguish between the studies. In each chapter, the specific model configuration and uncertainties are discussed before results are introduced and subsequently analysed. The case studies are ordered in increasing complexity.

- Local energy projects (chapter 7)
  - Cable pooling Nijmegen
    The first case study covers a cable pooling project. In this study, the cost-optimal configuration of solar PV and battery storage is determined based on wind turbines' installed capacity and grid capacity. Therefore, this study considers two design variables and two technology cost uncertainties. Moreover, there is no load component in this situation so that no additional complexity is introduced through a demand profile.
  - Electric mobility hub Deventer
    In the second case study, a fast-charging location near a highway close to Deventer is investigated. Based on traffic data, a demand profile is introduced. Under varying grid capacities, the optimal deployment of wind turbines, solar PV and battery storage is determined. Therefore, this case considers three design variables and respective technology capacity costs.
- Gelderland 2030 (chapter 8)
  - Renewable energy strategy regions
    In first part of this chapter, the renewable energy regions within the province of Gelderland are optimised in terms of deployment of wind turbines, solar PV, battery storage and hydrogen storage. In the first part of this chapter, the optimal configuration is determined based on the centre values of the projected cost ranges for each region. The same procedure is followed for the whole province of Gelderland. The result of the individual regions is aggregated and compared to the result of Gelderland as a whole. The following regions are located within Gelderland.
    - Achterhoek
    - Arnhem-Nijmegen
    - Cleantech
    - Foodvalley
    - Noordveluwe
    - Rivierenland
  - Province Gelderland
    In the second part of this chapter, the optimal system configuration for Gelderland in 2030 is determined based on the same four technologies. In addition to the first part, uncertainty

is introduced. Moreover, the optimisation model is further constrained by introducing renewability targets. Therefore, this section considers four technologies both in uncertainty and deployment.

- Gelderland 2050 (chapter 9) *To obtain insight into the future demand development within the region of Gelderland, the optimal configuration of the same four technologies as in the previous chapter is determined. Again, parametric uncertainty exploration is applied, but, this time the cost ranges are based on projections for 2050. Moreover, the optimisation model is constrained to generate only fully renewable energy systems. Four distinct scenarios are introduced that impact the demand for electricity. These are the same scenarios as used throughout the Dutch energy transition policies. By determining cost-optimal configurations for Gelderland in 2050, a view into the future is preserved. This can be used to validate whether the current policies are part of the no-regret investments needed to achieve a cost-optimal fully renewable power system in 2050.*
  - II3050 - Regional
  - II3050 - National
  - II3050 - European
  - II3050 - International

Chapter 7

Local energy projects optimisation

In this chapter, LESO is applied to study two local energy projects. Both studies are relevant to the bigger picture of the energy transition.

As stated in the chapter 4, LESO is not designed to calculate grid loads or optimise renewables' integration into existing infrastructure. Instead, this is reflected in energy system models as boundary conditions and thus an exogenous factor to the model. However, various parts of the Dutch grid infrastructure are becoming congested, thus preventing the development renewable energy projects.

In section 7.1, a possible solution direction is studied. This is the concept of cable pooling, where both solar PV and wind generation utilise the same grid connection. The concept is technically validated and recent amendments to the Dutch energy law introduce supporting legislation. In the case study on cable pooling, the concept is tested by applying cost-optimisation under uncertainty and varying context.

The scope of LESO is currently limited to the electricity sector. Other sectors are not modelled in LESO but in the ETM, to which LESO is coupled. However, considering that the transport sector is expected to electrify in the near future, it is relevant to address the possible forthcoming challenges. LESO can be used to generate insights for this topic by determining an expected demand profile as discussed in section 5.5.

In section 7.2, the possibility of meeting electricity demand emanating from fast-charger infrastructure through local energy generation in grid-constrained locations is assessed by investigation of an electric mobility hub. The cost-optimal configuration of a dependable energy system is evaluated under varying levels of grid connectivity and uncertainties regarding the cost level of technologies.

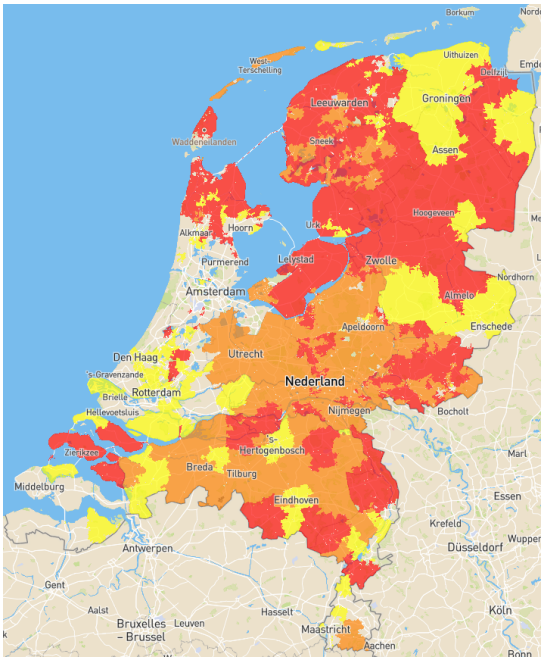

Figure 7.1: Visualisation of the current grid congestion challenges faced by grid operators and, subsequently, energy project developers. This map shows the congestion for delivery to the grid. Red means structural congestion and new permits for connecting energy projects are handed out. Orange and yellow indicated congestion to a lesser degree but still indicate the possibility of permit constraints due to grid congestion. [164]

7.1 Cable pooling

Grid operators are required by law to guarantee transport capacity when offering a grid connection point to a client [163]. This guarantee should also be upheld during the peak production of such an asset. If this guarantee can no longer be kept, grid operators have to imply a regime on the issue of new grid connection points for energy projects. When fossil dispatchable plants were the main energy source, this legislation did not necessarily lead to pressing issues. However, energy generation based on intermittent sources of renewable energy is highly volatile. I.e. the capacity factor is substantially lower, leading to short and high loads at peak power output. Replacing the current centralised fossil dispatchable generation assets with renewable energy plants has therefore led to an increasing demand on the grid transport capacity. As a result, project developers working on renewable projects already experience difficulty securing a grid connection. Between the various grid operators, there is a consensus that this situation is expected to become increasingly restrictive for new projects. The current situation with regards to the scarcity of possible locations for energy projects is illustrated in figure 7.1.

Now, because the Dutch National Climate Agreement specifies a certain share of the Dutch electricity mix to be completely renewable [8], grid operators are experiencing a very rapid influx of renewable energy projects on their infrastructure. On the long term, this project pipe-line is expected to be sustained by the enactment on the Regional Energy Stategies [30]. As a result, grid operators have alarmed national politics and regional policymakers that they cannot serve the needs of this sustained influx of renewable energy projects in terms of grid connection [165]. They state that they are able to serve only 35 TWh of renewable energy generation of the 55 TWh of renewable energy that is proposed across all RES regions [166].

There is an inherent conflict between the renewable energy goals captured in the RES and the transport capacity guarantee that grid operators have to offer. One is based solely on volume, while the latter is primarily concerned with peak power loads. It is crucial to overcome this barrier to reach the climate goals and renewable energy goals. This study investigates a concept known as cable pooling. From interviews with experts at grid operators (TenneT, Liander and Enexis) it can be concluded that they regard this concept as vital to cost-effectively reach high shares of renewable energy within a reasonable time span. Cable pooling is based on the combination of two energy generating assets that utilise the same grid connection point and thus pool their grid connection resource. Typically, this was done by combining wind and solar power plants, due to the fact that these technologies are anti-correlated in terms of the temporal relation in peak production [167]. A graphical representation of this concept is shown in figure 7.2.

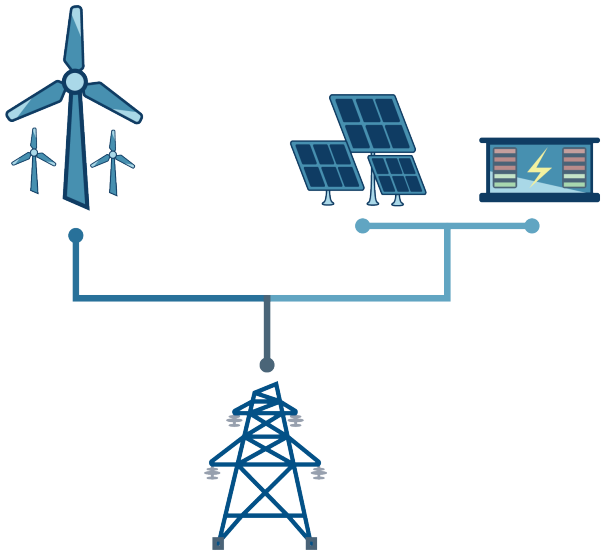

Figure 7.2: Abstract representation of cable pooling. The energy assets can be owned by the same developer, but recently passed legislation also allows multiple parties to pool on the same client station.

The branch organisation of the Dutch grid operators has already investigated the technical potential of cable pooling. They found cable pooling of renewable energy projects could increase the capacity factor of existing grid connections from 10% to as high as 42%, depending on the exact configuration of wind and solar components [168]. The first steps in putting in place the necessary enabling legislation have been taken by passing an amendment on the Dutch electricity law, allowing multiple parties to cooperate to increase the utilisation of a shared grid connection [169].

This section investigates the cost-optimal configurations of cable pooled centralised energy generation projects. This should reveal under what conditions - in terms of technology cost and applicable policies and context - cable pooling is sensible. In this optimisation study, a variety of solar PV and lithium battery energy storage configurations are considered. Results should reveal the effect of various cost developments on the viability of cable pooling.

7.1.1 Case description

This local energy project is loosely based on an existing centralised energy project in the RES region of Arnhem Nijmegen. It is a wind park called Nijmegen-Betuwe, which is a citizens' initiative and is owned by the local community. Currently, 4 Lagerwey L100 wind turbines of each 2.5 MW are readily feeding renewable energy to the grid but recently the initiative has announced that an additional 5 MW of solar PV will be connected on the same grid connection. The initiative states that an essential step was securing the SDE++ subsidy because it would otherwise not be possible to generate profit. Although cable pooling is known to lead to curtailment, the project initiative reports that using battery storage is not an economically viable option [170]. These two statements are evaluated in this case study, as well as the optimal amount of solar power to deploy, through optimisation under cost uncertainty.

In this study, a stylised representation of the wind park Nijmegen-Betuwe is considered. To this end, both a wind and grid component with a fixed installed capacity of 10 MW were included in the energy system model. The wind component bases its feed-in profile on the power curve of the Nordex N100 2.5 MW, which was the best matching turbine available. It has the same hub height and power rating as the original Lagerwey L100 and similar cut-in and cut-out speeds. Solar PV with a fixed tilt of 37 degrees is included in the model in three configurations based on varying orientations, namely South, East and West. Energy storage is included in the energy system by introducing three battery storage systems with a 4, 6 and 10-hour storage duration. The installed capacities of PV and lithium components are a parameter optimised by the optimisation algorithm. As such, it will determine the cost-optimal deployment of those technologies in the context of the existing wind capacity and grid capacity. An overview of the energy system and associated variables is given in table 7.1.

Table 7.1: Optimization set-up for the cable pooling case study.

Component	Configurations	Installed capacity
PV	South	*optimisation variable*
	East	*optimisation variable*
	West	*optimisation variable*
Battery storage	2 hours storage duration	*optimisation variable*
	6 hours storage duration	*optimisation variable*
	10 hours storage duration	*optimisation variable*
Grid capacity		10 MW
Wind	Nordex N100/2500	10 MW

7.1.2 Parametric uncertainty exploration

In order to investigate whether cable pooling will be a viable solution, cost projections of the included technologies are sampled. Since cable pooling is recognised as a solution that should offer relief on grid constraints within a reasonable time frame, cost projections up until 2030 are implemented in this study. Accordingly, the electricity price curve that was included in all models is based on a National ETM model for 2030. The method for deriving the curve is covered in depth in section 5.6.2. Assumptions specifically corresponding to the price profile in 2030 are introduced in section 6.1.2 The cost ranges for solar PV and lithium storage are presented in table 7.2. For lithium storage, only the energy capacity cost projection is sampled. The power capacity cost is linearly mapped to this sampling, based on the projection range corresponding to this variable.

Table 7.2: Uncertainties sampled in the cable pooling parametric uncertainty exploration

Component	Sampled parameters	Method	Cost range			Unit
PV	Capacity cost	LHS	388	-	867	€/kW
Lithium storage	Energy cost	LHS	114	-	194	€/kWh
	Power cost	*linear map*	108	-	208	€/kW

Other than the uncertainties, a set of policies was introduced in this study. These are listed below.

- **Policy 1 - Fixed-support subsidy**
  For current renewable energy generation plants, the Dutch government gives out fixed-fee subsidies through the Rijksoverheid voor Ondernemend Nederland (RVO) subsidy scheme "Stimulering Duurzame Energie" (SDE). This subsidy acts as a guarantee for investors and aims to attract capital investment for renewable energy projects. The subsidy is fixed-fee, which means that RVO makes up for the difference between the energy price on the market and the granted feed-in tariff. This form of subsidy has proven to be cost-effective, as it is only spent on actual renewable energy generated and not on installed capacity [155].

  In this policy, a stylised representation of a fixed-support subsidy on renewable energy is applied. This is done by setting a minimum value in the electricity price curve. The minimum value used on the price curve is therefore the height of the fixed-support subsidy. This is set at 28 €$/MWh$, which is roughly based on the 2022 SDE++ base fee and the corresponding correction factor projected on 2030 [171] [172]. It should be noted that this is not necessarily a realistic projection or probable value for the SDE++ in 2030 and should not be treated as such. Rather, it forms a stylised representation of the effect of such a fixed-support subsidy.
- **Policy 2 - No subsidy**
  This policy uses the same electricity curve but without the artificial minimum value that is induced by the fixed-support. This policy can be used to determine the effect of a fixed-support subsidy by comparing to the fixed-support subsidy policy. In addition, it can be used to determine the component cost level needed to support a subsidy-free business case for placing additional solar generation capacity on existing wind farms.
- **Policy 3 - Marked-down battery cost**
  This third policy was added later, after finding that the optimisation algorithm would not deploy battery storage under any of the sampled conditions. Policy is based on the first policy and has the same fixed-support subsidy in place. In the current case setup, the added value of storage is only to time-shift the production of the assets. As such, it can be used to store otherwise curtailed renewable energy to release at a later moment in time when there is either a better electricity price or when there is available grid capacity. This battery storage use case is called portfolio optimisation, as the only mode of operation is optimal dispatch of the projects generation portfolio.

  There are other substantial sources of income that can be generated by battery storage through ancillary services. These include day-ahead and intra-day energy arbitrage, i.e. trading on the energy market, frequency containment and restoration reserves, and congestion management on the new market platform GOPACS [173]. These sources of income are not included in this case setup. This gap between the realistic cost projection and the artificially marked-down cost should be interpreted as the necessary income generated by those income-generating activities other than the considered portfolio optimisation. The range of battery capacity cost that is sampled in this policy is shown in table 7.3. The remaining parameters are implemented as described in section 7.1.1.

Table 7.3: Marked down cost uncertainties sampled in policy 3

Component	Sampled parameters	Method	Cost range	Unit
Lithium storage	Energy cost	LHS	28 - 114	€/kWh
	Power cost	*linear map*	26 - 105	€/kW

Per policy, 200 samples were taken from the space spanned by the two cost uncertainties. This results in a total of 600 optimisation problems to be solved. In order to maintain the digestibility of these results, each set of results are first presented in a section according to each of the policies. Conclusions on the effect of policies and the sensitivity of the optimal solutions to cost uncertainties are formulated in section 7.1.6

7.1.3 Results policy 1 - Fixed-support subsidy

This section discusses the results that are generated by using a fixed-support subsidy on the cable pooling model. Due to the dimensionality of the results obtained through solving many iterations of the optimisation model over various dimensions of uncertainty, various plots were made and analysed to obtain insight. Key results are presented in this section.

Figure 7.3 displays all sampled uncertainties in the plane. This is the capacity cost for PV on the x-axis and the capacity cost for battery storage on the y-axis. Note that the cost of batteries is shown as power cost, although the optimisation variable is energy capacity. This is because the various battery configurations have a different cost of energy capacity in function of the storage duration - batteries configured to have a longer storage duration have a relatively lower cost per MWh. To reduce dimensionality, only the power cost component is used in plotting. The size and colour of the points in this scatter plot show the deployed capacity of PV. From the figure, it can be concluded that the deployment of PV is only related to the cost of PV. This is explained by the fact that over all sampled cost uncertainties in this policy, no deployment of battery storage occurred.

Figure 7.4 is used to display the relationship between the capacity cost of PV and the amount of PV capacity deployed by the optimisation algorithm. From this figure, it can be noted that when capacity costs of PV are below 720 €$/kWp$, it becomes viable to deploy PV capacity concurrent to the existing 10 MW wind capacity. When moving from right to left in the figure, thus from high to low cost, it can be noted that the angle of deployment is first very steep until roughly 10 MW of PV is deployed. After this point, the rate of deployment as a function of a further decreasing capacity cost progressively decreases. From this, two conclusions can be put forth. Firstly, at a fixed-fee subsidy of 28 €$/MWh$ capacity cost of PV should reach below 720 €$/kWp$ to become cost-competitive. Secondly, the ratio of solar to wind matters. Up until equal ratios of solar PV and wind, the deployment as function of solar PV capacity cost is very rapid. After reaching this equal ratio, deployment relative to PV cost reduction shows a notable reduction in PV deployment. From this same figure, it can also be noted that curtailment rapidly increases when the ratio of solar to wind reaches above 100%.

In order to further investigate the importance of the ratio between wind and solar when cable pooling, figure 7.5 was created. In both plots, a smooth line can be seen. This is not based on a theoretical relation, but is the result of the curtailment determined by the algorithm on various deployed capacities. Each of those capacities is in turn a result of optimisation for the sampled uncertainties. The relation between curtailment and total deployed capacity shows a shallow increase until a total deploy capacity of about 20 MW and a very steep increase for all capacities above that. The relation seems quadratic in the first region and additionally becomes exponential in the second region.

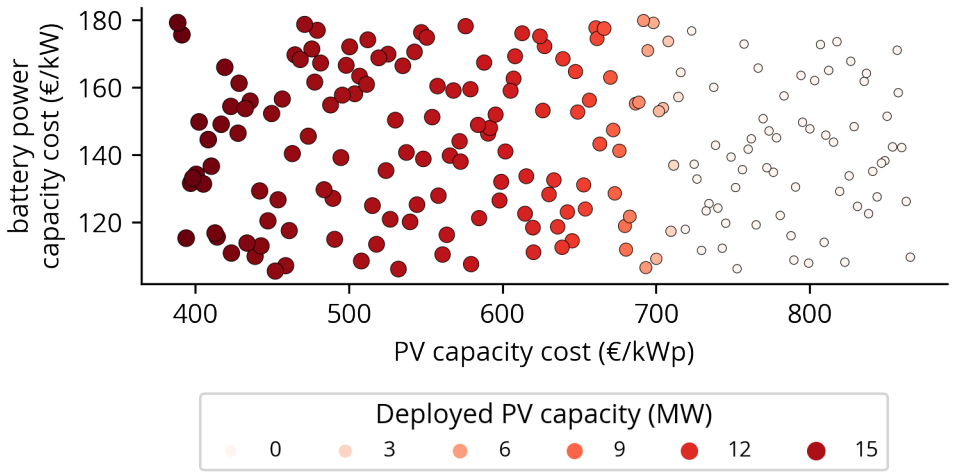

Figure 7.3: Deployment of PV plotted against the sampled uncertainties.

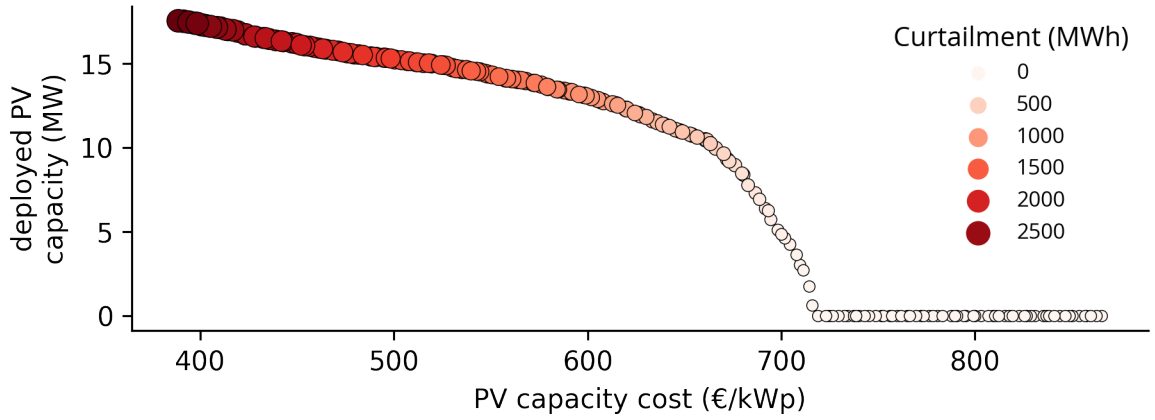

Figure 7.4: Cost-optimal PV deployment found by the optimisation algorithm and curtailment as a function of the sampled uncertain PV capacity cost.

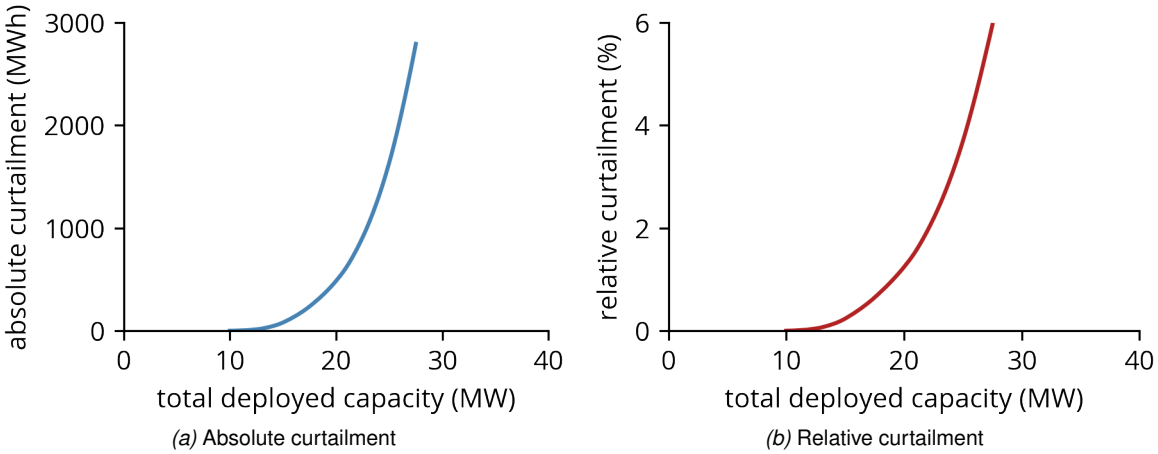

(a) Absolute curtailment *(b)* Relative curtailment

Figure 7.5: Curtailment as function of to the total deployed generation capacity.

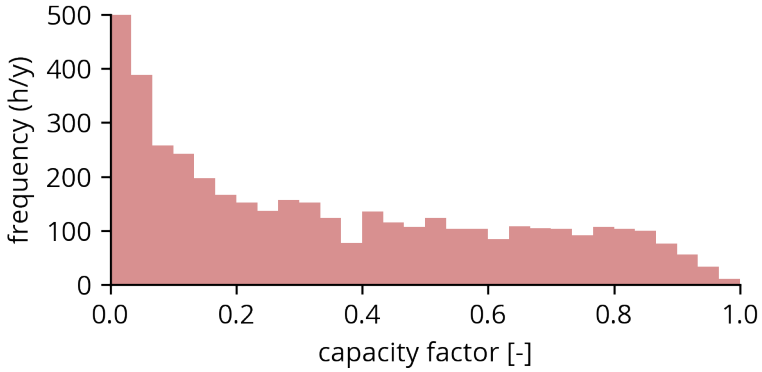

Figure 7.6: Histogram $n_{bins} = 30$ of the capacity factor of solar PV. Note that the sum of frequencies does not equal a year. For readability, the bin with the capacity factors closest to zero is cropped by imposing a y-limit. This lowest bin actually contains more than 4000 hours.

Two mechanisms are expected to drive the identified regions of curtailment. Below 100% solar-to-wind ratio, curtailment is driven completely by coinciding production by wind and solar. Whenever the feed-in power of wind and solar together is above the grid capacity, curtailment will occur. In the second region, where the solar-to-wind ratio is above 100%, curtailment is driven by the aforementioned effect and, additionally, clipping losses will occur. Clipping losses occur whenever the power output of the energy project is larger than the rated capacity of the grid connection point. The effect of clipping losses on total curtailment as a function of the total deployed capacity shows an exponential relation. This is a result of the frequency distribution of the capacity factor typical for PV. The highest capacity factors occur substantially less frequent when compared to lower capacity factors, as shown in figure 7.6 As a result, the total energy lost to curtailment increases rapidly.

7.1.4 Results policy 2 - No subsidy

In this section, the results from the second policy are presented. This policy has a different electricity price curve when compared to the first policy since the fixed-support subsidy is no longer in place. As a result, the electricity price curve contains many hours where the price is at or below 0 €$/MWh$. This decreases the profitability of generation assets substantially. As in the first policy, the sampled uncertainty space for battery cost did not include low enough values to allow for battery placement.

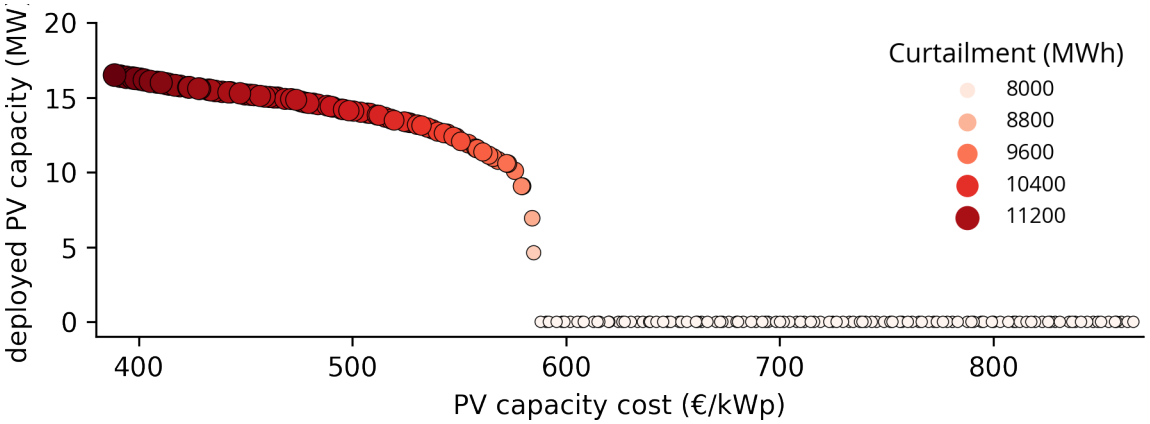

Figure 7.7: Deployment of PV and corresponding curtailment as a function of PV capacity cost without fixed-support subsidy

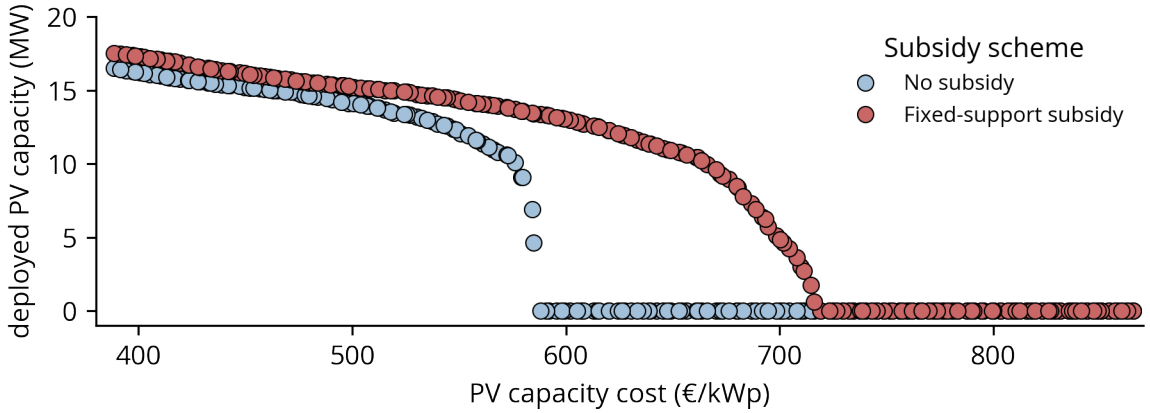

Figure 7.8: Comparison of PV deployment, with and without fixed-support subsidy

Therefore, the deployment of PV is only related to the PV capacity cost, which is shown in figure 7.7. From this figure, it can be concluded that viable implementation of PV in a cable pooling configuration starts when the capacity cost is lower than 585 €$/kWp$. This is substantially lower when compared to the first policy. In figure 7.8, this difference is depicted. The rate of deployment without subsidy is substantially steeper initially. Both policies seem to converge to the same rate of deployment as a function of the capacity cost and reach nearly the same maximum deployment of PV at the lowest capacity cost.

Electricity prices with values at or below zero has another effect. The levels of curtailment have increased substantially, even before additional PV capacity is placed. This is a result of the optimisation algorithm choosing rather to curtail the energy than to feed it to the grid at negative or zero return. The absolute curtailment follows a different pattern than the curtailment found in the first policy, as shown in figure 7.9a. This time, an additional mechanism drives curtailment, namely the occurrence of zero or negative energy prices concurrent with PV production. As a result, the initial range of curtailment below 20 MW shows a nearly linear relation between deployed capacity and absolute curtailment.

Interestingly, the relative curtailment (fig. 7.9b) first decreases when the solar-to-wind ratio is below one. Minimal relative curtailment is calculated to occur at 110% solar installed capacity relative to

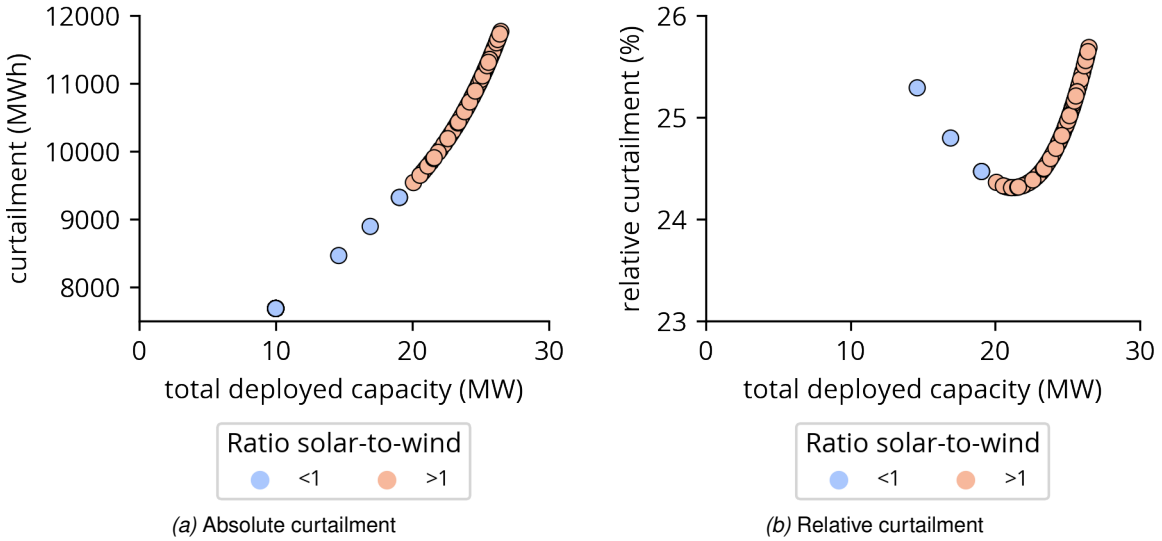

(a) Absolute curtailment

(b) Relative curtailment

Figure 7.9: Curtailment as a function of total deployed generation capacity.

wind capacity. The initial reduction of relative curtailment can be explained through the PV production curve which shows a lower correlation to hours with negative or zero prices for electricity in the price curve used. This is because the price curve is based on a national ETM model that reflects the Dutch national energy system in 2030 if current policies proceed. In this scenario, PV produces a total of 83 PJ in the energy mix while wind produces 265 PJ. As a result, prices are more often near or below zero when wind produces energy then when PV produces energy.

7.1.5 Results policy 3 - Marked-down battery cost

In this section the results of the third policy are discussed. In this final policy, the lower limit of the battery costs has been decreased far beyond what can realistically be expected by 2030. The upper limit of the battery cost range coincides with the lower limit of the realistic range for 2030. This decrease in battery cost was included to be able to find the tipping point for battery deployment and to assess the corresponding deployment dynamics. In all results, it was found that the optimisation algorithm only deploys battery storage configured to have a duration of 6 hours. Results are therefore plotted against the cost per MWh for a 6-hour battery.

Figure 7.10 shows the deployment of both PV and battery over all the sampled points in the uncertainty space. Contrary to the same visualisation for the first policy (fig. 7.3), in this policy both the deployment of PV and of battery is correlated to both axes spanning the uncertainty space. By observing this correlation to both axes, it can be concluded that some synergy exists between the battery storage deployment and PV deployment. It is fair to assume that this is a result of the temporal shifting that is possible using battery storage. As a result, peak production moments can be stored and later released when production no longer exceeds grid capacity. This allows for a higher deployed capacity of PV.

When looking at figure 7.10b, it can be noted that battery deployment is dependent on the capacity cost of PV. The highest deployed capacities of battery storage can be found in the lower-left corner of the figure, where both PV and battery storage are in the lowest range of the cost uncertainties. From this, it can be concluded that the low cost of PV is a qualifying factor for the substantial deployment

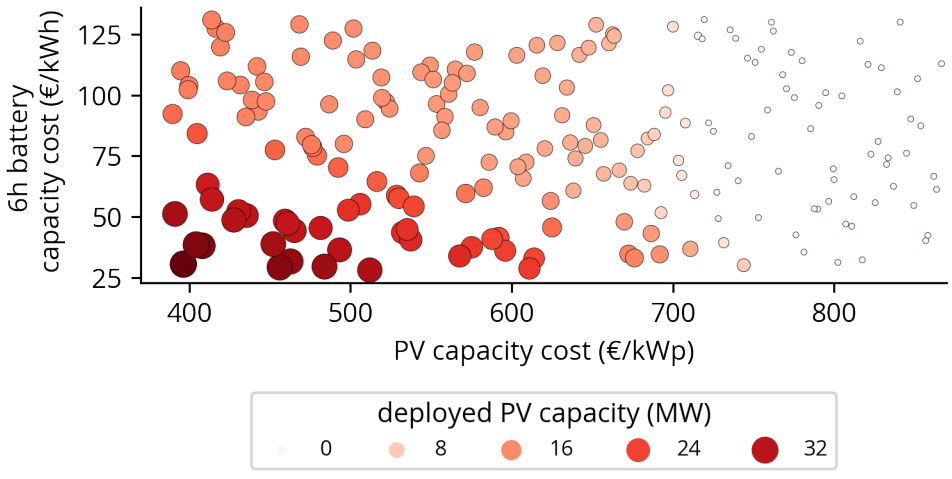

(a) Deployment of PV

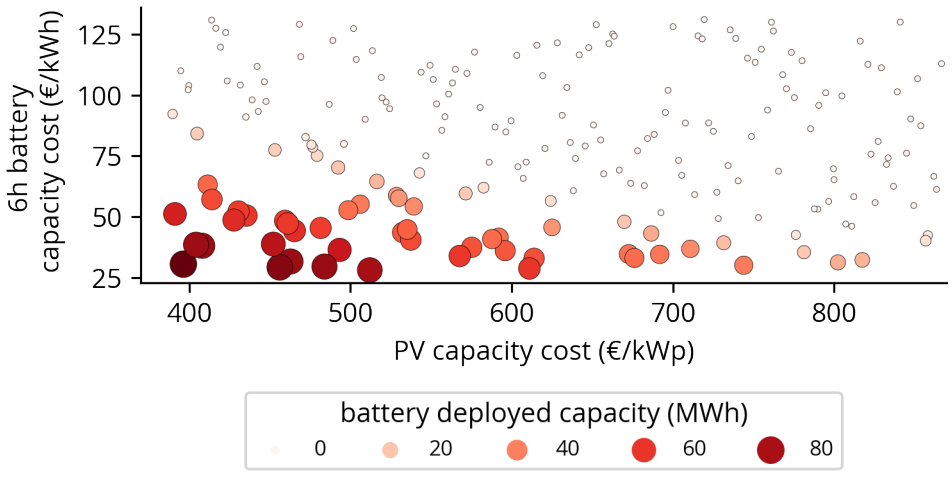

(b) Deployment of battery storage

Figure 7.10: Deployment of PV and battery storage plotted against the sampled uncertainties in the uncertainty space.

of battery storage. Only if oversizing PV relative to the grid capacity is sufficiently economical, large scale battery deployment is sensible. Interestingly, however, when battery capacity cost is sufficiently low there are some cases where battery storage is deployed without any additional solar capacity. From this, it can be concluded that it is possible to deploy batteries to allow for time-shifting of the wind production curve to increase the profitability of the existing wind assets.

The concurrent deployment dynamics are further detailed in figure 7.11. From this figure, it can be seen that battery deployment is indeed correlated with the deployment of PV and vice versa. It should be noted that the capacity cost for battery storage still is a significant factor as the deployment of battery storage only occurs when the price of the 6-hour battery drops below 95 €$/MWh$. This can be seen from the curve that can be traced to the lower deployed PV capacities in figure 7.11a. From this curve, all outliers show at least some deployment of battery capacity. The more substantial the deviation from the lower region of PV deployment, the higher the level of battery deployment. That a low cost for PV is a qualifying factor for high deployments of battery storage can be further substantiated using figure 7.11b. In the lowest-cost region, multiple samples of nearly the minimum capacity cost for battery storage exist. Only when high levels of PV deployment exist, higher levels of deployment for battery storage are found.

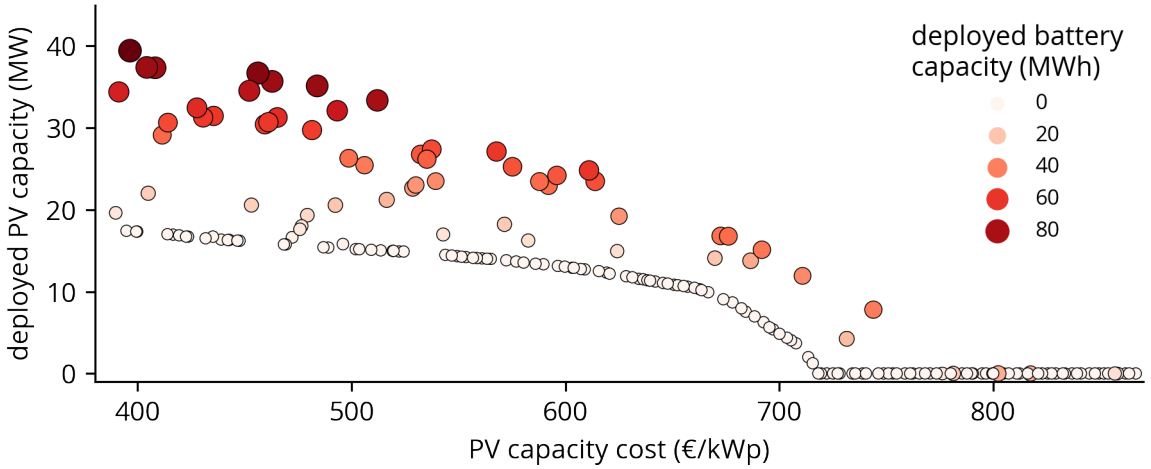

(a) Deployment of technologies against PV capacity cost

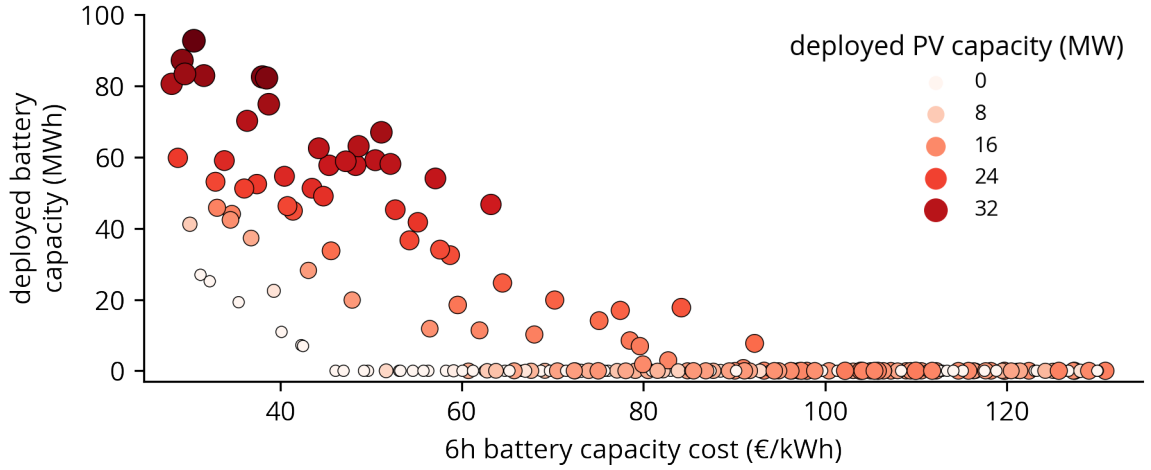

(b) Deployment of technologies against battery capacity cost

Figure 7.11: Deployment of PV and battery storage against a single technology capacity cost.

The curtailment found in this policy shows a new dynamic when compared to the two previous policies. This can be seen in figure 7.12. For most samples, curtailment shows the same relation as found in the first policy (fig. 7.5). In this policy, curtailment can be kept significantly lower at higher total deployed capacities based on the deployment of battery storage. It can be concluded that batteries are indeed deployed to temporally shift production from peak production moments to later moments to prevent curtailment. Under certain cost conditions, a total capacity of 500% of the grid capacity can economically be deployed in a cable pooling configuration. The optimisation algorithm cannot increase the deployed capacity of wind, as it is set to a fixed value. However, it is very likely that the total deployed capacity could even increase further relative to the grid capacity if the solar-to-wind ratio could be kept close to one, as found in 7.1.4.

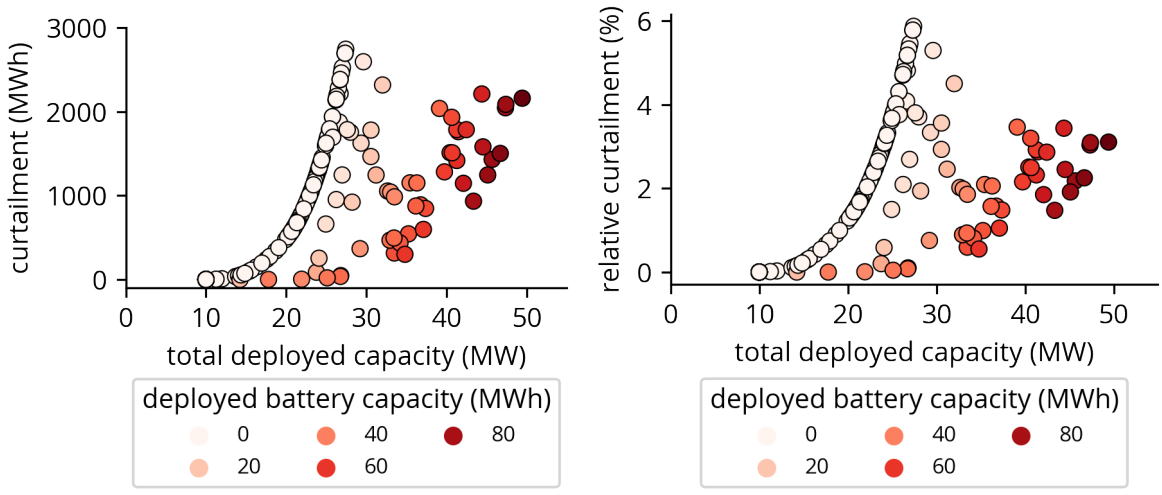

(a) Absolute curtailment

(b) Relative curtailment

Figure 7.12: Curtailment as a function of total deployed generation capacity.

7.1.6 Conclusion

This section presented the results of the optimisation study under uncertainty of the cable pooling concept. Grid operators recognize the importance of cable pooling to increase the share of renewable energy while minimising the impact on the grid. Cable pooling is a solution to increasing renewable energy generation in regions within the Netherlands that are marked as improbable for new renewable energy projects to obtain a grid connection within a reasonable time.

How can exploring energy system optimisation models under uncertainty provide insights into cost-optimal system configurations to support (robust) energy transition policy? This study contributes by generating key insights into the economical feasibility of cable pooling while considering the effect of a fixed-support subsidy and the development of technology costs. In addition, this chapter revealed the dynamics and modes of deployment of battery and PV technology in addition to existing wind capacity.

Development of solar PV in conjunction with existing wind power assets is economically viable with and without subsidy within the projected range of investment cost for PV. The effect of the fixed-support subsidy is significant in determining the point at which PV first becomes viable to deploy in cable pooling. With a fixed-support subsidy of 28 €$/MWh$, the cost tipping point for PV capacity cost is below 720 €$/kWp$. Without subsidies, the cost tipping point for PV capacity cost is below 585 €$/kWp$. Based on the projections, the fixed-support subsidy means that cable pooling becomes viable almost 10 years sooner if cost decline continues at the projected rates. In general, it can be concluded that by combining the two generating assets, more high-value production hours can be covered while utilising an undersized grid connection.

Battery deployment for portfolio optimisation, through energy re-dispatch, will only occur when battery prices are much significantly lower than the lower bound of the projected cost range. This indicates that even with subsidy the income of auxiliary grid services is vital to deploying battery storage at renewable energy projects within the projected cost ranges. From this, it can be concluded that policies that allow energy projects to participate more easily in frequency containment and capacity markets would support the business case for the deployment of battery storage. Once deployed, the battery storage can be utilised for multiple goals including portfolio optimisation through energy re-dispatch.

The policy with marked-down battery capacity cost revealed the deployment dynamics of PV and battery storage in cable pooling. The difference between realistic battery capacity cost and the marked down values depict the effective investment cost that needs to be achieved by revenue streams generated by ancillary services. It was found that battery and PV deployment is synergistic, high levels of PV deployment create a use case for temporal shifting which is realised by the battery storage.

Which cost-optimal system configurations can be identified for case studies within the province of Gelderland? With or without subsidy, solar PV is viable to deploy in conjunction with existing wind power assets. When a certain tipping point is reached in terms of PV capacity cost, the deployed capacity quickly reaches 10 MW and stabilises to reach a maximum of 15 MW of solar PV in both cases. When battery storage is deployed it leads to higher deployment of solar PV. Up to 40 MW of solar PV is deployed in the most extreme cases while curtailment is kept below 4%. In all, it can be concluded that cost-optimal system configurations exist that utilise cable pooling in substantial amounts.

7.2 Electric mobility hub

As climate goals aim to reduce overall greenhouse gas emissions it is becoming increasingly important to decarbonise sectors other than the electricity sector. In general, two routes can be taken to decarbonise a sector. One is to electrify, i.e. replace the energy source used by electricity. The other is to switch over to alternatives of fossil fuel sources, e.g. replacing fossil fuel with synthetically produced fuels either based on biomass or green or blue hydrogen. The Dutch government sets out to decarbonise the transport sector in considerable time, with an intensive focus on electric mobility. The aim is that 100% of all newly registered personal transport vehicles will be (hydrogen) electric by 2030 [8]. Already, the sales of electric vehicles have surpassed many of previous projections by as much as 400%. This exponential increase in the share of electric vehicles in the Dutch personal transport vehicles is expected to sustain and indeed reach 100% slightly before 2030 [152].

There is however a possible constraint that would prevent the massive adoption of this new technology. This constraint is the speed at which new fast-charging infrastructure can be rolled out. The roll-out of new fast-charging infrastructure to support the absorption of electric mobility because the availability of such infrastructure is regarded as a key factor for the market success of electric vehicles [149]. However, fast-charging infrastructure is very demanding on grid connection and requires investment in expanding or reinforcing existing grid capacities [150]. Even when the investment costs are covered by project initiatives, such as charging infrastructure operators, expanding grid capacities can take between 5 and 8 years. In some areas where grid capacity is severely constrained, grid connectivity will not improve before 2030 [174].

Since the electricity sector is already massively employing decentralised technologies such as wind and solar, it might be possible to still realise new fast-charging infrastructure, even on locations where the grid is severely congested. This study aims to research the possibility of providing an electric mobility hub, consisting of 20 fast chargers, local PV and wind generation, battery storage and no or a limited grid connection. In this way, LESO can be used to discover possibilities in a sector other than the electricity sector even though that the mobility sector is not endogenously considered in the framework. This is done by reflecting the mobility sector as a load generated through the fast-charging infrastructure, as described in section 5.5. LESO is then able to discover cost-optimal configurations of various local assets to meet this charging load curve.

In section 7.2.1, the details of this case study are covered in depth. Section 7.2.2 details the cost uncertainties and policies implemented in the various configurations of the optimisation model. Results are first presented per policy, in sections 7.2.3-7.2.6, after which the overall results are discussed in section 7.2.7. Additional analysis is done on the results in section 7.2.8 by applying cosine-distance clustering to identify patterns between similar design outcomes. This method is introduced following an in-depth analysis of the results and is presented as a tool to reduce the dimensionality of results and slink down the expansive analysis needed without it. Finally, section 7.2.9 concludes this chapter.

7.2.1 Case description

This local energy project has a location set close to the border of the province of Gelderland, on the other side of the river IJssel near Deventer. This location specifically is interesting since there are multiple local energy projects that struggle to secure a grid connection for feeding in the produced energy, i.e. grid congestion is a pressing issue near this city. Currently, the GROHW consortium actively researches suitable solutions to integrate more renewable energy by coupling the mobility and industrial sector through the use of hydrogen [175]. Deventer is located near the Dutch traffic

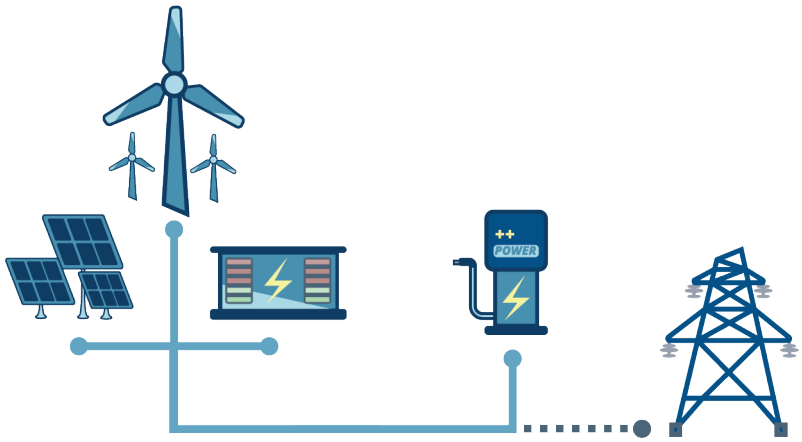

Figure 7.13: Abstract representation of the electric mobility hub. Local energy generation, battery storage and a (limited) grid capacity are used to meet fast-charging demand.

artery highway A1, which makes it a strategic location for fast chargers. In addition, there is currently no fast-charging infrastructure on the A1 Eastbound between Hoevelaken and Hengelo, a stretch of nearly 100 kilometres without fast chargers. Deventer lies almost perfectly centred between existing locations. Lastly, the A1 is a highway that travels from East to West, making it possible to place integrated PV in the sound barriers, which would face South, greatly reducing barriers for the spatial integration of PV.

The model under consideration is comprised of various generating components in varying configurations as shown in table 7.4. The components considered are nearly the same as in the previous study, only this time installed capacity of the wind component is an optimisation variable. In addition, the PV component is configured in a supplementary manner by introducing a South oriented sound wall integrated design. This component is assumed to have the same costs as the conventional set-up but is tilted at a steep angle of 70 degrees. Even though LESO does not consider spatial dimensions in finding cost-optimal configurations, it is possible that this configuration is better equipped for meeting the year-round charging demand as steep-angle PV setups have considerably less seasonal variance.

The charging load curve is determined based on traffic data measured over the same year as the historical meteorological data (2015). The procedure used for determining this fast-charging load curve is covered in detail in section 5.5. It reflects the charging demand for an electric mobility hub that facilitates the concurrent use of 20 high power chargers. This demand must be met completely for every hour of the year. The peak demand of these chargers on an hourly resolution is 2.2 MWh/h, while the maximum considered grid capacity is 1.5 MW. This means that the algorithm is tasked with meeting at least a part of the demand by installing a cost-optimal combination of solar, wind and storage.

The electricity price curve that is applied to the grid component is based on the Dutch national ETM scenario for 2030 based on current policy, as detailed in section 6.1.2. The price that is used for energy supplied to electric vehicles through the fast chargers is based on the lowest rate that is used by the biggest fast-charging infrastructure operator in the Netherlands (Fastned) and is set at 35 euro cents per kWh or 350 €$/MWh$. This rate is only applied to the energy that is actually absorbed by the vehicle and thus after applying the charging efficiency of 85% [153].

Table 7.4: Model set-up for the electric mobility hub study.

Component	Configurations	Installed capacity
PV	Sound wall integrated	*optimisation variable*
	South	*optimisation variable*
	East	*optimisation variable*
	West	*optimisation variable*
Battery storage	2 hours storage duration	*optimisation variable*
	6 hours storage duration	*optimisation variable*
	10 hours storage duration	*optimisation variable*
Grid capacity		*0-1.5 MW (defined in policies)*
Wind	Nordex N100/2500	*optimisation variable*
Fast chargers	150 kW	20 pcs

Table 7.5: Uncertainties sampled in the electric mobility hub parametric uncertainty exploration

Component	Sampled parameters	Method	Cost range			Unit
PV	Capacity cost	LHS	388	-	867	€/kW
Lithium storage	Energy cost component	LHS	105	-	180	€/kW
	Power cost component	*linear map*	116	-	224	€/kW
Wind	Capacity cost	*LHS*	900	-	1280	€/kW

7.2.2 Parametric uncertainty exploration

The parametric uncertainty exploration performed in this study is based on cost uncertainties and categorical sampling of the grid capacity. The grid capacity is categorically sampled in steps of 0.5 MW from 0 to 1.5 MW. This forms the basis for the four policies investigated in this study.

The cost uncertainties are based on the upper and lower range of the projected cost for 2030 of each technology, respectively. The cost projections are covered in detail in each component section as part of chapter 5. An overview of the sampled uncertainties is shown in table 7.5. All uncertainties are sampled using Latin hyper-cube sampling. The power cost component of the batteries is linearly mapped based on the sampled energy cost component.

Per policy, 200 samples were taken from the space spanned by the two cost uncertainties. This results in a total of 800 optimisation problems to be solved. In order to maintain the digestibility of these results, each set of results are first presented in a section according to each of the policies.

The first section covers the visualisations in-depth and aims to present a comprehensive introduction to support the reader in understanding the high dimensional result data, which can be quite overwhelming at first. The following sections stay closer to the core, to prevent repetition and to guard the compactness of this report. Whenever possible, additional results are moved to the appendix which can be consulted by the reader as supplementary figures (appendix C). A high-level overview of all results over the various policies is presented in sections 7.2.7. Lastly, extra analysis is done to cluster the system configurations in each policy is presented in section 7.2.8.

7.2.3 Results policy 1 - 0 MW grid capacity

The first variation of the electric mobility hub is denotative of a project where the grid is constrained to such a degree that connection to the grid is infeasible within a sensible budget or time frame. This set of experiments is also a situation where the level of autarky is highest, the hub will be completely self-sufficient. All consumed energy is locally generated by renewable energy assets.

Because of the vastly different cost conditions that the algorithm is exposed to, it is expected that at least a certain degree in variations of the optimal design is found. To give a quick overview of the playing field of design possibilities, the cost-optimal energy system configuration of various outcomes is given in figure 7.14. The reference system is the centre outcome, the resulting system configuration when all sampled costs are at or around the centre value of their respective ranges. This is also the system that, within some margin of variation occurs the most.

It can be seen that the total deployment is primarily dependent on vastly oversizing the total generation capacity with respect to the peak demand. This can be explained based on two observations. Firstly, the capacity factor of variable renewable energy sources is low when compared to conventional thermal generation plants. Moreover, the capacity of renewable energy sources varies uncontrollably over time. To be able to meet the demand at all moments in time, the system should be sized such that even in case of low capacity it is capable of meeting demand. Secondly, it is nearly always more cost-effective to oversize generation, than to expand the storage capacity. In the reference configuration, the total generation capacity is nearly exactly ten times the peak demand. The storage is sized such that the duration of storage is about 1.5 hours peak generation or about 15 hours peak demand.

The two other configurations are system design configurations where either maximum deployment of PV or wind is found. These configurations are found in the extremities of the cost ranges, as can be seen from figures 7.15 and 7.16. The configuration of maximum battery deployment coincides with the maximum deployment of PV, suggesting a synergy between these two technologies. By comparing the configuration with maximum PV deployment with maximum wind deployment, a trade-off between the deployment of these two technologies can be recognised. It seems that somewhere in the year, solar production is insufficient while wind production is better suited for meeting the demand. In order to reduce the wind capacity by 3 MW, an additional 9 MW of solar PV and 11 MWh of battery storage is required to meet demand. Similarly, by placing a marginally higher amount of wind capacity - not visible in the figure due to significance - the required amount of battery storage can be reduced by 3 MWh. It is important to note that each of these configurations are a result of optimisation. Therefore, each of these configurations from the cost-optimal configuration under certain costs combinations that lie within the range of projected costs for 2030.

With regards to the uncertainty space and the resulting configurations, a selection of visualisations is discussed in this section. Since there are three dimensions of cost uncertainty and three dimensions of optimisation variables a total of nine plots would be needed to show all relations. This section includes only the bivariate plots spanning the uncertainty plane between battery and PV capacity cost. The complete set of figures can be found in appendix C.1.1. When consulting the whole set of figures two conclusions can be formed. Firstly, it is seen that in most cases the final system configuration is very similar, switching between the reference and maximum wind configuration and a combination in between.

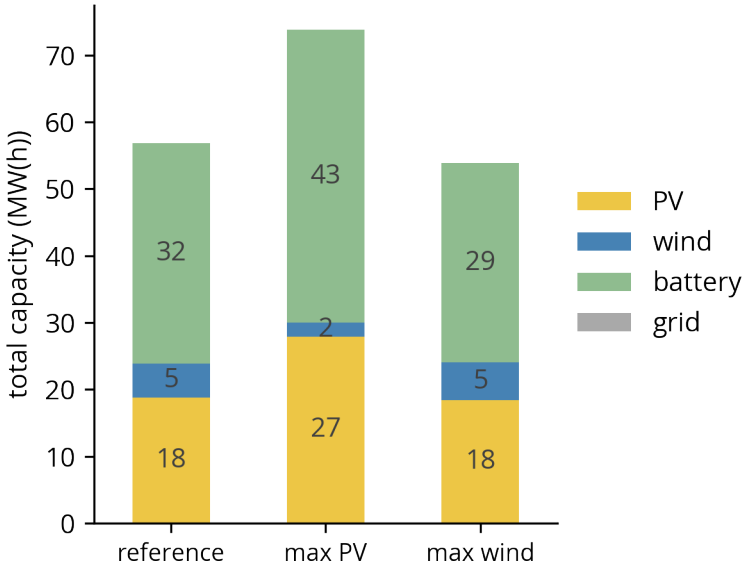

Figure 7.14: Various energy system configurations are found in the charging hub without grid connection (*policy 1*).

Secondly, it can be concluded that for wind and PV there exists a clear inverse relationship between the capacity cost and the deployed cost. This can be seen from the fact that deployment always increases with a decrease in cost over that axis, irrespective of the other cost axes. Wind does not show this same relation, it is very rigid in deployment along nearly all sampled sets of uncertainties with one exception. A diagonal can be recognised in all figures spanning a different combination of uncertainties. This is the situation where PV and battery are both economical while wind is close to the upper range of its cost projection. When considering the total occurrence of those configurations, they should be considered outliers. It is, however, still an interesting trade-off and should be analysed further.

From the set of results shown in figures 7.15-7.17, the trade-off between wind and solar PV plus storage can be identified. In both figure 7.15 and 7.16 the left bottom corner shows cases where the cost of PV and battery are sufficiently low that it leads to an increased deployment of both technologies. The fact that it happens only in this corner suggests co-dependence, the increased deployment of these technologies only poses competition when both are economically attractive options. From the same two figures, it should also be noted that it is not only the cost uncertainty of battery and PV that determines this trade-off. This can be seen from the fact that configurations with high and low deployment of PV and battery are very close to each other. This suggests that the third cost uncertainty dimension, which cannot be shown in the same figure, affects the deployment. This third cost uncertainty is that of wind. It makes complete sense that this sampled value would also affect the trade-off. When wind is sufficiently economical, there is not a configuration of PV and battery that is competitive, even when both the cost of PV and battery is near the lower limit of their respective cost ranges.

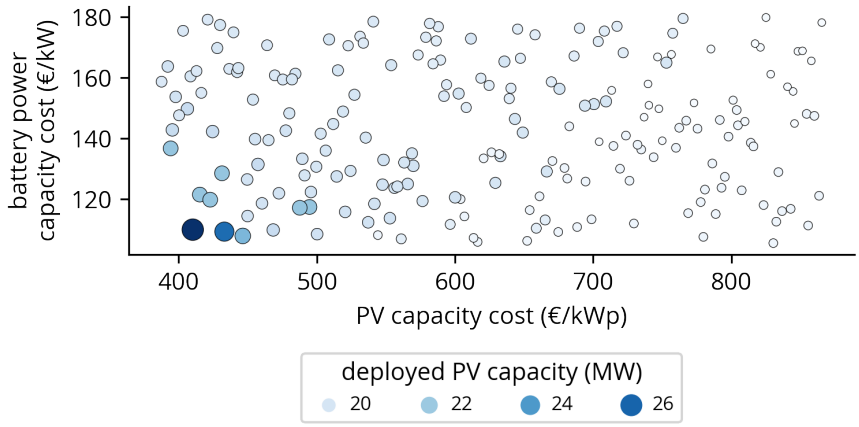

Figure 7.15: PV deployment on the uncertainty plane spanned by PV and battery capacity cost *(policy 1)*

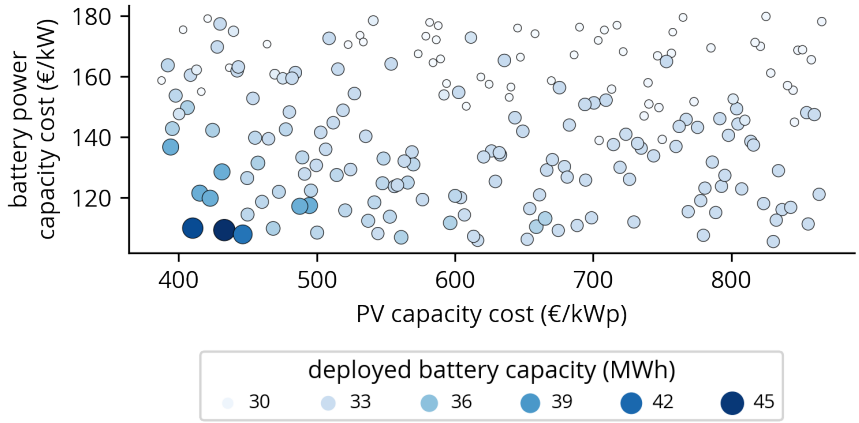

Figure 7.16: Battery deployment on the uncertainty plane spanned by PV and battery capacity cost *(policy 1)*

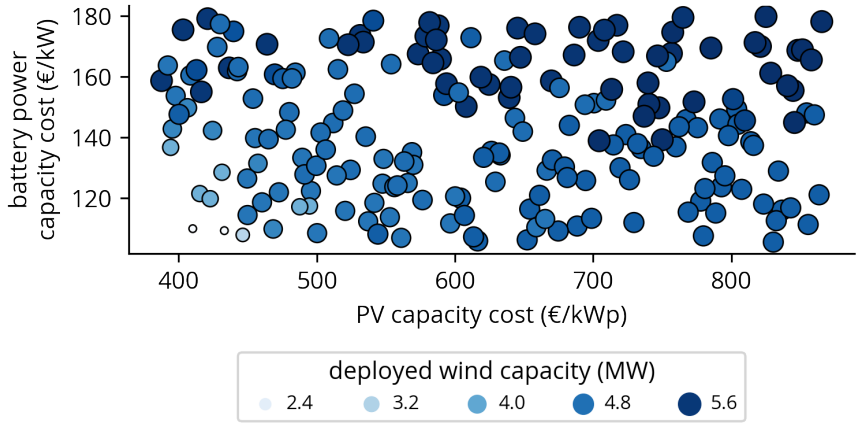

Figure 7.17: Wind deployment on the uncertainty plane spanned by PV and battery capacity cost *(policy 1)*

7.2.4 Results policy 2 - 0.5 MW grid capacity

This set of results are generated with consideration that the maximum grid capacity is 0.5 MW. This can be a result of lacking infrastructure or an imposed congestion mitigation measure. As introduced in the previous section, the configurations resulting from this set of experiments is shown in figure 7.18. Again, the same relation can be noted, albeit in different quantities. Most notably different is the range of deployed PV capacity, which in the most radical case only increases by 25% when compared to the reference system. Again, a marginal increase in wind decreases deployed capacity of PV and battery. It should be noted that in this case, the effect is more pronounced for battery deployment than for PV when compared to policy 1. Moreover, the addition of a 0.5 MW dispatchable energy source greatly impacts the installed generation to peak demand ratio. For this policy, the reference system deploys roughly seven times the peak demand in terms of generation capacity. Noteworthy is also the storage duration capacity, which decreases absolutely but increases relative to the deployed generation capacity. The storage duration is nearly two hours when related to the renewable generation capacity and about 10 hours of peak load. When compared to the first policy, the storage duration for on-site generation increases roughly by 50% while the storage duration for peak demand decreases by 50%.

Again, a total of nine bivariate plots cover the complete uncertainty space. Only two uncertainty spans are included in this section which show the most important relations in this policy. The complete set of figures can be found in appendix C.1.2 From figure 7.19 it can be concluded that the deployment of PV is indeed non-sensitive to the corresponding capacity cost in nearly all cases. Only in the extremity where both PV and battery are near their respective lower limits, a marginal increase in the deployed PV capacity can be noted.

When considering figure 7.19, it can be concluded that battery deployment is nearly solely dependent on the capacity cost of batteries themselves. This can be seen from the apparent gradient moving from the upper half to the lower half of the figure. When battery capacity cost approaches the upper limit, the optimal configuration switches to a system design with slightly less batteries. The majority of optimal configurations includes a higher level of battery deployment, however, which is mostly when the capacity costs for batteries stay below a certain threshold of around 160 €$/MWh$. The before mentioned synergistic configuration between PV and battery can be seen in the lower-left corner of this figure, where the battery deployment increases when PV capacity cost is sufficiently low.

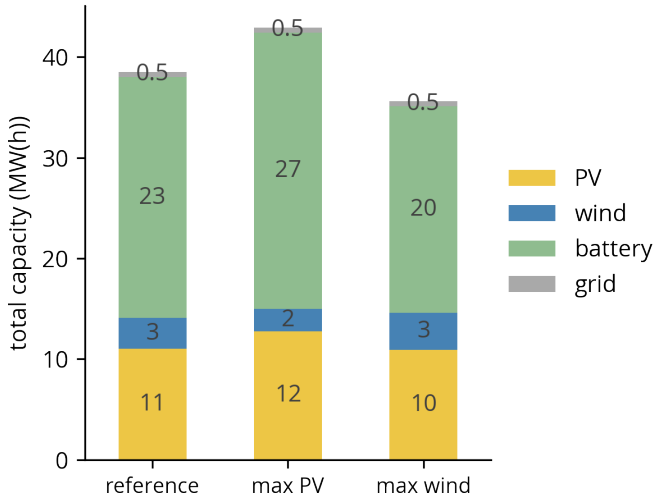

Figure 7.18: Various energy system configurations are found in the charging hub with a 0.5 MW grid connection (*policy 2*).

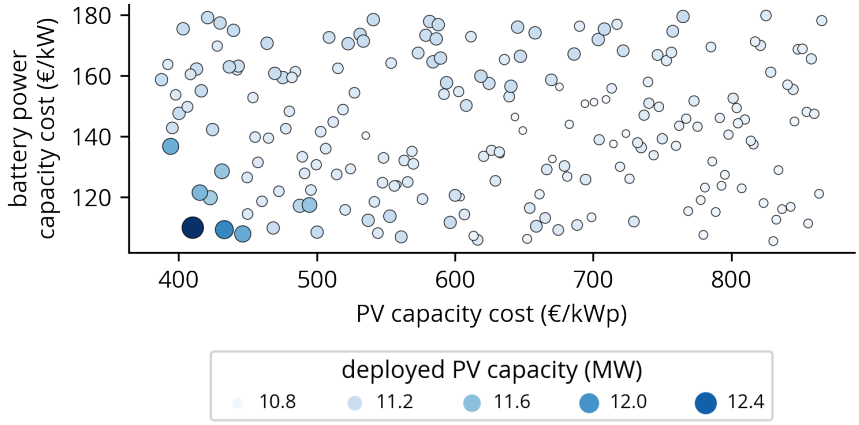

Figure 7.19: PV deployment on the uncertainty plane spanned by PV and battery capacity cost *(policy 2)*

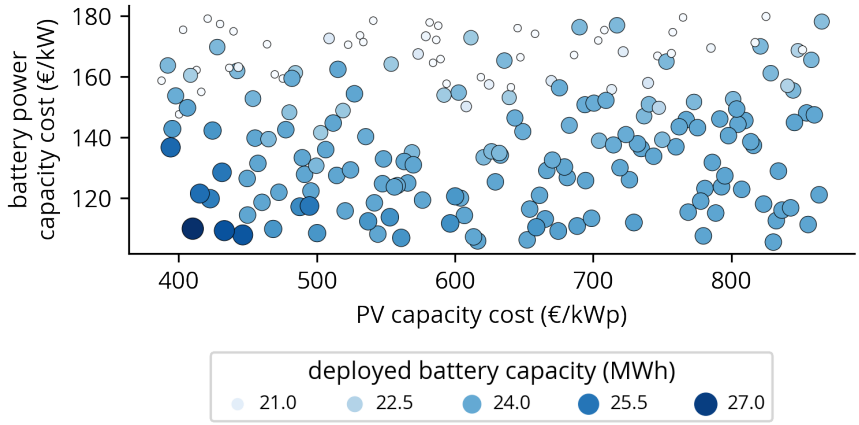

Figure 7.20: Battery deployment on the uncertainty plane spanned by PV and battery capacity cost *(policy 2)*

7.2.5 Results policy 3 - 1 MW grid capacity

This section covers the results of policy 3, where the grid capacity is 1 MW and therefore represents a situation with more relaxed constraints on the grid connectivity. As noted in the previous section, an increase in grid capacity yields cost-optimal configurations with a lower total generation capacity. When compared to the previous set of results, the difference between the reference and maximum PV configuration again shows a larger variance in the deployed capacity of PV. In policy 1, cost-optimal configuration with maximum PV deployment affected the deployment of battery storage more significantly than it affected the deployment of PV. Moreover, this set of results shows significantly less variance in the deployment of battery, where the range of battery deployment in all cost-optimal system designs varies by 30%.

The total deployed capacity in the reference system configuration is 3.5 times the peak demand. The storage duration of this policy's reference configuration is 2 hours when related to on-site generation capacity and about 5 hours of peak demand. Compared to the previous policy, this configuration has the same storage duration when related to the on-site generation capacity and half the storage duration when related to the peak demand. This implies that the cost-optimal ratio between storage and on-site generation is nearly identical between these policies, while the absolute required quantity of both on-site generation and storage decreases by half.

Since the total variation in deployed wind capacity is insignificant in terms of the share of total system costs, only the deployment of PV and battery are shown in this section's results. The complete set of figures can be found in appendix C.1.3. From figures 7.22 and 7.23, a relation can be seen that has not been identified in the policies before. In this policy, PV and battery deployed capacities form a trade-off against each other. In the two policies before, PV and battery deployment only showed a synergistic relation. In this policy, the deployment of PV is inversely related to its corresponding capacity cost, while battery deployment is positively related to the capacity cost of PV. This relation is nearly irrespective of the capacity cost of the battery. Still, a very select set of conditions shows the synergistic relation between PV and battery, when both technologies' capacity costs are sufficiently low to compete with deployed wind capacity.

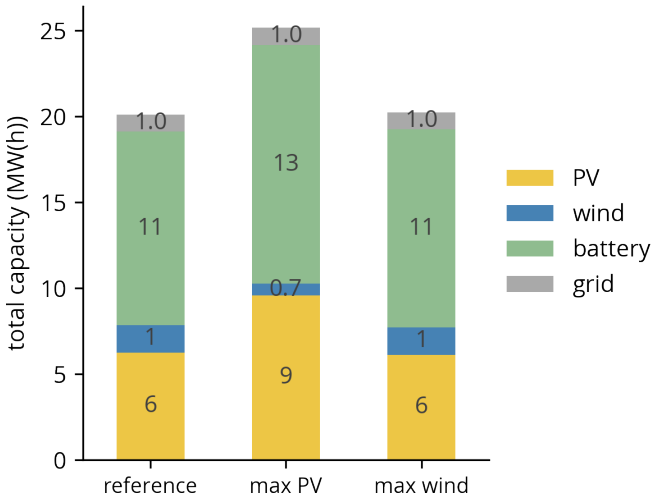

Figure 7.21: Various energy system configurations are found in the charging hub 1 MW grid connection (*policy 3*).

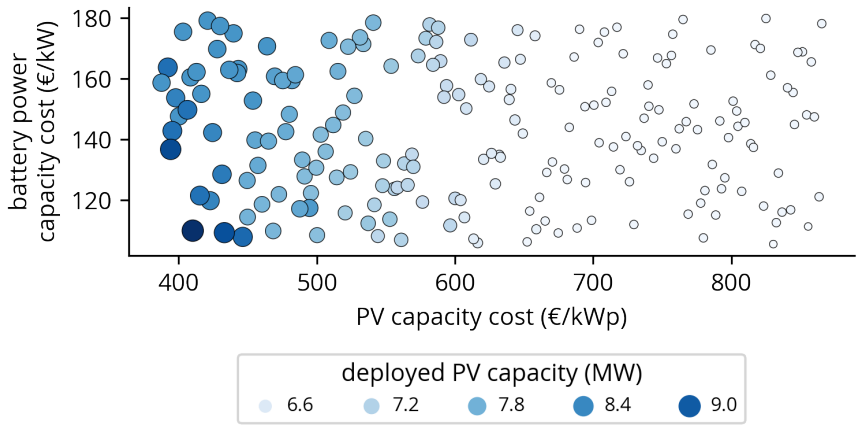

Figure 7.22: PV deployment on the uncertainty plane spanned by PV and battery capacity cost *(policy 3)*

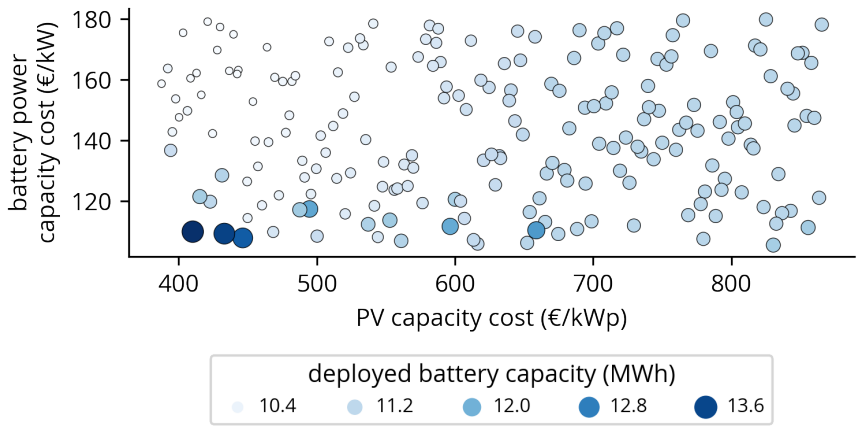

Figure 7.23: Battery deployment on the uncertainty plane spanned by PV and battery capacity cost *(policy 3)*

7.2.6 Results policy 4 - 1.5 MW grid capacity

This final set of results covers the situation where the grid capacity is rated at nearly 75% of the peak demand. The deployed capacity of on-site generation is similar to policy 3, but shows a clear favour for PV over wind deployment. The total deployed capacity in the reference system configuration is 3.5 times the peak demand. The total storage capacity decreases again with an increase in grid capacity. The storage duration is 1 hour when related to the on-site renewable generation capacity and just shy of 3 hours of peak load. When compared to policy 3, both these metrics show a drastic decrease, most notably for the storage duration of on-site generation. Again, the variation in deployed PV between the three configurations capacity increases while the deployed battery capacity shows less variation.

Similar to policy 3, this set of results shows that deployment of PV is completely independent of the other technologies capacity costs. This is not a new insight and thus the corresponding figures can be found in appendix C.1.4. Instead, figure 7.25 shows the deployment of battery capacity as a function of battery and wind capacity cost. It can be noted that there is an apparent diagonal gradient from the left upper corner to the right lower corner. In this gradient, wind and battery deployment are competitive and deployments of these two technologies are exchanged in the cost-optimal configurations.

It can be concluded that the span of battery and wind uncertainty does not include all factors driving the deployment of battery as there also exist very closely grouped points with varying levels of battery deployment. This can be attributed to the aforementioned relation of PV deployment proportional with the capacity cost of PV. Figure 7.26 shows the same but inverse gradient, where the maximum deployment of wind is found in the left upper corner.

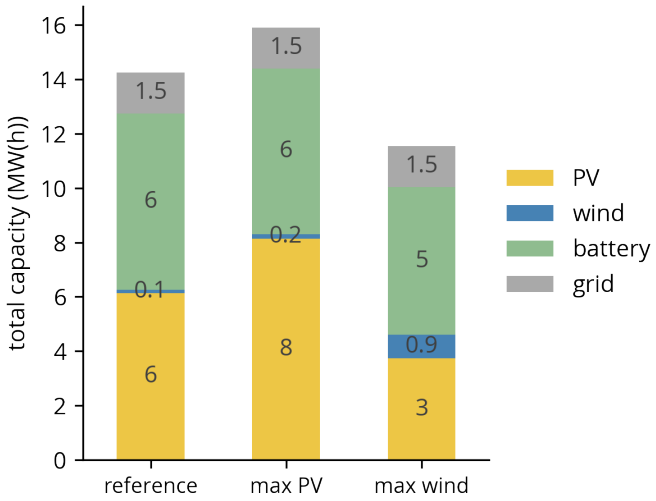

Figure 7.24: Various energy system configurations are found in the charging hub with a 1.5 MW grid connection (*policy 4*).

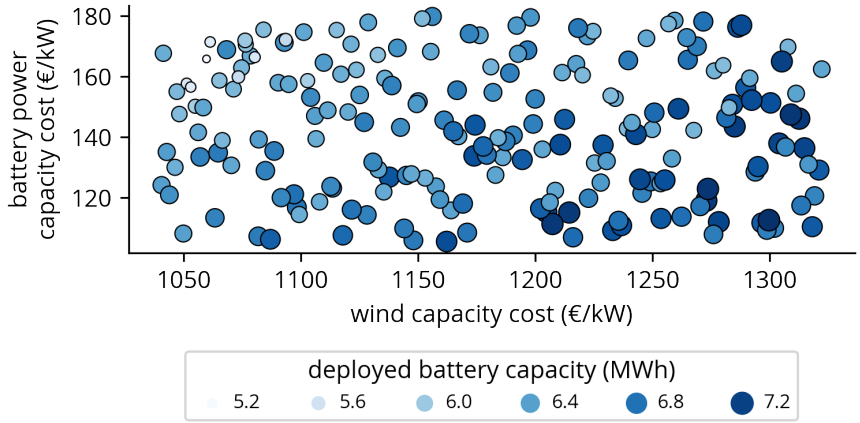

Figure 7.25: Battery deployment on the uncertainty plane spanned by wind and battery capacity cost *(policy 4)*

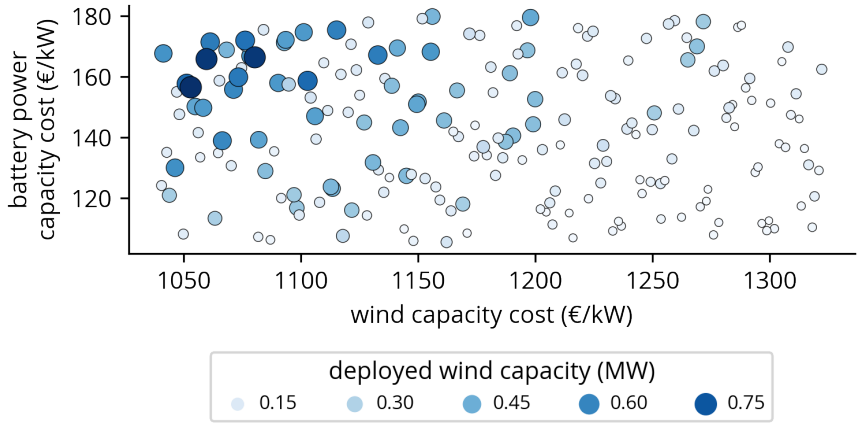

Figure 7.26: Wind deployment on the uncertainty plane spanned by wind and battery capacity cost *(policy 4)*

7.2.7 Results overview

This section presents an overview of all results and thus focuses less on the details of dynamics found in each policy result set. Instead, it relates the various policies to each other and distinguishes agreements and notable deviations. The cost-optimal reference configurations resulting from each of the four policies are depicted in figure 7.27. Two correlations can be deduced from this figure.

Firstly, the total installed capacity of all technologies decreases with an increase in grid capacity. The effect is most notable when the electric mobility hub would otherwise be (highly) self-sufficient, with less effect on the configurations that already include a more substantial grid capacity.

Secondly, the share of wind energy in the on-site energy generation assets decreases with an increase in grid capacity. From this, it is concluded that in many cases PV forms a more cost-effective way of generating electricity. However, it has a notably lower capacity factor and is more variable over time. Considering that the optimisation is constrained to meet the charging demand in all hours of the year, it seems that the generation curve of wind is better equipped to meet some hours of the years cost-effectively. Without the dispatchable power provided by the grid, at least some capacity of wind is found in the cost-optimal configuration as a result.

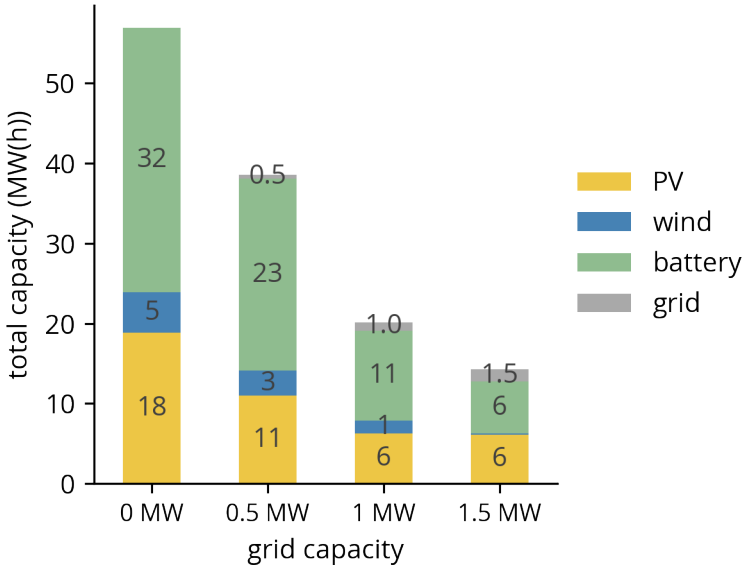

Figure 7.27: Reference energy system configurations for all policies compared

To depict all resulting cost-optimal technology deployment while maintaining the relationship to the sampled cost uncertainty requires a lot of bivariate plots to be generated and analysed, as a minimum of nine figures is needed to span all uncertainty planes and resulting technology deployment. The number of figures required to cover the results increases in function of the number combinations that can be made in sets of two (due to the two-dimensional plane) of the number of sampled uncertainties, which has a combinatorial relationship as shown in equation 7.1. I.e. a set of results that is based on four uncertainties can be combined to $\binom{4}{2}$ which yields six planes of uncertainty. If the number of distinct degrees of deployment included in optimisations is equal to the degrees of uncertainties this would require a total of $6 \cdot 4 = 24$ figures. To steer clear of this combinatorial relationship, an alternative visualisation technique is introduced.

$$C(n,r) = \begin{pmatrix} n \\ r \end{pmatrix} = \frac{n!}{(r!(n-r)!)} \tag{7.1}$$

This visualisation is called a strip plot and is shown in figure 7.28. A strip plot allows for plotting many data points on a single axis, which is the category of the data which in this case is the policy. As a result, the strip plot visualisation has a proportional relationship to the number of uncertainties. It does compromise on the relation to cost uncertainties due to the limited amount of dimensions that one can possibly fit into a single graph.

However, a strip plot visualisation is very suited to provide insight into the distribution of the cost-optimal configurations, both within a set of results corresponding to a single policy and between the various policies. Conventional visualisation techniques used for a similar purpose such as violin or box plots are not suited for optimisation results because the outcomes are not normally distributed, but rather forms distinct configurations that are able to meet the posed constraints.

From this figure, the deployment dynamics as discussed in the previous section can be still be distinguished to some extent. For instance, the continuous deployment relation between PV and its capacity cost described in policy 4 can also be seen in the top subplot of figure 7.28. The points are scattered nearly uniformly between the upper and lower bound of the PV deployment.

Another interesting observation that can be made using this diagram is how locked-in a certain model configuration is in relation to the sampled cost uncertainties. This can be seen from a high density of points at a single point at one of the axes. When a certain energy system configuration occurs often, it forms a pattern that nearly reassembles a vertical line in the strip plot. A suited example is the optimal deployed wind capacity in the policy where the grid capacity is 1 MW, as shown in the middle subplot of figure 7.28. Nearly all configurations have about 1.5 MW of wind deployed, only a few cases can be found where the capacity is lower.

Thus, by using the strip plot it is possible to visualise the cost-optimal configurations in such a way that it is possible to distinguish the configurations, their occurrence and distribution. This technique can be used to quickly visualise and analyse multi-dimensional data that describes energy system configurations resulting from optimisation. In this chapter, the relationships between costs uncertainties and energy system configurations have been investigated in great detail. This approach requires a lot of plots to be generated, analysed and discussed to generate insights, which is time-consuming. The strip plot contains similar information on deployment dynamics, only in less detail. It is advised to use strip plots in combination with other visualisation and dimension reduction techniques to achieve the key insights into optimisation results more effectively.

If only the strip plot visualisation is considered, the relationship between configurations and the cost uncertainties is lost. This is unfortunate since the cost uncertainties are the inputs that form the basis of the experiments. Reintroducing the correlation to the costs uncertainties and the relationships between other resulting variables while maintaining the overview can be achieved by applying statistics on the result set. A correlation matrix can be calculated and displayed using a heat map. Using this approach, the heat map shows the correlation between variables such as technology deployment and cost uncertainties. This visualisation strategy is valuable as it provides key relational insight in a single figure. The Pearson correlation was calculated for every policy independently, between various relevant variables. The resulting heat map figures are shown in figure 7.29.

This figure is very information-dense, and various interesting relations can be extracted from this single visualisation of which a select amount will be discussed. Firstly, there is a set of conclusions that are valid for all policies. Total generation capacity is always strongly negatively correlated with deployed storage capacity, i.e. oversizing generation capacity relative to the load decreases dependability on storage. Total generation capacity is the main driver for curtailment, while increased storage capacity decreases curtailment.

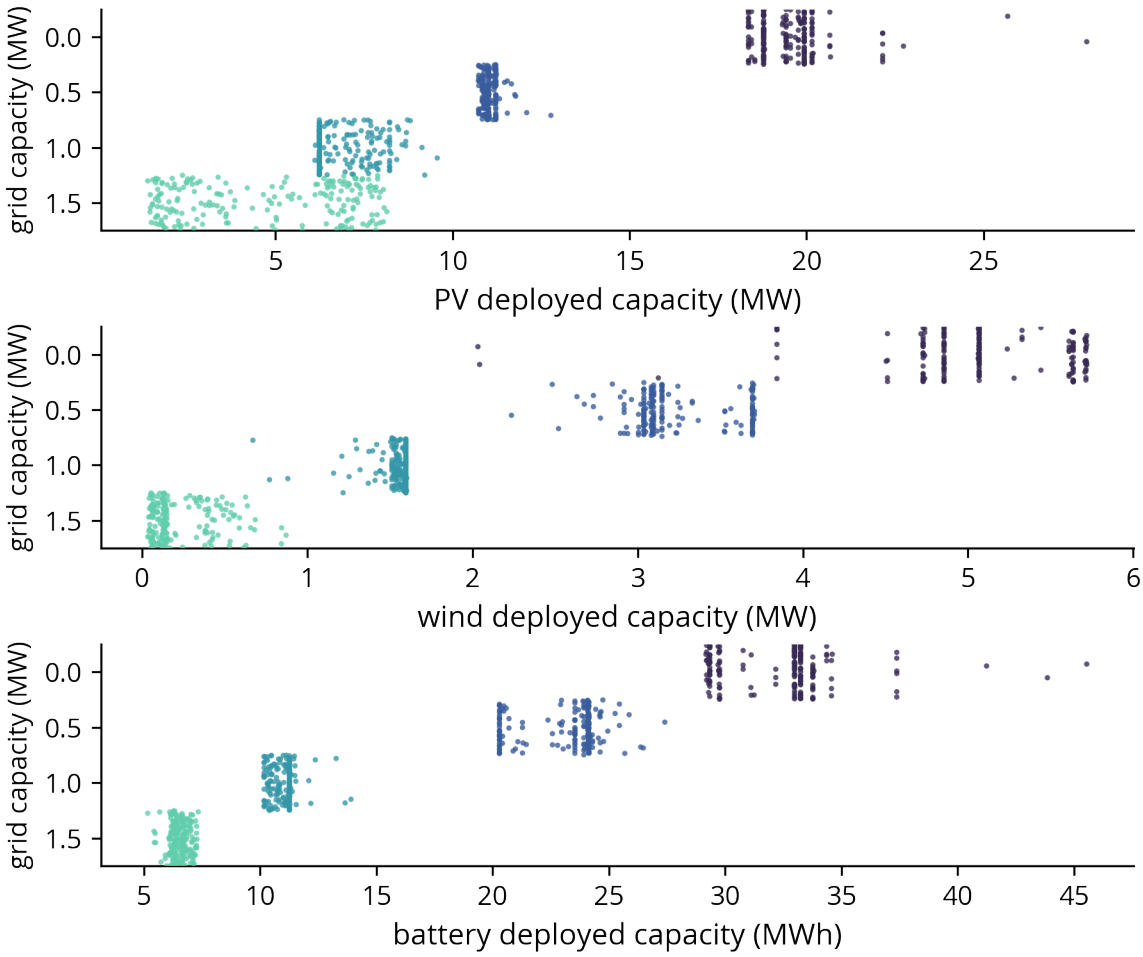

Figure 7.28: Deployment of PV, battery storage and wind for the four different grid capacities which is the y-category of the plot. The colour of the points is used to better separate the four categories.

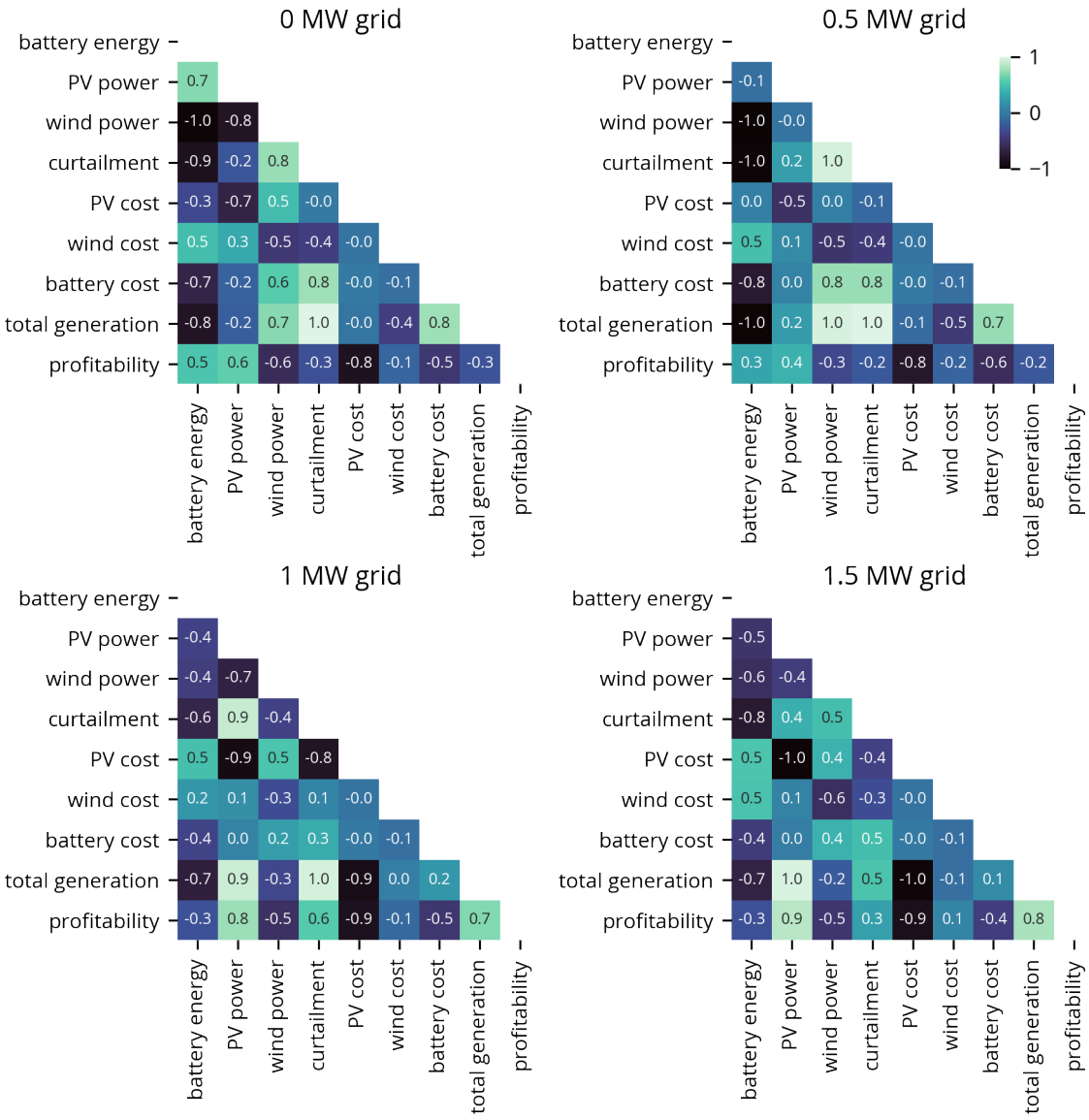

Figure 7.29: Correlation matrices for all grid configurations

More interestingly, the correlations between various variables can be vastly different from policy to policy. Take the relation between curtailment and deployed PV capacity. For the 0 MW results, curtailment is slightly negatively correlated with deployed PV capacity while there is a strong positive correlation between PV power and curtailment in the 1 MW case. Moreover, the deployment of PV is more strongly correlated to the price level for the higher grid capacity cases than for the lower grid capacity cases. The 1 MW case shows a positive relationship between the deployed wind capacity and the cost of PV capacity, implying that a lower cost of PV leads to a lower deployment of wind capacity. This while the 0 MW shows nearly no correlation between these variables.

By combining the strip plot visualisation with the correlation matrix, nearly all key information can be deduced from a much smaller set of figures. However, one key piece of information is not considered by using this method. This is the possibility to quantitatively relate the various cost-optimal energy system configurations to the underlying cost uncertainties and to compare various configurations against one another. For this purpose, section 7.2.8 present an approach to cluster the data set such that this relation can be observed in a reduced set of figures.

7.2.8 Clustering

This section covers another analysis to reduce the dimensionality of the set of results. The method applied in this section is inspired by a specific form of common unsupervised learning called agglomerative hierarchical clustering. This method is able to cluster similar energy system design configurations of any dimensionality based on the similarity between designs. This is achieved by minimising the cosine distance between the vectors that span the design, in each cluster. Agglomerative clustering starts by taking as many clusters as there are data points which subsequently move up in the hierarchy by finding the best pairs of existing clusters until either the number of desired clusters is achieved or when the distance threshold is reached.

The method applied in this thesis follows the approach of Fraiture, who suggests using hierarchical agglomerative clustering with complete linkage based on cosine distance after applying standardisation on each of the system design features independently [100]. In their work, this approach is applied to an optimisation model that optimises investment decisions over a time horizon spanning multiple years but only on account of yearly demand and supply. By implementing this approach, features can be used for clustering independently of their unit or values ranges and clusters are formed based on the similarity between the final designs. A comprehensive introduction to the clustering method can be found in appendix D.

In this chapter, clustering has been applied per policy such that the distinct configurations are maintained since the varying grid capacity has such a substantial effect on the cost-optimal configurations. The result of clustering was found to be best visualised using a pair plot when interest is mainly in the distribution of the clusters in relation to the cost uncertainties. When the interest is mainly towards the configurations of the various optimal designs the strip plot was found to be the best option to visualise clusters. Due to the fact that this chapter covers the dynamics of deployment as a function of uncertainties extensively already, the pair plots are kept outside of the main body of the text but can be found in appendix C.1. Figure 7.30 shows the strip plot of all resulting system configurations on which the described clustering method is applied to obtain the colour coding of every point in the plot.

By consulting the deployment graph of each of the technology the differences between the clusters can be recognised. For instance, the 0 MW grid results contain a cluster, marked by fluorescent green, with low deployment of PV, moderate deployment of battery and moderate deployment of wind on which it can be clearly distinguished from other clusters. This cluster contains 78 system configurations that are optimisation outcomes of unique sampled combinations of capacity costs.

The strip plot contains more specific information about the system configurations, now that various clusters can be identified from the same visualisation. The quantitative relationship between cost-optimal technology deployment and the cost uncertainties is visualised using pair plots. It can be concluded that this method of clustering is indeed very effective in identifying typical system configurations and that it can be applied to analyse optimisation results more efficiently. It is not only suitable for investment optimisation models but also applicable to optimisation models that provide a snapshot of cost-optimal energy systems configurations while considering a yearly energy balance on hourly resolution.

Altogether, it can be concluded that this method is suitable to improve the efficiency of analysis and forms a process robust to multidimensional results. The method processes data resulting from optimisation under cost uncertainty by applying cosine-distance based agglomerative clustering and calculating correlation matrices. This is visualised using strip plots, heat maps and pair plots. To this end, the proposed approach is able to provide key insights into deployment dynamics, while conserving the relation to the sampled cost uncertainties and providing a clear overview.

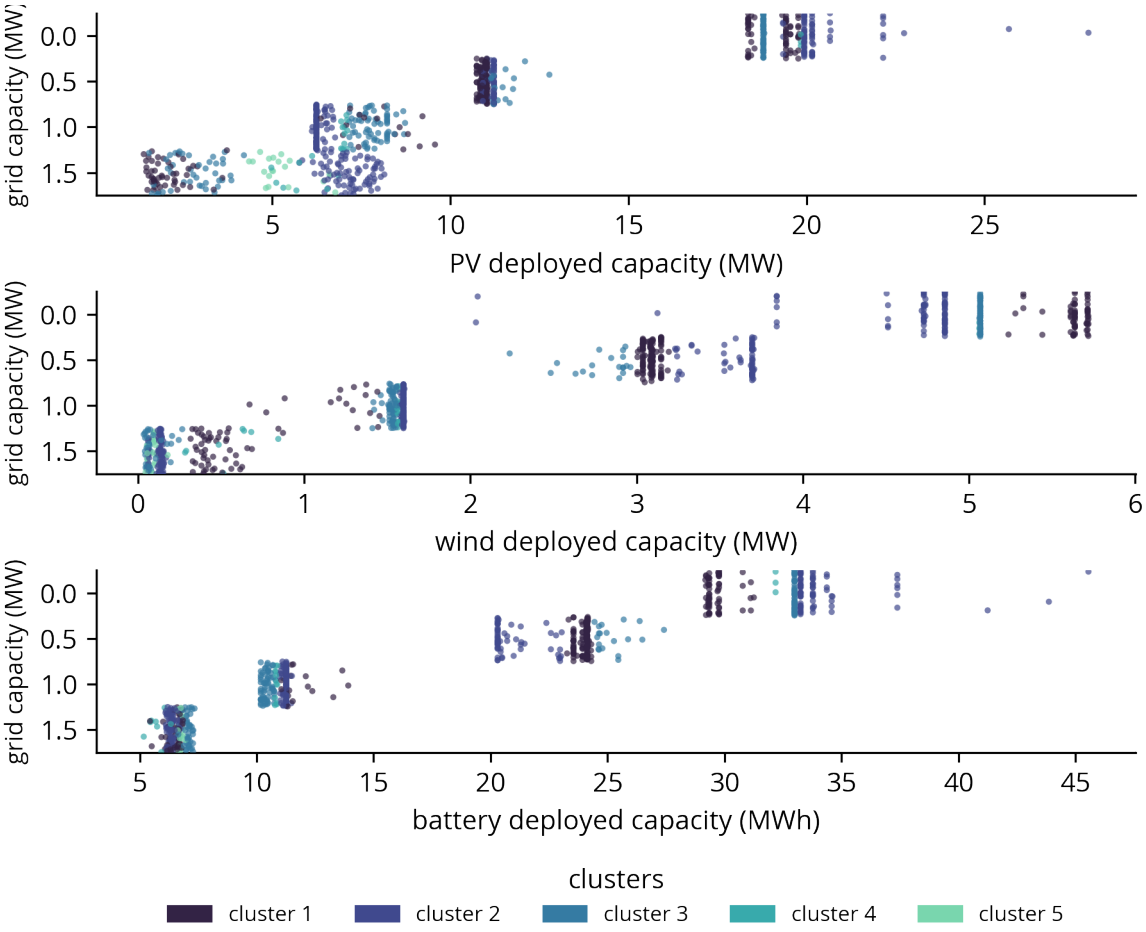

Figure 7.30: Deployment of PV, battery storage and wind for the four different grid capacities. The colour of the points is used to distinguish the various clusters found. The clusters can be used to identify certain patterns, which are most distinct for the 0 MW grid capacity policy.

7.2.9 Conclusion

In this section, it is found that it is technically possible to meet the demand of a large scale electric mobility hub in grid constrained areas by implementing various cost-optimal configurations of local renewable energy generation and storage. Moreover, it is also possible to find a cost-optimal configuration that supports a positive business case under all uncertainties.

How can exploring energy system optimisation models under uncertainty provide insights into cost-optimal system configurations to support (robust) energy transition policy? The cost-optimal configuration of the mobility hub depends primarily on the grid congestion since every policy investigated provided new relationships between the sampled cost uncertainties and the results. This is shown in the correlation matrices, calculated based on Pearson correlation between variables. Each of the grid configurations shows a unique sensitivity and response to the cost uncertainties. Specific deployment dynamics and sensitivity to cost uncertainties should therefore always be consulted in regards to the level of grid connectivity or desired level of energy autarky.

Moreover, it can be concluded that, although not visible in a single optimisation result, trade-offs between alternative system configurations are considered by the optimisation algorithm when exchanging competing technologies in their respective deployed capacities. These only become visible when exposing the model under consideration to a range of cost uncertainties. In some uncertainty sets, it is cost-optimal to reduce wind capacity in favour of increasing the deployment of both PV and battery storage which display a certain synergy. This phenomenon is observed in the 0 and 0.5 MW grid capacity cases. In the other cases, the deployed wind and battery capacities become more locked-in. Only the deployed PV capacity remains sensitive to the cost of capacity.

Which cost-optimal system configurations can be identified for case studies within the province of Gelderland? Depending on the available grid capacity and the underlying technology costs, different combinations of wind, solar PV and battery are implemented in the optimal system configuration to meet the charging demand. For the grid-isolated charging hubs, about 18 MW of solar PV is deployed with 32 MWh of battery storage and 5 MW of wind capacity. In the case with the highest grid connection capacity, only 6 MW of solar PV and 6 MWh of battery storage are required. By increasing the grid capacity by 1.5 MW, 12 MW of solar PV and 24 MWh of battery storage is no longer required to meet the charging demand. Although all configurations are in essence economically viable, it is likely that other combinations of local demand and generation are interesting. Future research into the possibilities of combined demand and generation grid connections is therefore recommended.

Finally, clustering was applied in an effort to reduce the time intensity of visualizing and analysing the results from optimisation under uncertainty. The approach implemented is based on the work of Fraiture and utilises cosine-distance based hierarchical agglomerative clustering after standardisation of relevant energy system design parameters [100]. The proposed approach can be applied to an arbitrary number of design and uncertainty dimensions.

Novel in this research is the combination of clustering, Pearson correlation matrices and visualisation through strip plots, heat maps and pair plots which is proposed as an effective alternative for analysis of optimisation results under uncertainty. Considering that visualisation and analysis of the complete uncertainty space and resulting deployment is achieved by spanning two uncertainties and one optimisation variable at a time, this approach is more dense and applicable to optimisation results of higher dimensions. It is therefore applied in the following chapters.

Chapter 8

Gelderland 2030

In this chapter, LESO is used to optimise the energy configuration for the province of Gelderland in 2030. This is done based on scenarios modelled in the ETM which are used by policymakers of the province to investigate future energy systems depending on large shares of renewable energy [17].

The ETM scenarios are implemented in optimisation problems by calculating the residual load for all categories modelled in the ETM as described in section 5.6. By using this approach, the regional specific demand curve depends on regional specifics such as the intensity and type of industry, the amount and composition of urban areas and the transport sector.

2030 is selected as the moment in time to provide an optimisation snapshot, as this year is an important milestone in Dutch climate policies. Gelderland consists of six RES regions. Each of these regions considers the spatial integration of renewable energy using a bottom-up approach. The RES are formed by a collective of municipalities, that in essence investigates the support for and possibilities of rolling-out renewable energy generation in their regions. System integration is only considered qualitatively.

For this reason, this chapter aims to provide key quantitative insights for policymakers with regards to optimal renewable energy configurations for each of these regions as well as for the whole province of Gelderland under various policies while considering cost uncertainty. To this end, two main sections are presented in this chapter.

Section 8.1 considers the RES regions individually. Demand curves, grid connectivity and current projections are based on each of their respective policies and regional specifics. For each of the six regions, the optimal deployment of PV, wind, battery and hydrogen storage is investigated for various renewability targets. This is compared against current policies. Aggregation of the regional results is measured against the optimisation of the whole of Gelderland, which forms the basis for the second section.

Section 8.2 introduced optimisation studies under uncertainty on the province of Gelderland as a whole. In this section, cost uncertainty can be taken into account since the spatial variation is reduced from six to one region. Cost-optimal systems are investigated under uncertainty and under various policies that impose renewability targets for the electricity sector. Finally, this chapter is concluded in section 8.3.

Figure 8.1: Overview of the six RES regions within the province of Gelderland.

8.1 RES regions

This section includes optimization based on each of the six RES regions that are part of Gelderland. Each of these regions has a specific scenario in ETM, which is tailored to that region. This means that it accounts for regional specifics such as housing stock, industry, mobility, agriculture and existing energy generation. Each of these scenarios has nearly 500 parameters, which have all been dialled in based on the most recent projections and region-specific data. The scenarios can be accessed through the ETM which provides a graphic interface. Links to these scenarios can be found in appendix E.2. The six RES regions that are part of the province of Gelderland are shown in figure 8.1.

In order to reflect the grid connectivity of each of the regions, the grid capacity is determined based on the capacity of the transformers from medium (10-20 kV) to high voltage (150 kV). This capacity is not necessarily fully representative of the actual inter-connectivity of the region since some regions are additionally connected to the bulk transportation infrastructure, which is at an even higher voltage level (380 kV). However, nearly all loads and sources of electricity are connected through the high voltage distribution network. It is therefore assumed that this approximation is valid enough if dependence on load flow calculations is to be prevented. The medium to high voltage transformer capacity for each of the regions is determined by querying ET local, the data management application connected to the ETM. The current transformer capacities are used for 2030. An overview is presented in table 8.1.

Each of these regions has a unique demand and generation profile based on the settings in the scenario, which include the RES policies for each scenario respectively. Using the ETM, the total energy generated using PV and wind is determined based on historical meteorological data from 2015. Based on the scenario-specific demand profile, a certain share of this electricity can be consumed in the region. Hours in the year where excess renewable energy exists, curtailment or export occurs. By subtracting curtailment and export from the regionally generated renewable electricity, the actual regional electric renewability target is determined. This is shown in table 8.1.

Table 8.1: Determined grid capacity and calculated renewable electricity target for the RES regions.

Region	Grid capacity (MW)	Current projection target
Achterhoek	219	68%
Arnhem Nijmegen	609	38%
Cleantech	299	40%
FoodValley	322	43%
Noord-Veluwe	147	49%
Rivierenland	590	53%

8.1.1 Model setup

An overview of the components in the model under consideration and their respective configuration can be found in table 8.3. Parametric uncertainty is not included in this set of experiments. Instead, costs are assumed at the centre values of projected ranges as shown in table 8.2. This reduces the dimensionality of the set of experiments by reducing the amount of possible variation therewith guarding the comprehensibility of the results.

Table 8.2: Cost centre values for the considered technologies

Component	**Parameters**	**Value**	**Unit**
PV	Capacity cost	632	€/kW
Wind	Capacity cost	1175	€/kW
Lithium storage	Energy cost component	155	€/kWh
	Power cost component	159	€/kW
Hydrogen storage	Power cost component	2871	€/kW
	Energy cost component	16	€/kWh

In the end, the six RES regions are optimised for three increasing renewable electricity targets, as shown in table 8.4. This results in a set of 18 experiments. This is modelled pragmatically by considering both the region and the targets as policies. This exposes all experiments to the EMA workbench, which is then used to sample all the experiments through a single interface. Since all considered policies are categorical, full factorial sampling is applied to obtain each desired configuration of the model as an experiment.

Table 8.3: Model set-up for the Regional Energy Strategy model runs.

Component	**Configurations**	**Installed capacity**
PV	South	*optimisation variable*
	East	*optimisation variable*
	West	*optimisation variable*
Battery storage	2 hours storage duration	*optimisation variable*
	6 hours storage duration	*optimisation variable*
	10 hours storage duration	*optimisation variable*
Hydrogen storage	350 hours storage duration	*optimisation variable*
	700 hours storage duration	*optimisation variable*
Wind	Vestas V90-2000	*optimisation variable*
Regional demand	RES regions	*sampled regions in Gelderland*
Grid capacity		*see table 8.1*

Table 8.4: Target renewability electricity share.

Target renewability electricity share	Value	Unit
Current projection	*region specific: table 8.1*	%
60% target	60	%
80% target	80	%

Results are presented divided per renewability target, which is numbered 1 through 3, from current policy to 80% renewable electricity. The results of the 18 experiments are discussed in section 8.1.2. In this section, differences between regions are addressed. Moreover, the energy system configurations resulting from the optimisation constrained by current projection renewable electricity targets is compared to the deployment of technologies proposed in the RES policies for each of the regions.

The same interface to the configured model is used to generate a single experiment for the whole province of Gelderland, implementing a target of 60% renewable electricity. Since the cost-optimal energy system configurations for the same target is known, this can now be compared to the cost-optimal system configuration of the whole province of Gelderland at once by taking the aggregate of all regions. The result is discussed in section 8.1.3.

8.1.2 Results Regional Energy Strategies

In this section, the results from optimising energy systems on a regional level are presented. Each energy system is configured to cost-optimality by deploying various quantities of renewable energy generation and storage technologies. This depends on the grid connectivity of the region under investigation, as well as the specific demand profile of that region.

An overview of the results with relation to the location of the various RES regions within the province of Gelderland is given in figure 8.2. In addition, figure 8.3 provides a comprehensive overview by grouping the various targets per region.

Based on the figures, it can be seen that throughout all renewability targets, the deployed PV capacity is very stable. Current policy targets (which vary per region, as based on the RES - see table 8.7) can be reached most cost-effectively by deploying nearly no wind capacity. In any case, the PV capacity is significantly oversized in relation to the grid capacity. During any hour of the year where demand is lower than the generated power from PV, export followed by curtailment occurs. From this, it can be concluded that under the cost assumptions used, oversizing PV generation is most cost-effective in reaching the lower percentages of renewable energy in electricity.

Another observation is that the optimally deployed wind capacity increases with an increase in the renewable electricity target. This occurs in all regions, although to varying degrees. When comparing Rivierenland and Arnhem Nijmegen for example, it is clear that the relative increase in wind capacity is more substantial for Arnhem Nijmegen. This can be attributed to the difference in the demand profiles of the two regions, which in part determine the most optimal configuration. When comparing Arnhem Nijmegen to Achterhoek, a similar but distinct observation can be made. The RES region of Achterhoek employs a combination of wind and battery storage to reach the 80% renewable electricity target while Arnhem Nijmegen reduces the small number of batteries deployed and switches to wind deployment.

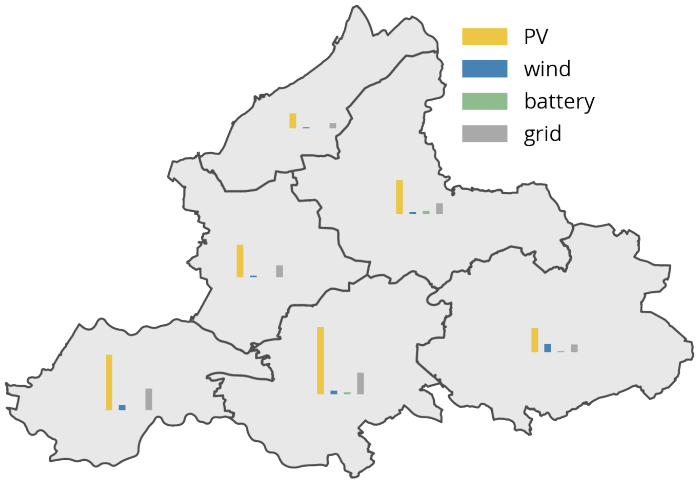

(a) Current policy renewability target

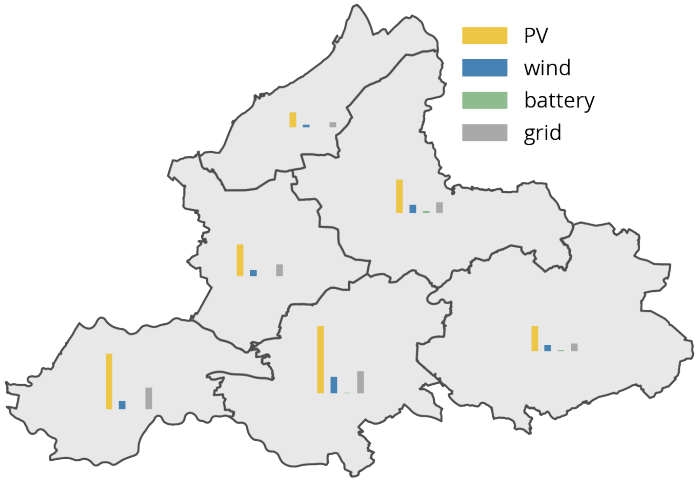

(b) 60% target

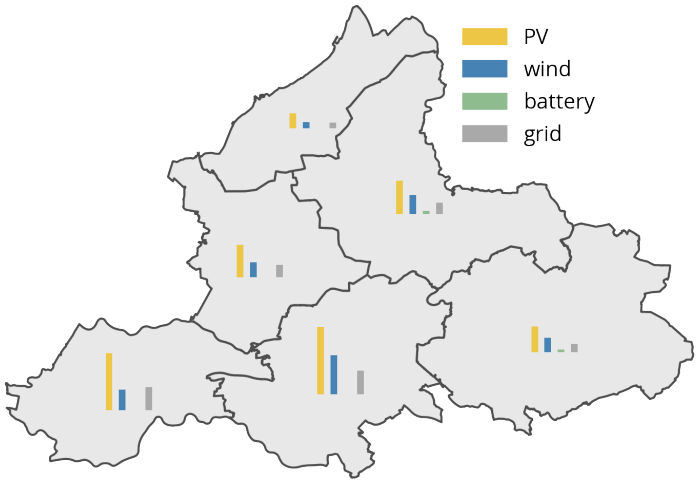

(c) 80% target

Figure 8.2: The resulting energy configurations are shown in a geographic plot for each of the renewable electricity policy targets.

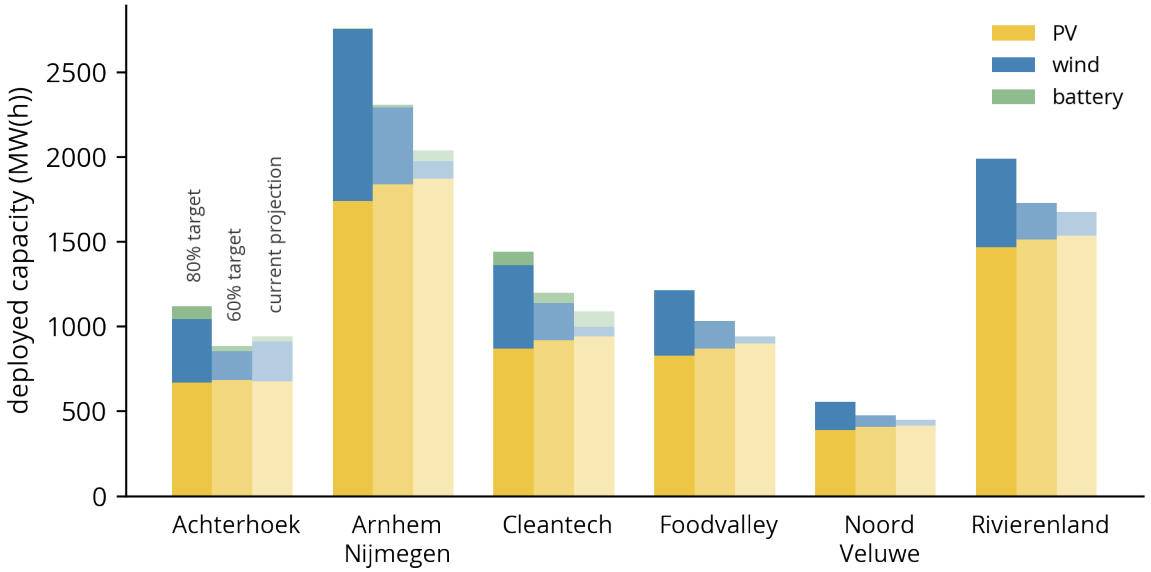

Figure 8.3: Overview of cost-optimal energy system configurations for various renewable electricity targets grouped per RES region.

Interestingly, only two RES regions deploy battery storage for reaching the 80% target. None of the regions employs hydrogen storage to any degree. From this, it can be concluded that on regional level storage does not fulfil a significant role in optimal configurations with up to 80% renewable electricity. This can be attributed to the backup capacity that is present in the national grid, which is more cost-effective at providing balancing power for intermittency and seasonality than regionally deployed storage. The target is implemented such that 80% renewable electricity for self-consumption means a maximum of 20% of consumed electricity from import on a yearly basis. It is more cost-effective to depend on the grid for closing the energy balance for 20% of the energy than to deploy more generation capacity or incorporate energy storage within the region.

Lastly, when imposing renewable electricity targets per region the deployment of renewable energy generation assets is correlated to regions of high electricity demand. This can be seen from figure 8.2, where the three most densely populated regions also have to deploy the largest amount of wind and PV to reach regional targets. Considering the land use of, and public aversion to large scale wind and solar PV projects, it could be noted that imposing regional self-consumption targets is not ideal. If more rural regions are able to supply more urbanized regions with their electricity, this barrier can in part be averted. This does pose a possible cost trade-off that cannot be evaluated in this model, which is the cost of increasing grid capacity between the regions to improve inter-connectivity.

In figure 8.4 the cost-optimal configuration of regional energy systems that reach the projected share of renewable electricity is compared to system configuration as proposed in the RES of each region. In this figure, the optimal deployed capacity has been translated to yearly energy yield based on the capacity factors of wind and PV in the considered configuration. As a result, the cost-optimal deployment of technologies can be compared to the expected energy yield from renewables as proposed in each of the RES regions.

From the figure, it can be observed that most regions are in fairly good agreement, both in terms of total yearly energy yield from renewable (depicted by the size of the pie) and the ratio of wind to solar PV. It can be seen that all regions but Cleantech deploy a larger share of wind energy in their

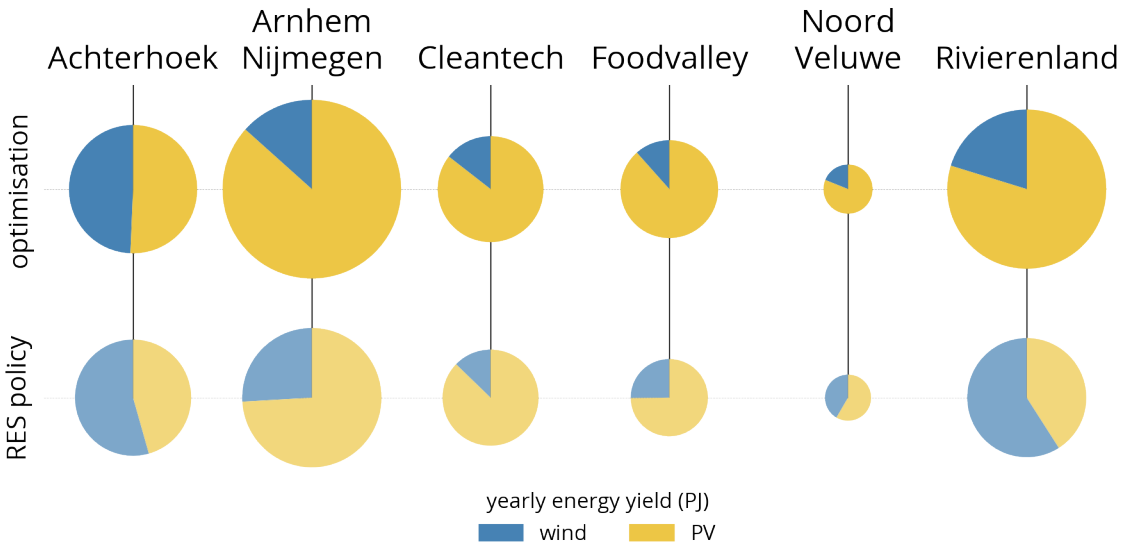

Figure 8.4: Current policy renewable electricity targets per region, comparison between the system configurations found by using optimisation and the configurations determined in the Regional Energy Strategies.

configurations. This is most notably in the RES region of Rivierenland. When observing this region, it can also be noted that the total yearly energy yield can also be substantially lower when the ratio of wind to solar PV is higher.

This can be coupled to observations on the results presented in section 7.1, where a ratio of 1:1 between solar and wind does not substantially increase curtailment. In that case, the constrained grid capacity can be interpreted as a baseload that does not need to be met at all times. In the regions, however, the load profiles exhibit seasonal variations and should be met by renewables for 60% of the yearly energy volume. Increasing the deployed wind capacity in the region of Rivierenland improves the correlation between demand and generation, reducing overall generated renewable electricity because less is curtailed or exported but instead consumed locally.

When considering the results presented in figure 8.3, it should also be noted that an increase in the share of wind in the energy mix is desirable for cost-optimally reaching higher shares of renewable energy in the locally consumed electricity. From this, it can be concluded that under the assumed static cost conditions in this set of experiments it is not sufficiently economical to deploy battery storage for intra-day power matching of otherwise curtailed energy and local demand. Neither does employing hydrogen-based storage for seasonal storage fulfil any role in reaching renewable electricity goals up to 80%.

8.1.3 Aggregation to Gelderland level

This section compares the aggregate energy system configuration of individually optimised RES regions to the energy system configuration determined by optimising Gelderland on a provincial level. This is done for a renewable electricity target of 60%, which is imposed both on the individual RES region models and the provincial model.

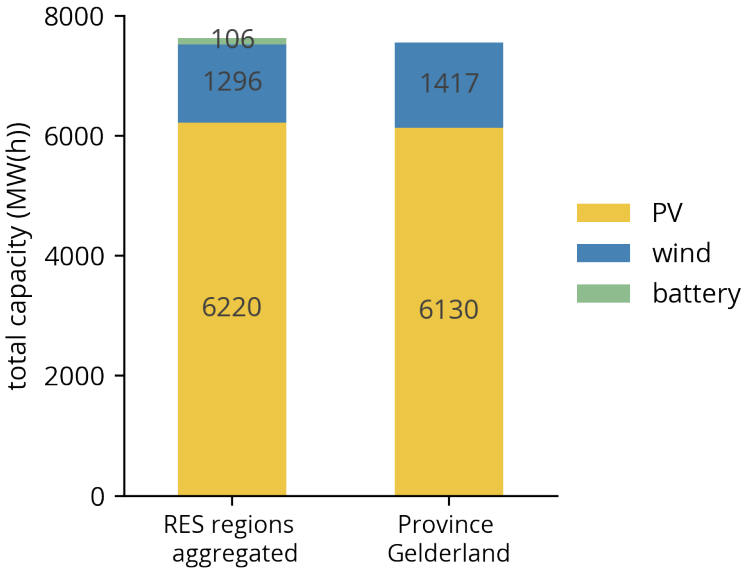

Figure 8.5: Energy system configurations are determined by optimisation of the individual RES regions versus optimisation of Gelderland on provincial level by imposing a 60% renewable electricity target.

The cost-optimal configurations for both approaches are shown in figure 8.5. From this figure it directly becomes clear that both configurations are in very good agreement in terms of deployed capacities of all technologies under consideration. There is a slight variation in deployment of storage, of which a relatively small quantity is deployed when optimising the RES regions which is not found in the provincial level optimisation. The lack of battery storage in the provincial level model is countered by a slight increase in the deployed capacity of wind. This can be explained by the fact that locally specific behaviour is slightly dampened by considering a larger region in a similar model. Peaks and variations of specific demand sectors are more subtle and balanced by other components in the system.

Optimising the energy system on a provincial level instead of for every region represents the aggregate outcome of optimising individual RES regions within the province accurately. Moreover, by reducing the regional models under consideration from six to one region, the dimensionality of experiments and subsequently results is reduced. This improves the transparency of the results and reduces computational demands significantly.

8.2 Gelderland

In this section the model under consideration is Gelderland in 2030 on a provincial level. In section 8.1.3, it was found that optimising on a provincial level leads to very similar outcomes when compared to cost-optimal system configurations found using models on RES regional scale. In addition, this approach greatly reduces computational requirements. This is important if the model under consideration is exposed to uncertainty, which requires solving the same model under slightly different conditions. Section 8.2.1 outlines the model configuration, cost uncertainties and their ranges, and defines the policies. In sections 8.2.2-8.2.5, the results of exposing the model under consideration to cost uncertainties and varying renewable electricity targets are presented. Section 8.2.6 present an overview of all experiments in this study. Finally, section 8.3 concludes this chapter.

8.2.1 Parametric uncertainty exploration

This section introduces the model under consideration and cost uncertainties applied to obtain the set of experiments that are optimised in this section. Because the approach is nearly identical to the method applied in 8.1, this description is brief to refrain from unnecessary repetition.

An overview of the components considered in this model and their respective configuration can be found in table 8.5. The regional demand is based on the ETM scenario that reflects the aggregate of all RES scenarios within the province. The link to the scenario can be found in appendix E.2, which can be browsed through a graphical interface to discover the parameters used in this scenario.

The grid capacity is determined based on the transformer capacity between the regional distributional medium voltage network and the higher voltage transport network (150 kV). This reflects the interconnectivity of the province under the assumption that the transformer capacity is the bottleneck for transporting electricity from outside the province to and from electricity sources and sinks.

Table 8.5: Model set-up for the Gelderland 2030 under uncertainty.

Component	Configurations	Installed capacity
PV	South	*optimisation variable*
	East	*optimisation variable*
	West	*optimisation variable*
Battery storage	2 hours storage duration	*optimisation variable*
	6 hours storage duration	*optimisation variable*
	10 hours storage duration	*optimisation variable*
Hydrogen storage	350 hours storage duration	*optimisation variable*
	700 hours storage duration	*optimisation variable*
Wind	Vestas V90-2000	*optimisation variable*
Regional demand	Provincial level	*Gelderland 2030*
Grid capacity		2150 MW

This set of experiments exposes the model under consideration to cost uncertainties regarding the technology capacity cost. An overview of the range and method of sampling of those uncertainties is given in table 8.6.

Table 8.6: Uncertainties sampled in the Gelderland 2030 parametric uncertainty exploration

Component	Sampled parameters	Method	Cost range			Unit
PV	Capacity cost	LHS	388	-	867	€/kW
Wind	Capacity cost	LHS	900	-	1280	€/kW
Lithium storage	Energy cost component	*LHS*	114	-	194	€/kWh
	Power cost component	*linear map*	108	-	208	€/kW
Hydrogen storage	Power cost component	LHS	2022	-	3720	€/kW
	Energy cost component	*linear map*	12	-	21	€/kWh

The policies that are implemented in this set of experiments impose a minimal share of renewable electricity on the optimisation problem. These are numbered 1 to 4, in increasing shares of renewable electricity. Per policy, a total of 250 experiments are created by sampling the uncertainty space spanned by the parameters shown in table 8.6. This yields a total of 1000 experiments.

Table 8.7: The renewable electricity targets applied to the model that forms the policies of this set of experiments.

Target renewability electricity share	Value	Unit
No target	-	%
60% target	60	%
80% target	80	%
100% target	100	%

To maintain readability and transparency, these results are presented separately per policy in sections 8.2.2-8.2.5. The clustering and visualisation pipeline proposed in this thesis (see section 7.2.8) is also applied to this set of results, as it greatly reduces the obscurity of results and enhances the transparency of results. An overview and comparison of the results per policy are presented in section 8.2.6.

8.2.2 Results policy 1 - No renewable electricity target

In this policy, no target is imposed on the minimal share of renewable electricity. As a result, the optimisation algorithm will only deploy technologies when the current grid capacity is insufficient for future peak demands or when it is more economical to locally generate electricity than it is to import it from the national grid.

In short, it can be stated that for a large region within the cost uncertainty range of PV it is economical to deploy a substantial amount of PV. When the capacity cost of PV drop below a certain threshold, at least 5 GW of PV is cost-optimal for the province of Gelderland. For the 250 experiments in this policy, 189 deploy anywhere between 5 and 8.5 GW of PV capacity. The other technologies are under no circumstance deployed without a renewability constraint in place.

Within this set of results, the proposed clustering approach was applied to identify similar energy system design configurations. In this set of results, two clusters were found which are shown in terms of technology deployment in figure 8.6 and in figure 8.7 the clusters are related to the sampled cost uncertainties.

- **Cluster 1 — PV deployment, 189 outcomes**
  PV deployment between 5 and 8.5 GW.
  PV cost factor below 0.75, corresponding to a capacity cost of 765 €/kWp.

- **Cluster 2 — no PV deployment, 62 outcomes**
  No PV deployment
  PV cost factor above 0.75, corresponding to a capacity cost of 765 €/kWp.

It is interesting to note that the cost-optimal system configuration for Gelderland in 2030 without renewable energy enforcing policies is in good agreement with the aggregate of the RES policies within the region, as shown in section 8.1.3. This conformity is in essence substantiation that deploying substantial quantities of PV is a no-regret decision.

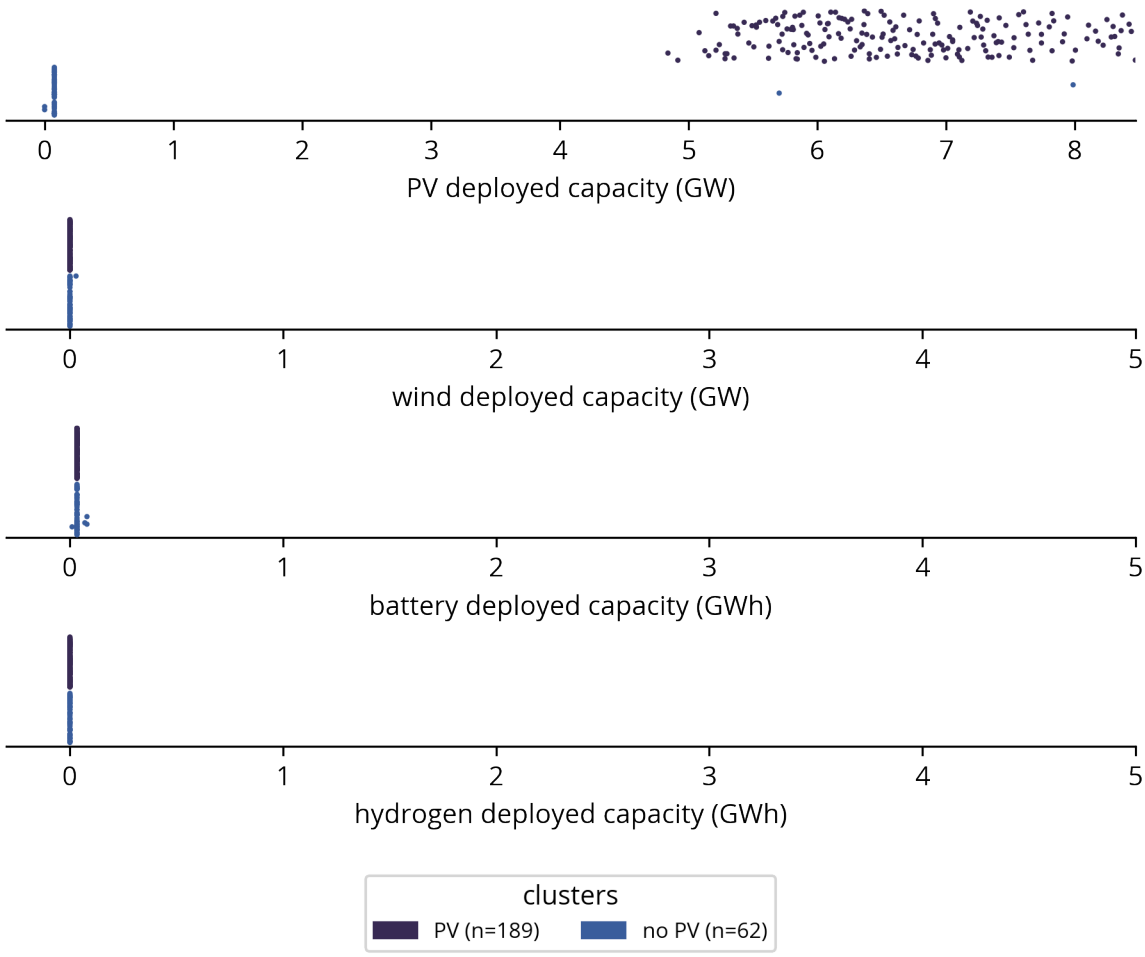

Figure 8.6: Strip plot of the various cost-optimal system configurations found under cost uncertainty, colour-marked by the determined clusters in the case where no renewable electricity target is imposed *(policy 1)*.

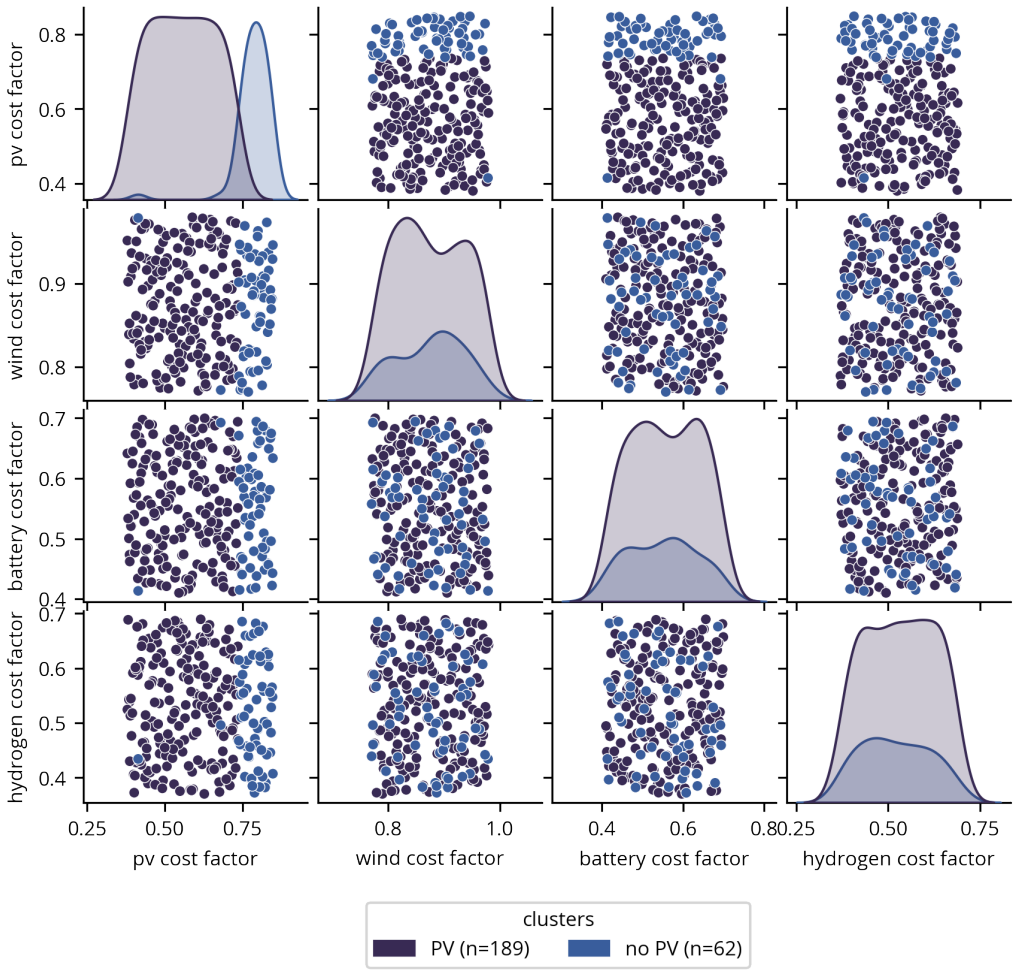

Figure 8.7: Pair plot depicting the identified system configuration clusters in relation to the sampled cost uncertainties in the case where no renewable electricity target is imposed *(policy 1)*.

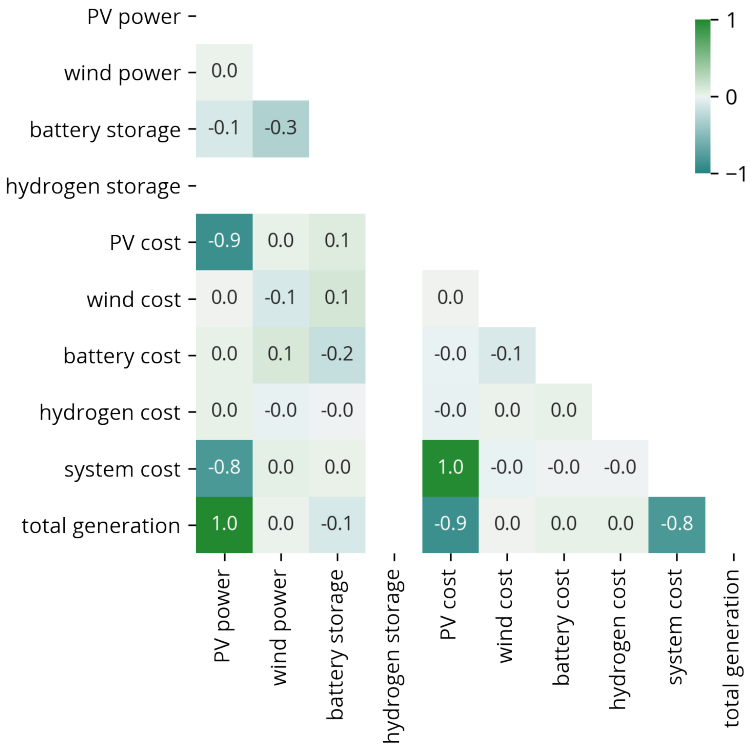

Figure 8.8: Correlation matrix with no renewable electricity target *(policy 1)*

As part of the proposed data handling procedure, figure 8.8 depicts the correlations between the cost uncertainties, deployed capacities and total system cost. However, since there is only one axis of variation, namely PV deployment, all variables are correlated to either PV capacity cost or deployed PV capacity.

Although not very dynamic, this outcome forms an approachable introduction to analysing and consulting results based on clustering and the applied visualisation strategy. Remember, all sampled uncertainty planes and corresponding technology deployments require 26 plots to fully unpack the dimensionality of the resulting data. Although some specific information is lost through the implementation of this approach, the transparency gain is substantial. If policymakers, project developers or consulting engineers are interested in these specifics, it is still possible to dive into those results since the underlying data remains unchanged.

8.2.3 Results policy 2 - 60% renewable electricity target

In this policy, a target of 60% is imposed as the minimal share of renewable electricity. Within this set of results, the proposed clustering approach was applied to identify similar energy system design configurations resulting in three clusters that each describe a distinct system configuration. These clusters are shown in terms of technology deployment in figure 8.9. Figure 8.10 relates the clusters to the sampled cost uncertainties.

- **Cluster 1 — maximum PV deployment, 75 outcomes**
  Maximum PV deployment, minimum wind deployment and the only cluster with battery deployment

- **Cluster 2 — moderate, 47 outcomes**
  Moderate PV and wind deployment without battery deployment

- **Cluster 3 — maximum wind deployment, 128 outcomes**
  Maximum wind, minimum PV, no battery deployment

Consulting the pair plot shown in figure 8.9 reveals that the various clusters are determined mostly by the PV cost factor because the clusters can be very clearly distinguished on all axes with the PV capacity cost factor. Cluster 1 contains configurations that nearly all result from the upper half of the uncertainty range of PV. This cluster shows clear uni-modality for the PV cost factor distribution and no evident mode for the other uncertainties. The inter-cluster variation of PV and wind is explained based on the various cost ratios that are found in this cluster since it contains samples in the complete range of wind capacity costs.

Cluster 0 and 2 can be distinguished from one another based on the tight grouping that is displayed by cluster 2 on one hand, and the range of inter-cluster cost-optimal configurations found in cluster 0. Moreover, cluster zero has the highest deployed capacities of PV and battery storage capacity. Finally, cluster 2 only occurs when wind capacity costs are relatively low and battery costs are relatively high.

In any case, the PV capacity deployed to reach this target is nearly the same as in the previous policy. However, to achieve a higher share of renewable electricity, additional wind capacity is deployed. Only when PV capacity is sufficiently economical, cost-optimal configurations can be found that reduce wind capacity while increasing PV capacity, when possible with battery storage.

Figure 8.11 depicts the correlation matrix of this policy. In contrast to the correlations calculated for the previous policy, this matrix reveals some interesting relations of which three are highlighted in the text. Firstly, the strongest correlations are found for wind and PV cost and deployed capacity. Deployed wind and PV capacity display a very strong negative correlation - implying a trade-off between the two technologies in any of the sampled combinations of cost uncertainties.

Another remarkable result is that the deployed wind capacity displays a stronger correlation to the price level of PV than to itself. This implies that wind deployment is more dependent on the cost of PV than on the cost of wind itself. Lastly, although battery storage only shows in a select set of system configurations, the system costs are still negatively correlated to battery deployment. This implies that any future system that is equipped with affordable battery storage is more cost-effective than similar systems without.

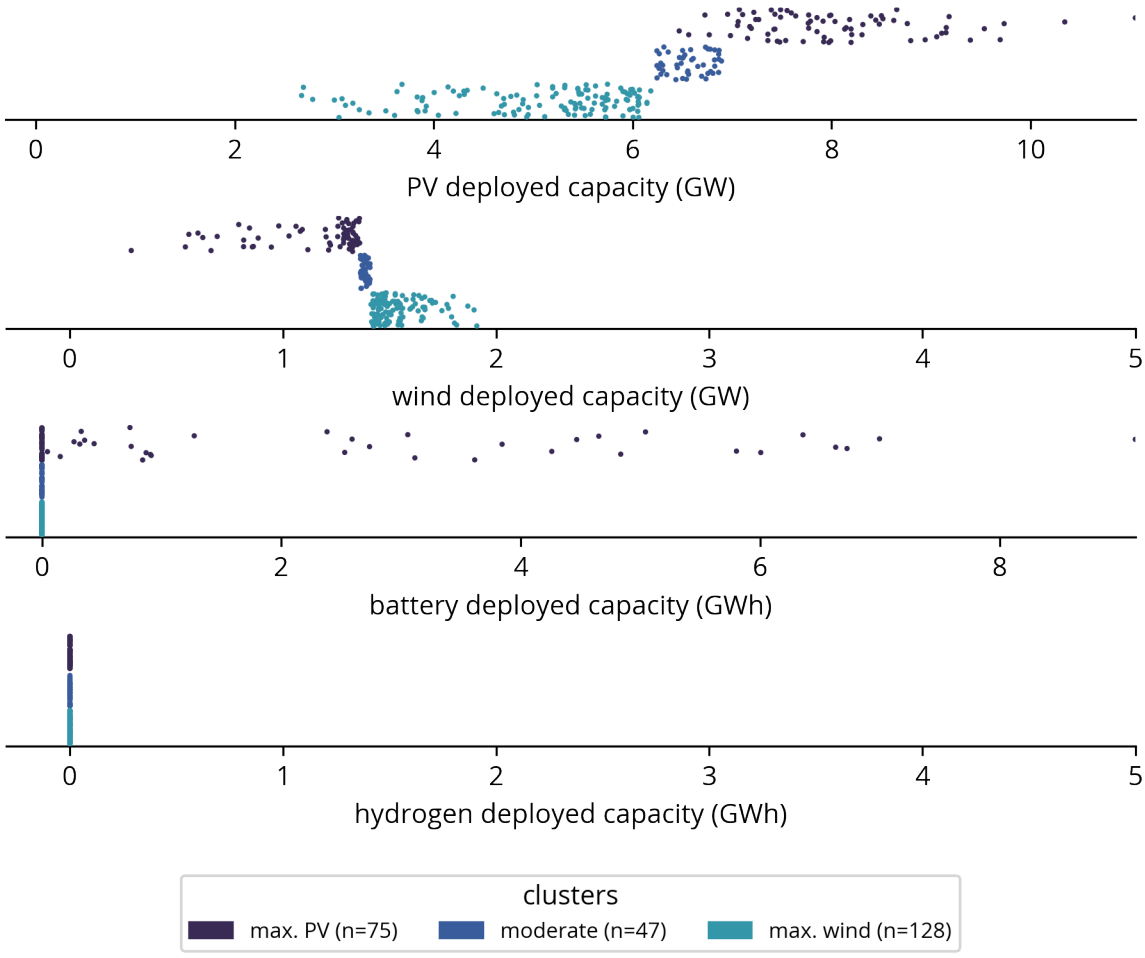

Figure 8.9: Strip plot of the various cost-optimal system configurations found under cost uncertainty, colour-marked by the determined clusters in the case where a 60% renewable electricity target is imposed *(policy 2)*.

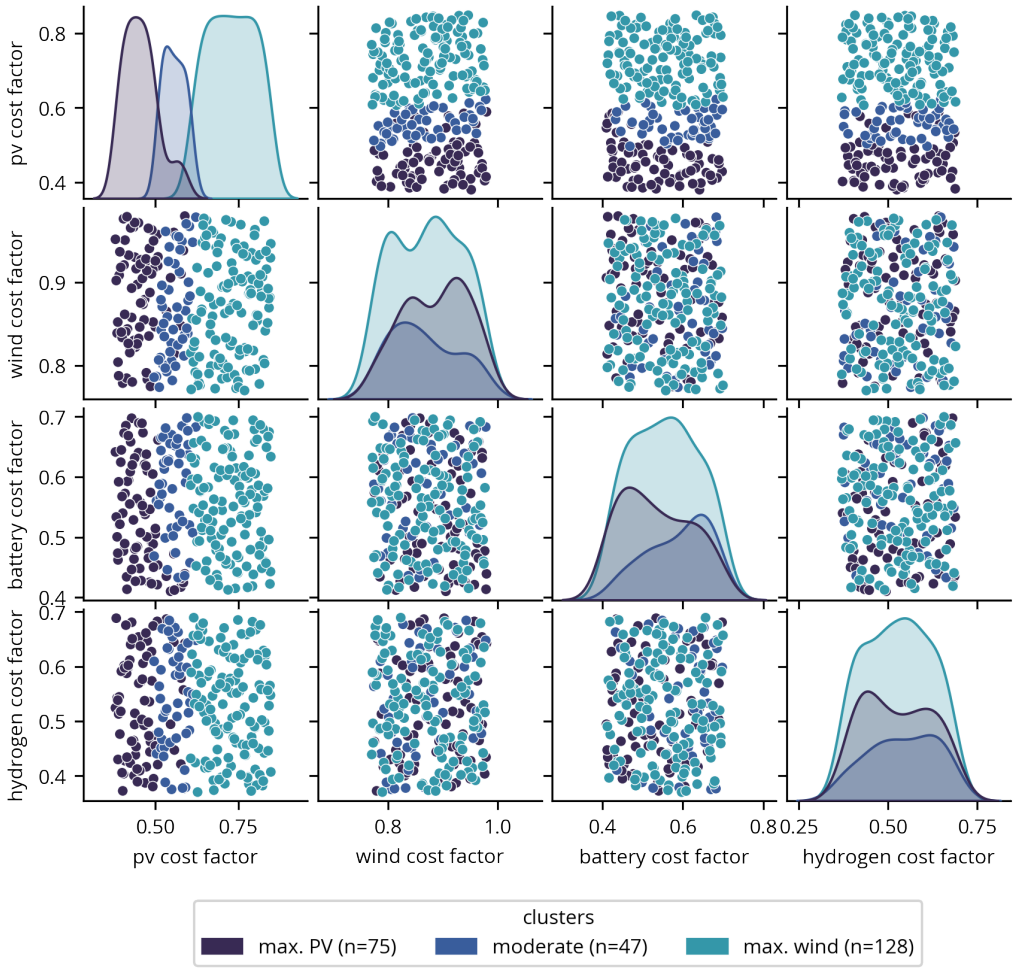

Figure 8.10: Pair plot depicting the identified system configuration clusters in relation to the sampled cost uncertainties in the case where a 60% renewable electricity target is imposed *(policy 2)*.

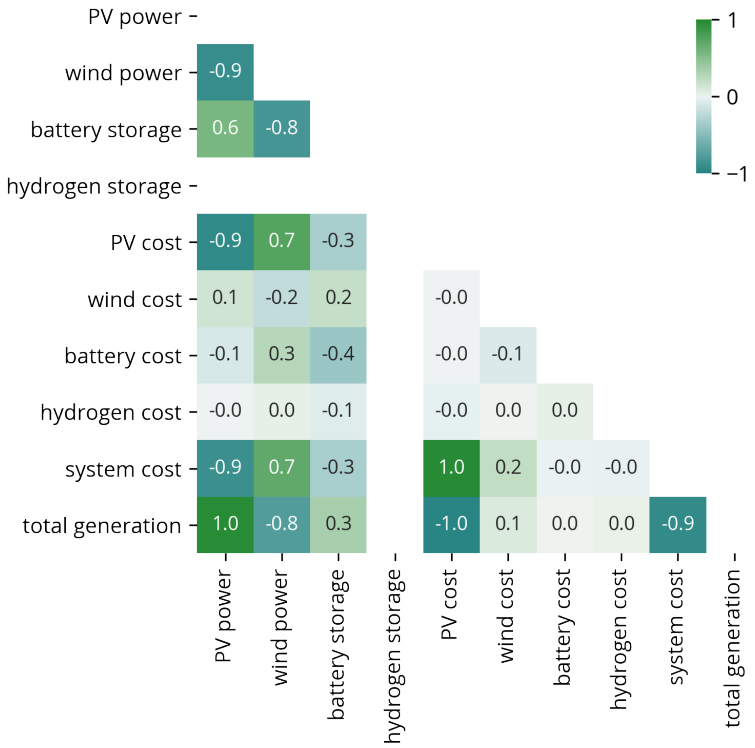

Figure 8.11: Correlation matrix with a 60% renewable electricity target *(policy 2)*

8.2.4 Results policy 3 - 80% renewable electricity target

This policy covers the cost-optimal system configurations found when a target of 80% is imposed as the minimal share of renewable electricity. Within this set of results, the proposed clustering approach was applied to identify similar energy system design configurations resulting in three clusters that each describe a distinct system configuration. The clusters are shown in terms of technology deployment in figure 8.12. Figure 8.13 relates the clusters to the sampled cost uncertainties.

A general observation that can be made is that a similar pattern starts to form as the renewability constraint increases. An increasingly higher share of renewable electricity leads to an incremental increase in deployed wind capacity, similar to cost-optimal configurations in the RES regions (section 8.1.2). However, exposing the model under consideration to cost uncertainty reveals an alternative route, where a substantial decrease in wind capacity is realised by deploying battery storage capacity under certain cost conditions.

- **Cluster 1 — maximum PV deployment, 75 outcomes**
  Maximum PV deployment, minimum wind deployment and the cluster with the highest battery deployment

- **Cluster 2 — moderate, 80 outcomes**
  Moderate PV and wind deployment, some battery deployment

- **Cluster 3 — maximum wind deployment, 95 outcomes**
  Maximum wind, minimum PV, minimum battery deployment

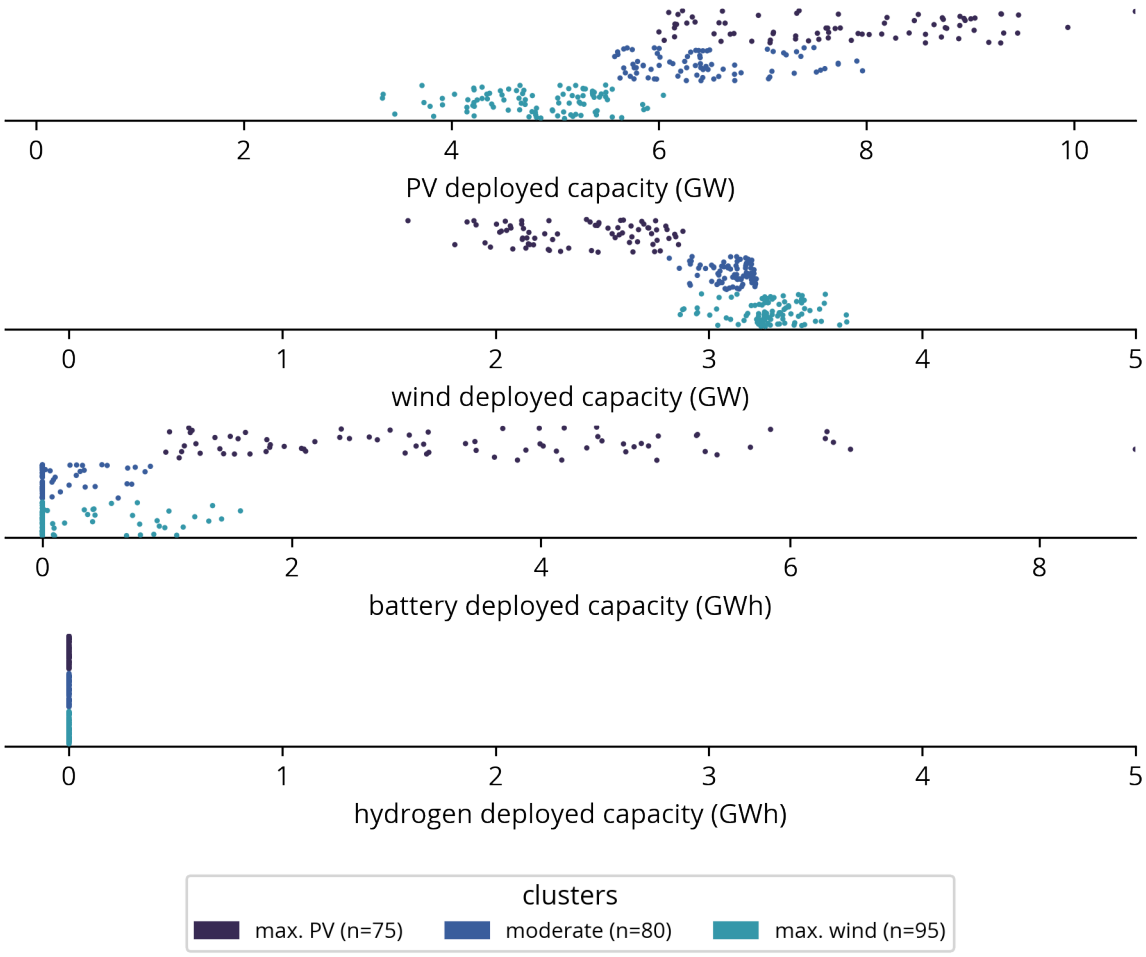

Figure 8.12: Strip plot of the various cost-optimal system configurations found under cost uncertainty, colour marked by the determined clusters in the case where an 80% renewable electricity target is imposed *(policy 3)*.

Utilizing figure 8.12 it is determined that a clear separation is found in the PV cost factor, where cluster 2 shows a clear mode in the upper-cost range. The other two clusters are found in the lower half of the cost range of PV. Not only in terms of cost of PV but also in terms of PV deployment clusters 0 and 1 display overlap in inter-cluster variations. The clear difference between clusters 0 and 1 is found in the deployment of wind and battery, where both cost and deployment of the technologies show clear modality.

In terms of inter-cluster configurations, the three clusters found in this policy set are well balanced. From this policy set, it can be concluded that high PV prices cast a dependency on deployed wind capacity or battery storage. Moreover, when battery capacity costs are sufficiently low, battery deployment is an option to reduce the deployed capacity of wind. In urban areas, this could remove spatial integration barriers while retaining high levels of self-sufficiency.

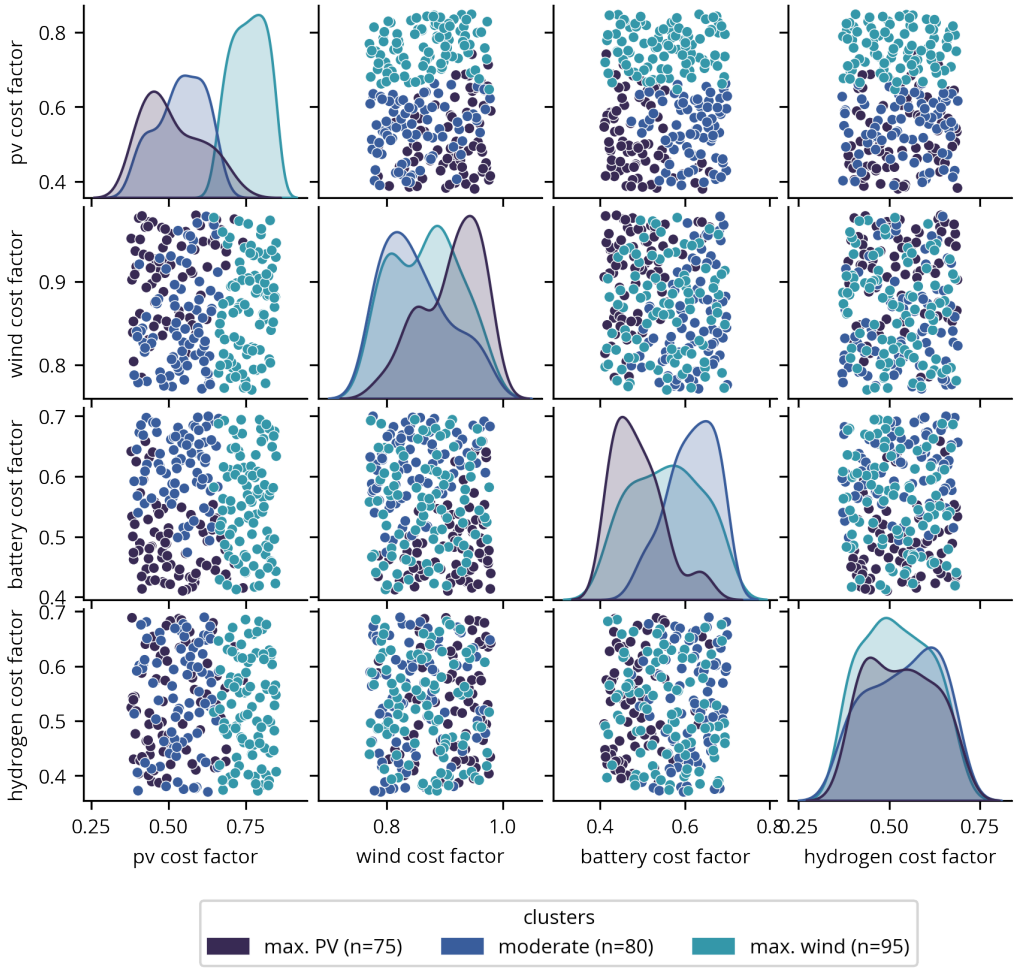

Figure 8.13: Pair plot depicting the identified system configuration clusters in relation to the sampled cost uncertainties in the case where a 80% renewable electricity target is imposed *(policy 3)*.

Figure 8.14 displays the correlation matrix calculated for this set of outcomes. This correlation matrix shows a number of specific relations of which a few are addressed in text. Firstly, there is a strong positive correlation between deployed PV capacity and battery storage capacity, indicating synergy between PV and battery deployment. The same strong negative correlation between wind deploy-

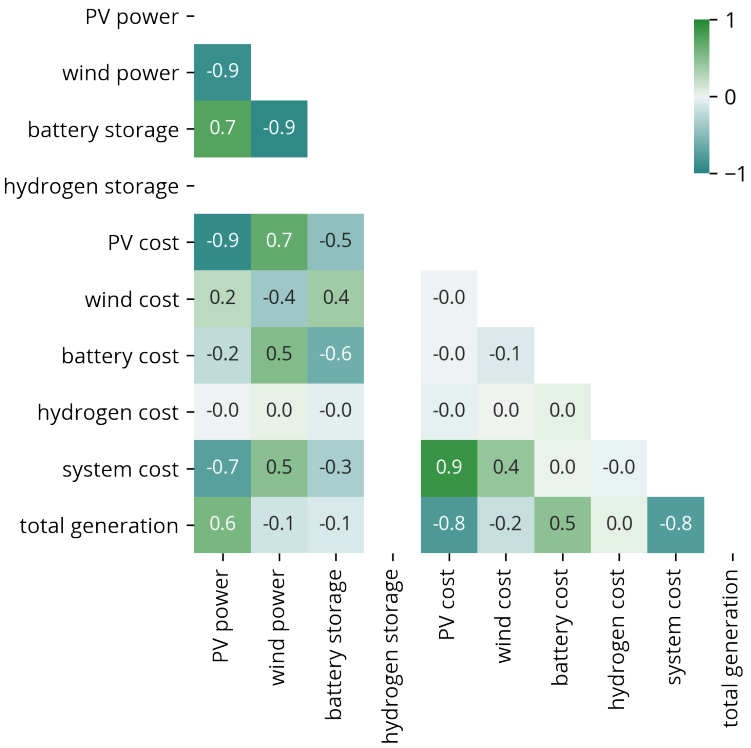

Figure 8.14: Correlation matrix with a 80% renewable electricity target *(policy 3)*

ment and PV deployment exists. Combining this observation with the synergistic appearance of PV and battery indicates that a trade-off exists between wind versus PV in some cases deployed with battery storage. Lastly, system costs are very strongly correlated to the cost of PV indicating that a cost reduction in PV has the biggest impact on reducing costs of all found cost-optimal system configurations.

8.2.5 Results policy 4 - 100% renewable electricity target

This section covers the result set that is based on optimisation of energy system configurations for Gelderland that comply with a target of 100% renewable electricity. The resulting energy system configurations have been clustered which yielded four clusters that each describe a distinct group of possible cost-optimal system configurations. The clusters are shown in terms of technology deployment in figure 8.12. Figure 8.13 relates the clusters to the sampled cost uncertainties. This set of results are the first that contain hydrogen storage deployment and substantial deployment of battery storage.

- **Cluster 1 — maximum PV deployment, 49 outcomes**
  Maximum PV deployment together with maximum deployment of battery storage. Hydrogen deployment is minimal, wind deployment is lower.

- **Cluster 2 — PV&hydrogen deployment, 35 outcomes**
  High deployment of PV and moderate wind deployment, lower battery and higher hydrogen deployment.

- **Cluster 3 — wind&hydrogen deployment, 103 outcomes**
  High deployment of wind and moderate PV deployment, minimal battery and maximal hydrogen deployment.

- **Cluster 4 — maximum wind deployment, 63 outcomes**
  Maximum wind deployment together with minimal deployment of PV. Both battery and PV deployment are moderate.

Comparing the deployment of PV in figure 8.15 between the various clusters, a separation can be made between clusters 0 and 3 against clusters 1 and 2. Clusters 0 and 3 span the high ranges of PV deployment and display significant overlap. However, the system configurations in cluster 0 mostly deploy a moderate amount of hydrogen and battery storage while cluster 3 deploys substantially more battery storage than hydrogen. Combining this insight with the pair plot (fig. 8.16), it can be noted that cluster 0 shows a clear unimodal distribution based on PV capacity cost, while cluster 3 spans a wider range. Moreover, cluster 0 displays no clear modalities on the other axes while cluster 3 shows a very clear modality in the lower range of the battery cost factor.

Cluster 2 shows high densities in the upper range of PV capacity costs and lower range of wind capacity in combination with high density in the upper range of hydrogen cost factors. This explains the observed higher deployment of wind in this cluster, which is unique when compared to the other clusters. As a result, configurations in this cluster display a lower hydrogen storage duration relative to the total installed capacity of generation. This implies that configurations in this cluster are dependent on the synergies in terms of seasonality between PV and wind.

Finally, cost-optimal configurations found in cluster 1 are uniquely defined based on their dependence on hydrogen as storage components. Inter-cluster configurations display the lowest deployment of battery storage deploying the highest quantity of hydrogen storage capacity.

Correlations between the various components in the found cost-optimal configurations and underlying cost uncertainties are computed and shown in figure 8.17. Remarkably, the strong negative correlation between PV and wind capacity found in all previous policies has weakened significantly. The strongest negative correlations are found between PV capacity cost and deployment, and between hydrogen and battery storage. Interestingly, hydrogen storage deployment shows a very strong negative correlation with total generation capacity while battery storage deployment displays a very strong positive correlation with total generation capacity. Since the system configurations display a substantial positive correlation with PV deployment, it is expected that hydrogen can be effectively employed to dampen seasonal dependence inherent to PV deployment and therewith reduce generation over-sizing effectively for PV.

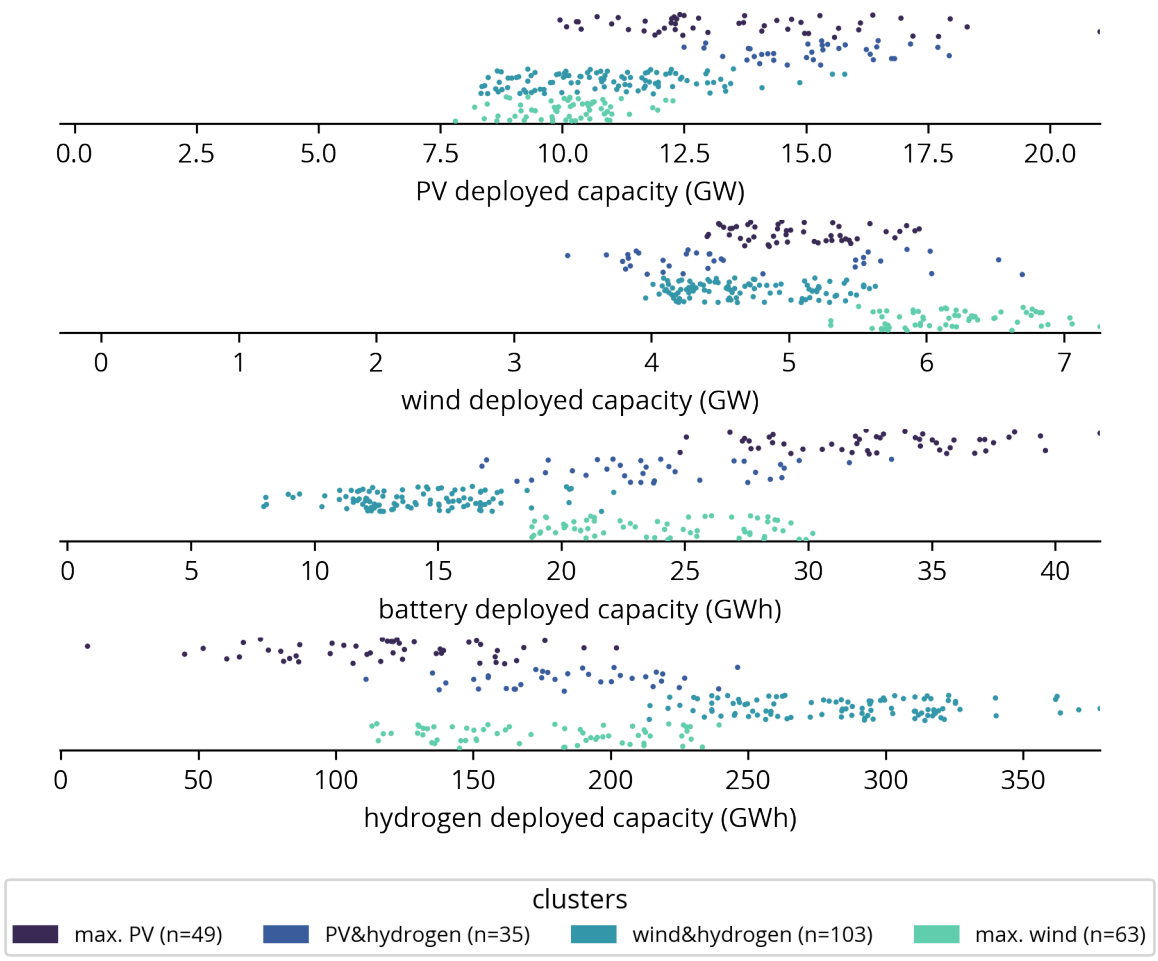

Figure 8.15: Strip plot of the various cost-optimal system configurations found under cost uncertainty, colour-marked by the determined clusters in the case where a 100% renewable electricity target is imposed *(policy 4)*.

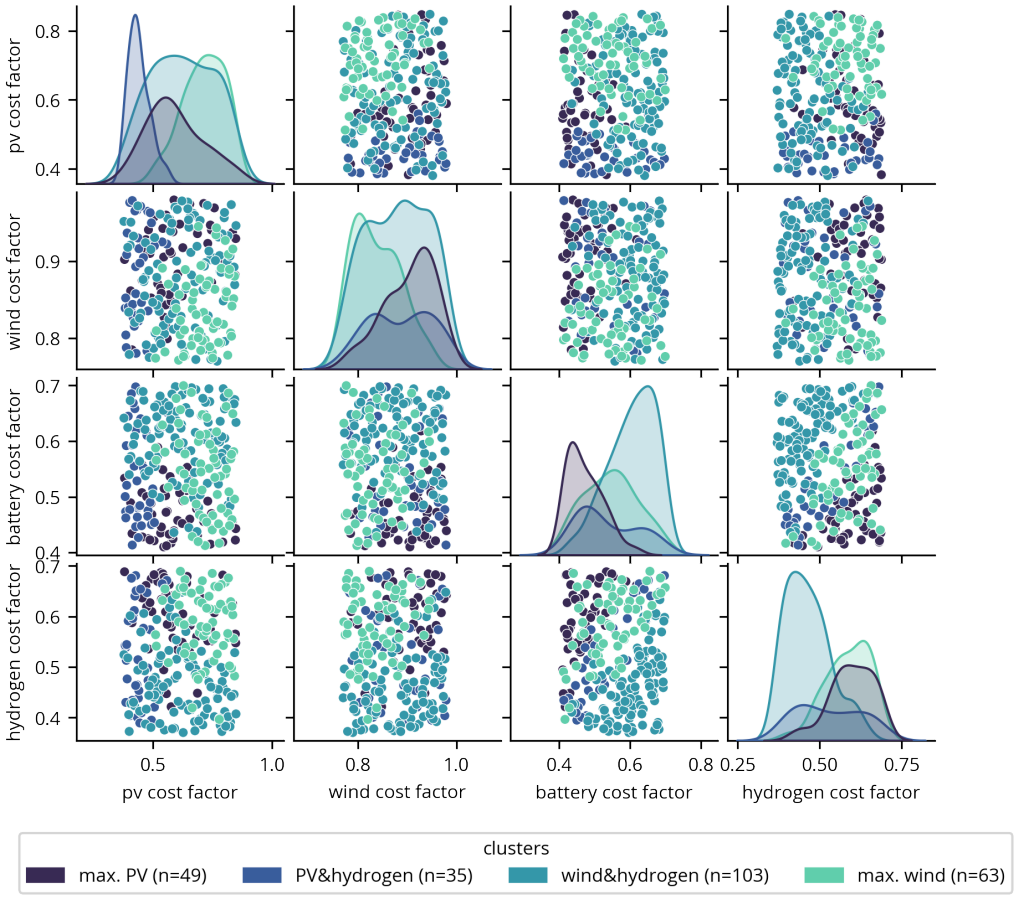

Figure 8.16: Pair plot depicting the identified system configuration clusters in relation to the sampled cost uncertainties in the case where a 100% renewable electricity target is imposed *(policy 4)*.

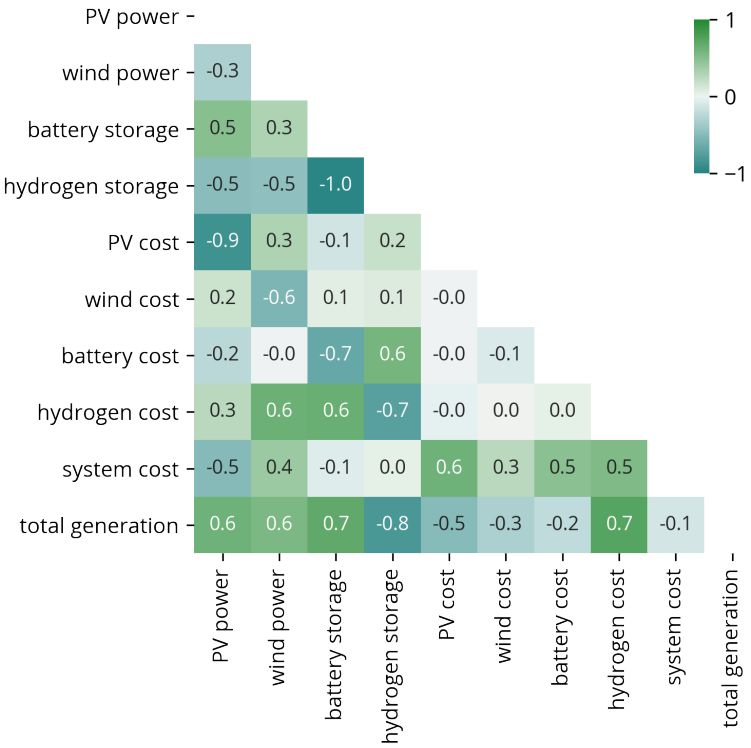

Figure 8.17: Correlation matrix with a 100% renewable electricity target *(policy 4)*

8.2.6 Overview

This section combines the insights of the previous sections to a higher level of abstraction as to provide an overview of all results generated in this section. As a graphically supporting reference, figure 9.1 displays the cost-optimal system configurations resulting from all four policies and all cost uncertainties.

Firstly, it should be noted that the no-regret capacity of PV to deploy is substantial. A minimum of 5 GW PV is found among nearly all outcomes, even without imposing a renewability constraint. Moreover, transitioning to a fully renewable and self-sufficient electricity system on a provincial level requires even more PV capacity to be deployed. This is a positive evaluation in terms of the proposed capacity of PV that RES policies aim to deploy in Gelderland.

Secondly, a clear trend in the amount of wind deployed in cost-optimal energy systems in relation to the renewability targets is observed throughout all sampled uncertainties. When the renewability targets increase, the minimal deployed capacity of wind also increases. However, the range of deployed capacity of wind in alternative cost-optimal also increases with higher renewability targets implying that the optimal deployment of wind is subject to change when storage options become competitive.

Considering the storage, substantial deployment is only required when the target is 100% renewable electricity. Battery storage is deployed to some degree when it is sufficiently low in capacity cost while hydrogen is only deployed in the 100% renewable electricity policy. On the other hand, there are no cost-optimal configurations within the sampled cost uncertainties that deploy no storage as soon as the 100% target is imposed.

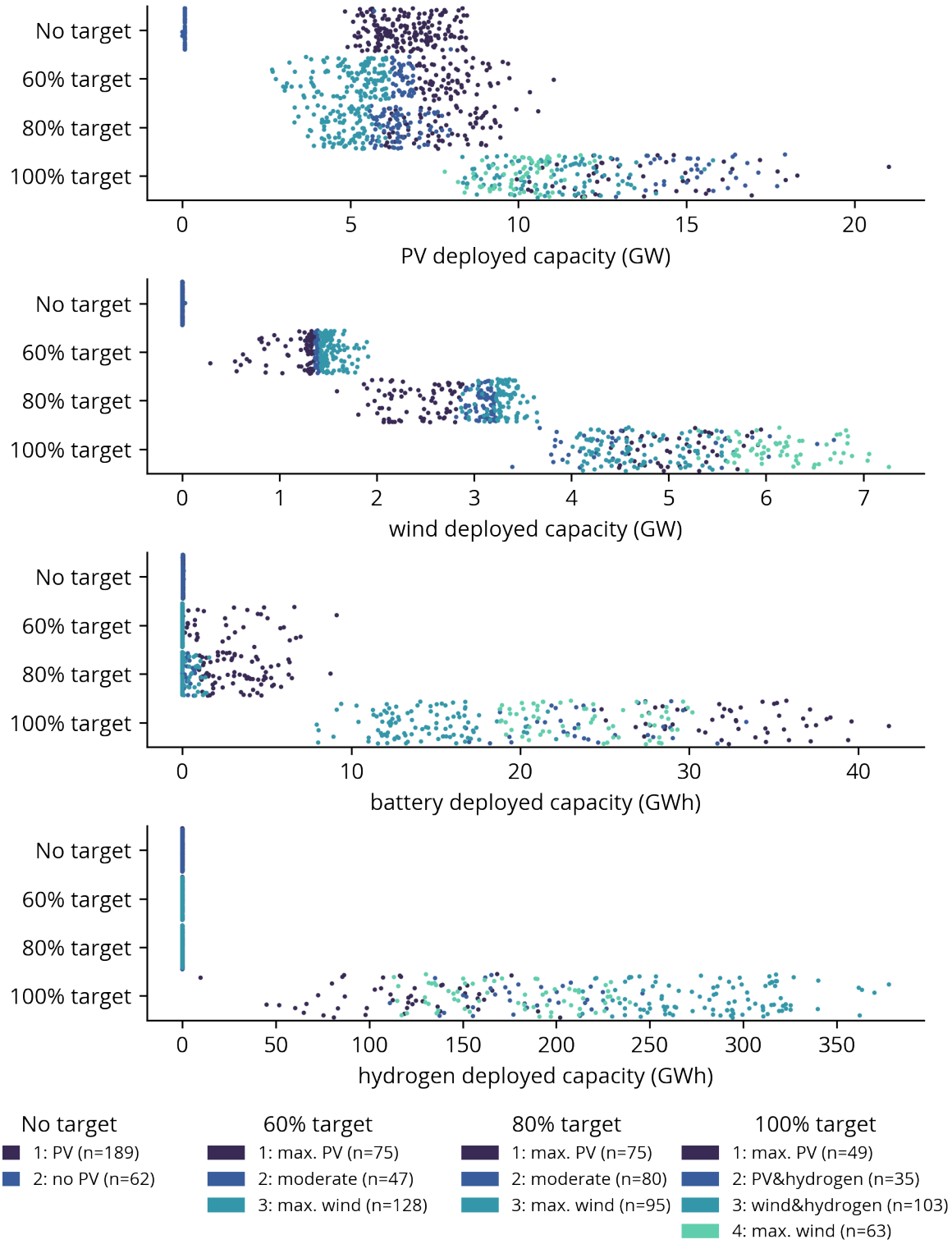

Figure 8.18: Strip plot of the various cost-optimal system configurations found under cost uncertainty, colour-marked by the determined clusters for all policies. Clusters are uniquely defined per policy, thus the combination of a policy and cluster colour denotes the identified clusters.

With regards to the clustering and visualisation pipeline as proposed in section 7.2.8, it should be noted that this approach is very effective at creating transparency and supplying insights in the response of cost-optimal deployment and correlations for higher-dimensional results. It is an effective method to dissect the complex deployment dynamics, correlations and the relationship to the cost uncertainties under various policies and large amounts of data.

Finally, by consulting 9.1 it is concluded that the traceability of clusters is obfuscated when the variation in the system configuration increases and the clusters display at least some overlap over some of the categories. This can be noted when comparing the 80% and 100% renewability targets and their respective clusters. While it is possible to locate clear segregation in the clusters found in the 80% target, it is very difficult to do so in the same figure for the 100% target. Characterizing the clusters using the strip plots per policy was still possible, as demonstrated in section 8.2.5.

8.3 Conclusion

In this chapter, two distinct optimisation studies were carried out on the province of Gelderland in 2030. In the first study, the regions of the Regional Energy Strategies were investigated. These regions each stipulate the deployment of renewable energy sources based on spatial integration. The achieved renewable electricity share was optimised under constant cost, without addressing uncertainty. To this end, the centre values of the ranges were applied.

How can exploring energy system optimisation models under uncertainty provide insights into cost-optimal system configurations to support (robust) energy transition policy? The results of optimisation were found in good agreement with the proposed deployment in the RES. In some regions, a notably larger share of wind energy was proposed by the RES when compared to the found cost-optimal configurations. As a result, the RES configuration has a lower total amount of renewable electricity generated that has a higher rate of self-consumption. The configurations found in optimisation imply a higher share of PV in cost-optimal configurations. This information can be used to provide an alternative pathway for more urbanized areas, where resistance to wind capacity is typically higher.

When the RES regions were exposed to more strenuous renewable electricity targets, the cost-optimal configuration increased in the ratio of deployed wind in relation to the deployed PV. For higher self-consumption, energy generation based on wind is more cost-effective than alternative configurations using PV and battery under centre cost values. Considering this increasing importance of wind for higher targets, deployment of a higher than optimal amount of wind for current targets will lead to a good basis for attaining higher shares of renewable electricity.

When comparing the resulting configurations of the six regions within Gelderland combined with the cost-optimal outcome of the province as a whole for the same target, good agreement was found between the configurations. The aggregate of the RES regions deployed only a slight amount of battery and slightly less wind. It is concluded that specifics on the RES regional level in terms of demand and grid capacity do not lead to substantially different results when compared to Gelderland on a provincial level.

Based on the observation that cost-optimal configurations on the provincial level are a suitable representation of the aggregate of configurations on the regional RES level, it is possible to expose only the provincial level model to cost uncertainty. In this way, key insights on the robustness of cost-optimal configurations are found. This was studied considering the cost uncertainties for PV, wind, battery and hydrogen under four increasing renewable electricity targets.

Even when no renewability constraint is in place, most cost-optimal configurations deploy substantial PV capacity in 2030. When the model is constrained to obtain higher shares of renewable electricity, the deployed capacity of wind increases for the whole range of possible cost-optimal outcomes. On the other hand, in all policies, a strong anti-correlation between deployed wind capacity and PV capacity is observed. In addition, the deployment of PV capacity shows a clear synergy of battery storage.

Enforcing a 100% renewable electricity target leads to the substantial deployment of storage in all cost-optimal outcomes. When the target is lower than 100%, the (seasonal) variability of renewable energy sources is resolved through import and export. Counter-intuitively, battery storage shows a positive relation to the total generation installed capacity while hydrogen displays a negative correlation. Additionally, it was found that the cost of PV capacity has the most substantial effect on system costs when considering all policies and all uncertainties.

The clustering and visualisation method as proposed in 7.2.8 was very effective in transparently presenting the resulting multidimensional data. The alternative approach of visualising every uncertainty plane and deployment of technologies would require a total of 26 plots for the result of this study, per policy. The clusters, based on the cost-optimal system configurations found, can be clearly distinguished in the strip plots. Through consultation of the respective pair plots, the relationship of those clusters to the cost uncertainties can be determined. Lastly, the correlation matrices give insight into deployment dynamics and inter-dependence at a glance.

Which cost-optimal system configurations can be identified for case studies within the province of Gelderland? By applying the clustering method, various patterns have been identified in terms of the deployment of renewable energy generation and corresponding storage. It was found that deploying 6 GW of solar PV that is proposed in the RES is a no-regret investment. Moreover, the slightly higher share of wind that is proposed in the RES forms the first step towards a fully renewable energy system of Gelderland. When the renewability target increases, wind increases per target. When the electricity system has to be fully renewable, solar PV deployment increases by at least another 4 GW. Depending on the costs, battery and hydrogen trade each other off. This is in part driven by the cost ratio between solar PV and wind. Wind is synergistic with hydrogen in most cases and ranges between 150 GWh and 300 GWh for most optimal configurations, while high deployment of solar PV leads to high deployment of battery storage (20 GWh).

It should therefore be concluded that in any case, a fully renewable energy system within Gelderland is dependent on higher amounts of wind than planned by the RES. Moreover, although not considered by the RES, storage technologies will play a substantial role in attaining higher shares of renewable electricity. Additionally, the optimal deployment of storage depends not only on the cost of the storage technologies but also on the cost of the generation assets. This means that the deployment of certain technologies now might determine the optimal constitution of storage technologies in the future.

Chapter 9

Gelderland 2050

This chapter exposes a model of Gelderland in 2050 under various scenarios to cost uncertainties. There are four scenarios that are considered, based on the fact that these four scenarios are currently widely adopted by both Dutch policymakers as grid operators (as described in section 2.2).

The model under consideration is configured in a nearly identical manner as done in section 8.2. The only substantial differences are that this chapter bases cost projections and the regional energy demand on the year 2050. Since there is such similarity in approach, this chapter is formulated aptly.

Section 9.1 presents an overview of the model under consideration, the cost uncertainties and the scenario's that have been implemented as policies. An overview of the results is presented in section 9.2. Finally, section 9.3 concludes this chapter.

9.1 Parametric uncertainty exploration

In this section, the configuration of the model under consideration is presented as well as the corresponding cost uncertainties. The approach of this study is very similar to the approach in section 8.5, but applied to 2050. The configuration of the model under consideration is shown in table 8.3. The grid capacity is determined based on the provincial transformer capacity between the regional distribution medium voltage (10-20 kV) and high voltage (150 kV) grid infrastructure. The regional demand is determined based on the corresponding II3050 tailored to Gelderland [17]. The corresponding ETM scenarios can be consulted through the graphical interface which is accessible through the links provided in appendix E.2.

Table 9.1: Model configuration for the Gelderland 2050 study.

Component	Configurations	Installed capacity
PV	South	*optimisation variable*
	East	*optimisation variable*
	West	*optimisation variable*
Battery storage	2 hours storage duration	*optimisation variable*
	6 hours storage duration	*optimisation variable*
	10 hours storage duration	*optimisation variable*
Hydrogen storage	350 hours storage duration	*optimisation variable*
	700 hours storage duration	*optimisation variable*
Wind	Vestas V90-2000	*optimisation variable*
Regional demand	Provincial level	*Gelderland II3050*
Grid capacity		2150 MW

Table 9.2 shows the range of capacity costs of all technologies considered in this study. These are all based on the upper and lower range of the projections as discussed in the respective component section in chapter 5.

The policies in these experiments are based on the four II3050 scenarios, specifically adopted for the province of Gelderland. Below a short overview of each of the scenario's is given. For a more extended overview of the scenario's either consult section 2.2.2 or the respective publications [17] [27] [30] [162].

Table 9.2: Uncertainties sampled in the Gelderland 2050 parametric uncertainty exploration

Component	Sampled parameters	Method	Cost range			Unit
PV	Capacity cost	LHS	255	-	734	€/kW
Wind	Capacity cost	LHS	905	-	1283	€/kW
Lithium storage	Energy cost component	LHS	69	-	194	€/kWh
	Power cost component	*linear map*	64	-	208	€/kW
Hydrogen storage	Power cost component	LHS	704	-	2871	€/kW
	Energy cost component	*linear map*	4	-	16	€/kWh

1. **Policy 1 - Il3050 Regional**
   This scenario is focused on regional control and energy autarky. Key concepts are high levels of decentralised power generation, by deploying high shares of on-land wind turbines and solar PV. The final energy demand from industry is assumed to shrink and electrify where possible. This results in a substantial reduction in energy demand.
2. **Policy 2 - Il3050 National**
   This scenario assumes strong leadership by the Dutch government. This allows for more centralized renewable energy sources, mainly an expanded capacity of offshore wind production. The industry remains roughly the same size. Energy self-sufficiency is achieved on a national level.
3. **Policy 3 - Il3050 European**
   Significantly less renewable energy is generated within the Netherlands leading to low self-sufficiency on a national level. Additionally, this scenario assumes a growing industry. The import of hydrogen, biomass and fossil fuels closes the energy balance. The scenario is centred around biomass and highly dependent on CO2 capturing technologies to mitigate or reduce emissions from fossil energy sources.

4. **Policy 4 - Il3050 International**
   This scenario displays the lowest self-sufficiency and renewability. This energy system configuration relies very heavily on the availability and import of green hydrogen. Additionally, this scenario assumes a growing industry and is the only scenario where the final energy demand increases. In this scenario, hydrogen and bio-gas could be feasible alternative energy sources for natural gas in gas plants.

Although the scenarios consider thermal plants based on alternative renewable energy sources a part of future energy systems, this is not considered in the model under consideration. This study is intended to provide insight into cost-optimal system configurations that are based on renewable energy sources, even when the considered scenarios are not strictly concerned with self-sufficiency.

A total of four policies is evaluated at 250 samples of the cost uncertainty space. This results in 1000 experiments that each produce a cost-optimal system configuration under the sampled conditions.

9.2 Results

This section presents and discusses the outcomes of the optimisation of Gelderland in 2050, based on four future scenarios for the province. When analysing the results it became clear that the effect that the different scenarios had on the model outcomes are substantially smaller than expected. This can be noted from the correlation matrices and the strip plots with clusters. The correlations are nearly similar and the strip plots display very similar patterns. However, some minor differences still exist between the regional and national scenario outcomes when compared to the outcomes of the European and international scenario, which to some extend can be seen from figure 9.1. Therefore, this only covers the results of policies 1 and 4, corresponding to the regional and international scenario. The results of all policies have been clustered and processed based on the approach proposed in section 7.2.8.

Based on analysis of the pair plots and strip plots in figures 9.3 and 9.2, respectively, the clusters resulting from the cosine hierarchical clustering are characterised for the regional scenario. The clustering on the Gelderland in the regional II3050 displays a very distinct mode in the density of the clusters over the various axes of cost uncertainty. In the corresponding pair plots, the density approximation shows a clear distinction between clusters 0 and 1 on the PV, battery and hydrogen axis. When one cluster is mostly found in the upper range, the other cluster shows a clear peak in the lower range. Most outcomes are found in these two clusters. The other two clusters show the same separability but on each of the axes.

Based on the densities that are shown in the pair plots, it can be concluded that the resulting clusters are indeed a unique result of the sampled cost uncertainties. Given the fairly well-distributed data, it is very positive that the clustering approach is still able to recognise patterns in design parameters. A quantitative description of the clusters found in the regional II3050 Gelderland scenario is given below.

- **Cluster 1 — maximum PV deployment, 90 outcomes**
  Maximum PV deployment together with maximum deployment of battery storage. Both hydrogen and wind deployment are minimal.

- **Cluster 2 — PV&hydrogen deployment, 34 outcomes**
  Moderate PV, low wind, low battery and high hydrogen deployment.

- **Cluster 3 — wind&battery deployment, 27 outcomes**
  Low PV, high wind, high battery and low hydrogen deployment.

- **Cluster 4 — maximum wind deployment, 99 outcomes**
  Maximum wind deployment together with maximum deployment of hydrogen storage. Both battery and PV deployment are minimal.

From this overview, it can be concluded that there are two sets of distinct opposite clusters. Clusters 0 and 1 inversely span the maximum and minimum range of PV and wind deployment. The same contrast is seen for the storage categories. Where cluster 0 deploys maximum battery and minimum hydrogen, cluster 1 opposes this deployment exactly. This is in good agreement with the observed relationship between the cluster and the cost uncertainty.

The second set of clusters is identified between clusters 2 and 3. Both clusters are more moderate in deployment ranges when compared to clusters 1 and 0. Cluster 2 combines high deployment of PV, with the high deployment of hydrogen, while the other capacities are deployed less. The opposite relation is noticed in the case of cluster 3, which deploys high quantities of wind and battery storage and less of the other two components. Remarkable is how well the clusters are separated, both in terms of the deployment modes and the relationship between the clusters and the cost uncertainties.

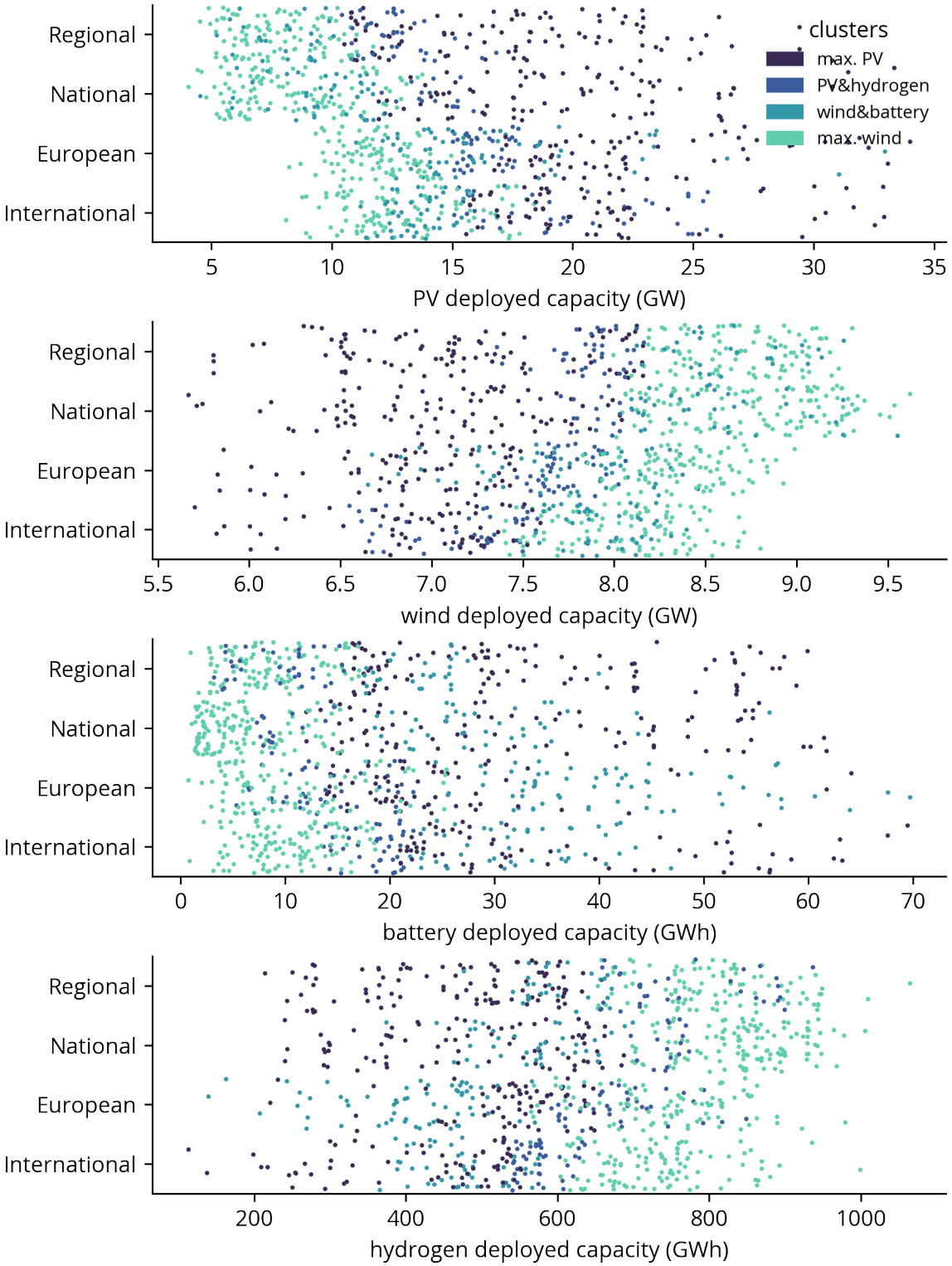

Figure 9.1: Strip plot of the various cost-optimal system configurations found in Gelderland 2050 study under cost uncertainty, colour-marked by the determined clusters for each of the policies. Clusters are uniquely defined per policy, thus the combination of a policy and cluster colour denote the identified clusters.

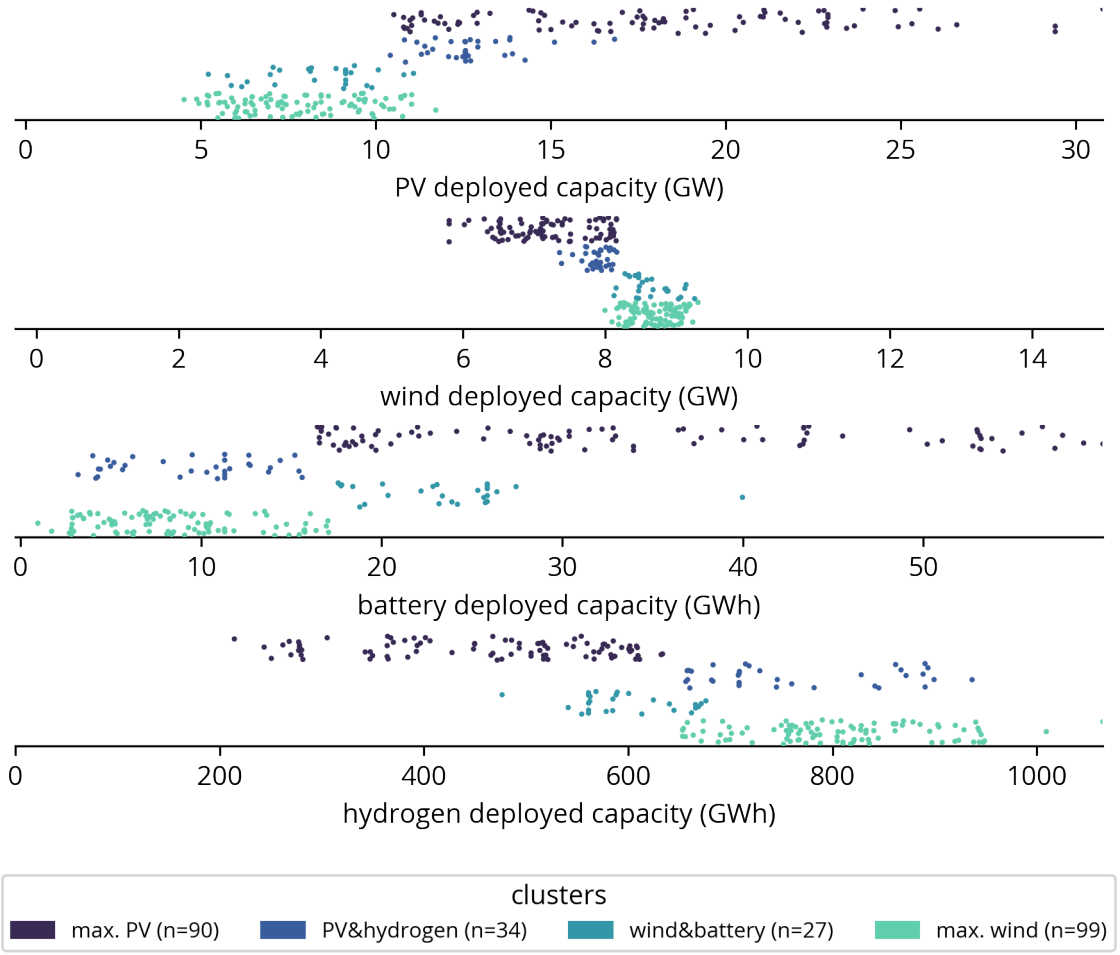

Figure 9.2: Strip plot of the various cost-optimal system configurations found under cost uncertainty, colour-marked by the determined clusters for the regional II3050 scenario (policy 1).

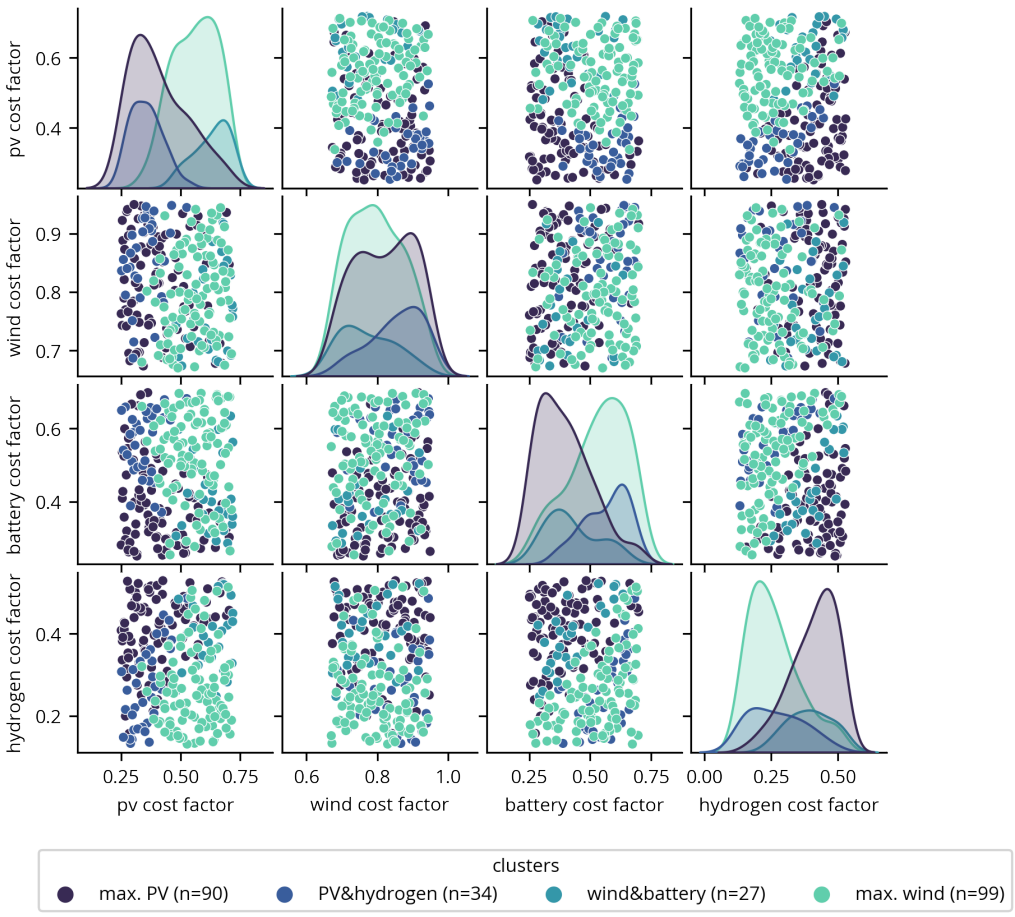

Figure 9.3: Pair plot depicting the identified system configuration clusters in relation to the sampled cost uncertainties for the regional II3050 scenario (policy 1).

Policy 4 is based on the international II3050 scenario of Gelderland. On the results within this policy, the same approach in identifying and characterizing the clusters is applied. A quantitative overview of the clusters is given below.

- **Cluster 1 — maximum PV deployment, 61 outcomes**
  Maximum PV deployment together with maximum deployment of battery storage. Both hydrogen and wind deployment are minimal.

- **Cluster 2 — PV&hydrogen deployment, 42 outcomes**
  Moderate PV, low wind, low battery and high hydrogen deployment.

- **Cluster 3 — wind&battery deployment, 43 outcomes**
  Low PV, high wind, high battery and low hydrogen deployment.

- **Cluster 4 — maximum wind deployment, 104 outcomes**
  Maximum wind deployment together with maximum deployment of hydrogen storage. Both battery and PV deployment are minimal.

Now, by comparing the quantitative description given for the clusters found in the regional scenario it is concluded that the same characteristic clusters occur in both scenarios. The number of inter-cluster configurations is different, implying that this scenario has a different impact on the most favourable system configuration, even when exposed to cost uncertainty.

Other than the quantitative description and the similarity in the found clusters in both scenarios, the absolute values are slightly different. PV deployment ranges from 5 to 25 GW in the regional scenario but ranges from 10 to 30 GW in the international case. Wind deployment shows agreement between the two scenarios, both ranges are centred tightly around 8 GW of wind. Battery storage shows a nearly similar range of deployment. Hydrogen storage is deployed in slightly higher amounts in the international scenario.

For each of the policies, a separate correlation matrix was created. However, they are nearly identical on all variables. Therefore, one single correlation matrix for all policies was calculated. This is shown in figure 9.4. A very strong negative correlation exists between wind and PV deployed capacity. Moreover, battery storage deployment is positively correlated with PV deployment and is negatively correlated with wind deployment.

From the quantitative description and analysis on clusters, it was determined that clusters exist that exhibit a contradiction to this correlation. These clusters are clusters 0 and 2 in the international scenario, and 2 and 3 in the national scenario. In both scenarios, these clusters are both less often present, and their deployment ranges are more constrained compared to the larger clusters.

Another interesting observation is that the deployment of wind still depends more on the cost of PV capacity than on the cost of wind capacity itself. This implies that wind is deployed because it is more effective at meeting the imposed constraints, but is less cost-effective. As soon as PV is sufficiently economical, a tipping point is reached where PV is over-sized to meet the constraint and is still more cost-effective than deploying wind capacity.

Finally, a big contrast when comparing this correlation matrix to the correlation matrix calculated for Gelderland 2030 with a 100% renewable target is that, in this study, the total system cost most

strongly correlates with the cost of hydrogen. This is most likely a result of the fact that the 2050 scenario's included various electrifying measures on heating, transport and industry. As a consequence, the seasonality of the demand profile increases and seasonal storage becomes more prominent in the energy configuration.

It should be noted that this set of experiments is the first of results that are quite uniformly distributed. As a result, the strip plot that is used to compare all scenarios (shown in fig. 9.1) no longer improves transparency, nor is an effective measure to support substantial analysis. In an attempt to improve on the visualisation, figure 9.7 was created. In this figure, every scenario still has a distinct axis. However, the resulting deployment values are not plotted directly but instead approximated using a kernel density approximation. This yields a distribution curve, that is better suited for visualising the more continuous data found in this data set. This is still a challenging graph to read, but it is way better equipped to visualise this sort of data. When investigated closely, the same cluster characteristics as described based on figure 9.2 and 9.5 can be recognized. It is recommended to use this chart over the strip plot when it is desirable to compare multiple policy results outcomes in one figure. However, whenever possible it is preferred to plot the strip plots per policy which are still very functional in visualising the data.

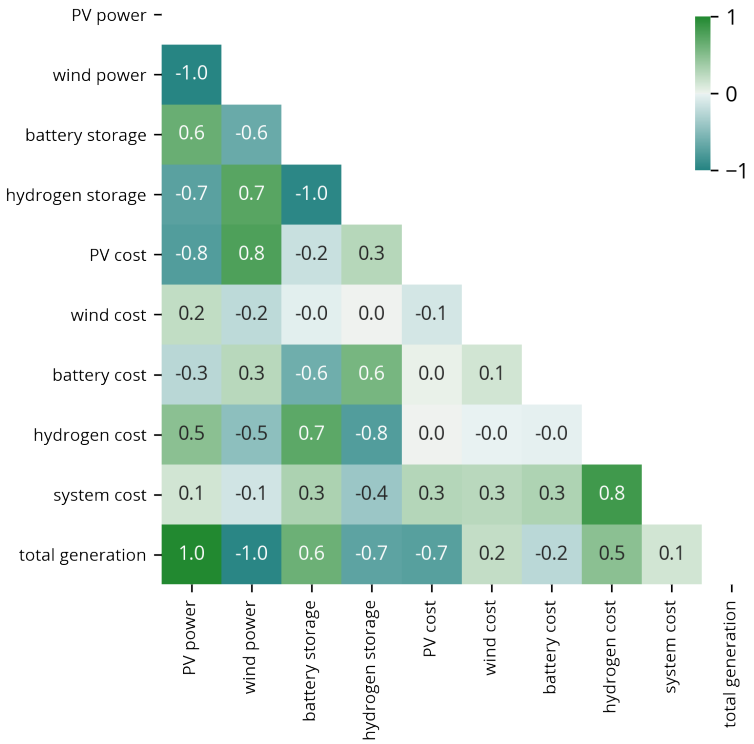

Figure 9.4: Correlation matrix for all Gelderland II3050 scenario's

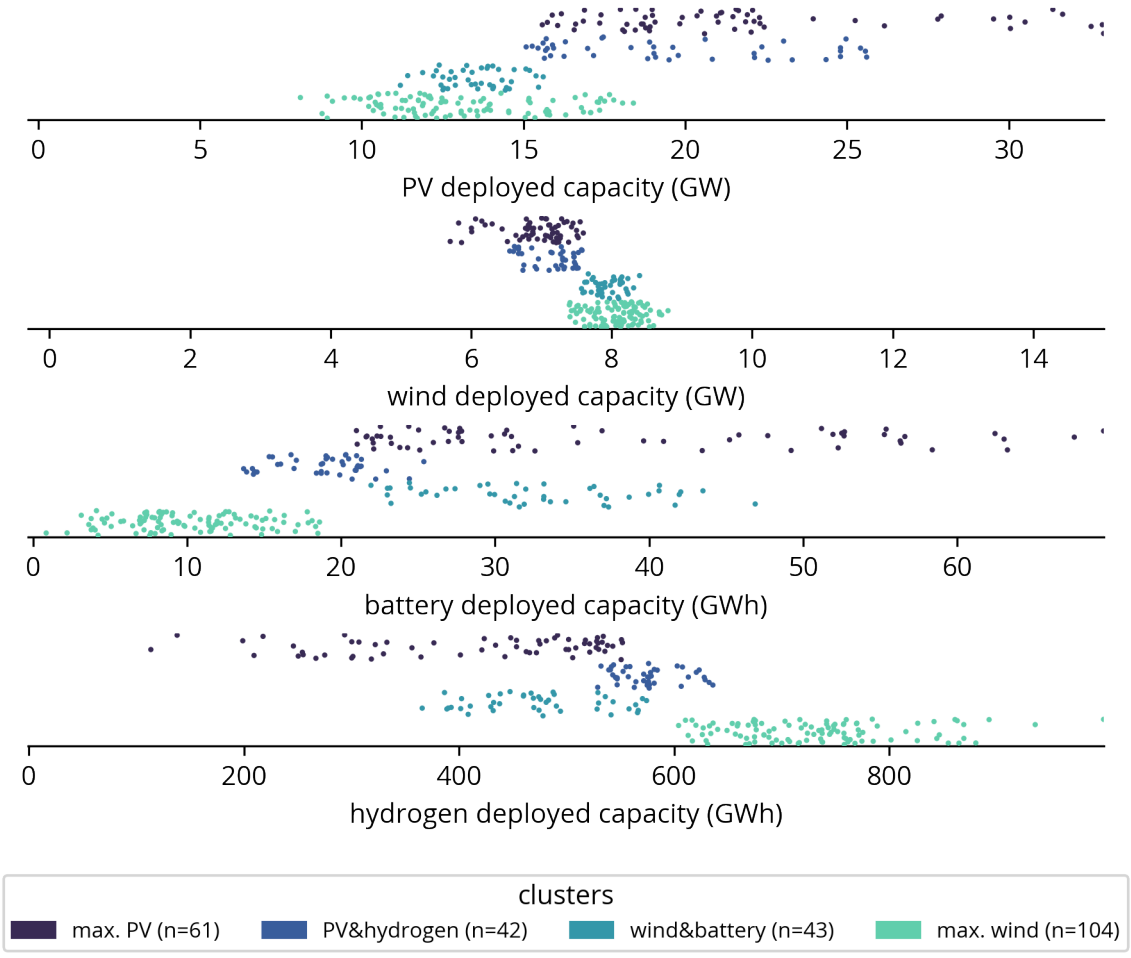

Figure 9.5: Strip plot of the various cost-optimal system configurations found under cost uncertainty, colour-marked by the determined clusters for the international II3050 scenario (policy 4).

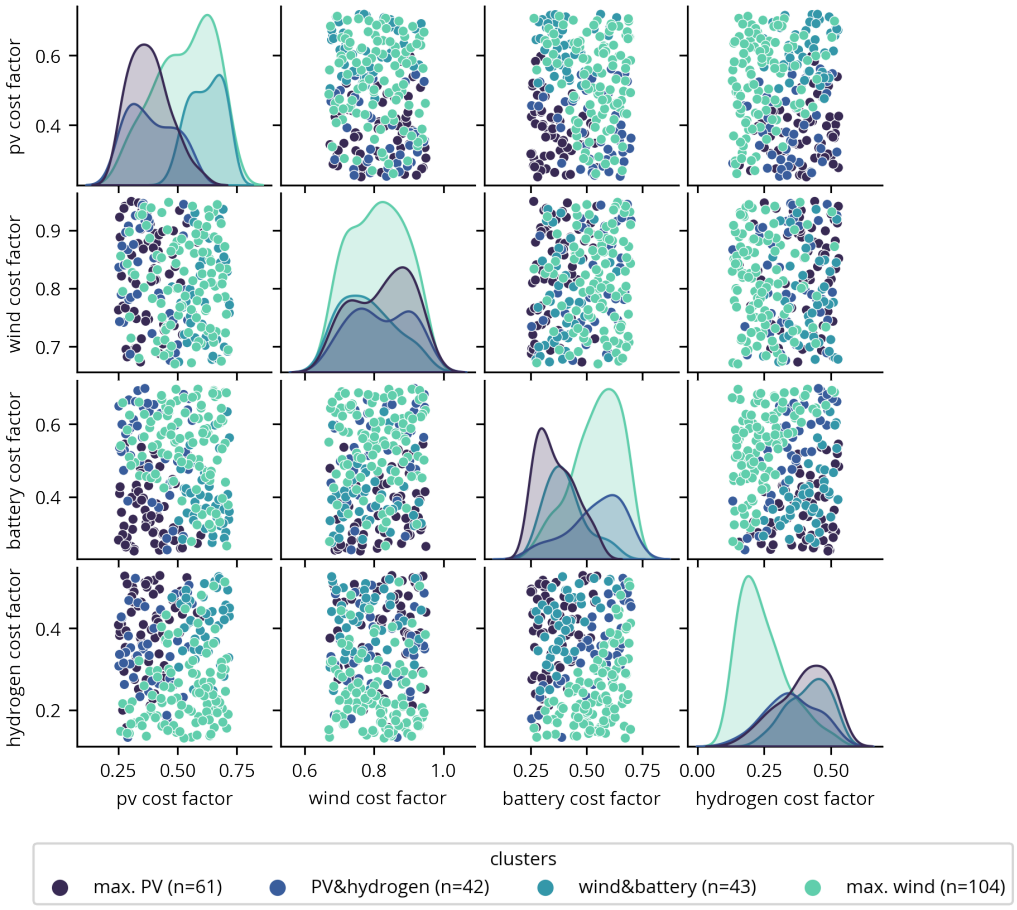

Figure 9.6: Pair plot depicting the identified system configuration clusters in relation to the sampled cost uncertainties for the international II3050 scenario (policy 4).

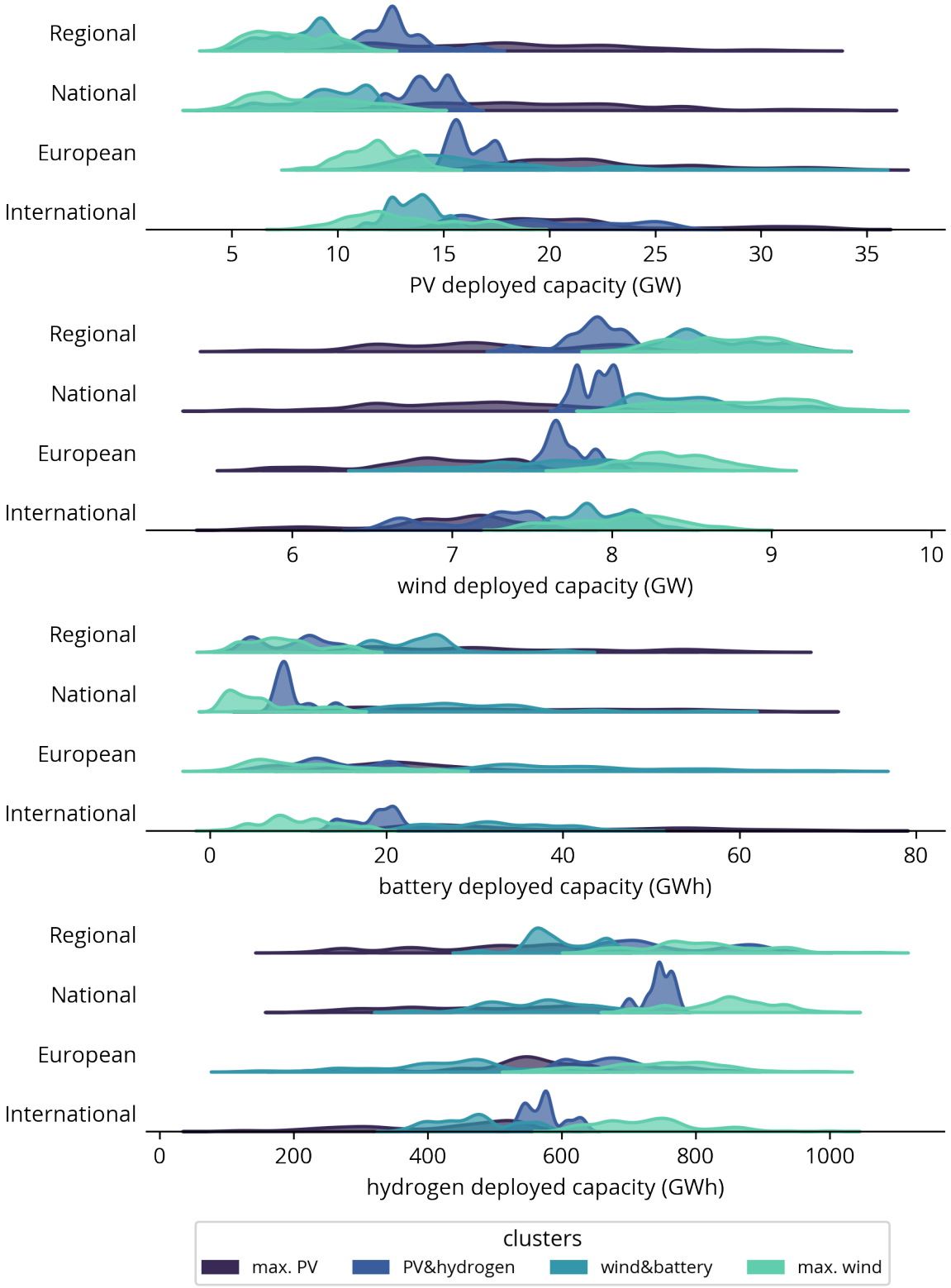

Figure 9.7: Deployment of PV, battery storage, wind and hydrogen storage for the four different II3050 scenarios plotted using a kernel density approximation. The height of the distribution at any point is directly related to the number of points fount at that point. The colour of the points is used to distinguish the various clusters found.

9.3 Conclusion

In this chapter, optimisation was applied to the province Gelderland in 2050 for four scenarios based on II3050. The model was configured identically to the model under consideration in section 8.2, where the energy system configuration of Gelderland was optimised for 2030.

How can exploring energy system optimisation models under uncertainty provide insights into cost-optimal system configurations to support (robust) energy transition policy? It was found that the cost-optimal configurations are very similar for the four scenarios. This indicates that the energy scenarios do not have the same influence on the optimal system configuration as the technology cost uncertainties. This indicates that policymakers should focus more on the deployment pathways to the clusters found and less on the uncertainty of future demand.

In general, the resulting cost-optimal configurations in both scenarios display shows very similar patterns. In both scenarios, the proposed clustering approach yielded similar clusters in terms of relative deployment of technologies and in terms of their relationship to the cost uncertainties. Both these properties were assessed effectively using the pair plot and strip plot.

The dominant clusters, with the highest in-cluster counts, exhibit similar relations as found in chapter 8, where PV and battery storage are synergistic and form an alternative to the other dominant cluster that consists of wind and hydrogen. However, in both scenarios, the same minority clusters were found that oppose this behaviour. These clusters exhibit more moderate ranges of deployment, but inverse deployment strategies to the majority clusters. Inter-cluster configurations of these minority clusters deploy a combination of PV and hydrogen storage versus a combination of wind and battery storage.

Which cost-optimal system configurations can be identified for case studies within the province of Gelderland? It can be concluded that the resulting system configurations as a whole display nearly the same pattern to the price uncertainties for Gelderland 2030 and Gelderland 2050. Even though both the demand profile and the cost ranges vary substantially between the two studies. Further extending on the observation made in chapter 8 that the current RES policy within the province of Gelderland forms a suitable stepping stone towards systems that are based on higher shares of renewable electricity, it can be concluded that this statement also applies to Gelderland in 2050.

It is interesting to note that the optimal deployment of PV found remains quite similar in 2050 when compared to 2030. However, the deployed capacity of wind increases substantially to about 8 GW in 2050. This is an increase of more than 2 GW to what was predicted using the 2030 demand profile and 2030 technology cost ranges to determine cost fully renewable optimal system configurations. This indicates, that even though costs of storage will decrease substantially towards 2050, wind remains important to overcome the seasonality of solar PV. For most system configurations found, the deployment of hydrogen nearly doubled compared to 2030. This slightly decreased the need for deploying battery capacity. This can be attributed to the fact that hydrogen is expected to see more substantial cost reductions towards 2050 when compared to 2030. In addition, the abundance of cheap renewable energy due to technology cost reductions help overcome the lower round-trip efficiency of hydrogen storage.

Finally, this study tested the proposed clustering and analysis procedure. The strip plots are still very useful, even when the data becomes more uniform and is less distinctly locked-in to specific configurations, but only when applied per policy. When using the strip plot to visualise clusters and

at the same time compare the various deployments found in clusters and policies, the visualisation becomes too obscure to be of any use. An alternative visualisation is presented that is based on kernel density approximations of the clusters, which is better suited to more uniform and overlapping data. However, it is recommended to use single policy strip plots primarily and only apply that plotting method restrictively as the level of abstraction can be quite challenging.

Chapter 10

Discussion

In this chapter, a discussion on the obtained results and insights is presented. This chapters is divided into three sections. Section 10.1 assesses all case study results to provide answers to research questions 4, 4.1 and 4.2. In section 10.2, based on experience gained from the application of the model on the case studies the implications of the obtained results and possible improvements to the model are addressed. Finally, section 10.3 presents directions of interest for future research into the explorative use of energy system optimisation models for policy relevance.

10.1 An overview of the case study results

The modelling framework developed during this thesis was applied to power systems of various scales and functionalities, each presenting a different possible use case for applying energy system optimisation models in an explorative manner. The experience, results and insights gained from the application of LESO in the case studies are used to formulate answers to relevant research questions.

With regards to research question 4.1 "*How can optimization models be utilized such that, in addition to uncertainty, the impact of various scenarios can be assessed?*", it can be stated that explorative use of energy systems models can be integrally applied with scenario-based assessment. For the local energy system projects presented in chapter 7, various scenarios in terms of grid capacity and subsidy schemes were investigated in addition to the explorative assessment of parametric uncertainties.

Moreover, LESO is coupled to the ETM using grid boundary conditions, electricity prices and residual power demand curves. The ETM is is an online interactive energy system modelling tool capable of simulation at various scale levels. In chapters 8 and 9, the ETM was used to reflect future energy scenarios for all sectors in the energy system as formulated in the provincial energy system integration study [17]. These scenarios were used to form an extra layer in the parametric uncertainty exploration in the form of policies. Policy is the terminology used in exploratory modelling and analysis for events that can be determined or controlled by the policymaker. The realisation of any of the Climate Neutral Energy Scenarios is in part dependent on Dutch national or European policy. The implementation of scenarios in this manner allows for scenarios-driven assessment in addition to the independent analysis of the deployment dynamics of optimal system configurations driven by technology cost uncertainties.

Which cost-optimal system configurations can be identified for case studies within the province of Gelderland? It can be stated within the cost uncertainty range for each of the case studies there are a lot of co-existing optimal energy system configurations. For the local energy projects, the configurations are more discontinuous and show more distinct behaviour. The case studies on Gelderland in 2030 and 2050 revealed that system configurations span whole ranges on each deployable technology axis. Some energy system configurations depend on the cost reduction of multiple technologies, such as battery storage and solar PV. Other configurations are more moderate in terms of deployed technology capacities and are more closely related to the centre values of the cost uncertainties.

Finally, main research question 4 "*How can exploring energy system optimisation models under uncertainty provide insights into cost-optimal system configurations to support (robust) energy transition policy?*" can be answered. As stated in the previous paragraph, a set of diverse energy system configurations exist within the projected cost ranges. Based on this, it can be stated that exploring those configurations under uncertainty is vital to obtain insight in the range of possible configurations in regards to the underlying cost uncertainties.

Moreover, by applying the clustering method a more general and high-level overview of the numerous results is obtained. The clusters are observed to exist to some degree in all scenarios for Gelderland in 2050 and are in generally good agreement with the clusters found in Gelderland 2030. From this, two conclusions can be drawn. Firstly, the clustering method can be applied to determine whether similar energy system configurations exist based on cost projections that are further in the future. Based on this, decisions that need to be made now can be aligned such that they either steer towards the desired or attainable system configuration or steer clear from locking in to a certain cluster until uncertainty resolves.

Secondly, it can be concluded that the used cost projections do not lead to substantially different clusters in 2030 compared to 2050. This is not necessarily intuitive as the cost projections of the considered technologies display large differences, which would suggest that the tipping points and trade-offs between technologies could substantially change over time. However, only applying energy system optimisation models for exploration of parametric uncertainty is insufficient since it does not reveal insight into the near-optimal solution space. This is a point for future research and is addressed in the following sections.

10.2 Application of the model

10.2.1 Implication of renewable electricity targets

As a result of the current model setup, imposing renewable energy targets was only possible by increasing the self-sufficiency in the region of scope. In the implementation used in this thesis, the targets are achieved by constraining the model with decreasingly lower allowed amounts of imported energy from the grid. The algorithm would then be forced to place more local generation assets, which were contained to only renewable energy.

However, it is known that regional autarky is not cost-optimal when compared to larger scales of demand balancing [60] [61]. Depending on the scale of balancing and tolerance on the level of self-sufficiency, total system costs can increase substantially when smaller geographic areas are tasked with achieving regional autarky. This could be overcome by applying a multi-nodal modelling approach that considers multiple connected regions within the Netherlands. Alternatively, a more representative implementation can be achieved by setting a CO2 target for the yearly average emissions

of electricity instead dictating of a minimal share of renewable electricity. In this implementation, it is possible to still use a single node representation of only the region of interest. This would require additional information on the grid boundary, namely the CO2 intensity of the electricity mix per hour.

10.2.2 Representation of cost uncertainties

In the case studies of this thesis, multiple data sources from various publication years were used to represent the range of parametric uncertainty of future technology capacity cost. Using a single publication or data source could be more favourable in terms of consistency in approaches. The cost uncertainties used in this thesis were based on various deployment scenarios, with exception of hydrogen storage [145] which is based on probabilistic sampling. Moreover, projections have historically underestimated the deployment rate of renewable technologies such as solar PV and wind [56].

Although the use of probability distributions as an input for energy systems modelling has been criticised for the lack of an empirical basis [88], probability distributions can be used to give an indication of the relative probability of the system configurations outcomes obtained through uncertainty exploration. In the current implementation of uncertainties, all model outcomes should be considered equally probable which means that it is not possible to quantitatively determine the best strategy to hedge against potential risks based on cost developments. It should rather be used as an indication of whether short-term deployment decisions will still align with potentially optimal future system configurations. Over time, uncertainty is expected to resolve. As such, period exploration of optimal energy system configurations based on parametric uncertainty should be used to reevaluate whether the current development trajectory can still be adapted towards optimal energy system configurations.

Recently, a pre-print was announced that addresses the historical underestimation of technology cost reductions and provides probability distributions based on empirical data. Moreover, this publication contains projections on all four technologies considered in this research (wind, PV, battery and hydrogen storage), meaning that a single data source with a coherent methodology could be used [176]. Still, perhaps an even more radical approach in determining the cost ranges is required, where an even lower range can potentially reveal interesting or unexpected optimal configurations. Finally, bounded use of predefined parametric uncertainties does not account for unforeseen technical innovation that disrupts the technological landscape completely. Perhaps an implementation-free approach to discover possible disruptive technologies as done for storage technology [66] should be considered.

10.2.3 Financial markets

Economic optimisation is in part driven by financial markets. Currently, only the energy market is included in a simplified manner that does not correspond to actual energy markets such as the day-ahead or spot market. In the current implementation, the ETM is used to determine the cost of electricity at every hour of the year, which is used as a grid-related boundary condition for the region under analysis. Moreover, the ETM models the electricity prices based only on marginal costs of electricity which are assumed to be homogeneous per technology group, which in itself is not a detailed representation of the actual market. Additionally, the price curve used was based on a single scenario that was deemed representative per respective case study. Strictly speaking, this scenario itself can be interpreted as a structural uncertainty, Or, by addressing the parameters assumed in the scenario (e.g. CO2 or fuel prices), as multiple parametric uncertainties. In following the logic of the last proposition, exploration of those parametric uncertainties could also be used to obtain insight into the effect of policies such as taxes or subsidies on fuels or electricity.

Moreover, each of the scenarios is based on either the currently planned or a predefined transformation of the energy system on a national level. As a result, it is potentially possible for the region under consideration to take the dominant route in the prisoners' dilemma in the energy transition: let the rest of the system bear the cost for deployment of renewable energy technologies and bear the fruit in terms of low energy prices for the hours where renewable energy is abundant. Addressing the scenarios themselves as parametric uncertainty might reveal more insight into the effect of this implementation.

Lastly, as noted in chapter 7, other energy markets such as the frequency restoration reserve, frequency containment services or balancing reserves have not been included in the optimisation model. This is in part due to the fact that these markets operate on a timescale much smaller than the hourly time resolution used. However, this leads to an underestimation of the potential modes of income and functionality of storage technologies. It is expected that modelling of those markets or by approximation of incomes from those markets will lead to increased deployment of storage.

10.2.4 Complete energy system

Arguably one of the shortcomings in the current approach is that only the power system is modelled endogenously. In the implementation used in this thesis, energy-consuming sectors such as housing, agriculture, transport and industry are not included in the optimisation model. Instead, the optimisation model is coupled to the ETM which models each of those sectors. As a result, the transition of those sectors is reflected in the optimisation model only as an electric demand curve. Therefore, the optimisation algorithm itself is not capable of assessing possible configurations where other sectors electrify in specific ways.

Although not applied in this thesis, it is possible to reflect possible transition pathways in the ETM, without introducing additional computational complexity in the optimisation model. Feedback between decarbonisation strategies of other sectors (e.g. heat pumps, electric boilers, electric vehicles, etc) can be explored in relation to optimal power system configurations by changing parameters used in the ETM. Since LESO is already coupled to the ETM, it is possible to use the parametric uncertainty exploration on parameters that model other sectors, in addition to cost uncertainty. This would for instance allow for a more continuous representation of the climate-neutral energy scenarios used throughout Dutch energy modelling and analysis. This would allow for a more integral assessment of policies throughout all sectors and would reveal the sensitivity of optimal power system configurations in relation to decarbonisation strategies applied in the energy system.

Optionally, only components that are relevant for optimisation (i.e. that can substantially impact the outcome and can, in reality, be addressed through policy or planning) can be included in the optimisation model. This potential is recognised for smart charging, sector coupling to heat and industry and demand-side management.

10.2.5 Energy system optimisation models for exploratory use

One of the research questions of this thesis is: *What design considerations are imperative to create an optimisation model that can be used to explore uncertainties and policy effects?*

An important consideration for using energy system optimisation models in an exploratory manner is the computational time of the model. On a rig with 2 dual-socket mounted octa-core Xeon processors and 32 GB of RAM, the computational time required for the results obtained in this thesis was between 10 and 150 hours per case study. Per perturbation i.e. model optimisation run, this took between 20-45 seconds per result or 250-500 seconds when parallel computing with 10 instances. When resources and knowledge for cloud computing are available this can be greatly reduced as single high-performance clusters with more than tenfold the computational power are available at reasonable prices.

Moreover, the framework used in this thesis is developed using Python. The optimisation is implemented in roughly two stages. First, the framework formulates the optimisation problem based on constraints, inequalities and the objective function using Pyomo. Consequently, the explicit formulation of the problem (a large system of equations, consisting mostly of sparse matrices) is written to a file and passed to the solver of choice. The reported computational times were obtained using Gurobi, an expensive commercial solver. Open-source solvers are available but are inferior in terms of performance [40]. In the current implementation, all constraints and inequalities that are formulated in the first stage are generated by iterating the time window used in the optimisation. Iteration or recursion in programming is inherently limited in terms of computational speed. Additionally, Python is a single-threaded language. This means that more computational power will not significantly improve this stage. However, it is possible to use set-based definitions for all constraints that are not time-coupled such as storage dynamics [82]. This will greatly reduce the time needed for the first stage.

10.3 Future research

10.3.1 Leverage on existing interface

An additional benefit that can potentially be explored is the use of the ETM to obtain insight into factors not addressed in the optimisation model. Factors that are also relevant for policymaking such as CO2 reduction, land use or grid expansion requirements [39] can be indicated by ETM. These results can be linked to the optimisation results obtained with parametric uncertainty exploration and included when evaluating model outcomes.

Moreover, ETM can be used with a general description of energy systems configurations and results. This can act as an interface between multiple specialized models and is called the Energy System Description Language (ESDL). As part of an ongoing project called the ”Multi-Model for integral decision making”, grid operators and commercial parties are currently implementing a model chain with ESDL as an interface. Implementation of this interface in optimisation models would leverage on this development, allowing grid operators to perform detailed studies on the effect of energy system configurations without the need for sharing sensitive information on grid infrastructure.

10.3.2 Meteorological conditions

The optimisation models used in this thesis have only been based on a single meteorological year. This is partly due to the computational demands and limited available resources and in part due to the coupling to the ETM, which only contains a limited set of meteorological data. However, as noted in the literature optimisation based on one year underestimates the total system cost due to the fact that the system is exposed to less interannual fluctuations and extreme weather events [72]. As a result, the resilience of the optimal energy systems is unknown but expected to be low. It is recommended to either implement multiple years at the cost of increased computational demand or by performing scenario-based sensitivity analysis using a predefined set of meteorological years. Moreover, studies indicated that climate change can potentially negatively impact the generation potential of renewable energy such as wind and solar [177]. This is a fairly new topic in energy systems optimisation and further research is needed to obtain insight into the robustness of energy systems with respect to climate change.

10.3.3 Multi-objective optimisation

Policymakers and energy planners have to consider multiple factors when deciding between alternative energy system configurations such as land use, emission reduction, water use, impact on biodiversity, spatial integration and societal acceptance. Optimal system configurations presented in this thesis are obtained by optimising only based on cost. It is possible to integrate multiple objective functions. However, this introduces another uncertainty as the implementation of multiple objective functions requires weighing between the objectives. Still, models developed to generate insight for policy based on multiple objectives exist. For example, a model has been developed especially to address the energy-water-food nexus [178].

On the other hand, routines such as modelling all alternatives and modelling to generate alternatives have been implemented in energy optimisation models. It is argued that these approaches provide a rigorous method of generating alternative system configurations in the feasible near-optimal solution space that can be used by policymakers to decide between competing system configurations based on objectives not included in the optimisation model [29], [35], [52], [97], [111]. In addition, methods exist that use modelling to generate spatially explicit, practically optimal solutions. This method can be used when policymakers need to decide on the spatial configuration of energy systems such that the systems align with political or societal acceptance [95].

10.3.4 Integral approach to structural and parametric uncertainty

Optimisation model outcomes should not be considered normative due to the lack of validation. Rather, energy system optimisation models should be applied in an exploratory manner to obtain robust insights for policymakers. All optimisation models inherently contain structural uncertainty due to the complexity of the energy system. Methods such as modelling to generate alternatives, already offer a suitable method to deal with structural uncertainty. This thesis applied a novel method to explore outcomes of energy system optimisation models based on parametric uncertainty. Optimisation models of energy systems inherently possess structural uncertainty. However, it is recommended that further research be carried out on combining methods for both structural and parametric uncertainty. Moreover, addressing uncertainty in energy system optimisation models should be integral to their application.

10.3.5 A new policy-model interface

Although energy modelling has acquired a crucial supporting role for policymaking, the current interface between modelling and policy has its limitations [41]. An interface that is better equipped to overcome existing barriers for perceived policy relevance should be investigated. Interventions such as aligning model development with policy cycles, forming expert groups for model outcomes and higher levels of stakeholder involvement can help overcome existing barriers [179].

As proposed in this thesis, energy system optimisation models should be used in an explorative rather than normative manner. Both structural and parametric uncertainty should be addressed integrally to the application of optimisation models. However, this introduces a challenge in terms of the dimensionality of results. Therefore, the new policy-model interface should facilitate interaction between policymakers, energy planners, analysts and modellers. To achieve dynamic interaction, models should be developed such that they can generate results that support such interaction. It should be possible to pre-compute various perturbations of system configurations with methods such as modelling to generate alternatives or exploratory modelling and analysis. However, due to the high dimensionality of energy systems, it might be more desirable that models are computationally tractable and suitable for deployment on high-performance clusters such that results can be generated on the fly, based on input from policymakers, stakeholders and other involved parties. Additionally, global sensitivity analysis should be applied beforehand such that model sensitivities are known.

10.3.6 Exploration and visualisation of results

The interpretation of results obtained with exploration remains a challenge. Even for the relatively low number of uncertainty dimensions, it is time-consuming to organise, visualise and analyse all obtained results to obtain comprehensive results. With a booming interest in machine learning and its applications, various new visualisation methods that deal with high dimensional data are introduced. Novel methods such as uniform manifold approximation or more conventional methods such as principal component analysis are promising methods for dimension reduction and can consequently provide more rigorous methods [180].

10.3.7 Clustering methods

Clustering was applied to reduce the dimensionality of results and determine patterns in model outcomes. However, the hierarchical clustering based on cosine distance with complete linkage produces diverse results based on parameters determined on the go by the analyst. The analysis either determines the desired number of clusters a priori or sets a distance threshold. Both parameters are thus dependent on the competence and interpretation of the analyst. Therefore, further investigation of other unsupervised clustering methods is recommended.

Chapter 11

Conclusion

This thesis presents an energy system optimisation modelling framework, results and data processing approach for explorative use of optimisation models in the context of presenting insights for policymakers in the energy transition. This contributes to filling the gap in current literature and substantiates the added value of using energy system optimisation models in an explorative manner for generating insights for the Dutch energy transition. Cost uncertainties are found to have a substantial impact on the outcome of optimisation studies which are typically not addressed when presenting results. Indispensable insight in deployment dynamics and correlation in optimised energy systems can be identified by exposing energy systems optimisation models to cost uncertainties. The presented modelling framework was proven to be capable of generating vital insights for policymakers through the application of the model on case studies at various geographic scales within the province of Gelderland.

Typically, optimisation models are complex and entail many details that do not guarantee the accuracy of the model or increase the relevance of its results. This thesis presents a comprehensive, extensible and representative framework developed conscious of computational tractability with which new possibilities arise. By configuring many iterations of the same model with slightly modified parameters the obtained configurations are optimised to reveal the response of the optimum to parametric uncertainties, such as technology cost. This is of great value to academics, policymakers and consultants in the energy transitions because, unlike with structural uncertainty, no formal methods exist that systematically address the parametric uncertainty of energy system optimisation models.

This thesis presents novel research on exploring optimisation model outcomes as a result of cost uncertainty for various types of power systems on various scale levels. From a local energy project to a whole provincial region, the model can be configured and subsequently exposed to uncertainties from within the same modelling framework. Additionally, the most time-consuming tasks encountered in energy systems modelling and analysis have been automatised within the framework and are available to the modeller through a low-code interface. This forms a unique proposition because in this way the optimisation model can be quickly repurposed and configured to generate insight for policymakers. Moreover, it provides insight into the robustness and dynamics of the determined optima through exploration of underlying uncertainties and scenarios, whereas conventional optimisation studies would typically deliver a single output.

In addition, this thesis incorporated, extended and validated a clustering approach recently introduced by Fraiture [100]. Validation of the approach is achieved by applying the procedure to the model introduced in this thesis, which is distinctly different from the model the clustering was originally proposed with. Moreover, the optimisation results generated in this thesis also included policies

besides cost uncertainties which adds extra value for policymakers. This thesis improves on the proposed clustering approach by standardizing the analysis pipeline and introducing visualisation methods that are capable of visualising complex relationships over multiple axes and categories comprehensively.

The framework and method were applied to various cases to obtain insight into the robustness of future energy system plans under uncertainty and to compose a set of valuable results on topics relevant to accelerating the energy transition. Through investigation of cable pooling, insight is obtained in the sensitivity of optimal cable pooled configurations based on the uncertainty of technology capacity cost. It was found that this concept has great potential to further extend renewable electricity shares while maximizing the utilisation of current grid capacities. The conditions for economically viable projects based on cable pooling have been quantified based on technology cost and subsidy policies.

Sectors that rely on fossil fuels will have to electrify to meet emission reduction goals. Electrification of the mobility sector is a development relevant to the transition. Considering the increasing number of grid constrained areas, barriers to exploiting fast-charging infrastructure arise. It is found that grid congestion can be overcome by incorporating optimal system configurations based partly on local energy generation. For self-sufficient variations, oversizing production is more cost-effective than deploying large quantities of storage.

By optimisation of RES regions within Gelderland for 2030, the direction of the path of current policies is evaluated in terms of robustness to cost uncertainties and suitability for supporting higher shares of renewable electricity. By applying the clustering method, a distinct set of optimal energy system configurations is found, of which the relation to the uncertainty of costs is known. Current policy is found suitable to support future power systems with higher shares of renewable electricity if the possibility for more wind deployment is guarded. Moreover, current deployment goals within the province of Gelderland are aligned with the ranges of possible cost-optimal configurations found in cost uncertainty.

In addition, Gelderland is optimised in four various stylized scenario-based representations of the energy system in 2050. The clustering method is successfully applied and reveals similar but distinct results, identifying similar cluster configurations in the two most different scenarios. Optimal system configurations are found to be significantly less reactive to the scenario than to uncertainties regarding component costs. An additional visualisation method is proposed based on this data set to visualise more sparse and uniform optimisation results.

Overall, it is advised that cost uncertainty evaluation should be regarded as integral of optimisation based policy evaluation as system configurations show a wide range of possible outcomes when exposed to uncertainties. As these uncertainties are outside of the control of policymakers and project developers, it entails key strategic information. Insight into the robustness of energy systems can be obtained using the developed framework and the improved method which is standardised to effectively generate insight in various energy systems.

Recommendations for future research

In the discussion presented in chapter 10, various methodological limitations of this research have been addressed. Based on this discussion, a set of recommendations for future research is formulated.

I Apply an alternative formulation for the targeted renewable electricity share that does not result in complete regional self-sufficiency. For example, based on a CO_2 target and using hourly CO_2 intensities for the external electricity market or by using a larger scale, multi-nodal model.

II Investigate the possibilities of better representing parametric uncertainties such as technology capacity cost based on uncertainty ranges with probability distributions with an empirical basis.

III Formulate optimisation models with implementation-free component groups to investigate possible effects of unforeseen technological breakthroughs.

IV Include more financial energy markets in the optimisation model or approximate the expected effects based on observations from existing literature or case studies. This includes markets such as frequency containment and capacity reserves.

V To be able to investigate the effects of transitioning sectors other than the electricity sector, more of the energy system should be endogenously included in the model because the transformation of for example mobility and transport, industry and housing can greatly affect the optimal energy system configuration.

VI Implement the Energy Systems Descriptive Language as an interface between energy system optimisation models, infrastructure models and descriptive models to move towards integrated assessment models or achieve greater coupling of existing energy modelling tools.

VII Structural and parametric uncertainty of energy system optimisation models should be addressed methodologically and seen as an integral part of the application of those models. Moreover, an explorative rather than normative use is recommended for energy system optimisation models.

VIII Temporal down sampling based on hierarchical clustering with time-coupling for storage components should be used to decrease computational demands of parametric uncertainty exploration.

IX More efficient mathematical formulations (e.g. set-based matrix construction) and programming approaches (e.g. resolving with slightly different parameters) should be investigated to reduce the computational burden of parametric uncertainty exploration.

X Research the application of knowledge from the data science and machine learning domain to improve the analysis and visualisation of the large quantities of results obtained with parametric and structural uncertainty exploration to increase accessibility and transparency of conclusions.

Recommendations on the application of energy systems optimisation models for policy relevance

Based on both the discussion in chapter 10 and the results obtained by applying the explorative use of the optimisation model on Gelderland in chapters 7-9, a set of recommendations for achieving policy relevance with energy systems optimisation models is formulated.

I Increase the use of energy system optimisation models in addition to the currently used scenarios and simulation energy models to obtain insight into the transition pathways to a desired future energy system. Based on that insight, policies can be put in place that leads to an orchestrated energy transition that is currently missing.

II Policymakers should aim to periodically apply energy system modelling and analysis in an explorative manner to reevaluate current policies and to adjust policies where needed or to hedge against potential risks.

III Invest in researching a new policy-model interface, where policy cycles and model development are better aligned such that it supports the interaction between modellers, analysts, energy planners and various other stakeholders.

IV Investigate the implications of using longer meteorological data i.e. evaluate the effects of different historical meteorological years to address the resilience of optimal energy systems to extreme events and interannual variations. Moreover, investigate the possible effects of climate change on the performance of the energy system.

Bibliography

[1] University Of Twente, "'Research Strategy 2020-2030 University Of Twente'," Ensc, 2020.

[2] V. Masson-Delmotte, P. Zhai, A. Pirani, S. L. Connors, C. Péan, S. Berger, N. Caud, Y. Chen, L. Goldfarb, M. I. Gomis, M. Huang, K. Leitzell, E. Lonnoy, J. Matthews, T. K. Maycock, T. Waterfield, O. Yelekçi, R. Yu, B. Zhou, and (eds.), "IPCC, 2021: Climate Change 2021: The Physical Science Basis. Contribution of Working Group I to the Sixth Assessment Report of the Intergovernmental Panel on Climate Change," *Cambridge University Press. In Press.*, p. 42, 2021. [Online]. Available: https://www.ipcc.ch/report/ar6/wg1/

[3] United Nations, Framework Convention on Climate Change, and Conference of the Parties (COP), "Paris agreement," 2015.

[4] United Nations, Framework Convention on Climate Change, and Conference of the Parties (COP), "Nationally determined contributions under the Paris Agreement," *EU*, 2021.

[5] European Commission, "The European Green Deal," *European Commission*, 2019. [Online]. Available: https://eur-lex.europa.eu/legal-content/EN/TXT/PDF/?uri=CELEX:52019DC0640&from=EN

[6] European Commission, "Synopsis report on the results of the 2030 Climate Target Plan consultation activities," Brussels, Tech. Rep., 2020.

[7] European Commission, "Decarbonising our energy system to meet our climate goals," Brussels, Tech. Rep. July, 2021.

[8] Netherlands Ministry of Economic Affairs, "National Climate Agreement," no. June, p. 247, 2019. [Online]. Available: https://www.klimaatakkoord.nl/documenten/publicaties/2019/06/28/national-climate-agreement-the-netherlands

[9] Rijksoverheid, "Klimaatakkoord," *Klimaatakkoord*, p. 250, 2019. [Online]. Available: https://www.klimaatakkoord.nl/binaries/klimaatakkoord/documenten/publicaties/2019/06/28/klimaatakkoord/klimaatakkoord.pdf

[10] Energieonderzoek Centrum Nederland, Centraal Bureau voor Statistiek, and Rijksdienst Voor Ondernemend Nederland, "Nationale Energieverkenning 2017," pp. 1–276, 2017. [Online]. Available: http://www.cbs.nl/NR/rdonlyres/C0F1D74C-1EB1-4E3B-9A46-ECA28ABFED7E/0/2015nationaleenergieverkenning.pdf

[11] Planbureau voor de Leefomgeving, TNO, and CBS, "Klimaat- en Energieverkenning 2019," PBL, Den Haag, Tech. Rep., 2019. [Online]. Available: www.pbl.nl/kev

[12] Planbureau voor de Leefomgeving, TNO, and CBS, "Klimaat- en Energieverkenning 2020," PBL, Den Haag, Tech. Rep., 2020.

[13] Planbureau voor de Leefomgeving, TNO, CBS, and Wageningen University and Research, “Klimaat- en Energieverkenning 2021,” PBL, Den Haag, Tech. Rep., 2021.

[14] European Commission, “Powering a climate-neutral economy: An EU Strategy for Energy System Integration EN,” 2020.

[15] Province of Friesland, “Regionale Energie Strategie 1.0 Fryslân,” 2021.

[16] Province of Flevoland, “Regionale Energie Strategie 1.0 Flevoland,” pp. 1–60, 2021.

[17] Berenschot and Witteveen+Bos, “Systeemstudie Gelderland,” Tech. Rep., 2021.

[18] CE Delft and Quintel Intelligence, “Systeemstudie Groningen en Drenthe,” Tech. Rep., 2020.

[19] Quintel Intelligence, TNO, and CE Delft, “Systeemstudie Limburg,” Tech. Rep., 2020.

[20] DNV, “Systeemstudie Noord-Brabant,” Tech. Rep., 2021.

[21] CE Delft and TNO, “Systeemstudie Noord-Holland,” Tech. Rep., 2019. [Online]. Available: https://www.ce.nl/publicaties/2323/rapportage-systeemstudie-energie-infrastructuur-noord-holland-2020-2050

[22] Berenschot and Quintel, “Systeemstudie Overijssel,” Tech. Rep. December, 2020.

[23] CE Delft and Quintel Intelligence, “Systeemstudie Utrecht,” Tech. Rep., 2021.

[24] CE Delft and Royal Haskoning DHV, “Systeemstudie Zeeland,” Tech. Rep., 2020.

[25] CE Delft, TNO, and Quintel Intelligence, “Systeemstudie Zuid-Holland,” Tech. Rep., 2020.

[26] CE Delft and Netbeheer Nederland, “Net voor de toekomst,” 2017.

[27] B. Den Ouden, J. Kerkhoven, J. Warnaars, R. Terwel, M. Coenen, and T. Verboon, “Klimaatneutrale energiescenario’s 2050,” Tech. Rep.

[28] J. H. Kwakkel and G. Yücel, “An exploratory analysis of the dutch electricity system in transition,” *Journal of the Knowledge Economy*, vol. 5, no. 4, pp. 670–685, 2014.

[29] H. Lund, F. Arler, P. A. Østergaard, F. Hvelplund, D. Connolly, B. V. Mathiesen, and P. Karnøe, “Simulation versus optimisation: Theoretical positions in energy system modelling,” *Energies*, vol. 10, no. 7, p. 840, jun 2017. [Online]. Available: http://www.mdpi.com/1996-1073/10/7/840

[30] Integrale Infrastructuurverkenning, “Het Energiesysteem van de Toekomst,” 2021.

[31] P. McCallum, D. P. Jenkins, A. D. Peacock, S. Patidar, M. Andoni, D. Flynn, and V. Robu, “A multi-sectoral approach to modelling community energy demand of the built environment,” *Energy Policy*, vol. 132, no. June, pp. 865–875, 2019. [Online]. Available: https://doi.org/10.1016/j.enpol.2019.06.041

[32] H. Bontenbal and S. Erkens, “Motie van de leden Bontenbal en Erkens over inzicht in een kostenoptimale energiemix in 2050,” jul 2021. [Online]. Available: https://www.tweedekamer.nl/kamerstukken/moties/detail?id=2021Z13025&did=2021D27957

[33] D. Bogdanov, J. Farfan, K. Sadovskaia, A. Aghahosseini, M. Child, A. Gulagi, A. S. Oyewo, L. de Souza Noel Simas Barbosa, and C. Breyer, “Radical transformation pathway towards sustainable electricity via evolutionary steps,” *Nature Communications*, vol. 10, no. 1, dec 2019.

[34] V. C. Gironès, S. Moret, F. Maréchal, and D. Favrat, "Strategic energy planning for large-scale energy systems: A modelling framework to aid decision-making," *Energy*, vol. 90, no. PA1, pp. 173–186, 2015.

[35] J. DeCarolis, H. Daly, P. Dodds, I. Keppo, F. Li, W. McDowall, S. Pye, N. Strachan, E. Trutnevyte, W. Usher, M. Winning, S. Yeh, and M. Zeyringer, "Formalizing best practice for energy system optimization modelling," pp. 184–198, may 2017.

[36] M. Child, D. Bogdanov, and C. Breyer, "The role of storage technologies for the transition to a 100% renewable energy system in Europe," in *Energy Procedia*, vol. 155. Elsevier Ltd, nov 2018, pp. 44–60.

[37] T. Ommen, W. B. Markussen, and B. Elmegaard, "Comparison of linear, mixed integer and non-linear programming methods in energy system dispatch modelling," *Energy*, vol. 74, no. 1, pp. 109–118, 2014. [Online]. Available: http://dx.doi.org/10.1016/j.energy.2014.04.023

[38] N. A. Sepulveda, J. D. Jenkins, F. J. de Sisternes, and R. K. Lester, "The Role of Firm Low-Carbon Electricity Resources in Deep Decarbonization of Power Generation," *Joule*, vol. 2, no. 11, pp. 2403–2420, 2018.

[39] A. Fattahi, J. Sijm, and A. Faaij, "A systemic approach to analyze integrated energy system modeling tools: A review of national models," *Renewable and Sustainable Energy Reviews*, vol. 133, p. 110195, nov 2020. [Online]. Available: https://linkinghub.elsevier.com/retrieve/pii/S1364032120304858

[40] S. Oberle and R. Elsland, "Are open access models able to assess today's energy scenarios?" *Energy Strategy Reviews*, vol. 26, p. 100396, nov 2019.

[41] M. Chang, J. Z. Thellufsen, B. Zakeri, B. Pickering, S. Pfenninger, H. Lund, and P. A. Østergaard, "Trends in tools and approaches for modelling the energy transition," *Applied Energy*, vol. 290, p. 116731, may 2021.

[42] H.-K. Ringkjøb, P. M. Haugan, and I. M. Solbrekke, "A review of modelling tools for energy and electricity systems with large shares of variable renewables," *Renewable and Sustainable Energy Reviews*, vol. 96, pp. 440–459, nov 2018. [Online]. Available: https://linkinghub.elsevier.com/retrieve/pii/S1364032118305690

[43] V. Krey, "Global energy-climate scenarios and models: a review," *Wiley Interdisciplinary Reviews: Energy and Environment*, vol. 3, no. 4, pp. 363–383, jul 2014. [Online]. Available: https://onlinelibrary.wiley.com/doi/10.1002/wene.98

[44] S. Sinha and S. S. Chandel, "Review of recent trends in optimization techniques for solar photovoltaic-wind based hybrid energy systems," pp. 755–769, jun 2015.

[45] A. Zerrahn and W.-P. Schill, "Long-run power storage requirements for high shares of renewables: review and a new model," *Renewable and Sustainable Energy Reviews*, vol. 79, pp. 1518–1534, nov 2017. [Online]. Available: https://linkinghub.elsevier.com/retrieve/pii/S1364032116308619

[46] M. G. Prina, G. Manzolini, D. Moser, B. Nastasi, and W. Sparber, "Classification and challenges of bottom-up energy system models - A review," p. 109917, sep 2020.

[47] P. Tozzi and J. H. Jo, "A comparative analysis of renewable energy simulation tools: Performance simulation model vs. system optimization," pp. 390–398, 2017.

[48] S. Pfenninger, A. Hawkes, and J. Keirstead, "Energy systems modeling for twenty-first century energy challenges," *Renewable and Sustainable Energy Reviews*, vol. 33, pp. 74–86, may 2014. [Online]. Available: https://linkinghub.elsevier.com/retrieve/pii/S1364032114000872

[49] S. Pfenninger, J. DeCarolis, L. Hirth, S. Quoilin, and I. Staffell, "The importance of open data and software: Is energy research lagging behind?" *Energy Policy*, vol. 101, no. October 2016, pp. 211–215, 2017.

[50] S. Pfenninger, L. Hirth, I. Schlecht, E. Schmid, F. Wiese, T. Brown, C. Davis, M. Gidden, H. Heinrichs, C. Heuberger, S. Hilpert, U. Krien, C. Matke, A. Nebel, R. Morrison, B. Müller, G. Pleßmann, M. Reeg, J. C. Richstein, A. Shivakumar, I. Staffell, T. Tröndle, and C. Wingenbach, "Opening the black box of energy modelling: Strategies and lessons learned," *Energy Strategy Reviews*, vol. 19, pp. 63–71, jan 2018.

[51] R. Morrison, "An Open Energy System Modeling Community," *Gen R*, 2019.

[52] J. Decarolis, K. Hunter, and S. Sreepathi, "The TEMOA Project : Tools for Energy Model Optimization and Analysis," *Energy*, no. June, pp. 1–18, 2010.

[53] S. Hilpert, S. Günther, C. Kaldemeyer, U. Krien, G. Plessmann, F. Wiese, and C. Wingenbach, "Addressing Energy System Modelling Challenges: The Contribution of the Open Energy Modelling Framework (oemof)," *Preprints*, 2017.

[54] S. Hilpert, C. Kaldemeyer, U. Krien, S. Günther, C. Wingenbach, and G. Plessmann, "The Open Energy Modelling Framework (oemof) - A new approach to facilitate open science in energy system modelling," *Energy Strategy Reviews*, vol. 22, pp. 16–25, 2018. [Online]. Available: https://doi.org/10.1016/j.esr.2018.07.001

[55] J. Priesmann, L. Nolting, and A. Praktiknjo, "Are complex energy system models more accurate? An intra-model comparison of power system optimization models," *Applied Energy*, vol. 255, p. 113783, dec 2019. [Online]. Available: https://linkinghub.elsevier.com/retrieve/pii/S0306261919314709

[56] C. Breyer, D. Bogdanov, S. Khalili, and D. Keiner, "Solar Photovoltaics in 100Science and Technology. New York, NY: Springer, New York, NY, 2021, pp. 1–30. [Online]. Available: https://link.springer.com/referenceworkentry/10.1007/978-1-4939-2493-6_1071-1

[57] D. F. Dominković, J. M. Weinand, F. Scheller, M. D'Andrea, and R. McKenna, "Reviewing two decades of energy system analysis with bibliometrics," *Renewable and Sustainable Energy Reviews*, vol. 153, no. December 2020, 2022.

[58] B. P. Heard, B. W. Brook, T. M. Wigley, and C. J. Bradshaw, "Burden of proof: A comprehensive review of the feasibility of 100systems," *Renewable and Sustainable Energy Reviews*, vol. 76, no. March, pp. 1122–1133, 2017. [Online]. Available: http://dx.doi.org/10.1016/j.rser.2017.03.114

[59] T. W. Brown, T. Bischof-Niemz, K. Blok, C. Breyer, H. Lund, and B. V. Mathiesen, "Response to 'Burden of proof: A comprehensive review of the feasibility of 100Sustainable Energy Reviews, vol. 92, no. April, pp. 834–847, 2018. [Online]. Available: https://doi.org/10.1016/j.rser.2018.04.113

[60] T. Tröndle, S. Pfenninger, and J. Lilliestam, "Home-made or imported: On the possibility for renewable electricity autarky on all scales in Europe," *Energy Strategy Reviews*, vol. 26, p. 100388, nov 2019.

[61] T. Tröndle, J. Lilliestam, S. Marelli, and S. Pfenninger, "Trade-Offs between Geographic Scale, Cost, and Infrastructure Requirements for Fully Renewable Electricity in Europe," *Joule*, vol. 4, no. 9, pp. 1929–1948, sep 2020. [Online]. Available: https://linkinghub.elsevier.com/retrieve/pii/S2542435120303366

[62] T. Trondle, "Supply-side options to reduce land requirements of fully renewable electricity in Europe," *PLoS ONE*, vol. 15, no. 8 August, pp. 1–19, 2020.

[63] K. Hansen, C. Breyer, and H. Lund, "Status and perspectives on 100energy systems," *Energy*, vol. 175, pp. 471–480, may 2019.

[64] O. Ruhnau and S. Qvist, "Storage requirements in a 100system: Extreme events and inter-annual variability," *ZBW - Leibniz Information Centre for Economics, Kiel, Hamburg*, 2021. [Online]. Available: www.econstor.eu

[65] S. Pfenninger and J. Keirstead, "Renewables, nuclear, or fossil fuels? Scenarios for Great Britain's power system considering costs, emissions and energy security," *Applied Energy*, vol. 152, pp. 83–93, aug 2015.

[66] N. A. Sepulveda, J. D. Jenkins, A. Edington, D. S. Mallapragada, and R. K. Lester, "The design space for long-duration energy storage in decarbonized power systems," *Nature Energy*, vol. 6, no. 5, pp. 506–516, 2021. [Online]. Available: https://doi.org/10.1038/s41560-021-00796-8

[67] W. P. Schill, "Electricity Storage and the Renewable Energy Transition," *Joule*, vol. 4, no. 10, pp. 2059–2064, oct 2020.

[68] J. Salpakari, J. Mikkola, and P. D. Lund, "Improved flexibility with large-scale variable renewable power in cities through optimal demand side management and power-to-heat conversion," *Energy Conversion and Management*, vol. 126, pp. 649–661, 2016. [Online]. Available: http://dx.doi.org/10.1016/j.enconman.2016.08.041

[69] J. P. Deane, G. Drayton, and B. P. Ó Gallachóir, "The impact of sub-hourly modelling in power systems with significant levels of renewable generation," *Applied Energy*, vol. 113, pp. 152–158, 2014. [Online]. Available: http://dx.doi.org/10.1016/j.apenergy.2013.07.027

[70] I. Dimoulkas, M. Amelin, and F. Levihn, "District heating system operation in power systems with high share of wind power," *Journal of Modern Power Systems and Clean Energy*, vol. 5, no. 6, pp. 850–862, 2017.

[71] C. O'Dwyer and D. Flynn, "Using Energy Storage to Manage High Net Load Variability at Sub-Hourly," *IEEE Power Systems*, no. October 2016, 2015.

[72] S. Pfenninger, "Dealing with multiple decades of hourly wind and PV time series in energy models: A comparison of methods to reduce time resolution and the planning implications of inter-annual variability," *Applied Energy*, vol. 197, pp. 1–13, jul 2017.

[73] L. Kotzur, P. Markewitz, M. Robinius, and D. Stolten, "Impact of different time series aggregation methods on optimal energy system design," *Renewable Energy*, vol. 117, pp. 474–487, mar 2018. [Online]. Available: https://linkinghub.elsevier.com/retrieve/pii/S0960148117309783

[74] P. Gabrielli, M. Gazzani, E. Martelli, and M. Mazzotti, "Optimal design of multi-energy systems with seasonal storage," *Applied Energy*, vol. 219, no. June 2017, pp. 408–424, 2018. [Online]. Available: https://doi.org/10.1016/j.apenergy.2017.07.142

[75] G. Limpens, S. Moret, H. Jeanmart, and F. Maréchal, "EnergyScope TD: A novel open-source model for regional energy systems," *Applied Energy*, vol. 255, p. 113729, dec 2019.

[76] L. Welder, D. S. Ryberg, L. Kotzur, T. Grube, M. Robinius, and D. Stolten, "Spatio-temporal optimization of a future energy system for power-to-hydrogen applications in Germany," *Energy*, vol. 158, pp. 1130–1149, 2018. [Online]. Available: https://doi.org/10.1016/j.energy.2018.05.059

[77] H. C. Gils, Y. Scholz, T. Pregger, D. Luca de Tena, and D. Heide, "Integrated modelling of variable renewable energy-based power supply in Europe," *Energy*, vol. 123, pp. 173–188, mar 2017.

[78] T. Brown, J. Hörsch, and D. Schlachtberger, "PyPSA: Python for Power System Analysis," *Journal of Open Research Software*, vol. 6, no. 1, jan 2018. [Online]. Available: http://openresearchsoftware.metajnl.com/articles/10.5334/jors.188/

[79] F. Steinke, P. Wolfrum, and C. Hoffmann, "Grid vs. storage in a 100renewable Europe," *Renewable Energy*, vol. 50, pp. 826–832, 2013. [Online]. Available: http://dx.doi.org/10.1016/j.renene.2012.07.044

[80] O. Kraan, G. J. Kramer, M. Haigh, and C. Laurens, "An Energy Transition That Relies Only on Technology Leads to a Bet on Solar Fuels," pp. 2286–2290, oct 2019.

[81] P. Denholm and M. Hand, "Grid flexibility and storage required to achieve very high penetration of variable renewable electricity," *Energy Policy*, vol. 39, no. 3, pp. 1817–1830, mar 2011.

[82] W. P. Schill and A. Zerrahn, "Long-run power storage requirements for high shares of renewables: Results and sensitivities," pp. 156–171, mar 2018. [Online]. Available: https://linkinghub.elsevier.com/retrieve/pii/S1364032117308419

[83] G. Limpens and H. Jeanmart, "Electricity storage needs for the energy transition: An EROI based analysis illustrated by the case of Belgium," *Energy*, vol. 152, pp. 960–973, jun 2018.

[84] A. Zerrahn and W. P. Schill, "On the representation of demand-side management in power system models," *Energy*, vol. 84, pp. 840–845, may 2015.

[85] A. Pappu, "Demand Side Management using Blockchain for Distributed Networks," Ph.D. dissertation, University of Twente, 2021.

[86] F. Scheller, F. Wiese, J. M. Weinand, and R. Mckenna, "An expert survey to assess the current status and future challenges of energy system analysis," 2021.

[87] H. A. Linstone, "Shaping the Next One Hundred Years: New Methods for Quantitative, Long-Term Policy Analysis: R.J. Lempert, S.W. Popper, and S.C. Bankes, Santa Monica, CA, The RAND Corporation, 2003," *Technological Forecasting and Social Change*, vol. 71, no. 3, pp. 305–307, mar 2004.

[88] S. Moret, V. Codina, M. Bierlaire, and F. Maréchal, "Characterization of input uncertainties in strategic energy planning models," *Applied Energy*, vol. 202, pp. 597–617, 2017. [Online]. Available: http://dx.doi.org/10.1016/j.apenergy.2017.05.106

[89] J. F. DeCarolis, "Using modeling to generate alternatives (MGA) to expand our thinking on energy futures," *Energy Economics*, vol. 33, no. 2, pp. 145–152, 2011. [Online]. Available: http://dx.doi.org/10.1016/j.eneco.2010.05.002

[90] J. F. DeCarolis, K. Hunter, and S. Sreepathi, "The case for repeatable analysis with energy economy optimization models," *Energy Economics*, vol. 34, no. 6, pp. 1845–1853, 2012. [Online]. Available: http://dx.doi.org/10.1016/j.eneco.2012.07.004

[91] G. Betz, "What's the Worst Case? The Methodology of Possibilistic Prediction," *Analyse and Kritik*, vol. 32, no. 1, pp. 87–106, may 2010. [Online]. Available: https://www.degruyter.com/document/doi/10.1515/auk-2010-0105/html

[92] K. K. Cao, F. Cebulla, J. J. Gómez Vilchez, B. Mousavi, and S. Prehofer, "Raising awareness in model-based energy scenario studies—a transparency checklist," *Energy, Sustainability and Society*, vol. 6, no. 1, dec 2016.

[93] X. Yue, S. Pye, J. DeCarolis, F. G. Li, F. Rogan, and B. Gallachóir, "A review of approaches to uncertainty assessment in energy system optimization models," *Energy Strategy Reviews*, vol. 21, no. June, pp. 204–217, 2018. [Online]. Available: https://doi.org/10.1016/j.esr.2018.06.003

[94] F. Neumann and T. Brown, "The near-optimal feasible space of a renewable power system model," *Electric Power Systems Research*, vol. 190, p. 106690, jan 2021.

[95] F. Lombardi, B. Pickering, E. Colombo, and S. Pfenninger, "Policy Decision Support for Renewables Deployment through Spatially Explicit Practically Optimal Alternatives," *Joule*, vol. 4, no. 10, pp. 2185–2207, 2020. [Online]. Available: https://doi.org/10.1016/j.joule.2020.08.002

[96] F. Neumann, "Costs of regional equity and autarky in a renewable European power system," *Energy Strategy Reviews*, vol. 35, p. 100652, may 2021.

[97] T. T. Pedersen, M. Victoria, M. G. Rasmussen, and G. B. Andresen, "Modeling all alternative solutions for highly renewable energy systems," *Energy*, vol. 234, no. October, 2021.

[98] X. Yue, N. Patankar, J. Decarolis, A. Chiodi, F. Rogan, J. P. Deane, and B. O'Gallachoir, "Least cost energy system pathways towards 100energy in Ireland by 2050," *Energy*, vol. 207, p. 118264, sep 2020.

[99] E. C, "Does cost optimization approximate the real-world energy transition?" *Energy*, vol. 106, pp. 182–193, jul 2016.

[100] J. Fraiture, "The Robustness of Energy Systems," *Delft University of Technology*, pp. 1–150, 2020. [Online]. Available: http://resolver.tudelft.nl/uuid:84cd083a-8bf8-4931-a75a-276e2d54c5cc

[101] S. Bankes, "Exploratory Modeling for Policy Analysis," *Operations Research*, vol. 41, no. 3, pp. 435–449, jun 1993.

[102] S. Collins, J. P. Deane, K. Poncelet, E. Panos, R. C. Pietzcker, E. Delarue, and B. P. Ó Gallachóir, "Integrating short term variations of the power system into integrated energy system models: A methodological review," *Renewable and Sustainable Energy Reviews*, vol. 76, no. January, pp. 839–856, 2017. [Online]. Available: http://dx.doi.org/10.1016/j.rser.2017.03.090

[103] K. Poncelet, E. Delarue, J. Duerinck, D. Six, and W. D'haeseleer, "The importance of integrating the variability of renewables in long-term energy planning models," *TME Working Paper - Energy and Environment*, no. October, pp. 1–18, 2014. [Online]. Available: https://www.mech.kuleuven.be/en/tme/research/energy_environment/Pdf/wp-importance.pdf

[104] Open Source Initiative, "The MIT License," p. 1, 2018. [Online]. Available: https://opensource.org/licenses/MIThttps://opensource.org/licenses/mit-license.php%0Ahttps://opensource.org/licenses/MIT

[105] S. W. P. van Wieringen, “Local Energy System Optimization (LESO) framework,” 2021. [Online]. Available: https://github.com/thesethtruth/LESO

[106] J. H. Kwakkel, “The Exploratory Modeling Workbench: An open source toolkit for exploratory modeling, scenario discovery, and (multi-objective) robust decision making,” *Environmental Modelling and Software*, vol. 96, pp. 239–250, oct 2017.

[107] J. Lavaei and S. H. Low, “Zero duality gap in optimal power flow problem,” *IEEE Transactions on Power Systems*, vol. 27, no. 1, pp. 92–107, feb 2012.

[108] N. Baumgärtner, B. Bahl, M. Hennen, and A. Bardow, “RiSES3: Rigorous Synthesis of Energy Supply and Storage Systems via time-series relaxation and aggregation,” *Computers and Chemical Engineering*, vol. 127, pp. 127–139, aug 2019. [Online]. Available: https://linkinghub.elsevier.com/retrieve/pii/S009813541831127X

[109] S. Pfenninger and B. Pickering, “Calliope: a multi-scale energy systems modelling framework,” *Journal of Open Source Software*, vol. 3, no. 29, p. 825, sep 2018. [Online]. Available: https://joss.theoj.org/papers/10.21105/joss.00825

[110] R. A. Rodriguez, S. Becker, and M. Greiner, “Cost-optimal design of a simplified, highly renewable pan-European electricity system,” *Energy*, vol. 83, pp. 658–668, apr 2015.

[111] D. P. Schlachtberger, T. Brown, M. Schäfer, S. Schramm, and M. Greiner, “Cost optimal scenarios of a future highly renewable European electricity system: Exploring the influence of weather data, cost parameters and policy constraints,” *Energy*, vol. 163, pp. 100–114, nov 2018.

[112] K. B. Lindberg, G. Doorman, D. Fischer, M. Korpås, A. Ånestad, and I. Sartori, “Methodology for optimal energy system design of Zero Energy Buildings using mixed-integer linear programming,” *Energy and Buildings*, vol. 127, pp. 194–205, sep 2016.

[113] G. Haydt, V. Leal, A. Pina, and C. A. Silva, “The relevance of the energy resource dynamics in the mid/long-term energy planning models,” *Renewable Energy*, vol. 36, no. 11, pp. 3068–3074, nov 2011.

[114] European Commission, Joint Research Centre, and EU Science Hub, “Photovoltaic Geographical Information System.” [Online]. Available: http://re.jrc.ec.europa.eu/pvgis.html

[115] European Commission, “TMY generator — PVGIS,” 2021. [Online]. Available: https://ec.europa.eu/jrc/en/PVGIS/tools/tmy

[116] R. Urraca, T. Huld, A. Gracia-Amillo, F. J. Martinez-de Pison, F. Kaspar, and A. Sanz-Garcia, “Evaluation of global horizontal irradiance estimates from ERA5 and COSMO-REA6 reanalyses using ground and satellite-based data,” *Solar Energy*, vol. 164, pp. 339–354, apr 2018.

[117] T. Huld, R. Müller, and A. Gambardella, “A new solar radiation database for estimating PV performance in Europe and Africa,” *Solar Energy*, vol. 86, no. 6, pp. 1803–1815, jun 2012.

[118] R. Urraca, A. M. Gracia-Amillo, E. Koubli, T. Huld, J. Trentmann, A. Riihelä, A. V. Lindfors, D. Palmer, R. Gottschalg, and F. Antonanzas-Torres, “Extensive validation of CM SAF surface radiation products over Europe,” *Remote Sensing of Environment*, vol. 199, pp. 171–186, sep 2017.

[119] T. Cebecauer and M. Suri, “Typical Meteorological Year Data: SolarGIS Approach,” in *Energy Procedia*, vol. 69. Elsevier Ltd, may 2015, pp. 1958–1969.

[120] G. Pernigotto, A. Prada, A. Gasparella, and J. L. Hensen, "Analysis and improvement of the representativeness of EN ISO 15927-4 reference years for building energy simulation," *Journal of Building Performance Simulation*, vol. 7, no. 6, pp. 391–410, 2014.

[121] S. Pfenninger and I. Staffell, "Long-term patterns of European PV output using 30 years of validated hourly reanalysis and satellite data," *Energy*, vol. 114, pp. 1251–1265, nov 2016.

[122] I. Staffell and S. Pfenninger, "Using bias-corrected reanalysis to simulate current and future wind power output," *Energy*, vol. 114, pp. 1224–1239, nov 2016.

[123] K. Gruber, P. Regner, S. Wehrle, M. Zeyringer, and J. Schmidt, "Towards global validation of wind power simulations: A multi-country assessment of wind power simulation from MERRA-2 and ERA-5 reanalyses bias-corrected with the global wind atlas," *Energy*, vol. 238, p. 121520, jan 2022.

[124] C. Jung and D. Schindler, "Integration of small-scale surface properties in a new high resolution global wind speed model," *Energy Conversion and Management*, vol. 210, p. 112733, apr 2020.

[125] L. Hayes, M. Stocks, and A. Blakers, "Accurate long-term power generation model for offshore wind farms in Europe using ERA5 reanalysis," *Energy*, vol. 229, p. 120603, aug 2021.

[126] A. Piasecki, J. Jurasz, and A. Kies, "Measurements and reanalysis data on wind speed and solar irradiation from energy generation perspectives at several locations in Poland," *SN Applied Sciences*, vol. 1, no. 8, pp. 1–8, aug 2019. [Online]. Available: https://doi.org/10.1007/s42452-019-0897-2

[127] J. Olauson, "ERA5: The new champion of wind power modelling?" *Renewable Energy*, vol. 126, pp. 322–331, oct 2018.

[128] Royal Netherlands Meteorological Institue, "KNMI Data Centre (KDC)," 2021. [Online]. Available: https://dataplatform.knmi.nl/

[129] I. L. Wijnant, B. V. Ulft, B. V. Stratum, J. Barkmeijer, J. Onvlee, C. D. Valk, S. Knoop, S. Kok, G. J. Marseille, H. K. Baltink, and A. Stepek, "The Dutch Offshore Wind Atlas (DOWA): description of the dataset," *The DOWA project*, 2019. [Online]. Available: http://bibliotheek.knmi.nl/knmipubTR/TR380.pdf

[130] P. Loutzenhiser, H. Manz, C. Felsmann, P. Strachan, T. Frank, and G. Maxwell, "Empirical validation of models to compute solar irradiance on inclined surfaces for building energy simulation," *Solar Energy*, vol. 81, no. 2, pp. 254–267, feb 2007. [Online]. Available: https://pureportal.strath.ac.uk/en/publications/empirical-validation-of-models-to-compute-solar-irradiance-on-inc

[131] H. Hottel and B. Woertz, "Performance of flat-plate solar-heat collectors," *Trans. ASME (Am. Soc. Mech. Eng.); (United States)*, 1942. [Online]. Available: https://www.osti.gov/biblio/5052689

[132] R. W. Andrews, J. S. Stein, C. Hansen, and D. Riley, "Introduction to the open source PV LIB for python Photovoltaic system modelling package," *2014 IEEE 40th Photovoltaic Specialist Conference, PVSC 2014*, pp. 170–174, 2014.

[133] European Commission Joint Research Centre Institute for Energy and Transport, "Energy Technology Reference Indicator projections for 2010-2050," 2014, p. 108. [Online]. Available: https://setis.ec.europa.eu/system/files/ETRI2014.pdf

[134] Ioannis Tsiropoulos, Dalius Tarvydas, and Andreas Zucker, *Cost development of low carbon energy technologies - Scenario-based cost trajectories to 2050, 2017 edition*, 2018.

[135] Fraunhofer ISE, "Current and Future Cost of Photovoltaics. Long-term Scenarios for Market Development, System Prices and LCOE of Utility-Scale PV Systems," Tech. Rep. February, 2015. [Online]. Available: www.agora-energiewende.de

[136] Manwell J. F., Mcgowan J. G., and Rogers A. L., *Wind Energy Explained: Theory, Design and Application, 2nd Edition*, segunda ed., 2010.

[137] G. Pleßman, "Open Energy Platform," 2015. [Online]. Available: https://openenergy-platform.org/

[138] S. Haas, F. Behrendt, J. Rieck, and B. Schachler, "Implementation and validation of an open source model for generating wind feed-in time series," Ph.D. dissertation, Technische Universitat Berlin, 2019.

[139] J. W. Ager and A. A. Lapkin, "Chemical storage of renewable energy," *Science*, vol. 360, no. 6390, pp. 707–708, may 2018.

[140] K. Mongird, V. Viswanathan, P. Balducci, J. Alam, V. Fotedar, V. Koritarov, and B. Hadjerioua, "An Evaluation of Energy Storage Cost and Performance Characteristics," *Energies 2020, Vol. 13, Page 3307*, vol. 13, no. 13, p. 3307, jun 2020. [Online]. Available: https://www.mdpi.com/1996-1073/13/13/3307/htmhttps://www.mdpi.com/1996-1073/13/13/3307

[141] C. Budischak, D. Sewell, H. Thomson, L. MacH, D. E. Veron, and W. Kempton, "Cost-minimized combinations of wind power, solar power and electrochemical storage, powering the grid up to 99.9Sources, vol. 225, pp. 60–74, mar 2013.

[142] M. Child, C. Kemfert, D. Bogdanov, and C. Breyer, "Flexible electricity generation, grid exchange and storage for the transition to a 100energy system in Europe," *Renewable Energy*, vol. 139, pp. 80–101, aug 2019. [Online]. Available: https://linkinghub.elsevier.com/retrieve/pii/S0960148119302319

[143] M. G. Rasmussen, G. B. Andresen, and M. Greiner, "Storage and balancing synergies in a fully or highly renewable pan-European power system," *Energy Policy*, vol. 51, pp. 642–651, dec 2012.

[144] A. Van Stiphout, K. De Vos, and G. Deconinck, "Operational flexibility provided by storage in generation expansion planning with high shares of renewables," *International Conference on the European Energy Market, EEM*, vol. 2015-Augus, 2015.

[145] O. Schmidt, S. Melchior, A. Hawkes, and I. Staffell, "Projecting the Future Levelized Cost of Electricity Storage Technologies," *Joule*, vol. 3, no. 1, pp. 81–100, jan 2019.

[146] N. A. Sepulveda, J. D. Jenkins, F. J. de Sisternes, and R. K. Lester, "The Role of Firm Low-Carbon Electricity Resources in Deep Decarbonization of Power Generation," *Joule*, vol. 2, no. 11, pp. 2403–2420, nov 2018.

[147] J. Moshövel, K. P. Kairies, D. Magnor, M. Leuthold, M. Bost, S. Gährs, E. Szczechowicz, M. Cramer, and D. U. Sauer, "Analysis of the maximal possible grid relief from PV-peak-power impacts by using storage systems for increased self-consumption," *Applied Energy*, vol. 137, pp. 567–575, jan 2015.

[148] W. Cole and A. W. Frazier, "NREL: Cost Projections for Utility-Scale Battery Storage," no. June, 2021. [Online]. Available: www.nrel.gov/publications.

[149] S. Funke, P. Jochem, S. Ried, and T. Gnann, "Fast charging stations with stationary batteries: A techno-economic comparison of fast charging along highways and in cities," in *Transportation Research Procedia*, vol. 48, 2020, pp. 3832–3849. [Online]. Available: www.sciencedirect.comwww.sciencedirect.comwww.elsevier.com/locate/procedia2352-1465www.sciencedirect.comwww.elsevier.com/locate/procedia2352-1465

[150] N. V. D. Werf, "Integration of public ultra-fast chargers for heavy-duty transport in the Dutch electricity grid," no. May, 2021.

[151] Rijkswaterstaat, "Dexter — Nationaal Dataportaal Wegverkeer." [Online]. Available: https://www.ndw.nu/

[152] BOVAG, "Update EV-onderzoek," no. april, 2021.

[153] A. Genovese, F. Ortenzi, and C. Villante, "On the energy efficiency of quick DC vehicle battery charging," *World Electric Vehicle Journal*, vol. 7, no. 4, pp. 570–576, 2015.

[154] Gasunie and TenneT, "Infrastructure Outlook 2050. A joint study by Gasunie and TenneT on integrated energy infrastructure in the Netherlands and Germany," Tech. Rep., 2019. [Online]. Available: https://www.tennet.eu/fileadmin/user_upload/Company/News/Dutch/2019/Infrastructure_Outlook_2050_appendices_190214.pdf

[155] R. J. Green and T.-O. Léautier, "Do costs fall faster than revenues ? Dynamics of renewables entry into electricity markets," *Toulouse School of Economics*, pp. 1–59, 2015. [Online]. Available: http://fs-unep-centre.org/publications/global-trends-renewable-energy-investment-2015.

[156] A. Savitzky and M. J. Golay, "Smoothing and Differentiation of Data by Simplified Least Squares Procedures," *Analytical Chemistry*, vol. 36, no. 8, pp. 1627–1639, jul 1964. [Online]. Available: https://pubs.acs.org/doi/abs/10.1021/ac60214a047

[157] Y. Sunak and R. Madlener, "The impact of wind farm visibility on property values: A spatial difference-in-differences analysis," *Energy Economics*, vol. 55, pp. 79–91, mar 2016.

[158] Quintel Intelligence, "etsource: Data source for the Energy Transition Model," 2021. [Online]. Available: https://github.com/quintel/etsource

[159] Kalavasta, "Uitwerking van een 2030 scenario op basis van het ontwerp Klimaatakkoord en vast en voorgenomen beleid," pp. 1–15, 2019. [Online]. Available: https://kalavasta.com/assets/reports/Kalavasta2030KEAenergiesysteemNL.pdf

[160] European Commission, *EU Reference Scenario 2020 — Energy*, 2021. [Online]. Available: https://ec.europa.eu/energy/data-analysis/energy-modelling/eu-reference-scenario-2016_en

[161] F. Simon, "Analyst: EU carbon price on track to reach €90 by 2030," jul 2021. [Online]. Available: https://www.euractiv.com/section/emissions-trading-scheme/interview/analyst-eu-carbon-price-on-track-to-reach-e90-by-2030/

[162] I. Infrastructuurverkenning, M. Afman, and M. Douwes, "Aanpassingen klimaatneutrale energiesysteem scenario ' s 2050," 2020.

[163] Ministerie van Economische Zaken en Klimaat, "Besluit leveringszekerheid Elektriciteitswet 1998," *Staatsblad*, 2018. [Online]. Available: https://wetten.overheid.nl/BWBR0019567/2018-10-01

[164] Netbeheer Nederland, "Capaciteitskaart invoeding elektriciteitsnet," 2021. [Online]. Available: https://capaciteitskaart.netbeheernederland.nl/

[165] D. Duijnmayer, “Netbeheerders: 35 TWh is het maximale dat we kunnen aansluiten,” jul 2021. [Online]. Available: https://energeia.nl/energeia-artikel/40094501/netbeheerders-35-twh-is-het-maximale-dat-we-kunnen-aansluiten

[166] N. programma regionale energie strategie, “Elektriciteitsproductie uit wind op land en grootschalige zon-pv,” pp. 1–18, 2021.

[167] S. Z. Golroodbari, D. F. Vaartjes, J. B. Meit, A. P. van Hoeken, M. Eberveld, H. Jonker, and W. G. van Sark, “Pooling the cable: A techno-economic feasibility study of integrating offshore floating photovoltaic solar technology within an offshore wind park,” *Solar Energy*, vol. 219, pp. 65–74, may 2021.

[168] Netbeheer Nederland, “Cable pooling: Update factsheet en verdieping,” Netbeheer Nederland, Tech. Rep., 2020. [Online]. Available: https://www.netbeheernederland.nl/_upload/Files/Netcapaciteit_60_5de4ca08ea.pdf

[169] Ministerie van Economische Zaken en Klimaat, “Wet van 10 juni 2020 tot wijziging van de Elektriciteitswet 1998 en Gaswet (implementatie wijziging Gasrichtlijn en een aantal verordeningen op het gebied van elektriciteit en gas),” *Staatsblad 236*, no. Juli, pp. 1–10, 2020.

[170] “Windpark Nijmegen-Betuwe, burgerinitiatief langs de A15.” [Online]. Available: https://www.windparknijmegenbetuwe.nl/http://www.windparknijmegenbetuwe.nl/

[171] A. Van Der Welle and H. Cleijne, “Conceptadvies basisbedragen SDE++ 2022 financieringsparameters en algemeen,” Planbureau voor de Leefomgeving, Tech. Rep. april 2021, 2022.

[172] CE Delft, “Scenario’s zon op grote daken,” *Gemeente Utrecht*, 2021. [Online]. Available: https://ce.nl/wp-content/uploads/2021/04/CE_Delft_200432_Scenarios_zon_op_grote_daken_Utrecht_DEF.pdf

[173] DNV and InvestNL, “Battery energy storage in the Netherlands: Market opportunities and financing challenges,” Tech. Rep., 2021.

[174] T. Scholten, L. van Cappellen, C. Jongsma, and F. Rooijers, “Doorlooptijden investeringen elektrificatie,” Tech. Rep., 2021. [Online]. Available: https://www.ce.nl/publicaties/2600/doorlooptijden-investeringen-elektrificatie

[175] Witteveen+Bos, Saxion Hogeschool, and MTSA, “GROHW Consortium.” [Online]. Available: https://grohw.nl/

[176] R. Way, P. Mealy, J. D. Farmer, and M. Ives, “Empirically grounded technology forecasts and the...,” *INET Oxford Working Paper No. 2021-01*, 2021. [Online]. Available: https://www.inet.ox.ac.uk/publications/no-2021-01-empirically-grounded-technology-forecasts-and-the-energy-transition/

[177] S. Jerez, I. Tobin, R. Vautard, J. P. Montávez, J. M. López-Romero, F. Thais, B. Bartok, O. B. Christensen, A. Colette, M. Déqué, G. Nikulin, S. Kotlarski, E. Van Meijgaard, C. Teichmann, and M. Wild, “The impact of climate change on photovoltaic power generation in Europe,” *Nature Communications*, vol. 6, 2015.

[178] A. Vinca, S. Parkinson, E. Byers, P. Burek, Z. Khan, V. Krey, F. A. Diuana, Y. Wang, A. Ilyas, A. C. Köberle, I. Staffell, S. Pfenninger, A. Muhammad, A. Rowe, R. Schaeffer, N. D. Rao, Y. Wada, N. Djilali, and K. Riahi, “The NExus Solutions Tool (NEST) v1.0: An open platform for optimizing multi-scale energy-water-land system transformations,” *Geoscientific Model Development*, vol. 13, no. 3, pp. 1095–1121, mar 2020.

[179] N. Strachan, B. Fais, and H. Daly, “Reinventing the energy modelling–policy interface,” *Nature Energy*, vol. 1, no. 3, pp. 1–3, 2016.

[180] L. McInnes, J. Healy, and J. Melville, “UMAP: Uniform Manifold Approximation and Projection for Dimension Reduction,” feb 2018. [Online]. Available: https://arxiv.org/abs/1802.03426v3http://arxiv.org/abs/1802.03426

[181] P. Ineichen, “Global irradiance on tilted and oriented planes: model validations,” *University of Geneva*, no. February, 2011.

[182] R. Perez, R. Seals, P. Ineichen, R. Stewart, and D. Menicucci, “A new simplified version of the perez diffuse irradiance model for tilted surfaces,” *Solar Energy*, vol. 39, no. 3, pp. 221–231, 1987.

[183] A. F. Souka and H. H. Safwat, “Determination of the optimum orientations for the double-exposure, flat-plate collector and its reflectors,” *Solar Energy*, vol. 10, no. 4, pp. 170–174, 1966. [Online]. Available: https://app.dimensions.ai/details/publication/pub.1053491128

[184] D. L. King, W. E. Boyson, and J. A. Kratochvil, “Photovoltaic array performance model, SANDIA Report SAND2004-3535,” *National Renewable Energy Laboratory*, vol. 8, no. December, pp. 1–19, 2004.

[185] A. P. Dobos, “An Improved Coefficient Calculator for the California Energy Commission 6 Parameter Photovoltaic Module Model,” *Journal of Solar Energy Engineering*, vol. 134, no. 2, may 2012.

[186] D. L. King, S. Gonzalez, G. M. Galbraith, and W. E. Boyson, “Performance Model for Grid-Connected Photovoltaic Inverters, SAND2007-5036,” *Sandia technical report*, vol. 38, no. September, pp. 655–660, 2007. [Online]. Available: http://www.ntis.gov/help/ordermethods.asp?loc=7-4-0#onlinehttp://jsedres.sepmonline.org/content/38/2/655.abstract

[187] P. Gilman, A. Dobos, N. DiOrio, J. Freeman, S. Janzou, and D. Ryberg, “System Advisor Model (SAM),” *National Renewable Energy Laboratory*, no. March, 2017. [Online]. Available: https://sam.nrel.gov/%0Ahttps://sam.nrel.gov/images/web_page_files/sam-help-2018-11-11-r4.pdf%0Asam.nrel.gov/content/downloads

[188] Huawei, “Smart String Inverter SUN2000-100KTL-USH0 technical reference sheet,” Tech. Rep.

[189] Jinko, “Eagle 72M-V 350 technical reference sheet,” Tech. Rep.

[190] Deutscher Wetterdienst, “Druckgradientkraft,” Tech. Rep., 2009.

[191] Deutscher Wetterdienst, “ICAO-Standardatmosphäre (ISA),” Tech. Rep. [Online]. Available: https://www.dwd.de/DE/service/lexikon/begriffe/S/Standardatmosphaere_pdf.pdf?__blob=publicationFile&v=3

Appendix A

Optimisation

This appendix contains a more elaborate mathematical introduction to the optimisation specifically as included in the modelling framework developed in this thesis. In section A.1, the objective function is introduced. First, a more comprehensive version of the objective function only based on capital cost is used. Later, an optimisation objective is introduced that includes discounted investment costs and variable costs. As such, this objective function represents overnight system cost and is used in this thesis. In section A.2, the energy balance that is a constraint for each of the system configurations is introduced and illustrated using an example case.

A.1 Objective function

For the objective function of the optimization problem at hand, various implementations exist, tailored to the scope and intended result of the research. Both a minimizing objective function and a maximisation objective function is possible, most typically implemented to reflect either cost or profit.

A.1.1 Capacity scaling factor

Within this research, optimal proportions of components within an energy system is of particular interest. These can be implemented in the optimization statement by introducing an optimization variable that scales the component capacity, which will be referred to as the Capacity Scaling Factor (CSF) and denoted by D_j for all components j in component set m. Component capacities include power supply, power demand and energy content for instance. The CSF is used to scale component capacities such that the applied constraints functions are met. The optimality of the CSF is assessed through the objective function, by computing the product of the CSF and the unit cost or profit scalar. Therefore, the CSF denotes the installed capacity of a specific technology feature.

This unit cost or profit factor can result from computing any arbitrary cost or profit function associated with that component, as long as all components return a scalar with the same dimension (e.g. Euros or $kg\ CO_2$). It is important that this cost or profit function is formulated in unit size, i.e. provides a linear cost scaling factor. The product of this unit cost/profit factor and the component scaling factor then represents the total cost/profit associated with a certain scaling decision. It is denoted by c'_j. The optimisation algorithm will then consider implicitly consider the possible configurations, assess their ability to meet the constraints and the objective function value. The best scoring configuration that is able to meet the constraint functions is selected as the optimal solution.

A.1.2 Capital cost

This simple objective function is based solely on the capital expenditure of an energy system. It is achieved by computing the sum of all component capital costs as can be seen from eq. A.1. The optimization sense will then be minimization. The solution resulting from this objective represents the lowest capital cost energy system that meets all constraint functions.

$$\min_{x} \qquad f(x) = \sum_{j=1}^{m} c'_j D_j \tag{A.1}$$

$$\text{with:} \qquad c'_j, \quad \text{unit capital cost factor} \quad \forall j \in m \tag{A.2}$$

$$D_j, \quad \text{installed capacity (CSF)} \tag{A.3}$$

Applying this objective function is rather straightforward. An advantage of this simple objective function is that it results in a solution that represents a comprehensive quantity; without any ponderous financial abstraction.

However, it strongly lacks the ability to incorporate variable costs or profits which are assumed and predicted to occur during the system lifetime (e.g. operation and maintenance cost or import and export costs). Moreover, money does not have a fixed value over time for instance due to inflation. One time expenses such as investment costs should be discounted to a yearly payment representing the capital cost in the same quantity as variable costs on a yearly basis.

A.1.3 Variable scaling factor

Energy sources can be either dispatchable or non-dispatchable. Solar PV and wind-based energy generation are considered non-dispatchable since their maximum power output is fully determined by meteorological conditions. Although production of these sources can be curtailed, such a renewable energy asset cannot be controlled in terms of output.

However, components such as the grid connection or storage elements can be controlled. This operation of assets should be included in the optimisation statement because without representation of the operation of these assets it is not possible to decide whether those components should be placed in the energy system. To the end, the variable scaling factor is introduced. This factor is used to represent the operation of dispatchable components and is an optimisation variable for every time step in the considered time horizon.

A.1.4 Overnight system costs

This objective function is an improvement over the capital cost function, due to two adjustments. Firstly, it includes both variable and fixed costs. Secondly, it does this by discounting and annualizing all costs to a common ground using the Capital Recovery Factor (CRF), shown in eq. A.4. By annualizing investment costs, the need to specify salvage values and modelling of end effects is avoided [52]. In this equation, the component values for (technical/financial) lifetime and the component real discount rate is used. The real discount rate is component-specific because different technologies can have a different required rate of return on the equity share. This is in part based on the risk aversion of investors and project developers.

$$CRF = \frac{i_c \cdot (1+i_c)^{\tau_s}}{(1+i_c)^{\tau_s} - 1} \tag{A.4}$$

with:

$$\tau_s, \quad \text{component lifetime} \tag{A.5}$$

$$i_c, \quad \text{component real discount rate} \tag{A.6}$$

The CRF is the inverse of annuity, thus multiplied by the CRF is equal to dividing by the annuity. The discounting is done by using the real discount rate, which is computed based on the nominal discount rate as shown in eq. A.7. In this formula, the nominal discount rate is set to equal to the Weighted Average Cost of Capital (WACC) which is shown in eq. A.10.

$$i = \frac{i' - f}{1+f} \tag{A.7}$$

with:

$$i', \quad \text{nominal discount rate (WACC)} \tag{A.8}$$

$$f, \quad \text{expteced inflation rate} \tag{A.9}$$

$$WACC = E \cdot R_e + D \cdot i(1 - T_c) \tag{A.10}$$

with:

$$E, \quad \text{Equity share} \tag{A.11}$$

$$D, \quad \text{Debt share} \tag{A.12}$$

$$R_e, \quad \text{Required rate of return of equity} \tag{A.13}$$

$$i, \quad \text{Debt rate e.g. loan cost} \tag{A.14}$$

$$T_c, \quad \text{Corporate tax rate} \tag{A.15}$$

The objective function is then formed by including the investment cost in a similar manner as with the capital cost objective function. Only this time, the cost scaling factor includes the component operational and variable cost. Both are assumed to be able to scale linearly. New in this formula are the variable cost function and the CRF, which is included in the unit cost factor c'_j as shown in eq. A.21. The overnight system cost objective function is shown in eq. A.16. The objective function now contains two parts which are both annual expenses. The left-hand component reflects the discounted and annualized cost of capital investments and the right-hand component contains all variable costs of operation for every time step in the considered time horizon.

$$\min_{D_j, E_{j,t}} \quad f(D_j, E_{j,t}) = \sum_{j=1}^{m} c'_j D_j + \sum_{j=1}^{m} \sum_{t} V_{j,t} \Delta t \tag{A.16}$$

with:

$$c'_j, \quad \text{unit cost factor} \quad \forall j \in m \tag{A.17}$$

$$D_j, \quad \text{installed capacity (CSF)} \tag{A.18}$$

$$V_{j,t}, \quad \text{variable cost function} \quad \forall t \in [t_{min}, t_{max}] \tag{A.19}$$

(A.20)

New variables are introduced in formula A.16, which should be unpacked further to fully describe this objective function. Firstly, the annualized discounted unit cost factor is shown in eq. A.21. This is now the sum of the discounted and annualized lifetime unit investment cost (CAPEX) and yearly fixed unit operation cost (OPEX) factor. The lifetime unit CAPEX has to account for the component lifetime which is included in the CRF as shown in A.4. This implicitly assumes linear replacement costs for any year after the component lifetime, which is an assumption that includes the scrapping value of

the component. If component lifetime exceeds the system lifetime, scrapping value is represented as a negative fraction of the replacement cost. As a result, investment cost can be reflected as a single figure for various components that each have a respective technological lifetime.

$$c'_j = c'_{CAPEX,j} \cdot CRF + c'_{OPEX,j} \tag{A.21}$$

The variable cost function is component-specific, but can further be decomposed in a general sense as seen in eq. A.22. This variable cost function includes all profits or costs that are associated with the variable operation of assets such as the grid or storage components. For components that have a variable income component but that are not controlled by the optimisation algorithm, such as demand components, this same formula can be used to account for generated income. The integral that surrounds the variable cost function sums over all time instances within the time scope — typically the 8760 hours of a year.

$$V_{j,t} = c^v_{j,t} \cdot E_{j,t} \tag{A.22}$$

Further decomposition of the variable cost function is used to make a component-specific distinction. To demonstrate the implementation of such a variable cost function, two examples are shown. This is that of the grid component and of a storage component, shown in eq.A.24 and eq. A.23, respectively.

$$V_{j,t} = \begin{cases} c^v_{cost} \cdot E_{j,t} & E_{j,t} \geq 0 \\ -c^v_{cost} \cdot E_{j,t} & E_{j,t} < 0 \end{cases} \tag{A.23}$$

From the storage variable cost function, it can be noted that it scales linearly with the energy flow in the component. Because of the convention used for energy flows, a condition has to be implied such that the product of cost and flow is always positive. This means that when the power output is positive i.e. the storage is discharging. When the energy flow is negative the cost is multiplied by -1 such that the result of the product is positive, meaning that also charging has costs associated. This represents some abstract generalization of increased battery wear-out associated with charging and discharging which is necessary to incentivise the algorithm against overusing storage components.

$$V_{j,t} = c^v_{j,t} \cdot E_{j,t} \tag{A.24}$$

For the grid component, it can be deduced that it is simply the cost of import multiplied by its import energy flow and vice versa for income due to the export of energy. Due to the convention of the energy flows, the same cost factor can be used both for profit and cost. These cost variables can be assumed constant over the system lifetime (if a Power Purchase Agreement (PPA) is installed, for instance). Alternatively, a time series of energy markets can be fed to this function; allowing it to represent energy scarcity and abundance through the price signal. It is possible to split the cost factors for import and export by applying a condition on the value of the energy flow as done for the storage components in eq. A.23

Finally, the energy flow of the component can be either predefined or an optimisation variable based on the fact whether the component is dispatchable or not. This is shown in eq. A.25. If the operation of the asset is an optimisation variable, the variable scaling factor is used. This is modelled in the framework with an indexed optimisation variable using Pyomo ($Pyo.Var$). Otherwise, it is assumed that a predefined time series exists for that component. This can be used for demand components that generate income, such as the fast-charger component for instance.

$$E_j, t = \begin{cases} predefined & \text{if not dispatchable} \\ VSF(pyo.Var()_j, t) & \text{if dispatchable} \end{cases} \tag{A.25}$$

A.2 Energy balance

Since all energy systems in this modelling framework are modelled using predefined constant temporal resolution, it is possible to discretely formulate the power balance. In the developed framework, a convention is used that states that all loads (i.e. electricity demands) should be expressed as negative values while all generators are expressed as positive values. As a result of this convention, the sum of loads and generators determines the energy balance. For all time instances t in τ the sum of all loads and generators should be exactly equal to zero. I.e., all components should be exactly balanced. This is shown in eq. A.26.

$$0 = \sum_{j=1}^{n} p_j(t) \cdot x_j + E_{j,t} \tag{A.26}$$

with:

$$c_j, \quad \text{capital cost} \quad \forall i = 1, m \tag{A.27}$$

$$x_j, \quad \text{installed capacity} \quad \forall j = 1, n \tag{A.28}$$

A sample optimisation problem is used to supply context to the formulation of an energy balance in LESO. To this end, let us consider an energy system consisting of 5 components, as shown below.

Source components

1. Solar PV
2. Wind turbine
3. Grid import

Sink components

1. DC fast chargers
2. Single industrial consumer
3. Grid export

Collector components

1. Local network

Storage components

1. Lithium battery storage

The problem at hand is to find the most cost-effective configuration of wind, solar and battery storage system given a limited grid connection and 2 must-meet loads. This makes the sizing of those components the design variable D_j and the operation of the dispatchable assets the operation variable $E_{j,t}$. The must-meet loads are sufficiently large (2.2 MW) for the grid connection alone (1.5 MW) to be inadequate, forcing at least some implementation of local renewable energy generation and storage.

Looking at the energy balance equation shown in A.26, it can be concluded export of energy, charging of the storage component and curtailment should be used to balance the power system whenever the generating assets are producing more energy than is consumed. Similarly, When the generating assets are not generating enough energy to meet the local demand import and storage discharge should be operated such that the energy balance is met. Whenever the operation of the dispatchable assets is not sufficient, the design variables of a set of components should be increased such that the energy balance is met.

A visual representation of the energy balance obtained based on the implemented constraint is shown in figures A.1-A.4 for four week-long periods on hourly resolution. These energy balances were obtained based on optimisation of the described system for a whole year. From these visualisations, it can be seen that the components below zero (loads) are perfectly reflected by the components above zero (generators). Whenever necessary, curtailment, charging or discharging of the storage component and export or import through the grid component is used by the optimisation algorithm to close the energy balance. It should be noted that the algorithm has found a way to import electricity

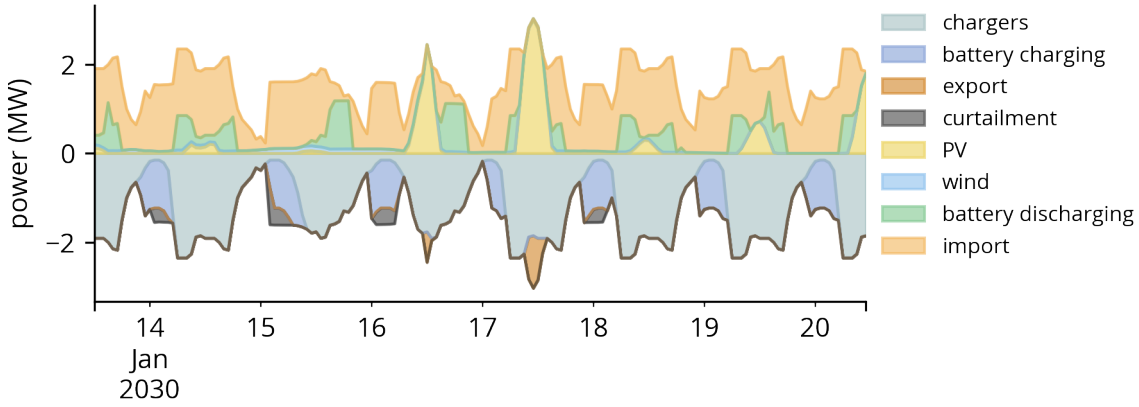

Figure A.1: Visual representation of the energy balance for the calculated system configuration for one week that starts at the 300th hour of the year

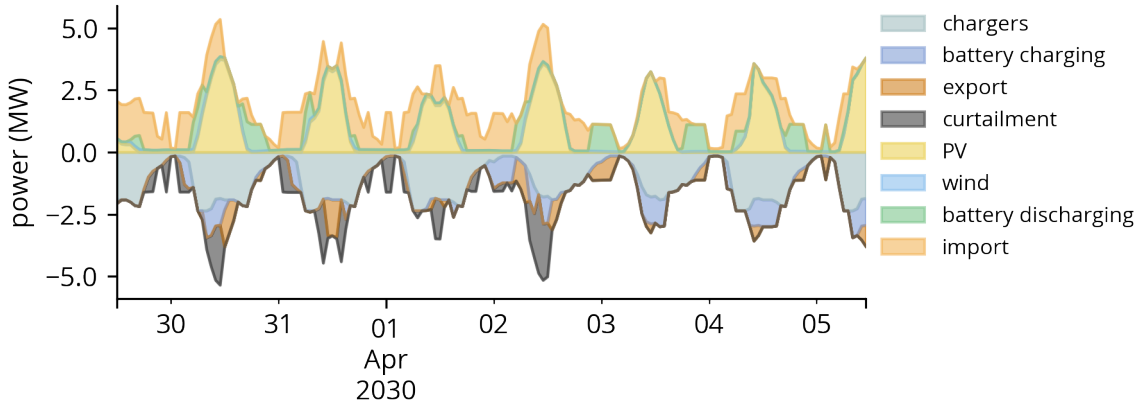

Figure A.2: Visual representation of the energy balance for the calculated system configuration for one week that starts at the 2100th hour of the year

at negative rates and curtail the local generation because that is more profitable. In reality, this will not be possible in most situations.

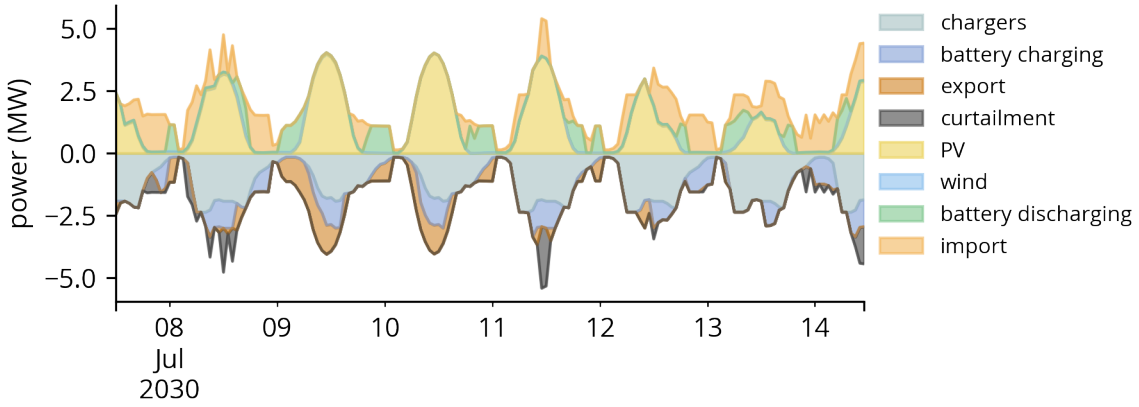

Figure A.3: Visual representation of the energy balance for the calculated system configuration for one week that starts at the 4500th hour of the year

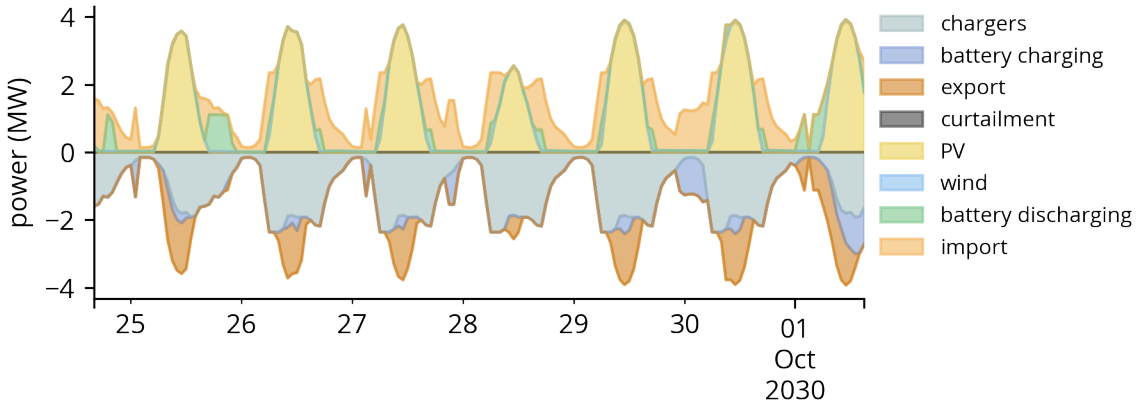

Figure A.4: Visual representation of the energy balance for the calculated system configuration for one week that starts at the 6400th hour of the year.

Appendix B

Submodels

B.1 Advanced PV modelling approach

Advanced diffuse transposition model — The isotropic transposition is a simple approach, which does not truly represent the physical phenomena of diffuse radiation. Even though no exact formula exist for transposition of diffuse radiation, various models have been formulated to better approximate diffuse radiation on arbitrary planes. [181] One well-known and often applied model is the Perez-transposition, shown in eq. B.1.

$$I_{\text{diffuse},\, poa} = I_{\text{diffuse},\, h} \cdot \left[(1 - F_1) \left(\frac{1 + \cos(\beta)}{2} \right) + F_1 \left(\frac{a}{b} \right) + F_2 \sin(\beta) \right] \tag{B.1}$$

With $a = max(0, \cos(aoi))$ and $b = max(\cos(85°, \cos\theta_z)$. Without considering too much of the specifics of this transportation, $F1$ and $F2$ represent complex functions that were empirically fitted to describe both circumsolar and horizon brightness. [182] This transposition circumstantially outperforms the isotropic diffuse transposition, when compared to measured data on various sites and system configurations. [181]

In the simplified PV power output model introduced in section 5.2.1 all system losses are simplified to a single efficiency factor. In reality, various effects contribute to this efficiency loss and display dynamic behaviour over time. Various of these components which are included in the detailed model approach are introduced below.

Effective irradiance — In reality not all irradiance reaching the surface of the array will be effectively absorbed by the photoactive layer in part due to reflectance. Eq. B.2 introduces a factor to be used to account for this reflectance, called the incident angle modifier (IAM), which is a function of the angle of angle of incidence (aoi). [183]

$$IAM = 1 - b_0 \left(\frac{1}{\cos(aoi)} - 1 \right) \tag{B.2}$$

Temperature model — Power output of a module is temperature dependent. In order to account for this effect, the module temperature should be calculated using eq. B.3. In this equation the effective radiation $(I_{\text{effective}})$ is correlated to the wind speed (s_w) and the temperature of the ambient air (T_a) using two empirical model parameters $(a\&b)$ which are determined for various system configurations. In addition to the macroscopic module temperature, the temperature on cell level is also of relevance to determining the dynamic power output. This is captured using eq. B.4, which also includes an empirical model parameter ΔT. For an open-field PV power plant this is best represented

using the model parameters of an open rack configuration and glass-glass module. This results in $a = 3.47$, $b = -0.0594$ and $\Delta T = 3$. [184]

$$T_m = I_{\text{effective}} \times \exp(a + b \times s_w) + T_a \tag{B.3}$$

$$T_C = T_m + \frac{I_{effective}}{I_{STC}} \Delta T \tag{B.4}$$

Temperature DC losses — Electric losses due to temperature effects are a substantial contributor to the total system losses. Eq. B.5 relates the DC output of the module to the temperature of the cells. The temperature of the cells is determined based on eq. B.3 and eq. B.4. This is a linear approximation of the effect of temperature on power output based on the modules parameters under STC. This relation is captured by γ_{pdc}, which is the temperature coefficient of power. This is a module specific parameter and reflects the sensitivity of the module to increasing temperature and as a result is a negative number. E.g. a higher temperature typically leads to a lower power output. [185]

$$P_{dc} = \frac{I_{\text{effective}}}{1000} P_{STC} \left(1 + \gamma_{pdc} \left(T_{\text{cell}} - T_{\text{STC}}\right)\right) \tag{B.5}$$

Inverter electrical losses — Losses at the inverter are another contributor to the total system efficiency losses. The relation used to model the inverter efficiency dynamically as function of the actual load in relation to the load under reference conditions is shown in eq. B.6. In this equation P_{dc0} is defined as the maximum input DC power of the inverter and is thus a inverter specific parameter. P_{ac0} is defined as the nominal AC output power of the inverter, which can be calculated by multiplying P_{dc0} by the DC power input limit. This variable therefore represents the maximum AC power output of an inverter under maximum DC load. Finally, power output of the inverter is defined as shown in eq. B.7. Other than purely efficiency losses, this correctly reflects possible clipping losses at an inverter level i.e. when DC power input cannot be fully converted to AC power. [186]

$$\eta = \frac{\eta_{\text{nom}}}{\eta_{\text{ref}}} \left(-0.0162\zeta - \frac{0.0059}{\zeta} + 0.9858\right) \tag{B.6}$$

With $\zeta = P_{dc}/P_{dc0}$ and $P_{dc0} = P_{ac0}/\eta_{\text{nom}}$.

$$P_{ac} = \min\left(\eta P_{dc}, P_{ac0}\right) \tag{B.7}$$

Selected modules, inverter and configuration — As noted in the above equations, some module specific parameters are needed to use the extensive modelling approach. It should however be stated, that also the configuration specifics of the PV systems should be considered such as the string configuration. To come to a sensible design that reflect current industry standards, a design of a recent solar park in the Netherlands was used. The respective parameters for both the module and inverter used in this configuration were taken from the CEC module and inverter databases. [187] These supply all needed parameters to use the described models in the correct format. The final PV system design uses a Huawei SUN2000-100KTL-USH0 smart string inverter [188] wired up to 12 strings each with 32 Jinko Eagle 72M-V 350 mono crystalline modules [189].

B.2 Detailed wind modelling approach

Density model — Since the power output of the wind turbine is in part proportional to the density of the passing air, it is relevant to use the density as found in the meteorological data. However, for

this it is required that this density is valid at the hub-height. As it is very unlikely that the measured or reanalyzed data height is exactly equal to the height of the turbine, the ideal gas law can be applied to transform the data point to the correct height. This is shown in eq. B.8. In this equation, the density is determined using the ideal gas law based on the pressure and temperature at the hub. The pressure at the hub level is approximated using B.9. [190] The temperature at the hub-height is a result of the temperature model. Alternatives to the ideal gas law approximation are barometric approximation or using interpolation/extrapolation if multiple height levels are available.

$$\rho_{hub} = p_{\text{hub}} \,/\, (R_s T_{hub}) \tag{B.8}$$

$$p_{hub} = \left(p/100 - (h_{hub} - h_{\text{ data}}) \cdot \frac{1}{8} \right) \cdot 100 \tag{B.9}$$

Temperature model — Since the ideal gas law is applied to determine the density at the hub height, it is necessary to determine the temperature at the height of the turbine hub. This is implemented in the form of a linear gradient assumption based on the ICAO-Standardatmosphäre (ISA), as shown in eq. B.10. In this implementation, a linear temperature gradient of -6.5 K/km is applied. [191] An alternative approach is to use interpolation/extrapolation if more height levels are available in the data used.

$$T_{hub} = T_{\text{air}} - 0.0065 \cdot (h_{\text{hub}} - h_{\text{ data}}) \tag{B.10}$$

Appendix C

Supplementary figures

C.1 Electric mobility hub

C.1.1 Policy 1 cost uncertainty and technology deployment

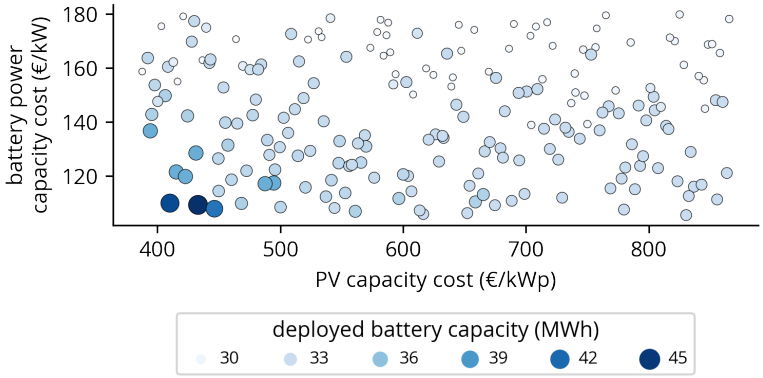

Figure C.1: Battery deployment on the uncertainty plane spanned by PV and battery capacity cost for 0.0 MW grid capacity *(policy 1)*

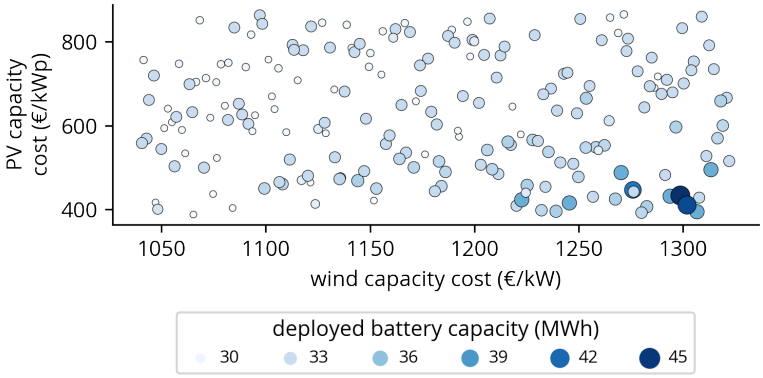

Figure C.2: Battery deployment on the uncertainty plane spanned by wind and PV capacity cost for 0.0 MW grid capacity *(policy 1)*

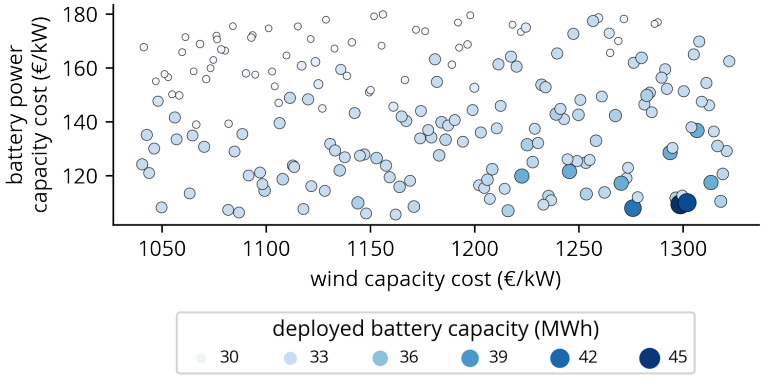

Figure C.3: Battery deployment on the uncertainty plane spanned by wind and battery capacity cost for 0.0 MW grid capacity *(policy 1)*

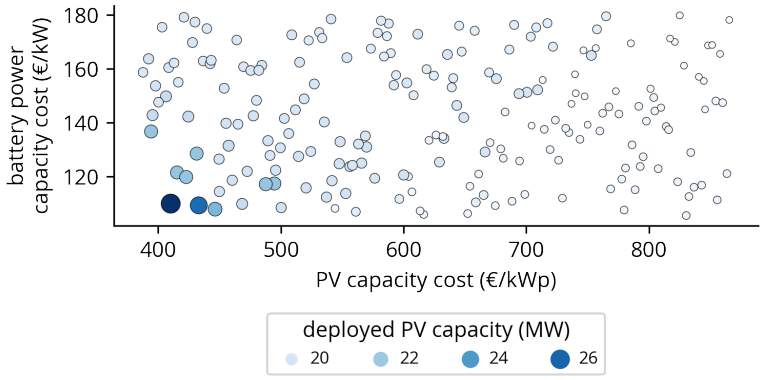

Figure C.4: PV deployment on the uncertainty plane spanned by PV and battery capacity cost for 0.0 MW grid capacity *(policy 1)*

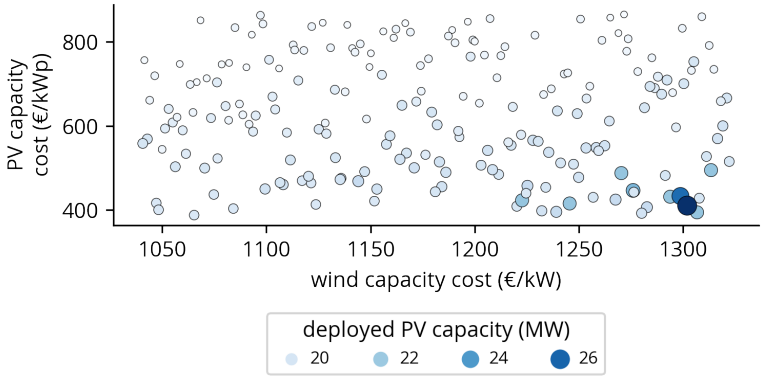

Figure C.5: PV deployment on the uncertainty plane spanned by wind and PV capacity cost for 0.0 MW grid capacity *(policy 1)*

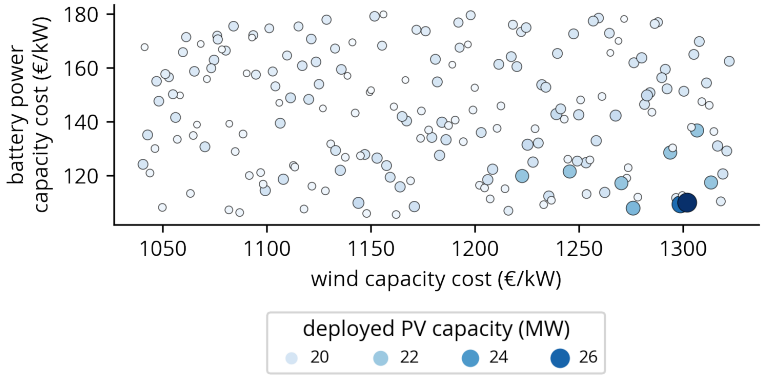

Figure C.6: PV deployment on the uncertainty plane spanned by wind and battery capacity cost for 0.0 MW grid capacity *(policy 1)*

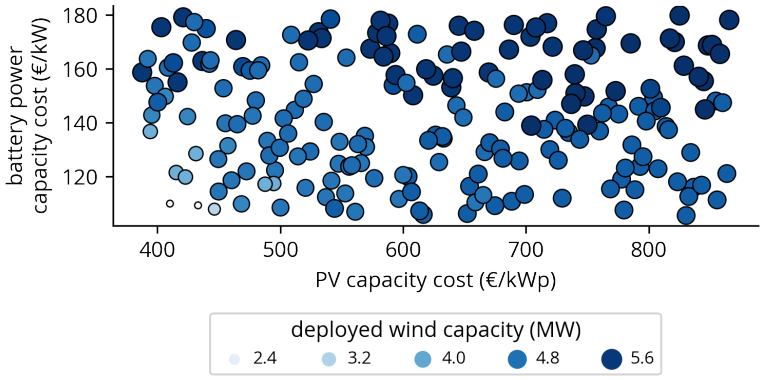

Figure C.7: Wind deployment on the uncertainty plane spanned by PV and battery capacity cost for 0.0 MW grid capacity *(policy 1)*

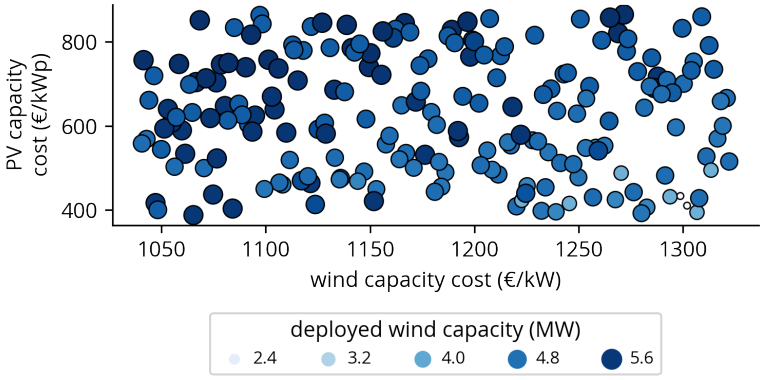

Figure C.8: Wind deployment on the uncertainty plane spanned by wind and PV capacity cost for 0.0 MW grid capacity *(policy 1)*

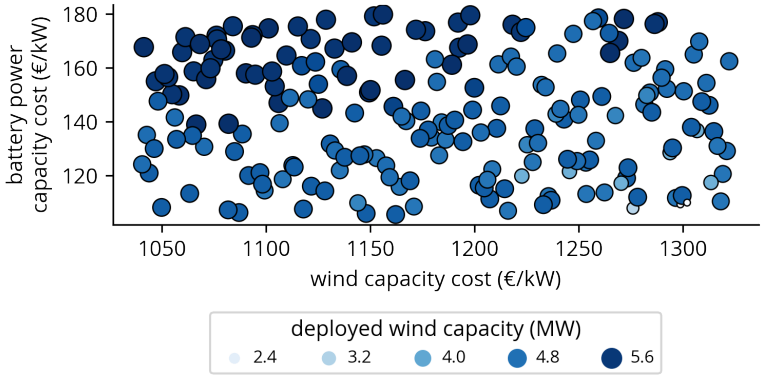

Figure C.9: Wind deployment on the uncertainty plane spanned by wind and battery capacity cost for 0.0 MW grid capacity *(policy 1)*

C.1.2 Policy 2 cost uncertainty and technology deployment

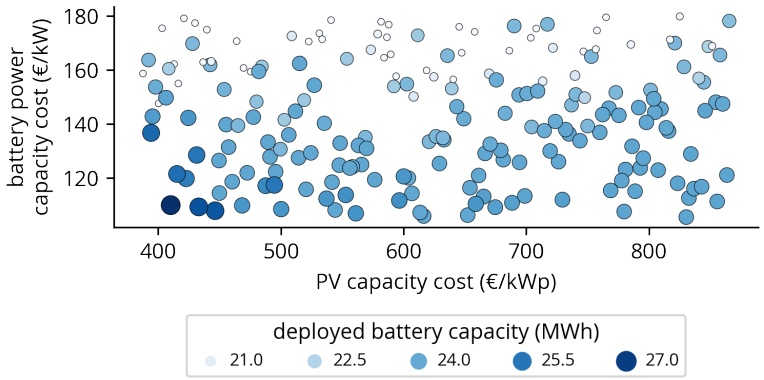

Figure C.10: Battery deployment on the uncertainty plane spanned by PV and battery capacity cost for 0.5 MW grid capacity *(policy 2)*

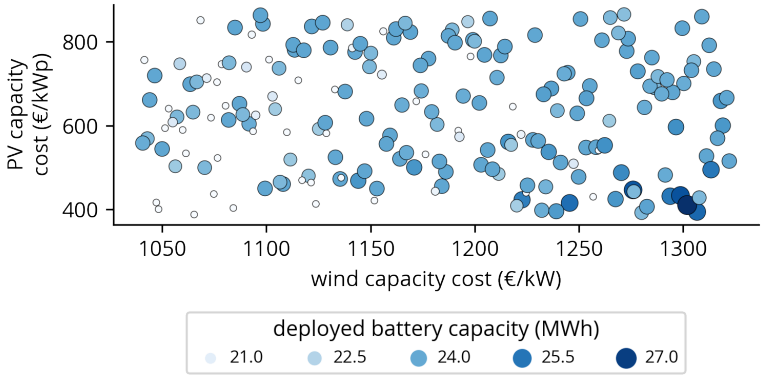

Figure C.11: Battery deployment on the uncertainty plane spanned by wind and PV capacity cost for 0.5 MW grid capacity *(policy 2)*

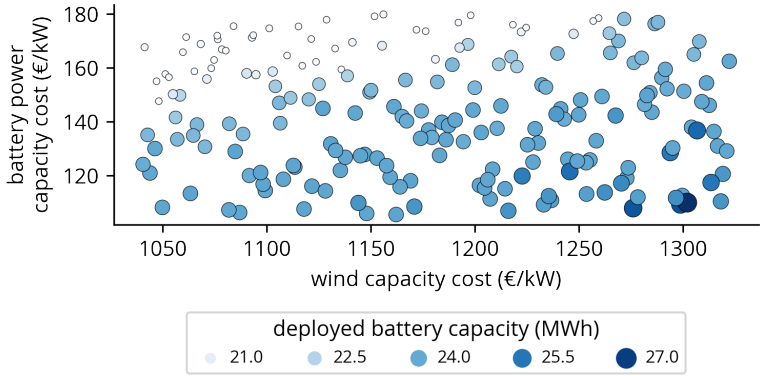

Figure C.12: Battery deployment on the uncertainty plane spanned by wind and battery capacity cost for 0.5 MW grid capacity *(policy 2)*

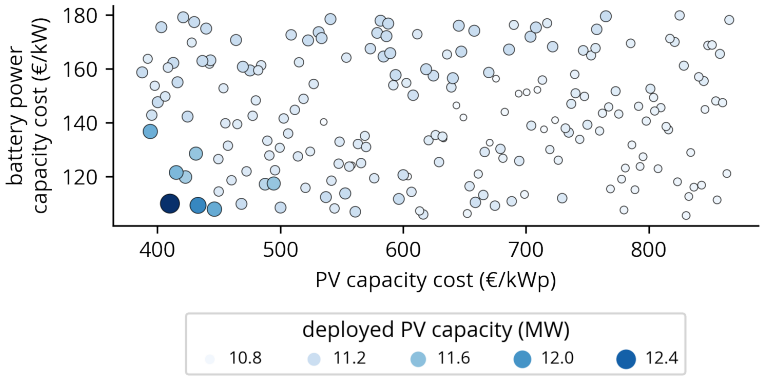

Figure C.13: PV deployment on the uncertainty plane spanned by PV and battery capacity cost for 0.5 MW grid capacity *(policy 2)*

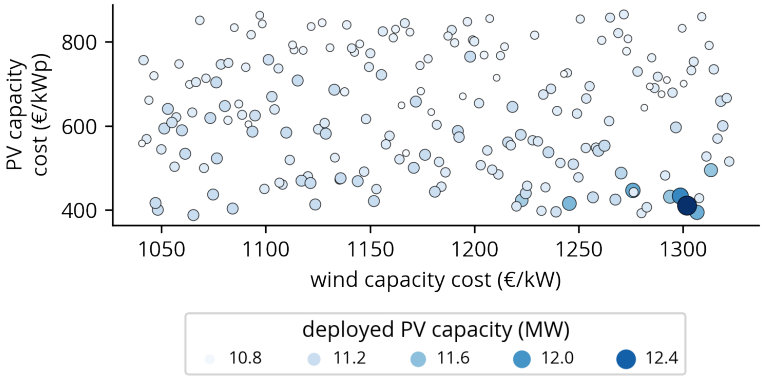

Figure C.14: PV deployment on the uncertainty plane spanned by wind and PV capacity cost for 0.5 MW grid capacity *(policy 2)*

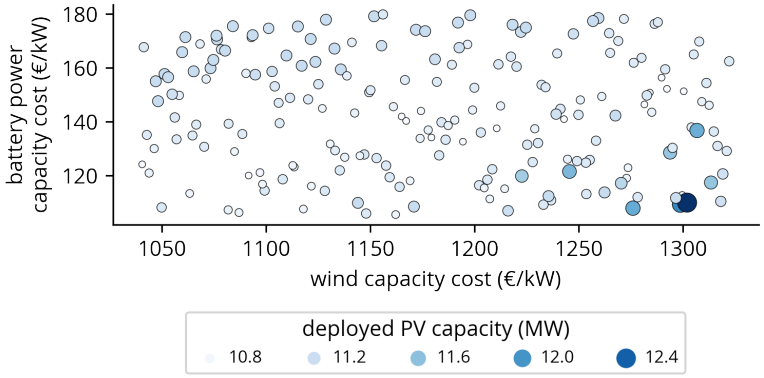

Figure C.15: PV deployment on the uncertainty plane spanned by wind and battery capacity cost for 0.5 MW grid capacity *(policy 2)*

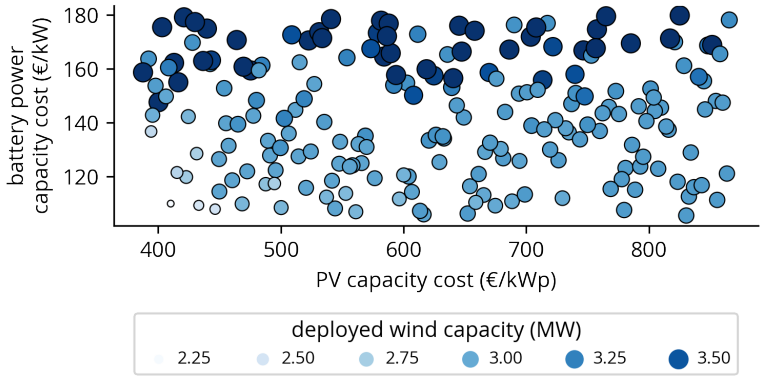

Figure C.16: Wind deployment on the uncertainty plane spanned by PV and battery capacity cost for 0.5 MW grid capacity *(policy 2)*

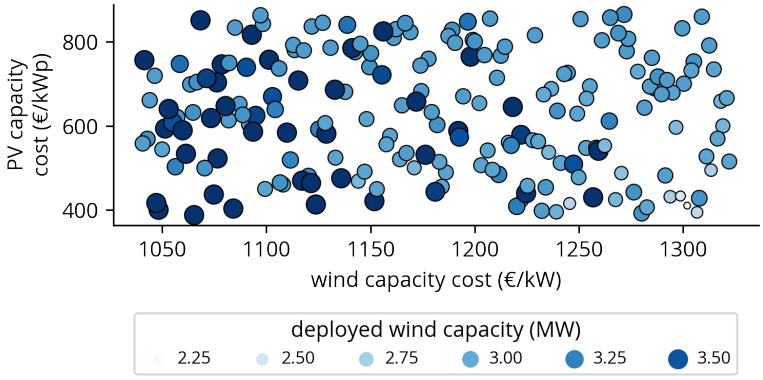

Figure C.17: Wind deployment on the uncertainty plane spanned by wind and PV capacity cost for 0.5 MW grid capacity *(policy 2)*

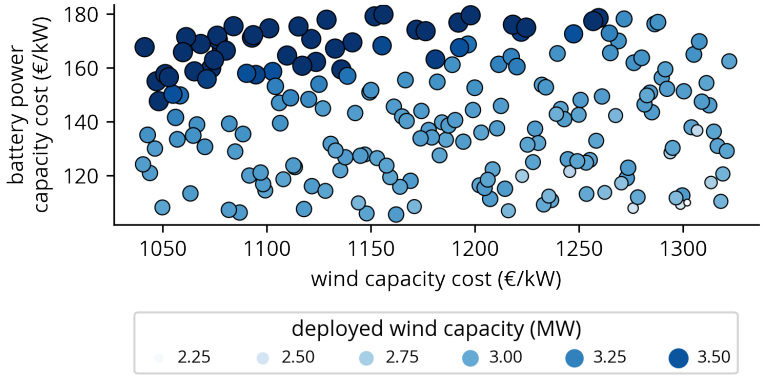

Figure C.18: Wind deployment on the uncertainty plane spanned by wind and battery capacity cost for 0.5 MW grid capacity *(policy 2)*

C.1.3 Policy 3 cost uncertainty and technology deployment

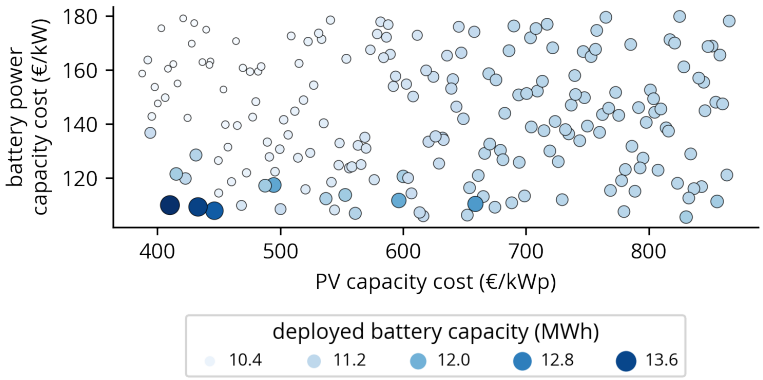

Figure C.19: Battery deployment on the uncertainty plane spanned by PV and battery capacity cost for 1.0 MW grid capacity *(policy 3)*

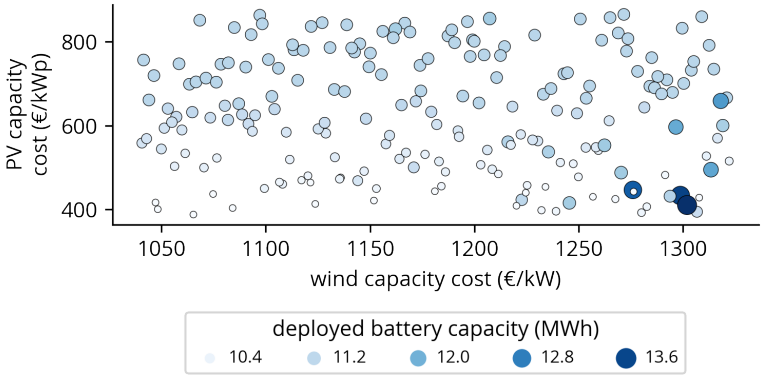

Figure C.20: Battery deployment on the uncertainty plane spanned by wind and PV capacity cost for 1.0 MW grid capacity *(policy 3)*

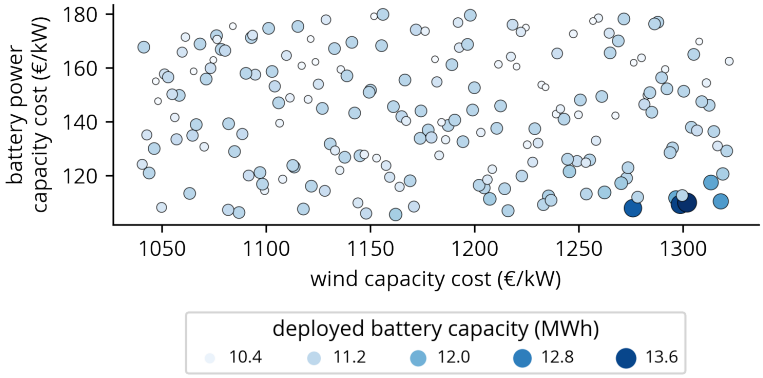

Figure C.21: Battery deployment on the uncertainty plane spanned by wind and battery capacity cost for 1.0 MW grid capacity *(policy 3)*

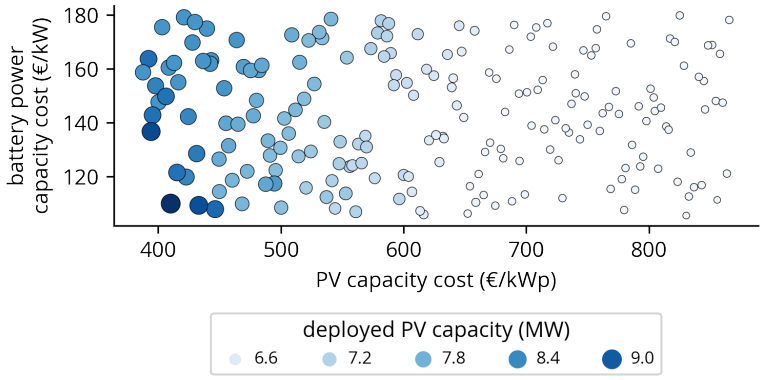

Figure C.22: PV deployment on the uncertainty plane spanned by PV and battery capacity cost for 1.0 MW grid capacity *(policy 3)*

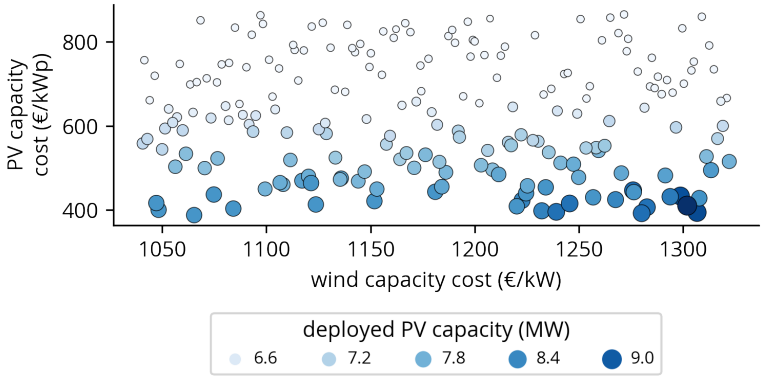

Figure C.23: PV deployment on the uncertainty plane spanned by wind and PV capacity cost for 1.0 MW grid capacity *(policy 3)*

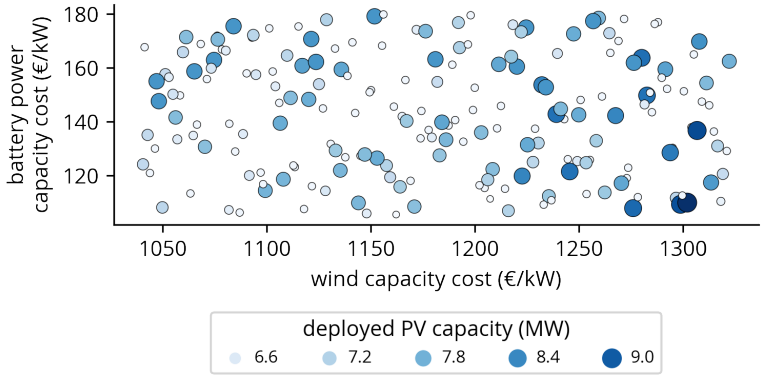

Figure C.24: PV deployment on the uncertainty plane spanned by wind and battery capacity cost for 1.0 MW grid capacity *(policy 3)*

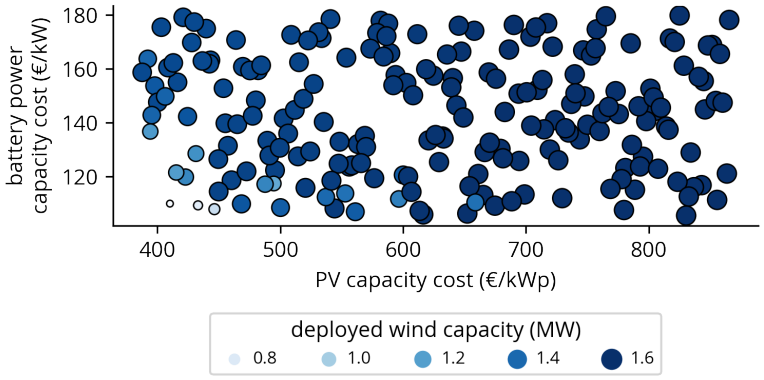

Figure C.25: Wind deployment on the uncertainty plane spanned by PV and battery capacity cost for 1.0 MW grid capacity *(policy 3)*

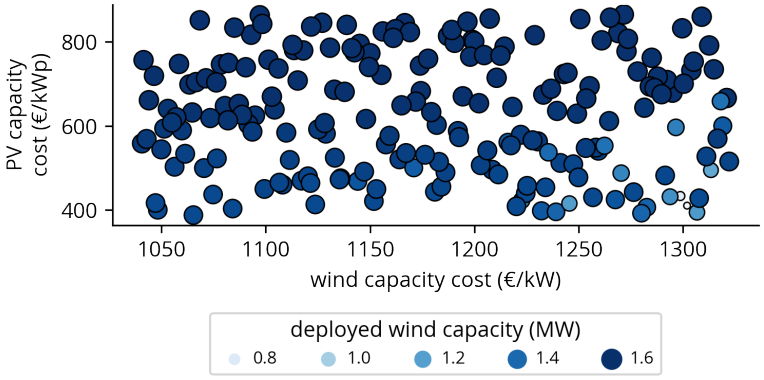

Figure C.26: Wind deployment on the uncertainty plane spanned by wind and PV capacity cost for 1.0 MW grid capacity *(policy 3)*

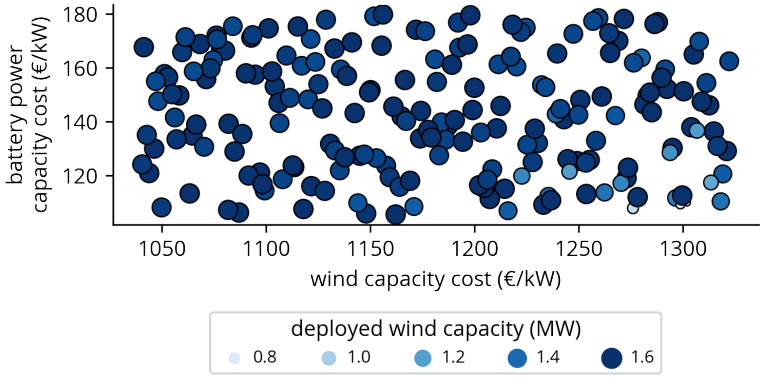

Figure C.27: Wind deployment on the uncertainty plane spanned by wind and battery capacity cost for 1.0 MW grid capacity *(policy 3)*

C.1.4 Policy 4 cost uncertainty and technology deployment

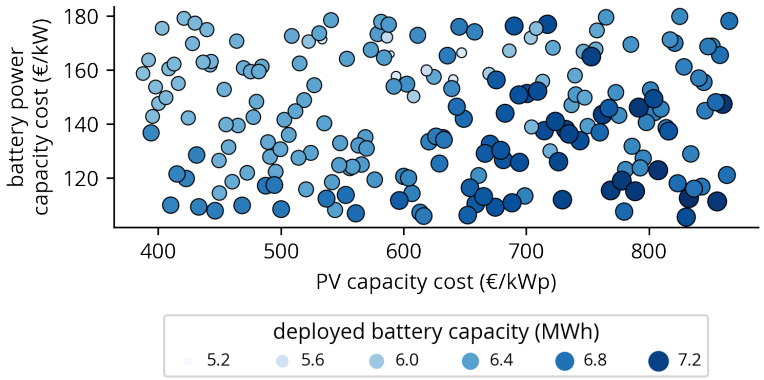

Figure C.28: Battery deployment on the uncertainty plane spanned by PV and battery capacity cost for 1.5 MW grid capacity *(policy 4)*

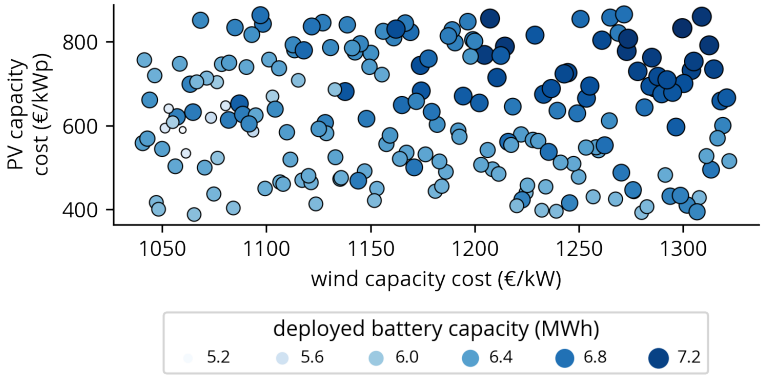

Figure C.29: Battery deployment on the uncertainty plane spanned by wind and PV capacity cost for 1.5 MW grid capacity *(policy 4)*

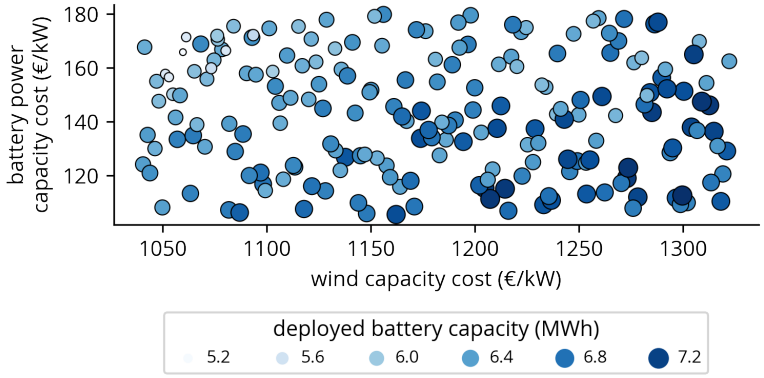

Figure C.30: Battery deployment on the uncertainty plane spanned by wind and battery capacity cost for 1.5 MW grid capacity *(policy 4)*

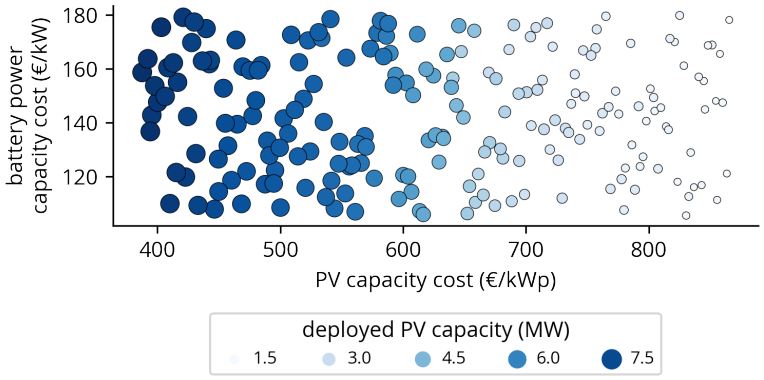

Figure C.31: PV deployment on the uncertainty plane spanned by PV and battery capacity cost for 1.5 MW grid capacity *(policy 4)*

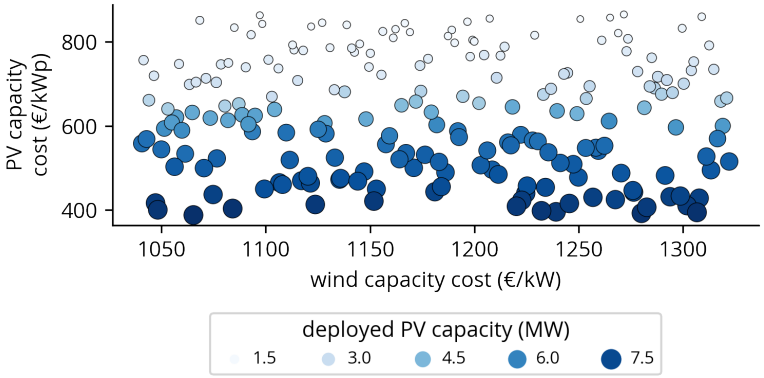

Figure C.32: PV deployment on the uncertainty plane spanned by wind and PV capacity cost for 1.5 MW grid capacity *(policy 4)*

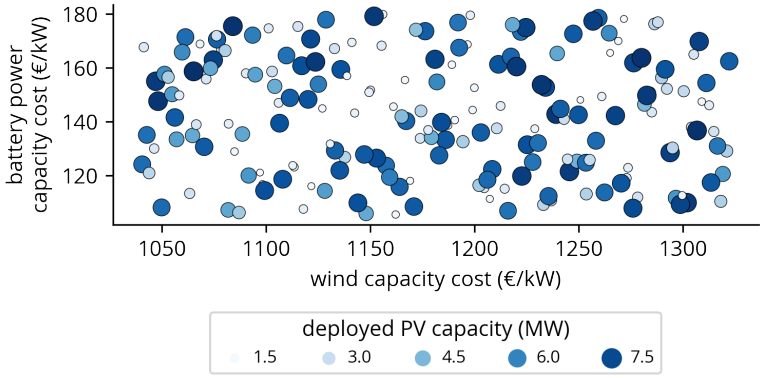

Figure C.33: PV deployment on the uncertainty plane spanned by wind and battery capacity cost for 1.5 MW grid capacity *(policy 4)*

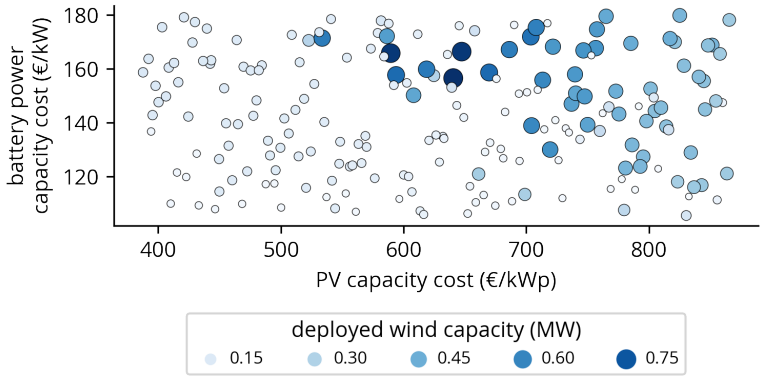

Figure C.34: Wind deployment on the uncertainty plane spanned by PV and battery capacity cost for 1.5 MW grid capacity *(policy 4)*

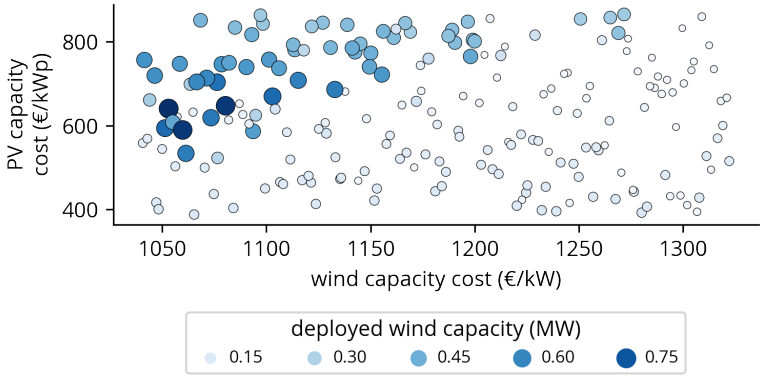

Figure C.35: Wind deployment on the uncertainty plane spanned by wind and PV capacity cost for 1.5 MW grid capacity *(policy 4)*

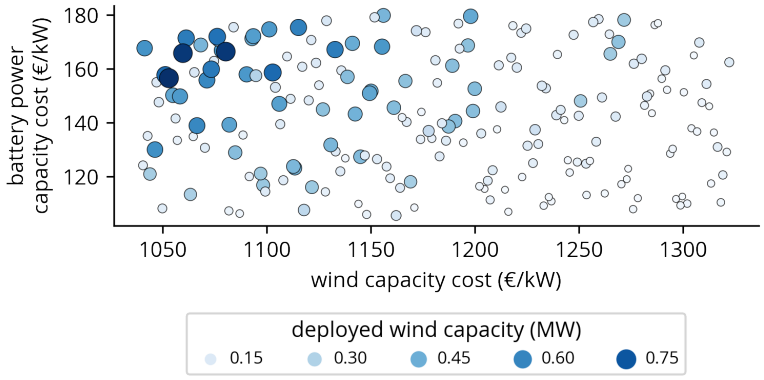

Figure C.36: Wind deployment on the uncertainty plane spanned by wind and battery capacity cost for 1.5 MW grid capacity *(policy 4)*

C.1.5 Cluster pair plots

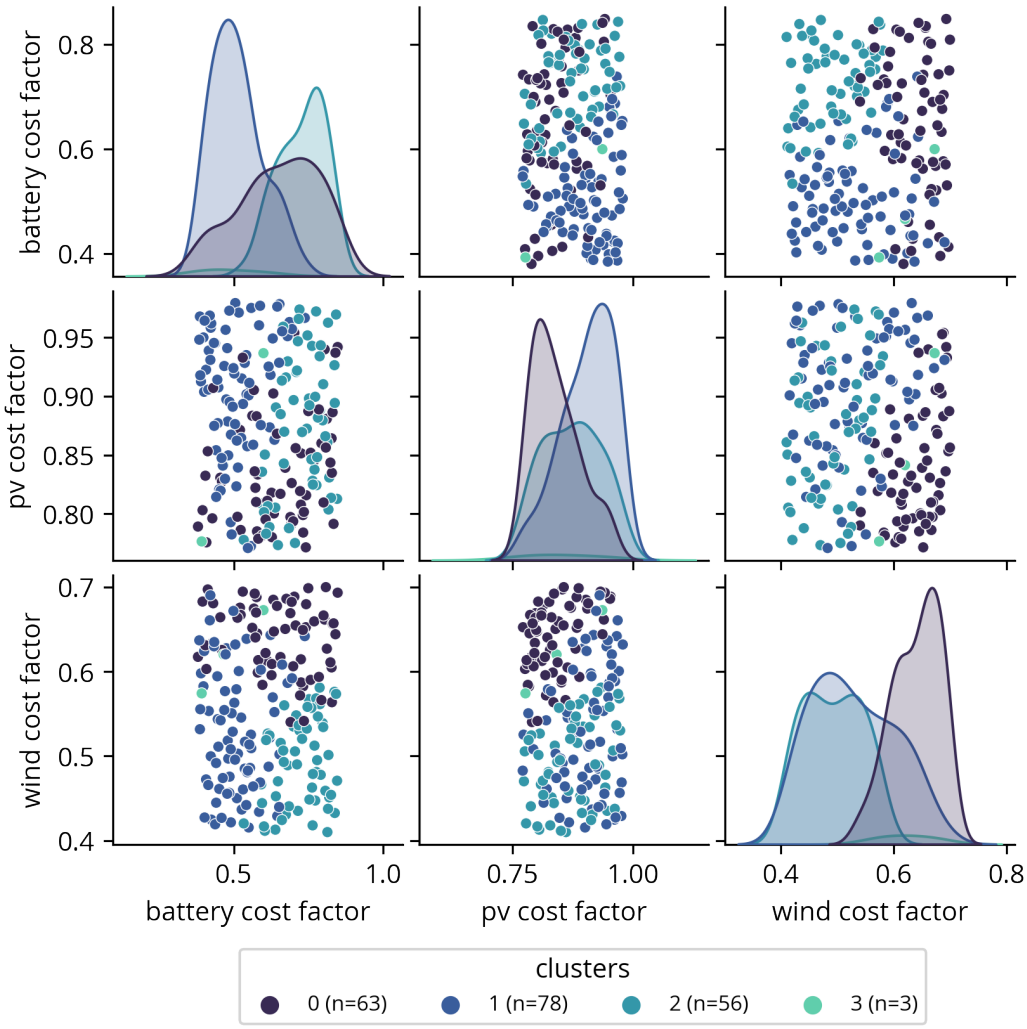

Figure C.37: Pair plots of the cost uncertainties related to the clusters obtained through cosine-distance based agglomerative clustering for the charging hub with 0 MW grid connection (policy 1)

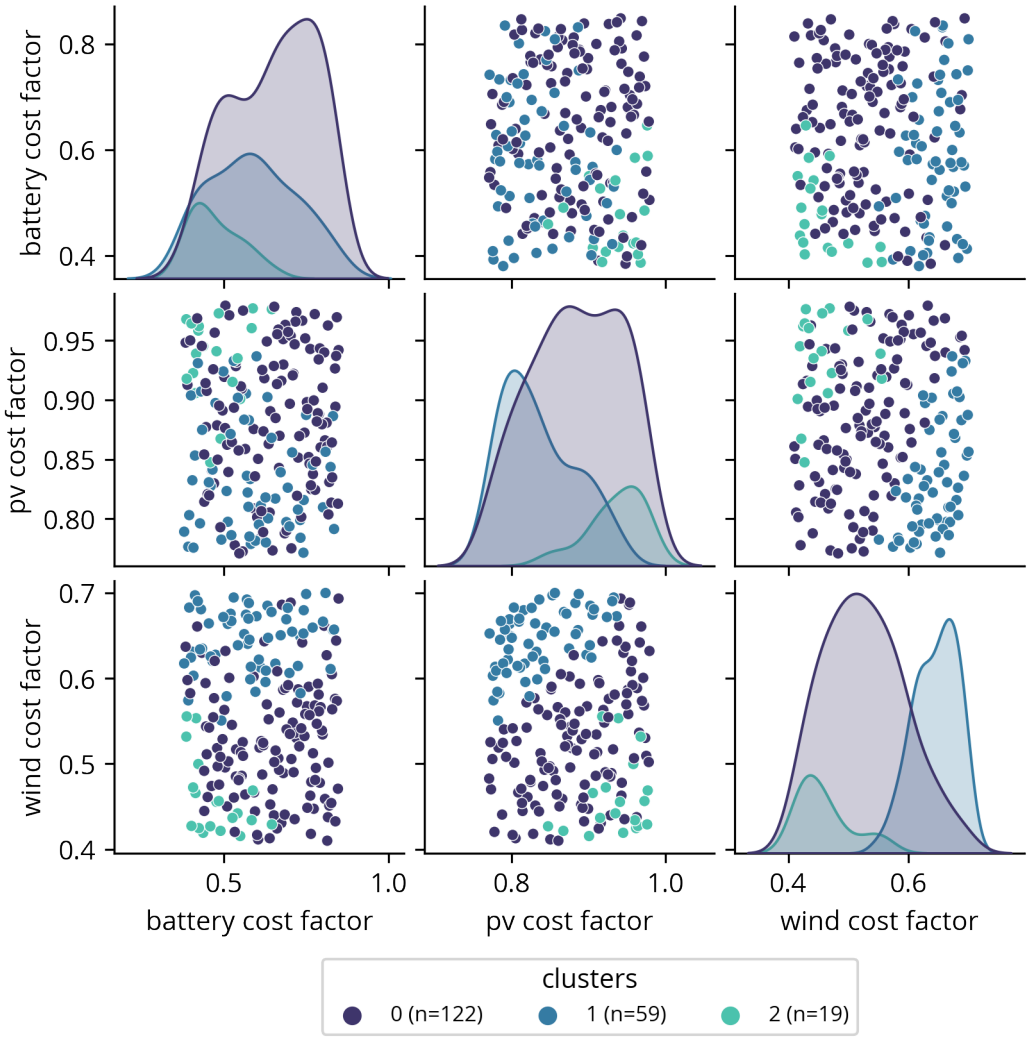

Figure C.38: Pair plots of the cost uncertainties related to the clusters obtained through cosine-distance based agglomerative clustering for the charging hub with 0.5 MW grid connection (policy 2)

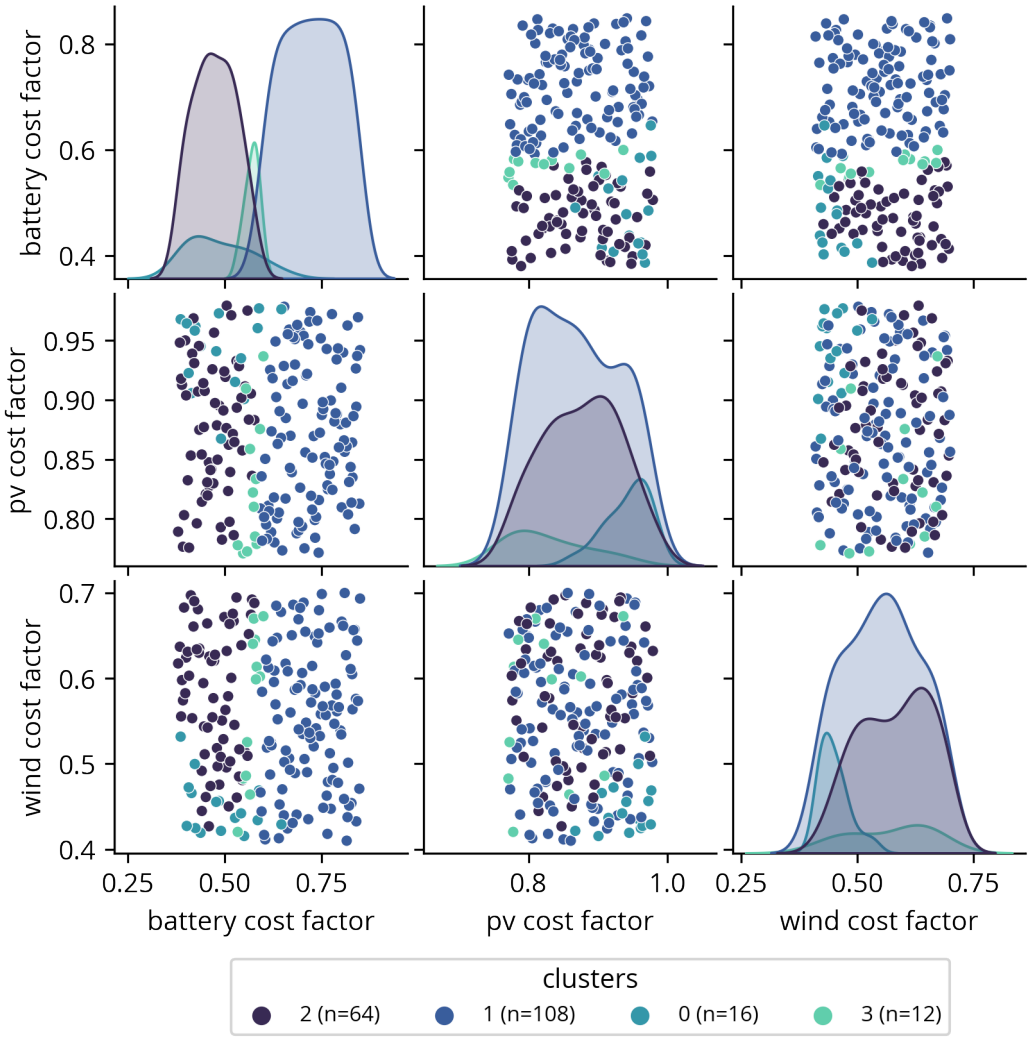

Figure C.39: Pair plots of the cost uncertainties related to the clusters obtained through cosine-distance based agglomerative clustering for the charging hub with 1 MW grid connection (policy 3)

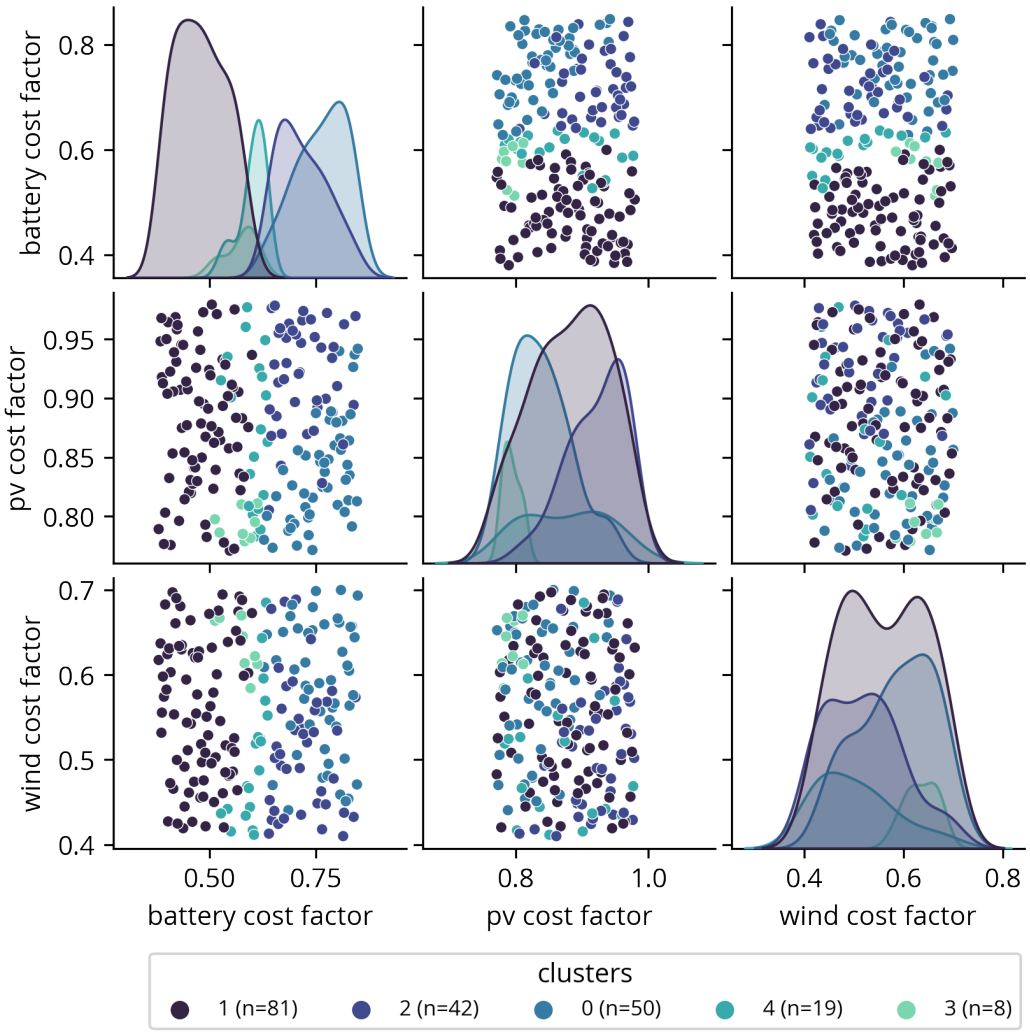

Figure C.40: Pair plots of the cost uncertainties related to the clusters obtained through cosine-distance based agglomerative clustering for the charging hub with 1.5 MW grid connection (policy 4)

C.2 Gelderland 2050

C.2.1 Results policy 2 - II3050 National

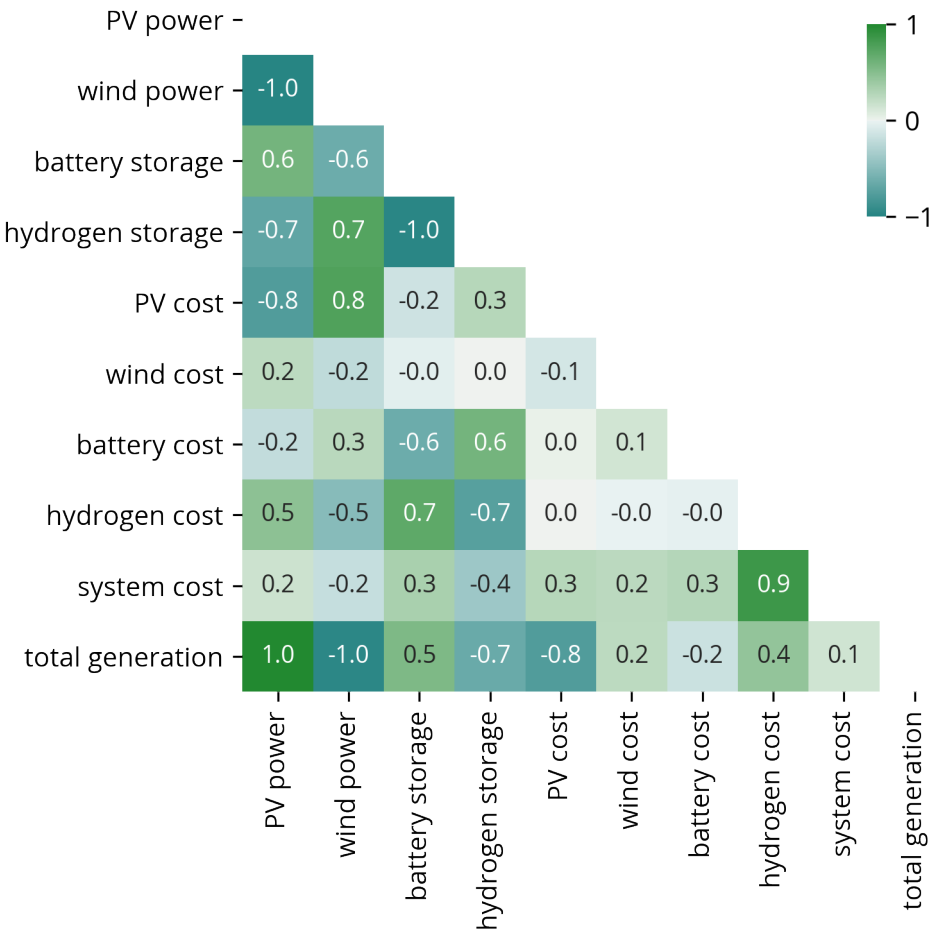

Figure C.41: Correlation matrix for the Gelderland in the national II3050 scenario (policy 2).

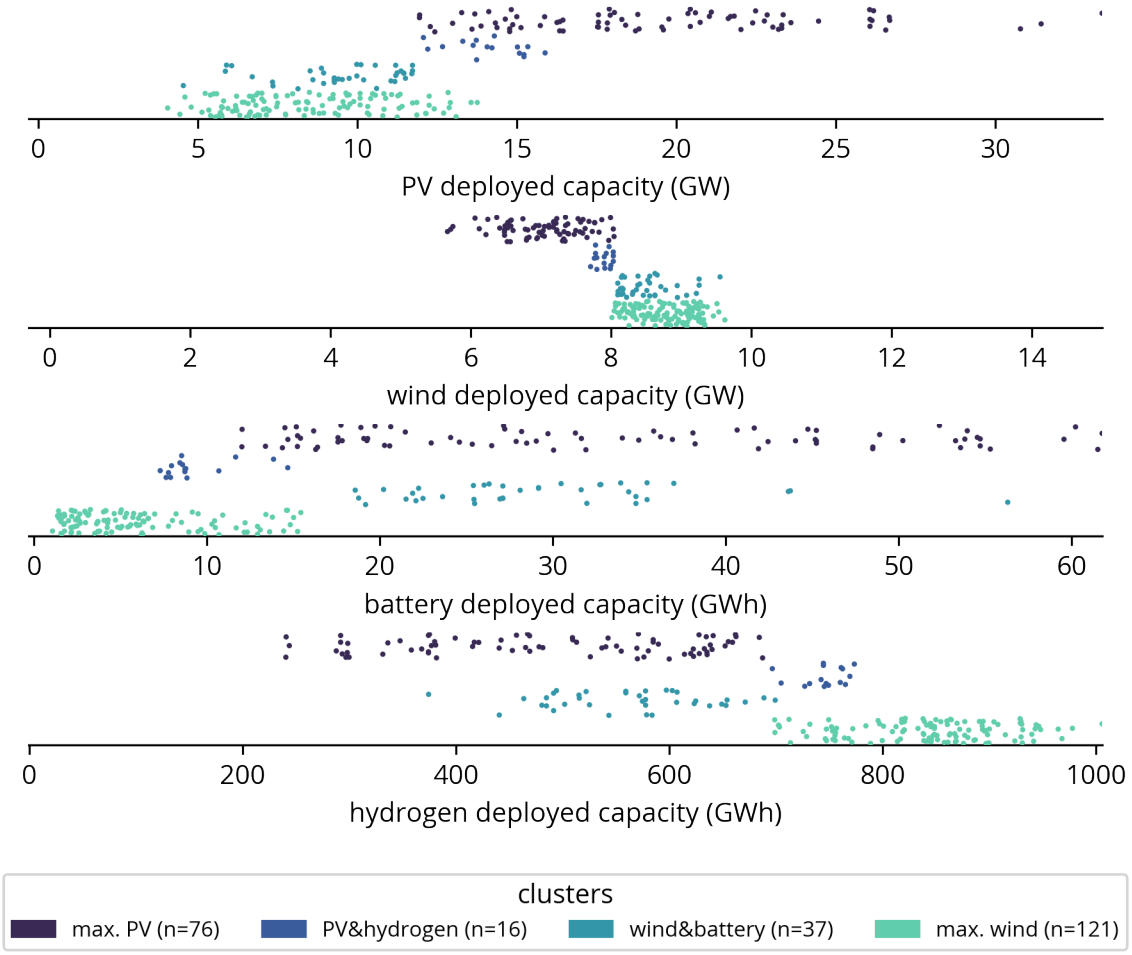

Figure C.42: Strip plot of the various cost-optimal system configurations found under cost uncertainty, colour-marked by the determined clusters for the national II3050 scenario (policy 4).

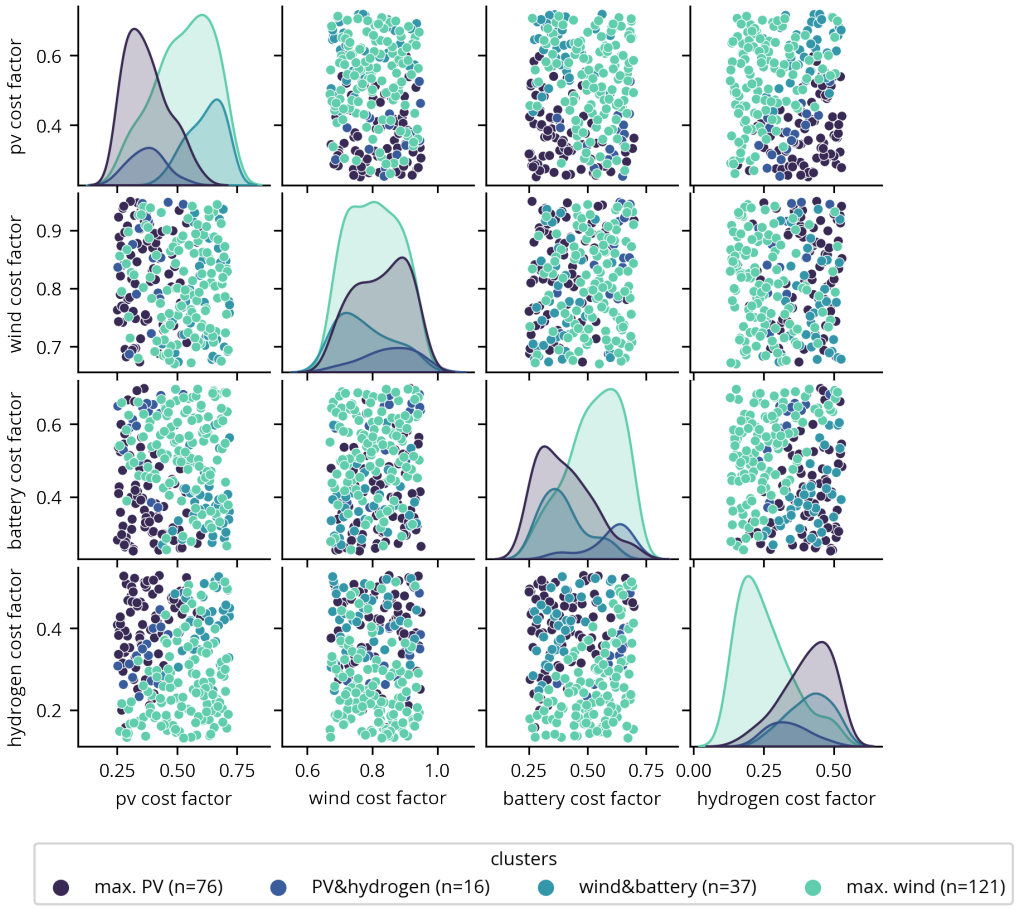

Figure C.43: Pair plot depicting the identified system configuration clusters in relation to the sampled cost uncertainties for the national II3050 scenario (policy 2).

C.2.2 Results policy 3 - II3050 European

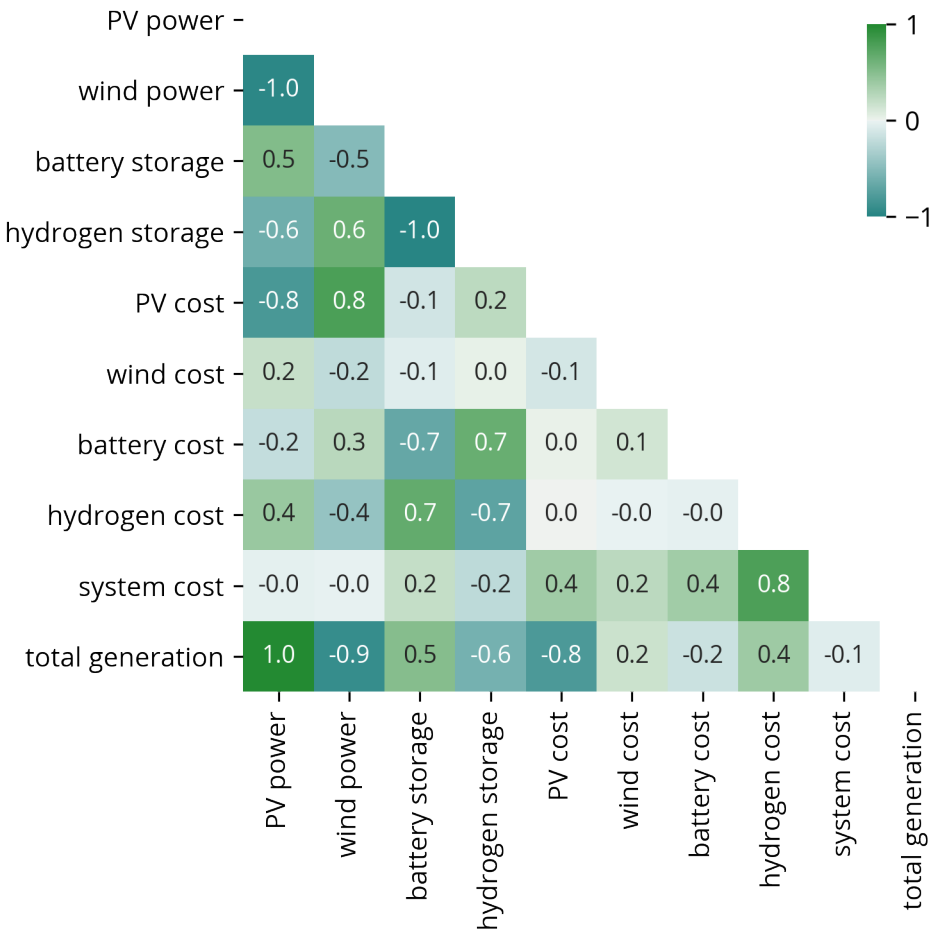

Figure C.44: Correlation matrix for the Gelderland in the European II3050 scenario (policy 3).

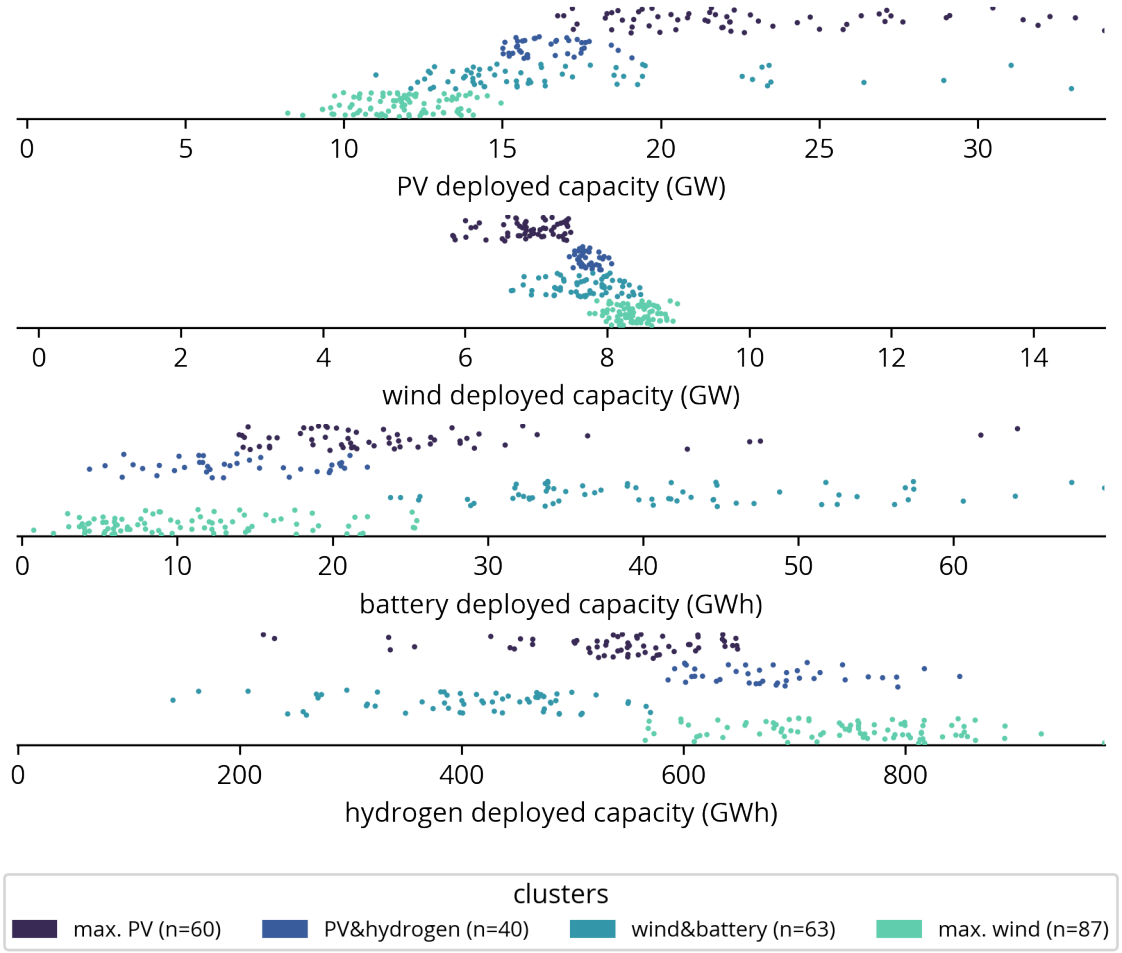

Figure C.45: Strip plot of the various cost-optimal system configurations found under cost uncertainty, colour-marked by the determined clusters for the European II3050 scenario (policy 3).

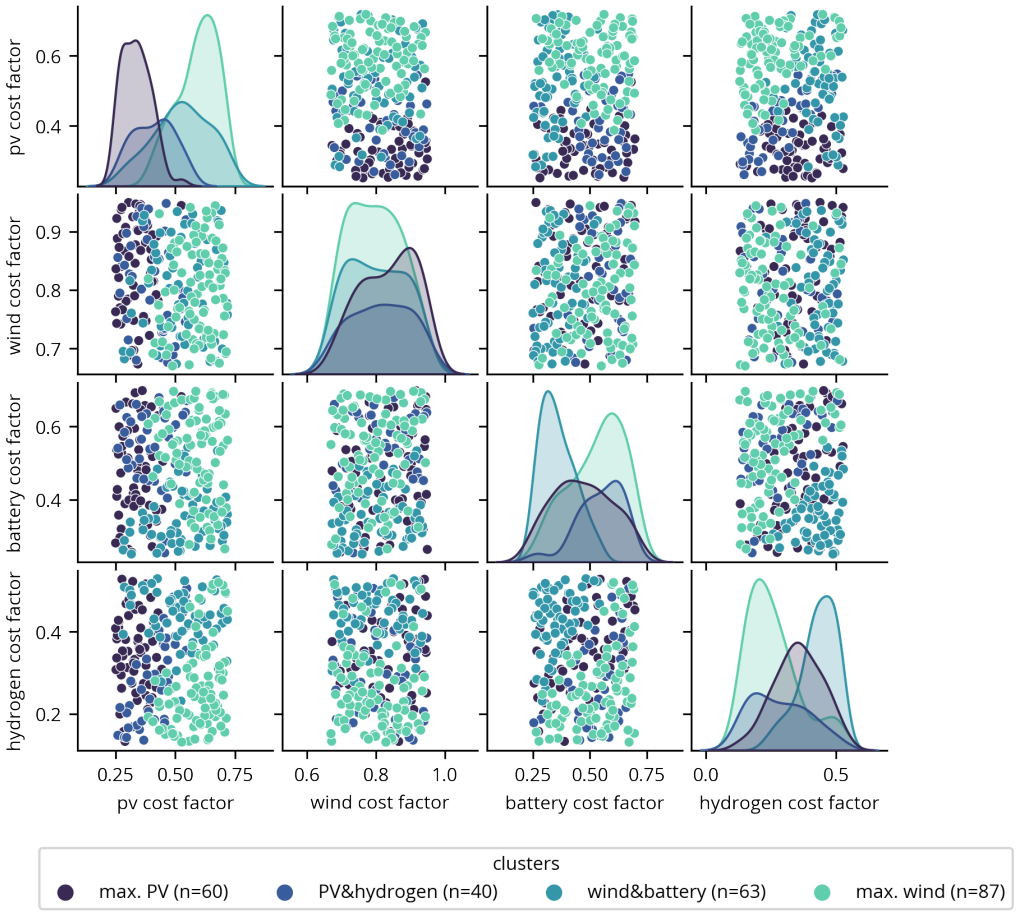

Figure C.46: Pair plot depicting the identified system configuration clusters in relation to the sampled cost uncertainties for the European II3050 scenario (policy 3).

Appendix D

Clustering

In this thesis, clustering is applied to the model outcomes to obtain insights into the patterns that occur in terms of the resulting system configurations. The method that is implied is inspired by the work of Fraiture [100], who applied this manner of clustering on an energy system optimisation model that optimises the investment in an energy system over multiple years based on a yearly resolution. The most important difference between this thesis' model and the multi-year model that was used by Fraiture is the fact that system configurations obtained in this thesis are not bound to a specific investment year or to a specific node in the system since the model in this thesis is of the snapshot category. This means that the clustering can be applied more direct, without the need for various processing steps to aggregate results.

Clustering is a form of unsupervised learning, where an algorithm is utilized to identify similarities in data. Based on the grouping that is obtained, specific attributes of the groups can be identified. When dealing with high dimensional data and large numbers of results, this method can be applied to reduce the number of data points to consider. As a result, the analyst can focus on the patterns that are found within the groups or how the groups compare against each other.

In this thesis, we are mostly interested in the cost-optimal system configurations that are obtained based on a wide range of technology costs. Based on the number of optimisation design variables, the results will span a solution space of N-dimensions. To cluster the outcomes in the solution space effectively, a standard procedure is used. This procedure is shown in figure D.1

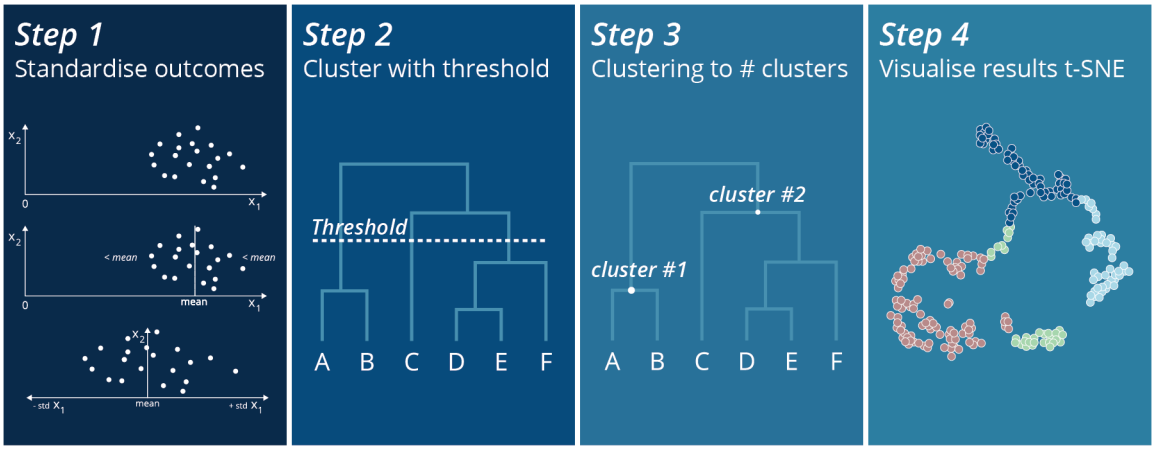

Figure D.1: Abstract overview of the clustering method applied in the case studies.

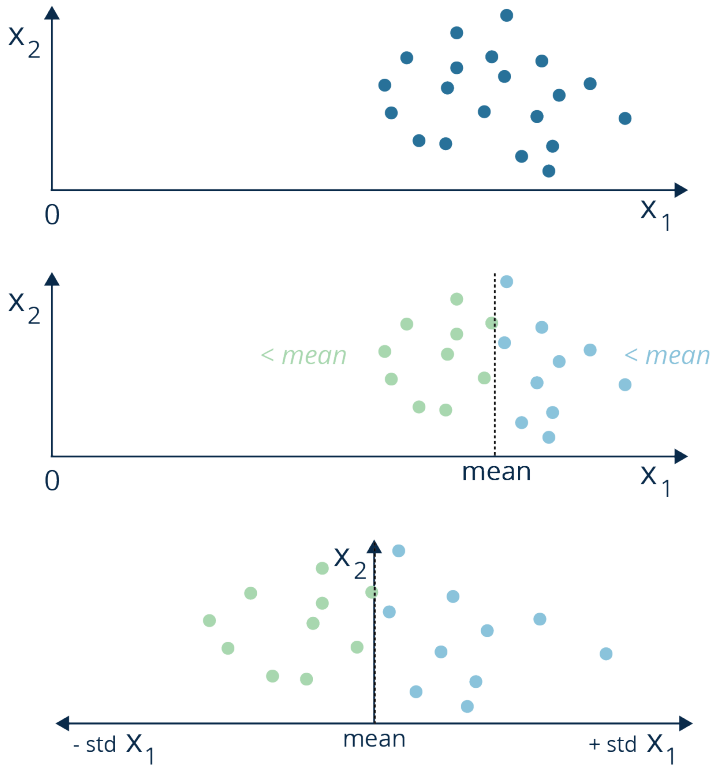

Figure D.2: Abstract illustration of standardisation for one feature for a set of 2-dimensional features.

D.1 Step 1 - Standardisation

The goal of the clustering is to identify similar system configurations. Therefore, the clustering method used is based on the connectivity of outcomes, i.e. the distance between outcomes. Any distance function can be implemented (e.g. Euclidean, Manhattan, higher-order P-norms, etc.) but because the ratio of implemented technologies is more relevant than the absolute numbers, this thesis implements a distance function that calculates the cosine distance. which is the inverse of the similarity criteria. The cosine distance is calculated after standardising results. Standardisation is a procedure that is applied per feature of the solution space. First, the feature mean of all outcomes is subtracted from each of the outcomes. Second, all outcome features are divided by the standard deviation of all outcome results. As a result, all standardised outcomes will be dimensionless and the resulting points in vector space are no longer skewed towards one of the design features. A visual representation of this procedure is shown in figure D.2.

D.2 Step 2 - Threshold clustering

The clustering algorithm implemented is a hierarchical agglomerative procedure. This means that it starts with all outcomes each in a single cluster and hierarchically merges clusters based on their distance until the termination condition is met. In this step the termination condition is the distance threshold. For most cases it was found that a threshold of 0.1 was sufficient to obtain distinct clusters, but to exclude the possibility for excessive amounts of clusters.

Hierarchical agglomerative clustering can be visualised using a dendrogram, which displays the hierarchical order in which clusters are formed based on their distance criteria. An abstract visual

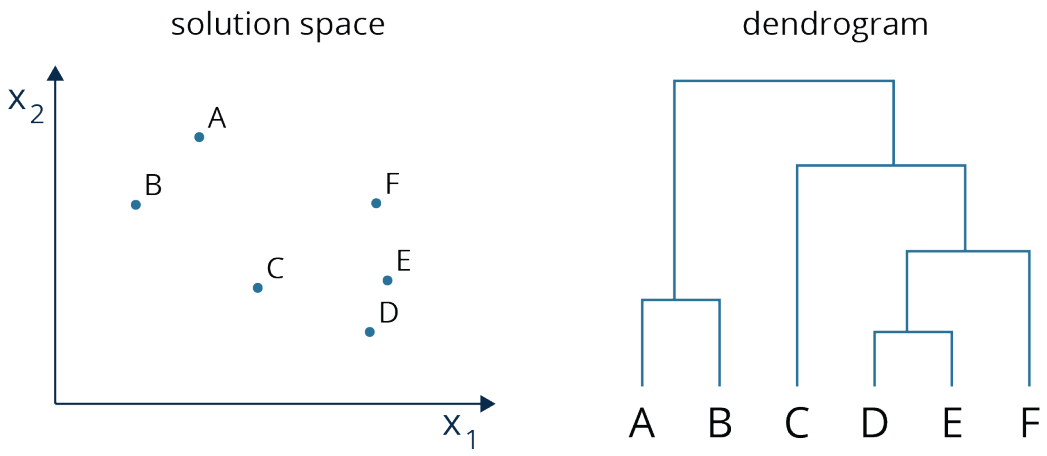

Figure D.3: An abstract representation of a possible solution space and the corresponding dendrogram for full-linkage clustering.

representation of such a dendrogram is shown in figure D.3. From the figure it can be seen that points E and D are most similar in the solution space. When consulting the dendrogram, it can be seen that these two outcomes are indeed merged to form the first cluster of more than 1 point. At a slightly higher point in the dendrogram, points A and B are merged to form the second cluster. Following this dendrogram up the ladder represents the agglomerative method applied. If we follow the dendrogram from the top to the bottom, it is a divisive clustering method.

D.3 Step 3 - Clustering with predefined number of clusters

Based on the clusters found in step 2, this step considers the resulting clusters and compares them based on the range that is covered in the cost uncertainties and system design outcomes. Most importantly, the amount of clusters is reduced until the total number of clusters contain a sufficient number of configurations in each cluster.

D.4 Step 4 - Visualize clusters with t-SNE

Fraiture recommends future research to implement t-SNE to visualise the resulting clusters in reduced dimensions as a shortcut to more extended analysis using various visualisations. This method is very well suited to data sets of high dimension and that contain a lot of results. However, the operation can be quite tedious and outcomes are unique due to the stochastic nature. Moreover, the clusters that can be visualised using t-SNE are strongly influenced by the parameters chosen. Tweaking the parameters is time-consuming and requires good understanding of the impact of the various parameters. If used incorrectly, the method can reveal non-existing clusters.

Sometimes this visualisation was useful, but most of the time it did not contain any new information and the strip plots and pair plots revealed more insights. Moreover, t-SNE is based on distribution of data and not on the distance between points and thus, it is not necessarily well-suited to use with cosine distance based clustering. As a result, during this thesis the proposed visualisation pipe-line with pair plots and strip plots was favoured over t-SNE. An example of a t-SNE visualisation is shown in figure D.4.

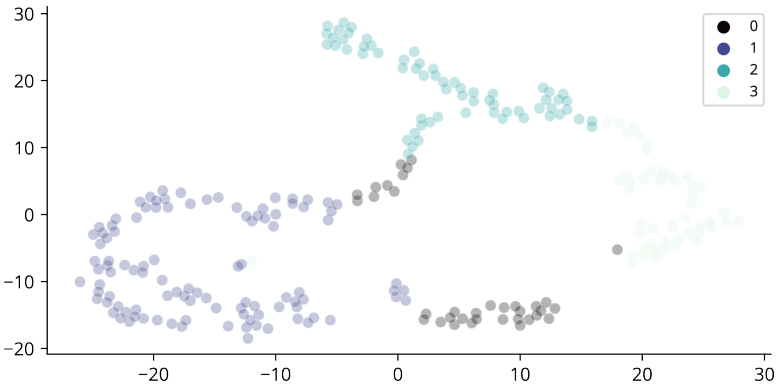

Figure D.4: An example visualisation of clusters using the t-SNE dimension reduction method.

Appendix E

Supplementary material references

E.1 EMA experiments code references

Cable pooling
Version: `https://github.com/thesethtruth/LESO/tree/b3239d6bd5`
Folder: LESO/thesis scripts/experiments/cablepool

E-mobility hub
Version: `https://github.com/thesethtruth/LESO/tree/eab19194f1`
Folder: LESO/thesis scripts/experiments/evhub

Regional Energy Strategies 2030
Version: `https://github.com/thesethtruth/LESO/tree/9e439cf395`
Folder: LESO/thesis scripts/experiments/2030

Gelderland 2030
Version: `https://github.com/thesethtruth/LESO/tree/d3a1b28218`
Folder: LESO/thesis scripts/experiments/2030

Gelderland 2050
Version: `https://github.com/thesethtruth/LESO/tree/8e12081ca8`
Folder: LESO/thesis scripts/experiments/2050

E.2 ETM scenarios references

RES Achterhoek 2030
URL: `https://pro.energytransitionmodel.com/scenarios/815753`
Scenario number: 815753

RES Arnhem/Nijmegen 2030
URL: `https://pro.energytransitionmodel.com/scenarios/815754`
Scenario number: 815754

RES Cleantech 2030
URL: `https://pro.energytransitionmodel.com/scenarios/815755`
Scenario number: 815755

RES FoodValley 2030
URL: https://pro.energytransitionmodel.com/scenarios/815756
Scenario number: 815756

RES Noord-Veluwe 2030
URL: https://pro.energytransitionmodel.com/scenarios/815757
Scenario number: 815757

RES Rivierenland 2030
URL: https://pro.energytransitionmodel.com/scenarios/815758
Scenario number: 815758

Gelderland 2030
URL: https://pro.energytransitionmodel.com/scenarios/815716
Scenario number: 815716

Gelderland 2050 - Regional
URL: https://pro.energytransitionmodel.com/scenarios/815695
Scenario number: 815695

Gelderland 2050 - National
URL: https://pro.energytransitionmodel.com/scenarios/815696
Scenario number: 815696

Gelderland 2050 - European
URL: https://pro.energytransitionmodel.com/scenarios/815697
Scenario number: 815697

Gelderland 2050 - International
URL: https://pro.energytransitionmodel.com/scenarios/815698
Scenario number: 815698